Analyse fonctionnelle de la famille OCTOPUS chez Arabidopsis thaliana

Pauline Anne

UNIVERSITE PARIS-SUD

ÉCOLE DOCTORALE : SCIENCES DU VÉGÉTAL
Institut Jean-Pierre Bourgin

DISCIPLINE : BIOLOGIE

THÈSE DE DOCTORAT

Soutenue le Vendredi 05 Décembre 2014

par

Pauline ANNE

Analyse fonctionnelle de la famille OCTOPUS chez *Arabidopsis thaliana*

Composition du jury :

Directeur de thèse :	Jean-Christophe PALAUQUI	CR1 (IJPB, INRA Versailles)
Rapporteurs :	Niko GELDNER	Professeur (DBMV, UNIL Lausanne)
	Teva VERNOUX	DR2 (RDP, CNRS-ENS Lyon)
Examinateurs :	Marianne DELARUE	Maître de Conférence (IBP, PSUD11 Orsay)
	Herman HOFTE	DR1 (IJPB, INRA Versailles)
	Yvon JAILLAIS	CR1 (RDP, CNRS-ENS Lyon)

Mes premières pensées vont évidemment à JC (Jean-Christophe Palauqui) pour m'avoir accueillie dans son laboratoire et confié l'étude de la famille *OPS*. Je te remercie tout particulièrement pour avoir cru en moi et pour m'avoir préparée efficacement au concours de l'Ecole Doctorale. Merci pour m'avoir encadrée au cours de ces trois années et transmis ton savoir-faire en cytologie et en microscopie, des compétences qui m'accompagneront pour la suite. Je te remercie également pour ta sympathie et ton grand cœur, ce très fut agréable de travailler avec toi. ☺
Je remercie du fond du cœur mon Kiankian (Kian Hématy) sans qui cette thèse n'aurait jamais été la même. Merci pour tes conseils au quotidien, ton implication technique dans mon travail thèse, dans design expérimental et pour les discussions scientifiques qui ont animées nos conversations au cours de ces trois années. Merci (quand même) pour les « remontages de bretelles ». Et merci de m'avoir transmis ta rigueur et ta passion, mon succès, je te le dois en partie. Merci ♥♥♥
Un grand merci à ma copine biochimiste préférée Mariannou (Marianne Azzopardi) qui a mené avec une grande efficacité (et non toujours sans peine) l'ensemble des expérimentations biochimiques. Tu fais partie des gens que je vais regretter ! ☺ **<3**
Je remercie bien évidemment Katia Belcram pour sa bonne humeur légendaire, pour ses financiers, sa tarte tatin et pour tous les conseils qu'elle a pu m'apporter tant en cytologie qu'en analyse d'image. J'en profite pour remercier Olivier Grandjean et Daniel Zaharia pour leur aide au microscope (les débuts ne sont pas toujours facile derrière ces grosses machines !).
Merci à Lionel Gissot pour m'avoir formée à la manipulation de la levure, je me sens désormais une âme de boulangère ! Merci également pour tous les petits conseils que tu as pu me donner en réponse à mes questions de thésarde perdue ! Je remercie également Yannick Bellec toujours prêt à aider et toujours de bon conseil ! J'espère que mes jolis protocoles te seront de bon usage. Je te remercie JD (Jean-Denis Faure) pour les discussions que nous avons pu avoir en réunion d'équipe. Ton recul et ton esprit de synthèse ont beaucoup apporté lors de l'écriture du papier. Je te remercie également d'avoir fait de mon projet de thèse un sujet d'étude pour le Master Sciences du Végétal au cours duquel j'ai eu l'opportunité d'intervenir. Merci à Sébastien Beaubiat et Julie Gervais qui ont participé à ce projet. J'aurai aimé vous le dire en langage R, mais mes compétences restent encore trop mauvaises pour cela : merci à l'ensemble de l'équipe informatique pour leur aide sur l'analyse statistique de mes données, et plus particulièrement à Jasmine, Éric et David. Mon p'tit Célinou (Céline Morineau). Merci d'avoir partagé avec moi tes collations lors de la pause de quatre heures, pour m'avoir remonté le moral quand je l'avais dans les chaussettes et juste pour m'avoir comprise en tant que thésarde dans la même galère ! Un grand merci à l'ensemble des membres du sous-sol (encore présents ou déjà parti) avec qui j'ai pu partager les repas du midi, les pots du vendredi soir, les gouters d'anniversaire et encore nos chaleureux repas de Noël ☺. La bonne humeur, les rires (mais aussi le travail !) résument parfaitement l'ambiance qui règne au sous-sol du bâtiment 2 (à la cave pour d'autres) et qui donne vraiment envie de venir y travailler. Merci à vous tous**.**
Je remercie également et très chaleureusement Kian, Patrick Laufs, Richard Sibout, Sebastian Wolf pour avoir participé activement à la correction de ce manuscrit. Chacun d'entre vous sait combien votre aide m'a été précieuse. Merci à l'ensemble des personnes qui ont participé à la réflexion sur ce projet en apportant leur expertise lors de discussion: Olivier Hamant, Grégory Vert, Catherine Rechenmann, Nicolas Arnaud, Sébastian Wolf, Patrick Laufs, Herman Höfte, Niko Geldner, Sébastien Mongrand. J'en profite pour remercier Sébastien pour sa bonne compagnie à Manchester. Nous nous sommes rencontrés par hasard au congrès SEB 2014 et j'ai passé une agréable semaine en ta compagnie. Je garderai un très bon souvenir de mon premier congrès ! Merci à Annouch (Anne Guiboileau) et Sebastian Wolf de m'avoir permis de présenter mon travail en public à l'extérieur de l'institut. Merci aux membres du Jury SEB pour m'avoir attribué le prix de meilleur poster de la session « Plants ». Cela fait toujours plaisir de voir ses efforts récompensés.
Je remercie également les « fournisseurs » de graines, de cDNA qui n'ont pas hésité à partager leur matériel : Yanhai Yin pour son anti-corps BES1 ; Zhi Wong Wang pour les graines *cdl1-1*, *cdg1-2*, le

double mutant *cdl1 cdg1* ainsi que sa lignée CDG1-YFP ; Sebastian pour la collection de mutants brassinostéroïdes et les cDNA BRI1 et BAK1.
Je remercie aussi les personnes qui font partie des coulisses mais sans qui rien ne serait possible (ou en tout cas serait bien plus difficile) : les serristes avec une mention particulière pour Bruno Letarnec, Hervé Ferry, Patrick Grillot, Joel Talbotec et Amélie Degeueuse ; l'équipe administrative toujours très conciliante et très efficace; le personnel de la laverie ; l'équipe du magasin ; les agents d'entretien. Merci à toutes celles et ceux que j'ai pu croiser, qui ont pu me venir en aide (Ivan Le Masson, Martine Pastuglia pour ne citer qu'eux).
Merci à *OPSL1*, *OPSL2* et au système Gateway qui, au travers de clonages, m'ont donné l'opportunité de connaitre un peu mieux Kian... ;-)
Merci à ma chouette bande de copains, ma famille (Tata Corinne et Tonton José en particulier) pour m'avoir toujours soutenue jusqu'à aujourd'hui et d'avoir cru en moi. **<3**
Pour finir, je tiens à remercier les membres de mon jury de thèse qui ont accepté de reviewer mon travail et pour la discussion stimulante que nous avons eu pendant ma soutenance : Herman Hofte, Niko Geldner, Teva Vernoux, Yvon Jaillais et Marianne Delarue.

Je terminerai ces remerciement par un poème de Jacques Prévert auquel j'ai repensé en rédigeant ce manuscrit et qui me tient à cœur de partager avec vous. Ne croyez surtout pas que je suis une grande littéraire… je l'avais juste appris quand j'étais enfant !

Pour faire le portrait d'un oiseau

Peindre d'abord une cage
avec une porte ouverte
peindre ensuite
quelque chose de joli
quelque chose de simple
quelque chose de beau
quelque chose d'utile
pour l'oiseau
placer ensuite la toile contre un arbre
dans un jardin
dans un bois
ou dans une forêt
se cacher derrière l'arbre
sans rien dire
sans bouger …
Parfois l'oiseau arrive vite
mais il peut aussi bien mettre de longues années
avant de se décider
Ne pas se décourager
attendre
attendre s'il le faut pendant des années
la vitesse ou la lenteur de l'arrivée de l'oiseau
n'ayant aucun rapport
avec la réussite du tableau
Quand l'oiseau arrive
s'il arrive
observer le plus profond silence
attendre que l'oiseau entre dans la cage
et quand il est entré
fermer doucement la porte avec le pinceau
puis
effacer un à un tous les barreaux
en ayant soin de ne toucher aucune des plumes de l'oiseau
Faire ensuite le portrait de l'arbre
en choisissant la plus belle de ses branches
pour l'oiseau
peindre aussi le vert feuillage et la fraîcheur du vent
la poussière du soleil
et le bruit des bêtes de l'herbe dans la chaleur de l'été
et puis attendre que l'oiseau se décide à chanter
Si l'oiseau ne chante pas
c'est mauvais signe
signe que le tableau est mauvais
mais s'il chante c'est bon signe
signe que vous pouvez signer
Alors vous arrachez tout doucement
une des plumes de l'oiseau
et vous écrivez votre nom dans un coin du tableau.

Jacques Prévert, *Paroles*

Table des matières

INTRODUCTION

Plants are everywhere, even in the most hostile regions. It's difficult to imagine land without plants, however land conquest starts there are only 500 million years ago for a earth that is 4.5 billion years-old! Today, plant kingdom counts almost 298 000 predicted species (Sweetlove, 2011) occupying diverse biotopes: cold or warm, dry or humid and from shaded zones to the most enlighten (Campbell and Reece, 2007).

A myriad of plants traits emerged from evolution permitting plants to colonize all types of environments. Way from unicellular to multicellular organisms and later organogenesis and tissues specification permitted specialization of activities. Pluricellularity and division of tasks require intra- and inter-cellular communications ensuring by plasmodesmata acquisition and mobile signal molecules such as hormones. Otherwise, land conquest needs a control of water flux and exchanges to overcome dehydration. Thus cuticle, a hydrophobic layer on the surface of plants and stomata development permitted plants to control water loss while allowing gas exchange necessary for photosynthesis. One of the adaptive characters selected by evolution is "the emergence of vascular tissues that played a central role in the plant conquest of land" (Rodriguez-Villalon et al., 2014). Plants possessing vascular tissues are called vascular plants or "Tracheophytes". Acquisition of vasculature solved the problem of long distance transport, permitting plants to grow in height. Some trees, such as giant sequoias, can even reach 100 meters height!

My thesis objective was to study the function of OCTOPUS protein. OCTOPUS is known to be involved in vascular tissues formation, but its function remains unclear. My work permitted to replace OCTOPUS in a hormonal signaling pathway. Therefore, I will develop in this introduction (1) organization and ontogenesis of vascular tissues insisting more specifically on phloem; (2) the signaling pathway of brassinosteroids and (3) involvement of brassinosteroids during development.

1 Vascular tissues: generalities, organogenesis, ontogenesis

1.1 What are vascular tissues?

Water, minerals and CO_2 are directly available for aquatic plants: all cells are directly in contact with their environment. In contrast, land plants are sessile and in consequence they have to face dehydration due to the low content of water in the atmosphere (Campbell and Reece, 2007). This constraint was progressively solved by the creation of conductive tissues which connect organs together and allow exchanges between autotrophic source (mature leaves able to ensure photosynthesis) and heterotrophic sink organs (Figure 1.1). At first glance, the vascular network is made of two kinds of tissues: xylem and phloem. By opposition to analogous vascular tissues in animal which correspond to a close system, plant vascular tissues is an open system with necessity to control the entrance and exit of sources (water, carbon and nutrients). Xylem conduces sap charged in water and minerals from the soil to the upper parts of plant. Phloem is a central actor of nutrition. It conduces sap charged in photoassimilates from source organs (mature leaves) to sink organs like roots, fruits or organs in development (Figure 1.1) (Lucas et al., 2013).

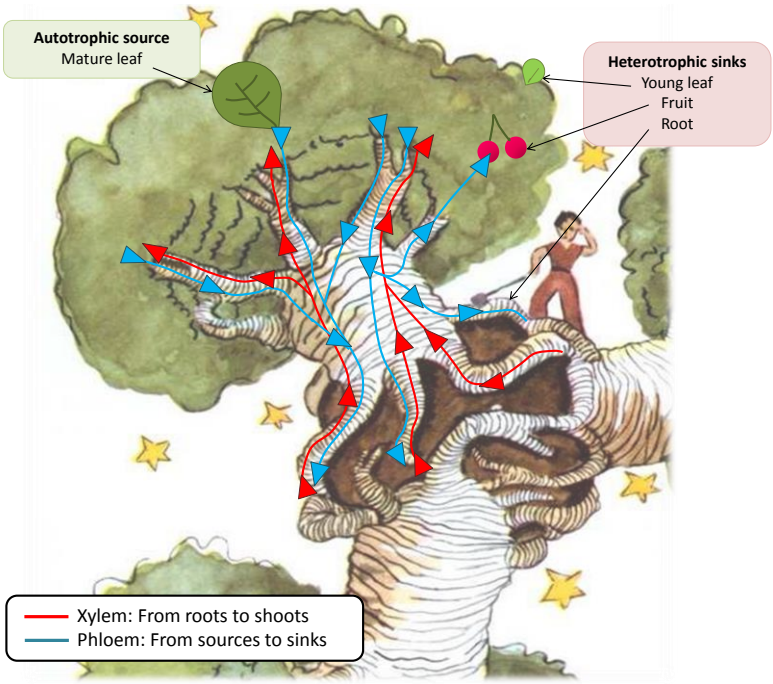

Figure 1.1: Sap movements across the plant
Illustration presenting the nutrients and photoassimilates fluxes within a vascular plant. Nutrients are absorbed by the roots and transported to the shoots through xylem vessels (red path). Photosynthetic organs (sources) produce photoassimilates dispatched (blue path) to the fruits and growing organs (sinks). Adapted from (De Saint Exupery, 1943)

1.1.1 Evolution of vascular tissues

To elucidate the progressive steps of vascular tissues acquisition, studies are focused on fossils and actuals plants observations.

In red algae, it is speculated that the central elongated cells act as sieve elements. Despite the presence of numerous connections and a polar organization, there is no obvious long distance transport, thus one cannot talk about vascular tissues in red algae (Van Bel, 1999). In brown algae, photosynthate translocation has been described. For example, the medullary zone of laminariales presents pores in transverse walls, reminiscent of the phloem sieve plates. Pretracheophyta plants simply developed pipes with smooth wall and small pores derived from plasmodesmata (Lucas et al., 2013).

Similar structures to vascular tissues are present in moss (Bryophytes): the water conducting cells and food conducting cells. The most complex forms of first sap conducing systems are hydroids and leptoids for xylem and phloem analogous respectively (Lucas et al., 2013). During development, hydroids undergo a succession of morphological modifications such as thickening of wall and cell death (Figure 1.2B). Leptoids are elongated cells files, aligned, presenting cytoplasmic modifications (Figure 1.2A): cytoplasmic polarization, organelles alignment in a longitudinal pattern, loss of the large central vacuole and high density of plasmodesmata. Generally hydroids and leptoids are associated: leptoid surrounding a hydroids core, called amphicribal organization in opposite to amphivasal organization (Figure 1.2C) (Van Bel, 1999). In Bryophyte, there is no mechanical strengthening of vascular tissues because of the lack of lignin deposition. This is a brake to size increase, but a real asset minimizing cavitation. Cavitation corresponds to the formation of gas inside sap as a consequence of a too strong evapotranspiration without water uptake to compensate this loss of water. Indeed, flexible walls allow collapse during tissue desiccation and to adapt cell diameter to the sap volume but also rapid rehydration following a resupply of water. In contrast, xylem is resistant to collapse and acquired mechanical strength permitting an increase in the size of land plants.

Pteridophytes are Tracheophytes with “real” vascular tissues. Pteridophytes is a large phylogenetic group (with high diversity in anatomic structures), including fern, horsetail and spikemoss. In fern, there is a continuous network connecting root to shoot. There is no difference between vascular tissues of leaf, rhizome or root. Fern vascular tissues are randomly distributed in the organ (Figure 1.2D), but they always display an amphicribal

organization with a lignified tracheids core surrounded by sieve elements (Pittermann et al., 2011; Van Bel, 2003).

As Dicots, Gymnosperms produced secondary vascular tissues: xylem inward, phloem outward thanks to cambial tissue activity. Conifers evolved a system permitting to struggle against emboli: the torus (Figure 1.2E). It acts like a little pillow permitting to close pores: conifers are thus more resistant to cavitation compared to Angiosperms (Lucas et al., 2013).

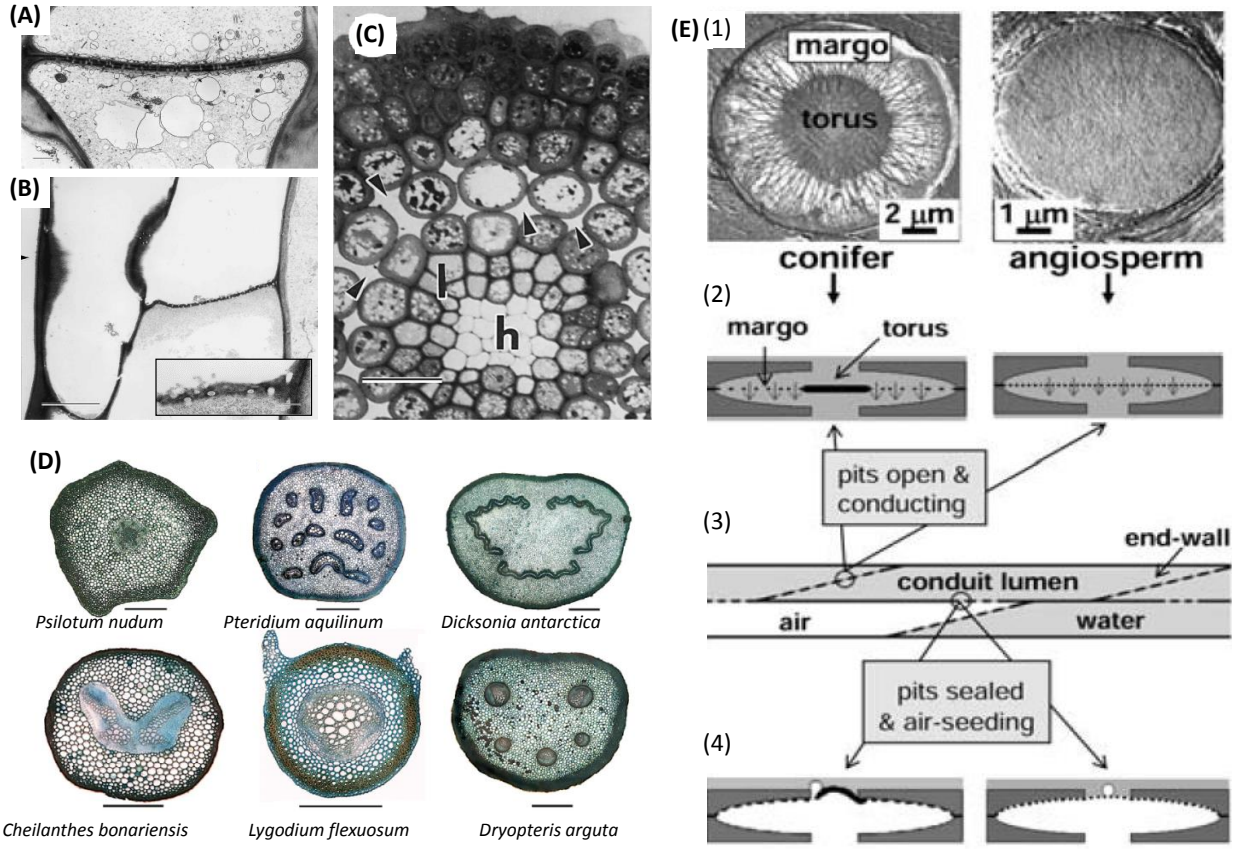

Figure 1.2: Diversity of vascular system across the plant kingdom

(A) Cytological details in a leafy stem leptoids observed in transmission electron microscopy in *Sphagnum cuspidatum* moss. Cells present abundant plasmodesmata in cell walls and most of the organelles are at the distal (top) end of the lower cell. Bar = 4µm. **(B)** Image of longitudinal section in moss hydroid observed by transmission electron microscopy *Takakia* species. Water conducing cells have transverse septa containing numerous plasmodesmata-derived pores. Scale bar: 5µm; 0,5µm for inset of details of the pores in an end wall. **(C)** Light micrographs showing conducting tissue with amphicribal disposition in sporophyte foot of *Pogonatum aloides* moss. Note the intercellular spaces (arrow) between the parenchyma cells. l: leptoid; h: hydroid; scale bar = 50µm. (A-C) Adapted from (Ligrone et al., 2000) **(D)** Cross sections of six fern stipes illustrating the variability of vascular tissues organization in ferns. Toluidine blue staining. Bar = 1mm. From (Pittermann et al., 2011) **(E)** Torus to avoid cavitation. (1) Scanning electron microscopy of pit membrane in conifer (left) and angiosperm (right). (2) Side view schematic of membranes . Pits open and functioning in water transport. (3) Pit location within schematic conduit network. (4) Side view of pits in sealed position showing proposed air-seeding process. From (Pittermann et al., 2005)

1.1.2 Histology of vascular tissues in Angiosperms

Like all tissues, vascular tissues display their own morphological characteristics. We defined differentiated cell as a result of a change in genes expression that leads to the acquisition of a new cell identity. Depending on their position (continually specified by signals from surrounding cells or by long distance signals), these cells can enter in a differentiation program and acquire their own identity (Bennett and Scheres, 2010). Vascular tissues are composed of two kinds of differentiated tissues in Dicots: xylem and phloem and a vascular meristematic tissue called (pro)cambium that ensure production of new xylem and phloem cells (Lucas et al., 2013).

In root, procambial cells are directly produced by root apical meristem that ensures the primary growth. In leaf, the precursors of procambial cells are the preprocambial cells that are produced de novo within the mesophyll cells.
By a gradual mechanism, preprocambial cells elongate, becoming procambial cells (Scarpella et al., 2004). This step is the anatomical clue of the future vascular bundles position that can be easily observed in leaf. Probambial cells divide anticlinaly to ensure stem cells pool autorenewal. Then it divides periclinaly in two daughter cells to give xylem cell precursor and phloem cell precursor. By successive divisions, precursor cells generate the different cells constitutive of xylem tissues and phloem tissues respectively (Figure 1.3) (Schuetz et al., 2013).

The vascular cambium, ensuring secondary growth, consists of a centrifugal layer of secondary phloem and a centripetal layer of secondary xylem. Secondary tissues are produced by periclinal divisions of cambium and permit plants to growth in thickness. Secondary tissues are found only in Dicots taxon: Monocots have no secondary meristem (Schuetz et al., 2013).

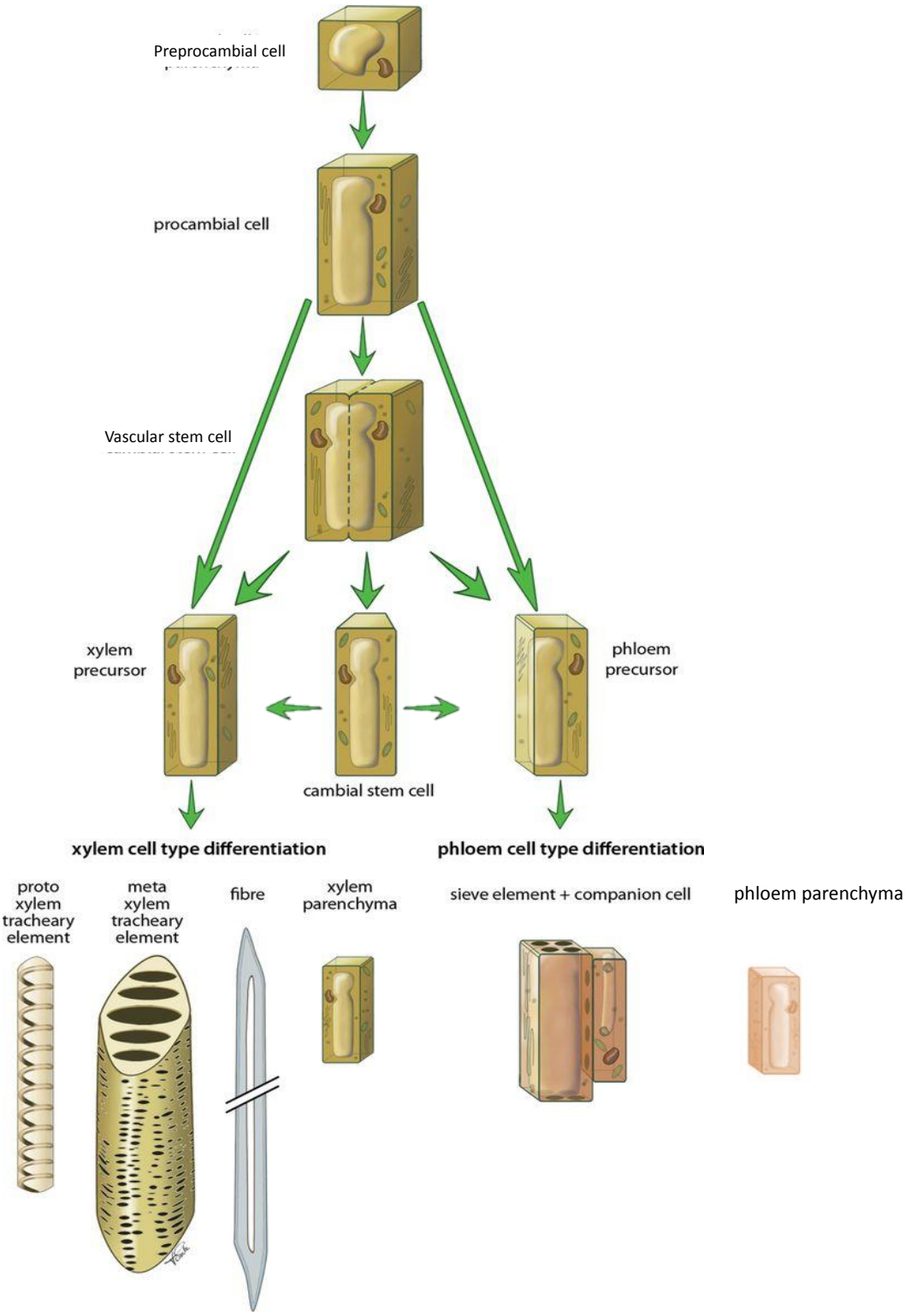

Figure 1.3: From preprocambium cells to vascular cells: a succession of divisions followed by differentiation
Preprocambial cells undergo an anticlinal division to give procambial cells and to ensure their own renewal. Procambial cells undergo next a periclinal division to generate vascular stem cells (xylem and phloem precursors). Xylem precursors produce tracheary elements, fibers and parenchyma by periclinal divisions. Similarly, phloem precursors produce sieve elements, companion cells and phloem parenchyma. Adapted from (Schuetz et al., 2013)

Xylem is composed of three cell types (Figure 1.4A):

- *Tracheary elements* are the functional unit of xylem. They are elongated cells with lignified and thick wall permitting cells to resist to pressure caused by surrounding cells and transpiration. Tracheary element precursors remain immature cells before they undergo Programmed Cell Death and acquire their functionality only when they are dead. Only lignin deposition subsist after tracheary element differentiation forming an inert tube wherein water and nutrients can move from one cell to another using special formation: perforation plates (for vertical movements) and pits (for horizontal movements). The shape of lateral lignin depositions permits to class xylem. Annular and spiral deposits correspond to protoxylem, whereas metaphloem display a reticulate deposition.
- *Wood parenchyma* with very thick wall (Turner and Sieburth, 2003). These cells could product lignin precursors to contribute to treachery elements lignification (Smith et al., 2013).
- *Xylary fibers* are long and fin cells. They mainly present a structural role in the solidity of stem.

During development, protophloem is the first phloem formed after germination and in new organs. Later, protophloem disappears because it is compressed by the other tissues in development especially metaphloem (Esau, 1969). Mature metaphloem is composed of four cellular types (Figure 1.4B):

- *Sieve element* is the unit of sieve tube that ensures sap transport from mature leaves to the whole plant. Sieve elements are living cells that lost the most part of their cellular components during differentiation (Cf §1.3). Either sides of a sieve element, sieve plates permit vertical communication between cells and to let sap move between two adjacent sieve elements. The sieve plates are region with high density of modified plasmodesmata (Figure 1.4C,E) (Esau, 1969).
- *Companion cells* are the “baton of life” of sieve elements. They are sieve elements neighboring cells which feed them in molecules necessary for their survival. One companion cell is specific to a sieve element but a sieve element can be bordered by two companion cells. Together, companion cells and sieve elements communicate by lateral plasmodesmata (Van Bel, 2003).

- *Phloem paremchyma* is composed of elongated cells. By the presence of big vacuoles in these cells, we supposed a storage role for phloem paremchyma cells and maybe a support function for the whole phloem tissue.
- In some species, one can also found *phloem fibres*. The cell wall in these cells is very thick giving them a support role in the plant.

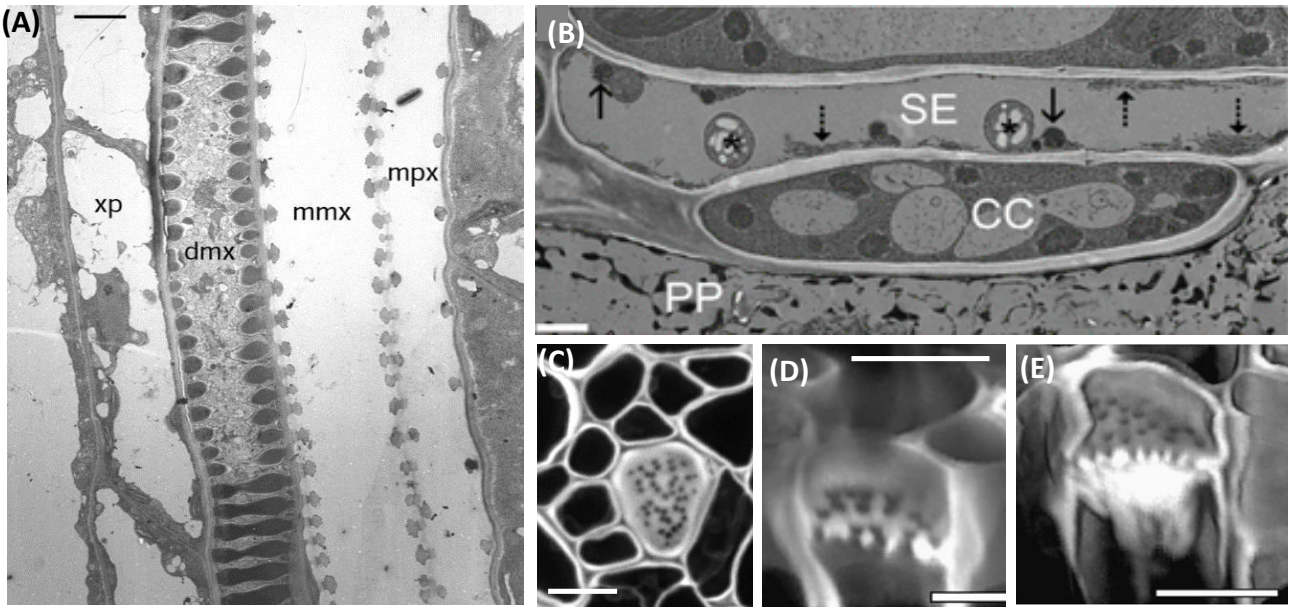

Figure 1.4: Histological structure of vascular tissues
(A) Xylem structure in Arabidopsis stem (Transmission electron microscopy). mpx: mature protoxylem; mmx: mature metaxylem; dmx: developing metaxylem; xp: xylem parenchyma. Bar = 7µm. From (Turner and Sieburth, 2003) **(B)** Transmission electron micrograph of Arabidopsis phloem in leaves. SE: sieve element; CC: companion cell; PP: phloem parenchyma; star: plastids; arrows: mitochondria. Bar = 500nm. From (Froelich et al., 2011) **(C)** Arabidopsis sieve plates in stem cross section stained with Propidium iodide. **(D-E)** 3D-reconstruction of sieves plates with (D) or without callose plug (E). Bar = 5µm. (C-D) From (Truernit et al., 2008).

1.1.3 Description of vascular tissues organization in Dicots

Vascular organization is different in root, shoot and leaf of Monocots and Dicots. One of the most important difference is the absence of cambium in Monocots that have no secondary growth. Moreover, vascular bundles are disposed along a ring in Monocots' root, scattered in stem and striate in leaves. In Dicots, vascular bundles are placed on a unique ring in stem, root phloem is surrounded by xylem arms and draw a network in leaves (Caño-Delgado et al., 2010). In this paragraph, I will describe vascular tissues architecture in Dicots which includes *Arabidopsis thaliana*, the plant model of my study.

Two publications from Lucas et al. (Lucas et al., 2013) and Cano-Delgado et al. (Caño-Delgado et al., 2010) nicely summarize knowledge concerning vascular tissues architecture in root, stem and leaf.

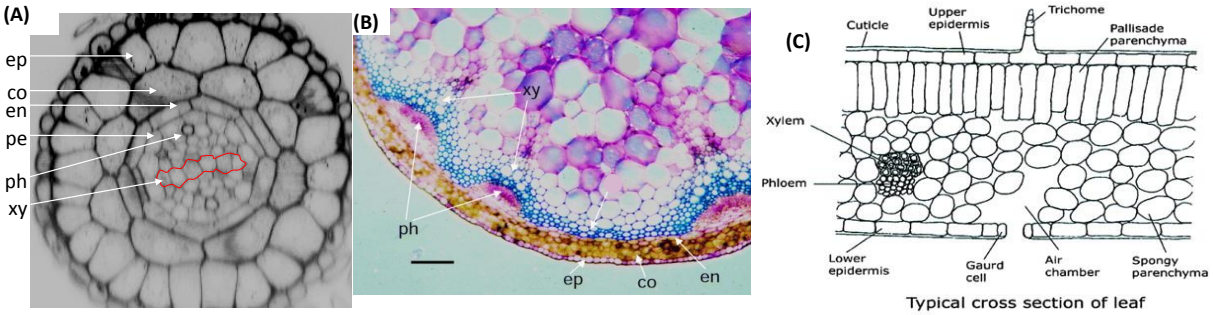

Figure 1.5: Vascular tissues patterning in different organs of *Arabidopsis thaliana*
Transversal section in arabidopsis organs **(A)** Reconstitution of root section from longitudinal optical acquisitions of 11 days old root stained by propidium iodide. ph: phloem, xy: xylem; ep: epiderm; co: cortex; en: endodermis; pe: pericycle **(B)** Cross section in stem . Scale bar: 100nm From (Turner and Sieburth, 2003) **(C)** Schematic representation of the leaf cross-section. From (Boyko et al., 2006)

The primary organization of vascular tissues in both root and the bottom of hypocotyl is roughly the same. As observed in a mature embryo or a young plantlet, the stele is composed of pericycle, procambium, xylem, phloem and parenchymal cells (Figure 1.5A).
In Arabidopsis, despite the radial organization of the external layers of these organs including pericycle, the vascular tissues display bilateral symmetry. The diarch organization of vascular tissues describes two poles of phloem that are separated perpendicularly by a xylem plate (Figures 1.5A, 1.6). The xylem plate is located in the frontal plane (Figure 1.7) whereas the phloem poles are located on both sides of the xylem plate in the sagittal plane (Bauby et al., 2007).

In stem, vascular bundles can be distributed as isolated structure inside the stem or can describe a continuous ring depending of the development stage of plant (Figure 1.5B, 1.6). From outward to inward, vascular bundle is composed of phloem, cambium and xylem in a collateral organization. Xylem growths in a centrifugal direction: protoxylem is oriented inward.

The limb is traversed by a well-organized network of vascular tissues covering the total surface of the leaf. The vascular tissues in leaf present a collateral organization as found in

stem (Figure 1.5C, 1.6). Xylem is turned up (adaxial), phloem is turn down (abaxial). There is a high hierarchy in leaf bundles organization depending on organ maturity, leaves position in the plant and species. In terms of branching type, we can determine different kinds of vascular patterning (or venation): pinnate, reticulate and palmate-veined. Midvein is branched by secondary veins, themselves by third veins constituting a dense network. Major and secondary veins present high diameter and are only allocated to transport. The highest orders are blind end veins that finish their way in mesophyll. High order veins (than third) ensure loading and unloading sap compounds.

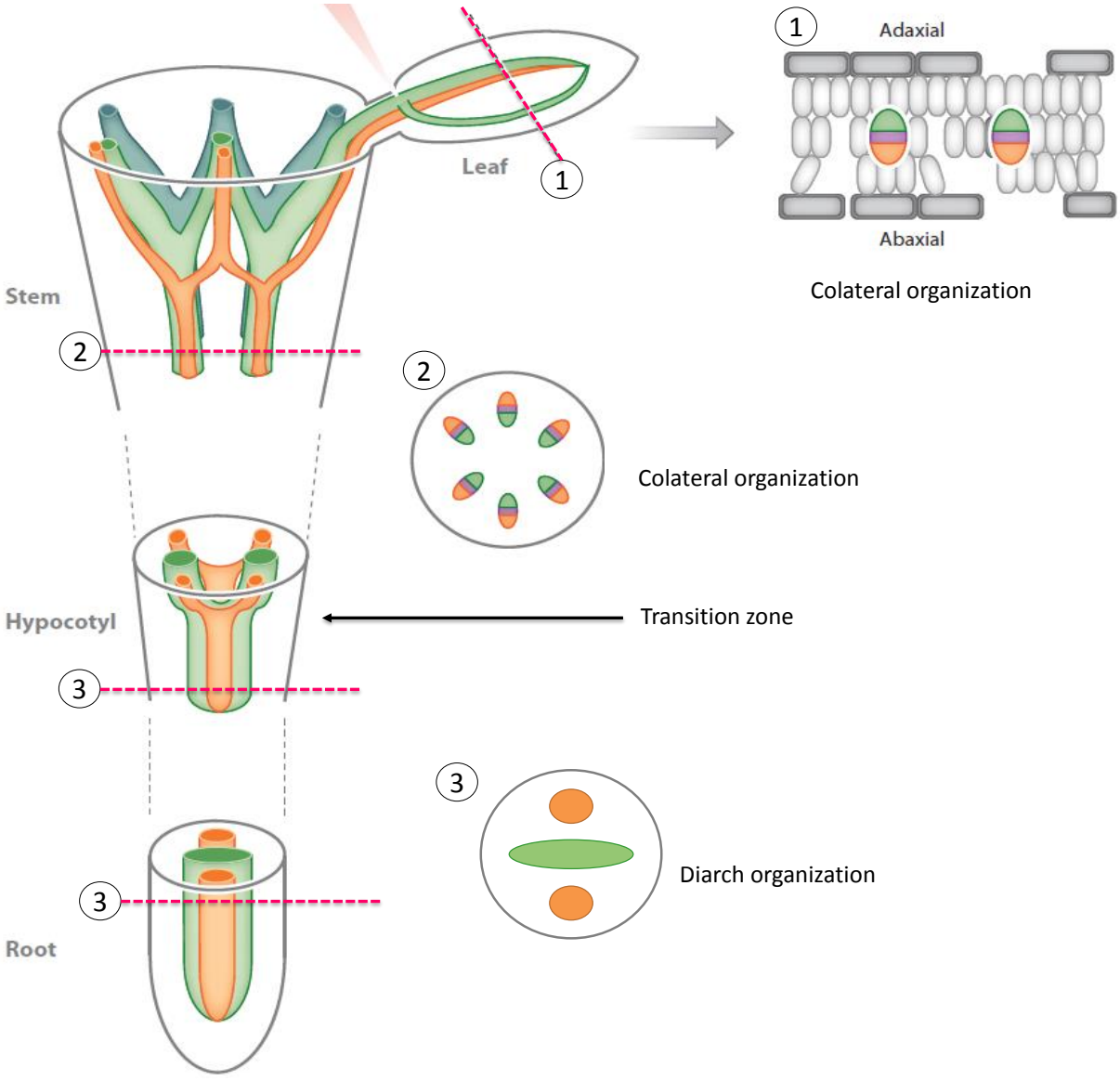

Figure 1.6: Post-embryonic vascular tissues patterning, a connecting network with variable organization. Vascular tissues are connected in a single network; however their organization changes depending on the plant organ. Orange: Phloem; Green: xylem; Purple: cambium. Adapted from (Caño-Delgado et al., 2010)

Vascular tissues are connected in a continuous network between organs, however their organization differs from root to shoot (Figure 1.6) and requires anatomical adjustments. This step is called vascular transition and takes place at the top of hypocotyl in the transition zone. Vascular tissues undergo remodeling from an alternate diarch organization in root to collateral organization in the stem and leaves. The opening of the xylem plate marks the beginning of transition zone. Each phloem strand divides in two strands in the direction of their respective cotyledons to form four phloem poles. Both strands of phloem are visible in each cotyledon until the branching of the distal loop of secondary veins. These phloem strands are located on the abaxial side (lower face) of the cotyledon whereas the xylem strand is located on the adaxial side (upper face) (Figure 1.6; 1.7) (Bauby et al., 2007).

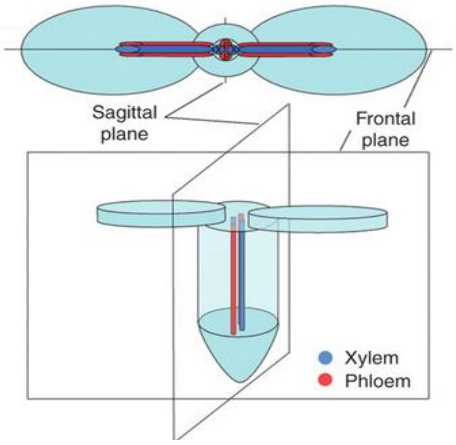

Figure 1.7: Organization of the vasculature in the mature *Arabidopsis thaliana* embryo
Scheme of the symmetry planes (frontal and sagittal) of a mature embryo of *Arabidopsis. thaliana* (Bauby et al., 2007)

1.2 Vascular tissues patterning establishment: an hormonal duality between auxin and cytokinin

The establishment of the vascular pattern is a complex mechanism that involves a spatio-temporal coordination the specification of tissue and the positioning of these tissues inside the different organs of the plant. First analyzes have pointed out the important role of both auxin and cytokinin hormones in establishing this pattern.

1.2.1 Vascular tissues are implemented during embryogenesis

During plant development, most preexisting vascular cells derive from vascular founder cells established during embryogenesis. Thus, the positioning of each vascular cell during embryogenesis determines the future position of differentiated vascular tissues after germination. Vascular tissues are implemented early as the globular stage while embryo is only composed of 32 cells. In the lower tier of globular embryo, asymmetric divisions of inner cells occur to give outside four cells of ground tissues precursors and four cells of procambium inside (Figure 1.8A). The formation of the four procambial cells coincides with expression of vascular specific markers (Scheres et al., 1994; De Rybel et al., 2014b). The founder procambial cells produce pericycle and provascular cells after successive peryclinal cell divisions (Scheres et al., 1994).

Provascular cells formation seems to result of geometric constraints. De Rybel et al. (De Rybel et al., 2014a) constructed a mathematical model to study which elements are essential for correct embryo development. They concluded that auxin is not uniformly distributed inside the four provascular founder cells. The founder cells aligned with cotyledons receive more auxin that their neighbors. Moreover, these two “high auxin level” cells are connected by a kind of communication bridge which results of first cell divisions planes occurring during two to four-cell embryo transition. The two other cells with “low auxin level” are meanwhile unable to directly communicate together. However, a change in simulation of cell communication between the two “high auxin cell” has no impact on embryo development whereas the bridge needs to connect the “high auxin level” cells to ensure a correct development. This indicates that the bridge only imposes a geometric constraint to next cell division (De Rybel et al., 2014a).

Interestingly, the bilaterally of Arabidopsis embryo is early specified during transition from late globular stage to triangular stage as evidence by a bisymmetric auxin maxima (Figure 1.8D) whereas the global shape of embryo does not indicate (De Rybel et al., 2014a). High auxin concentration promotes transcription of the cytokinin signaling inhibitor *ARABIDOPSIS HISTIDINE PHOSPHOTRANSFER PROTEIN6* (*AHP6,* (Mähönen et al., 2006)) in the future cotyledon tips (Figure 1.8B,C). This bisymmetry is propagated to the root and specifies

protoxylem in a bisymmetric pattern. Thus, cytokinin maxima are established perpendicularly to determinate protophloem position (Figure 1.8E) (Bishopp et al., 2011).

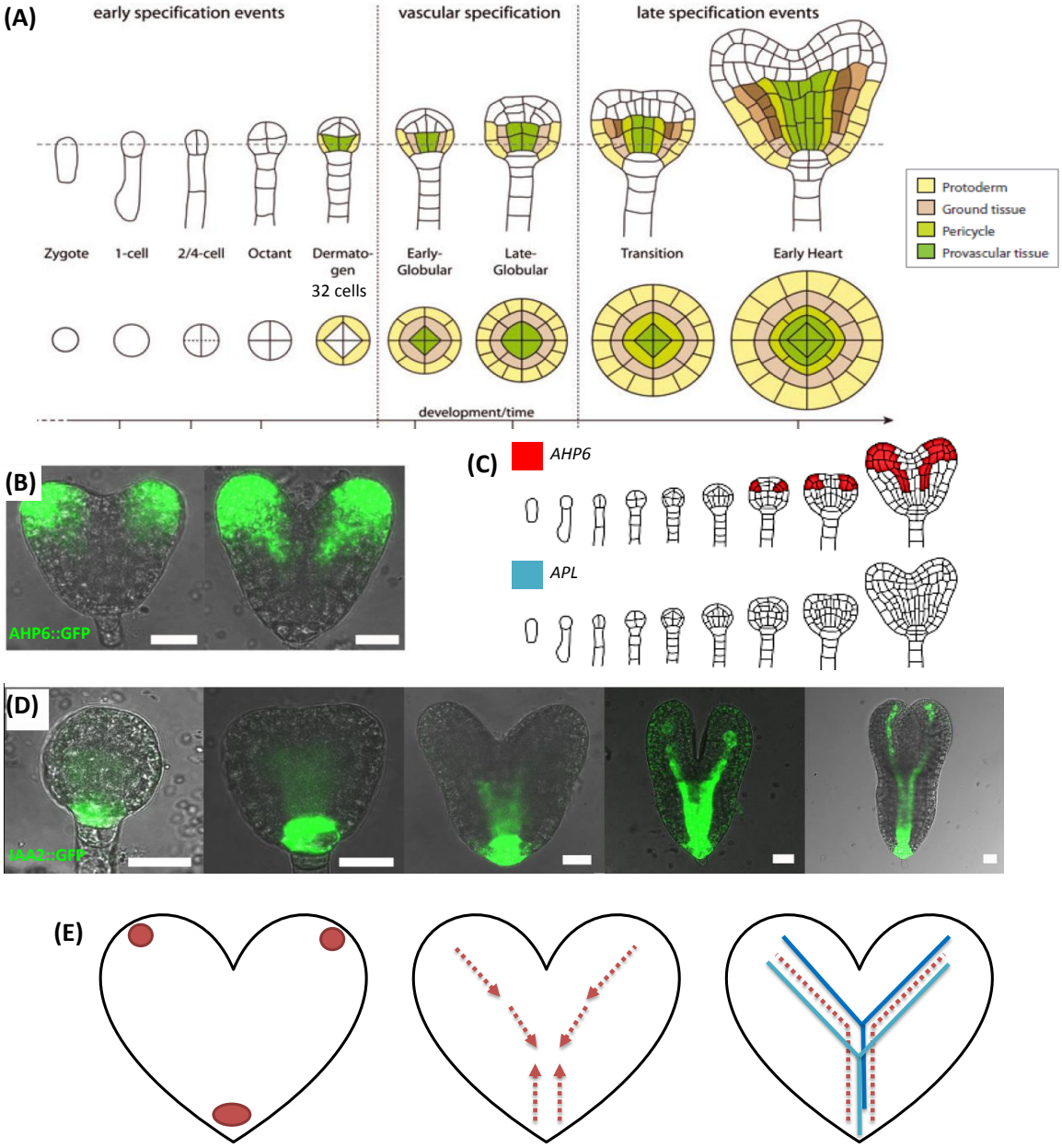

Figure 1.8: Vascular tissues patterning establishment during embryogenesis
(A) Schematic representation of embryo development in *Arabidopsis thaliana*. Longitudinal sections are shown on top of corresponding transverse cross sections at he embryo basal part (indicated gray by the dotted line). **(B)** During the early heart stage of embryogenesis, AHP6 expression is confined to the cotyledon apices. During the mid to late heart stage, the AHP6 response migrates toward the promeristem in two strands. Bar = 20µm. **(C)** AHP6 and APL expression patterns during early stage of embryogenesis. Whereas expression of AHP6 starts at late globular stage, APL expression only appears around late heart to torpedo stage **(D)** I*AA2* is expressed in the root promeristem in a radially symmetric pattern in heart-stage embryos. The promeristem is a minimal set of initial cells that later gives rise to the root structure seen in the root. During the torpedo stage of embryogenesis, IAA2 can be seen forming two signaling maxima at the position in which the protoxylem will form. **(E)** Auxin maxima are established early during embryogenesis. These maxima are aligned with cotyledons in a frontal plane and prefigure xylem tissues. Cytokinin maxima are established perpendicularly in a sagittal plane and prefigure phloem tissues. (A,C) From (De Rybel et al., 2014b) (B,D) From (Bishopp et al., 2011)

During embryogenesis, protoxylem seems to be first determinate as evidence by *AHP6* (a protoxylem marker induced by auxin) and *APL* (ALTEREDPHLOEMDEVELOPMENT, a phloem marker, (Bonke et al., 2003)) expression patterns (Figure 1.8C) (Bishopp et al., 2011).

Hormones play a fundamental role for vascular establishment during embryogenesis. Indeed, several mutants of vascular pattern were identified (Berleth and Jürgens, 1993; Mähönen et al., 2000). Many of them are involved in regulation, transport and signaling of auxin but also in cytokinin signaling during embryogenesis.

1.2.2 Auxin involvement in vascular patterning

Auxin has long been thought to play a fundamental role for vascular establishment. Early experiments (Sachs, 1981) showed that auxin is able to induce transdifferentiation of parenchyma closed to wounded vascular tissues (Figure 1.9E). Transdifferentiation corresponds to the reprogramming of cell identity where a differentiated cell (parenchymal cell) transforms into another cell (vascular cell). Parenchymal cell undergoes a dedifferentiation with a loss of parenchyma identity before to acquire its new characteristics of vascular cell identity. Thus under the influence of auxin, parenchyma is able to transdifferentiate in vascular tissues, reforming a continuous strand (Sachs, 1981).

However auxin also plays a main role during plant development such as embryo apico-basal organization as describe above, cell elongation and cell differentiation. MONOPETROS (MP) is an Auxin Response Factor (ARF) transcription factor early expressed during embryogenesis in provascular cells. *mp* mutant shows a reduced vasculature and discontinuous strands (Figure 1.9A) (Scheres et al., 1994; Hardtke and Berleth, 1998; Wenzel et al., 2007). MP regulates several targets: PIN1 an auxin efflux transporter (Wenzel et al., 2007); TMO5 a bHLH transcription factor controlling periclinal division (see below) (De Rybel et al., 2014a). Their corresponding mutants display vascular defects suggesting auxin involvement during vascular embryogenesis.

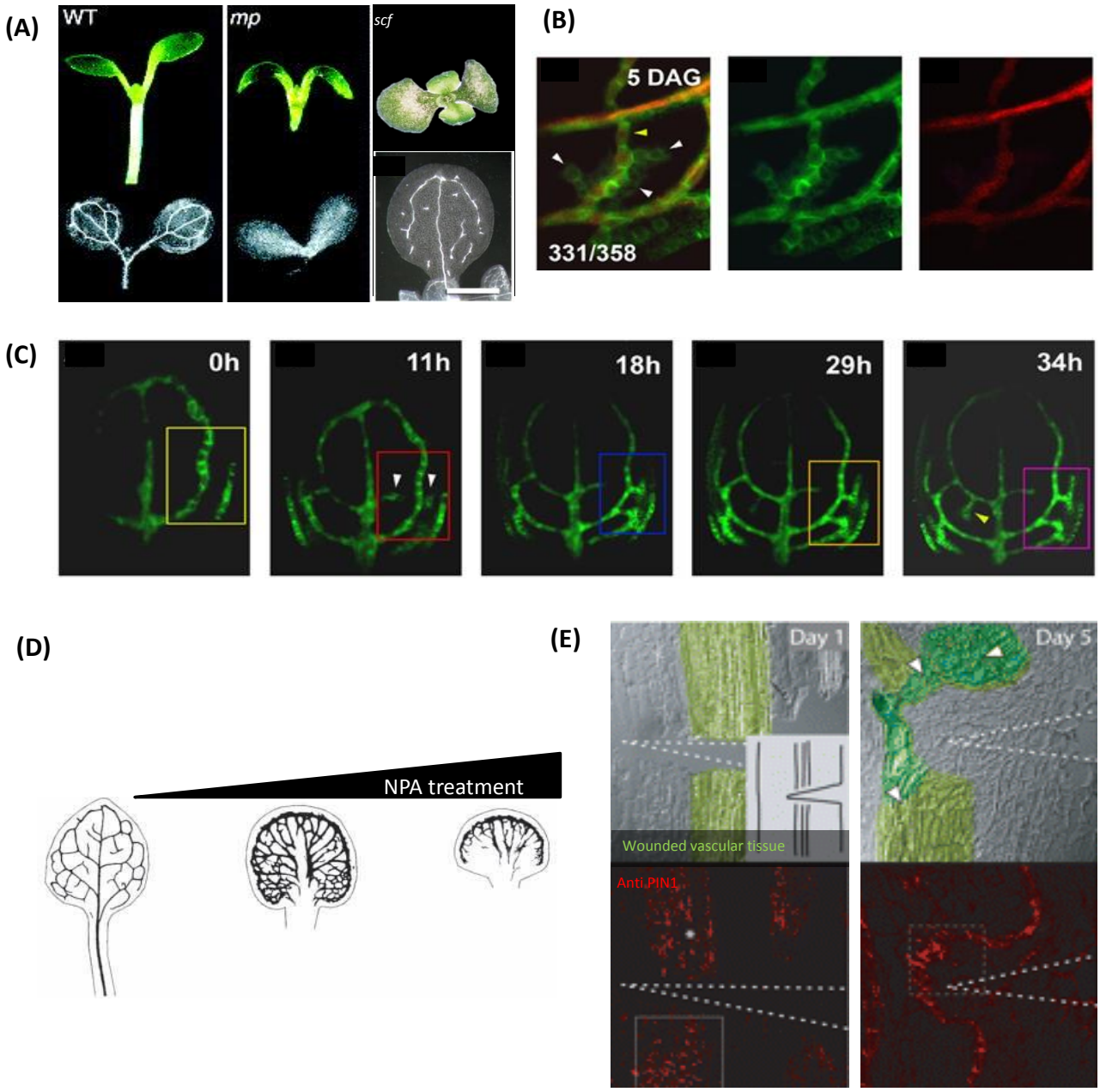

Figure 1.9: Auxin involvement and distribution during phloem ontogenesis
(A) Vascular system in WT, *mp* and *scf* mutants. From (Berleth et al., 2000; Sieburth et al., 2006). **(B)** Overlapping (yellow) of pPIN1::GFP (green) and pATHB8::YFPer (red) a preprocambial marker. From (Marcos and Berleth, 2014). **(C)** Time laps of pPIN1::GFP expression in leaf from 3 to 4,5 DAG permitting to follow vascular tissues formation; scale bar:20µm. From (Marcos and Berleth, 2014). **(D)** Vascular patterning and inhibition of auxin transport treatment (NPA). From (Berleth et al., 2000). **(E)** Regeneration of wounded vascular tissues in pea epicotyl and PIN1 localization. Adapted from (Berleth et al., 2000)

After germination, auxin continues to ensure a primordial role for vascular tissues formation. Increasing NPA treatment (1-naphthylphthalamic acid an auxin transport inhibitor) results on an abnormal vascular patterning in leaves (Figure 1.9D) (Berleth et al., 2000).

Auxin is synthesized in apex of leaf primordia and transported to young developing organs. Leaves in development perceive two opposite auxin fluxes: one comes from the leaf apex, the second comes from the petiole. Together they determine vascular patterning in leaves. In response to auxin flow, MP activates *ATHB8* expression that in turn induces *PIN1* expression in preprovascular cells (Scarpella et al., 2006). *MP*, *ATHB8* and *PIN1* expression are aligned and delineate the development of future vascular bundles (Figure 1.9B) (Wenzel et al., 2007; Marcos and Berleth, 2014). PIN1 is required to canalize auxin flux, to determine vascular strands position and arrangement by inducing differentiation of near preprocambial cells in leaves (Figure 1.9C) (Wenzel et al., 2007). PIN1 correct localization is coordinated by trafficking mechanisms necessary to ensure the bundles formation (Geldner et al., 2003). Indeed, PIN recycling is abnormal in *scarface* mutant (*scf*) (Sieburth et al., 2006) and it results in fragmented disconnected veins in cotyledons and leaves (Figure 1.9A).

1.2.3 Cytokinin involvement in vascular patterning

Pre-procambial cells lead to emergence of vascular tissues. Their division in procambial cells is the first step of vascular tissues formation and is ensured by cytokinins that are known to positively control cytokinesis. Tissues morphogenesis in root is established by asymmetric division involving *WOL/AHK4* (*WOODEN LEG* (Scheres et al., 1995; Mähönen et al., 2000)). *WOL* is specifically expressed in vascular cylinder and very early during globular stage of embryogenesis. WOL is a histidine kinase cytokinins receptor (Inoue et al., 2001). In *wol* mutant, there is no more phloem (Figure 1.10B). The mutant only presents xylem in stele with a decrease of cell number explaining its name "*wooden legs*". *WOL* induces phloem formation through cytokinin signaling (Mähönen et al., 2000).

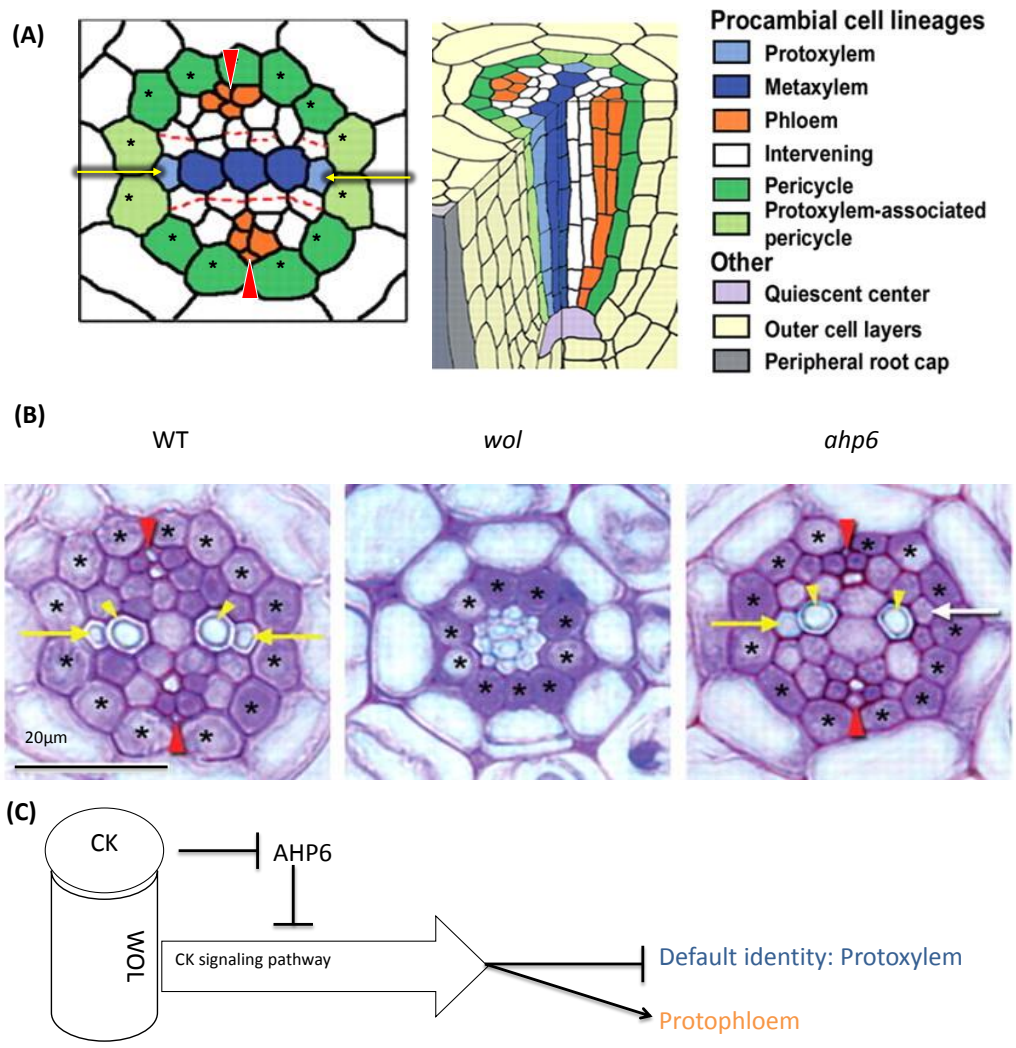

Figure 1.10: Cytokinin involvement during phloem ontogenesis
(A) Schematic of *Arabidopsis* stele root (transverse section and three dimensional representation). **(B)** Histological analysis of root vasculature stained with toluidine blue indicates that protoxylem is more present in *wol* and *apl* mutants; and protoxylem less presents in *ahp6* mutant. **(C)** Schematic signaling pathway that regulated phloem differentiation. Stars: pericycle; Red arrow: protophloem; Yellow arrow: protoxylem; White arrow: abscence of protoxylem
(A,B) Adapted from (Mähönen et al., 2006)

Oppositely to *wol*, *ahp6* (*arabidopsis phosphotransfer protein 6* (Mähönen et al., 2006)) mutant (a *wol* suppressor) shows less xylem tissues suggesting that AHP6 induces protoxylem formation (Figure 1.10B). AHP6 is a pseudo-AHP which participates to xylem specification by exerting a negative repression on cytokinin signaling. In absence of cytokinin signaling, protoxylem is considered as a default identity (Figure 1.10C). Interestingly, an exogenous cytokinins treatment down-regulates *AHP6* expression suggesting that the system is controlled by a reciprocal action between cytokinin and *AHP6* to specify the

differentiated nature of procambial cell files (Figure 1.10C). In conclusion, cytokinins inhibit protoxylem formation and allow differentiation of phloem.

1.2.4 Auxin and cytokinin antagonist effects to control vascular identity

As detailed above, vascular tissues identity is the result of a fine hormonal control involving auxin and cytokinins. Interestingly, auxin and cytokinins pathways interact to define vascular patterning. *AHP6* induces xylem formation by preventing cytokinins signaling (Mähönen et al., 2006). *AHP6* expression is enhanced by auxin as shown by RT-q-PCR analysis on plant treated by auxin (Figure 1.11A) (Bishopp et al., 2011).

The cytokinin response gene *ARR5* is normally expressed in phloem pole (Figure 1.11B). In *ahp6* mutant, its domain expression is enlarged to xylem (Bishopp et al., 2011). Similarly, *IAA2* auxin reporter gene is normally restricted to xylem pole in root (Figure 1.11C). When treated with CK, *IAA2* expression pattern is reduced. In cytokinin signaling mutant such as *wol* mutant, *IAA2* expression domain occupies the entire stele (Bishopp et al., 2011). These data suggest existence of a negative regulation loop between auxin and cytokinins.

Furthermore, MP and indirectly PIN1, are inhibited by SHORT HYPOCOTYL 2 (SHY2 (Weijers et al., 2005)). SHY2 is an AUX-IAA protein that is induced by cytokinin (Dello Ioio et al., 2008). AUX/IAA proteins interact with ARF (AUXIN RESPONSE FACTOR) proteins (MP in this case) to repress auxin-induced genes expression (Reed, 2001). This example illustrates how cytokinins inhibit auxin signaling during development (Figure 1.11D).

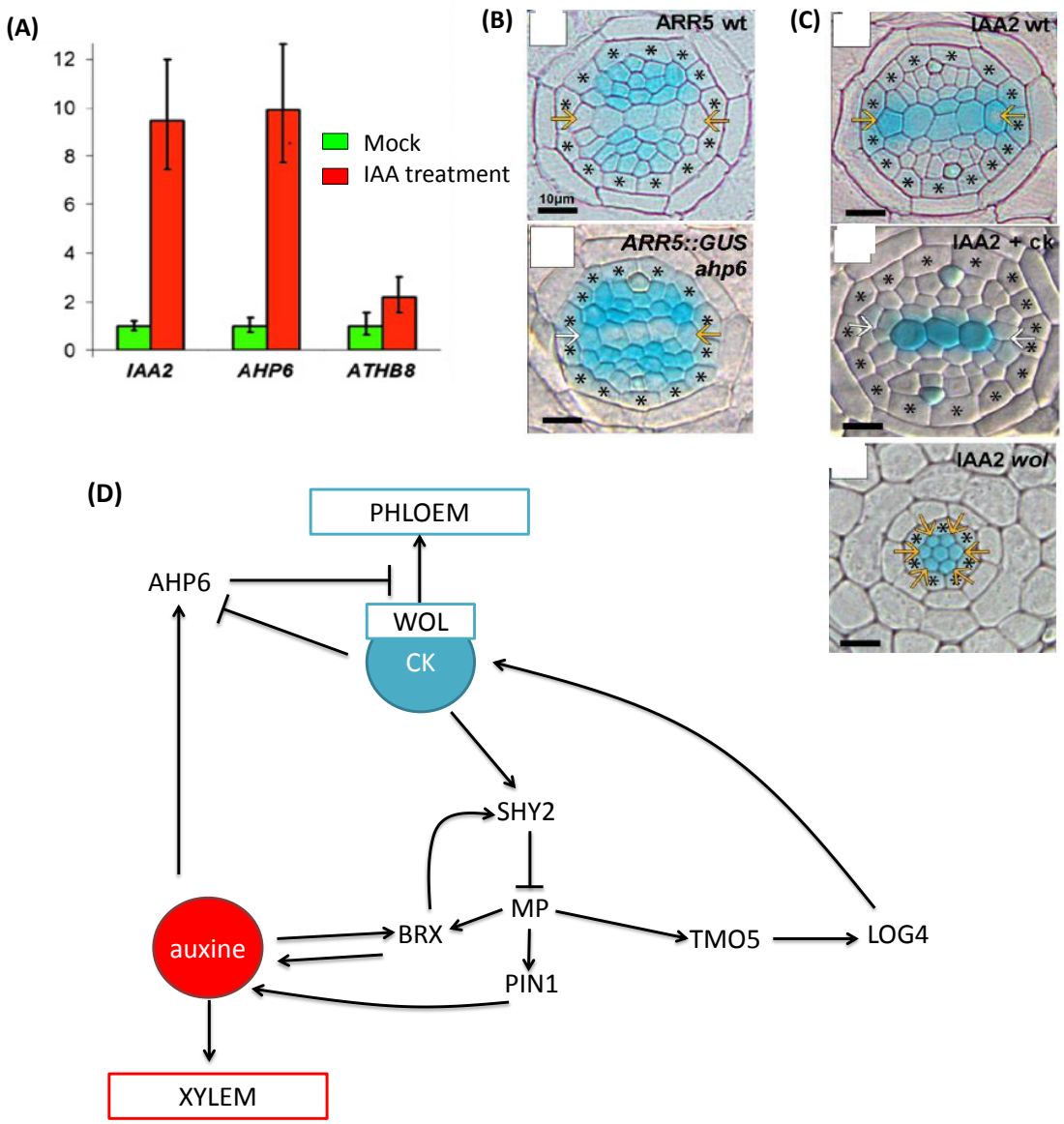

Figure 1.11: Cytokinin/Auxin mutual inhibition to control vascular development
(A) Auxin induces AHP6 expression. RT-q-PCR on 5 days old seedlings treated (red) or not (green) with IAA. **(B)** GUS staining on root section. ARR5::GUS expression in WT and *ahp6* mutant. ARR5 is a CK reporter gene. Scale bar: 50µm; yellow arrows: xylem pole; Stars: pericycle. **(C)** GUS staining on root section .IAA2::GUS expression in WT treated or not with cytokinin and *wol* mutant. IAA2 is an auxin reporter gene. When treated with CK, IAA2 expression pattern is reduced, whereas in *wol* mutant (a CK signaling mutant) IAA2 occupies the whole stele. Scale bar: 50µm; yellow arrows: xylem pole; Stars: pericycle. **(D)** Model of auxin and cytokinin crosstalk to control vascular patterning. (A-C) From (Bishopp et al., 2011)

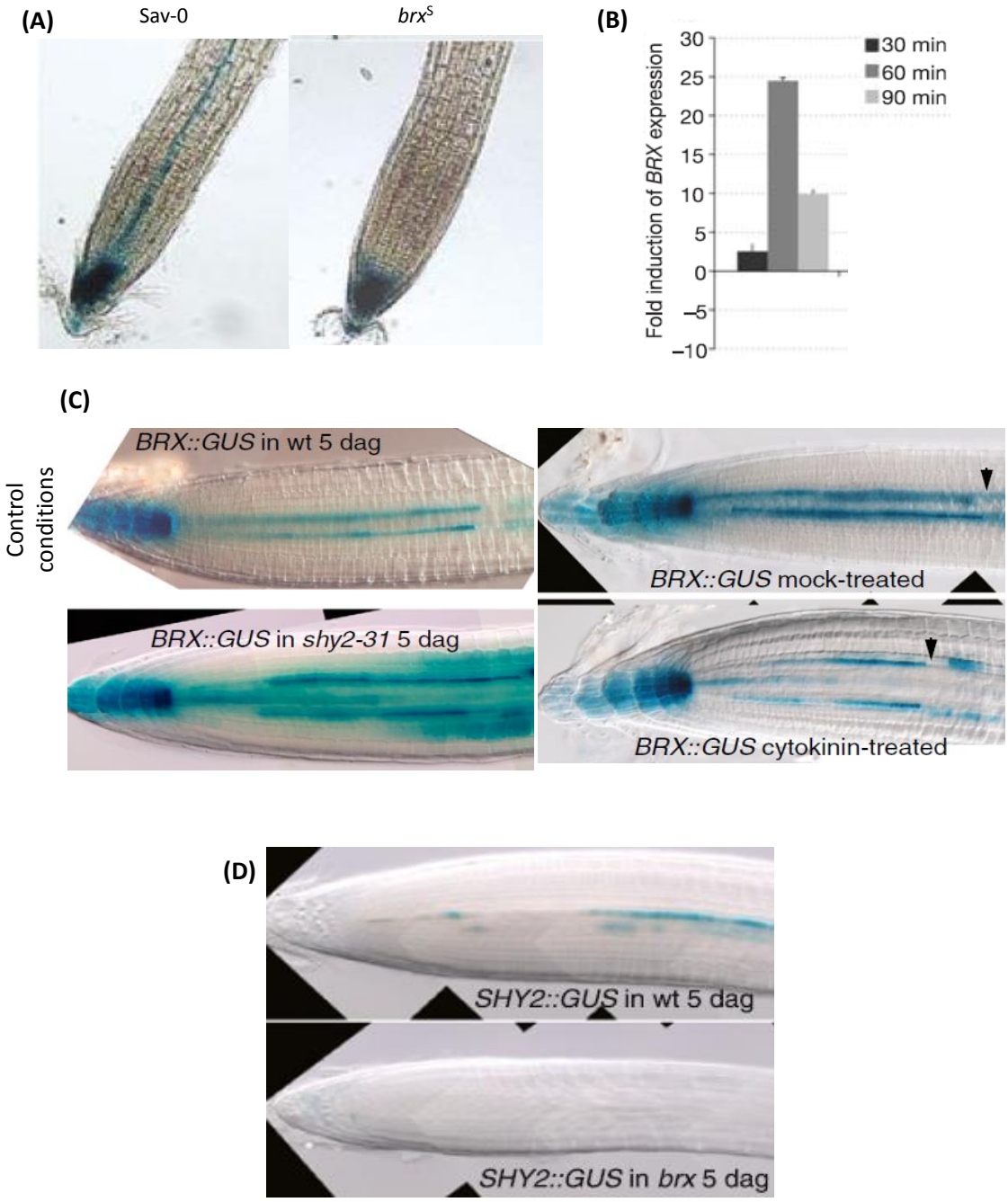

Figure 1.12: *BRX* involvement in cytokinin and auxin signalings

(A) BRX induces auxin signaling. DR5::GUS expression in Sav-0 and brx^{S} roots. **(B)** Auxin induces BRX expression. BRX transcript levels measured by RT-qPCR on young seedlings treated with auxin (fold change expression level 30, 60 or 90 minutes after auxin treatments) . **(C)** BRX expression is regulated by cytokinins. BRX::GUS expression in *shy2-31* loss of function mutant background and in response to cytokinin treatment (6h after 5µM of transzeatin treatment). 5 days old seedlings. **(D)** BRX acts positively on SHY2 transcription. SHY2::GUS expression in WT and *brx* in 5 days old seedlings. (A,B) Adapted from (Mouchel et al., 2006) (C,D) From (Scacchi et al., 2010)

In addition, *BREVIS RADIX (BRX*) gene, involved in phloem differentiation, seems to crosstalk the cytokinin and auxin signaling. Transcriptomic analysis revealed that 4000 genes are impaired in the line *brx*^{S} (Mouchel et al., 2006). Many of them are involved in auxin signaling. In *brx* mutant, the level expression of DR5::GUS (a reporter construct relating auxin level in cell (Ulmasov et al., 1997)) is decreased when compared to control (Figure 1.12A) which would suggest that *BRX* acts positively on auxin signaling. Oppositely, auxin treatments induce *BRX* gene expression suggesting the mutual positive effect between BRX and auxin (Figure 1.12B) (Mouchel et al., 2006). Furthermore, *BRX* displays similar pattern expression to *MP* (Hardtke and Berleth, 1998). In vitro analysis reveals that BRX is a target of MP confirming interaction between *BRX* and auxin signaling (Scacchi et al., 2010).
Otherwise, the *shy2-D* gain of function mutant displays the same phenotype as *brx* (Mouchel et al., 2004; Dello Ioio et al., 2008). Interestingly, *BRX* and *SHY2* expressions overlap in few cells of the transition zone of root tip. When *BRX* expression decreases, *SHY2* expression increases. Their expressions are mutually exclusive except in the few cells where they overlap, *SHY2* being expressed later than *BRX* (Figure 1.12C,D). *SHY2* downregulates *BRX* expression as evidence by extension of *BRX* expression domain in *shy2-31* loss-of-function mutant (Figure 1.12C). Moreover, SHY2 expression decreases in a *brx* mutant background (Figure 1.12C). These findings suggest that *BRX* expression is cytokinin responsive (because SHY2 is induced by cytokinin). This is confirmed by cytokinin treatments that induce a repression of *BRX* where *SHY2* is expressed (Figure 1.12C,D). Beside, a feedback loop between BRX and SHY2 permits to control the auxin/cytokinin signaling balance (Scacchi et al., 2010).

To summarize (Figure 1.11D), *BRX* expression shifts in favor to *SHY2* expression along the root in response to cytokinin signaling that act in opposite manner on *BRX* and *SHY2*. Moreover, auxin signaling is induced by *BRX* and repressed by *SHY2*. In conclusion, *BRX* and *SHY2* antagonize in a spatio-temporal sequence dependent of auxin and cytokinins concentrations to regulate vascular development (Scacchi et al., 2010). This example illustrates again how cytokinins inhibit auxin signaling during development.

By the way, there are not only repression relationships between auxin and cytokinins. In some case, auxin can induce cytokinin. Indeed, TARGET OF MONOPTEROS 5 (TOM5, a

transcription factor), regulated by auxin through MP activity, controls *LONELY GUY 4* (*LOG4*) expression (a cytokinins biosynthesis gene). Thus, auxin acts positively on cytokinin pathway through the MP/TMO5/LOG4 set (Figure 1.11D) (Schlereth et al., 2010; De Rybel et al., 2014a).

To summarize, there is a fine regulation of hormonal balance between auxin and cytokinins to control vascular identity. Auxin induces xylem formation and cytokinins control phloem differentiation by its inhibition on protoxylem formation by repressing auxin pathway via SHY2. Auxin presents an ambivalent behavior on cytokinins pathway repressing its signaling pathway through AHP6 activity and inducing cytokinins biosynthesis. All these examples demonstrate that auxin and cytokinin are mutually inhibited and cooperate to regulate vascular patterning and development during embryogenesis and post-embryogenesis stages of development (Figure 1.11D).

1.2.5 Xylem and phloem position in vascular bundle: adaxial or abaxial identity?

Vascular tissues are organized in a recurrent pattern in stem and in leaf. Xylem is present inward the stem (adaxial), phloem is outward (abaxial) and are generated by (pro)cambium mitotic activity.

In each meristem, cell proliferation is controlled by the CLAVATA/WUSCHEL (CLV/WUS) like regulatory loops. In shoot apical meristem, the system is led by a complex involving the peptide ligand CLAVATA 3 (CLV3) and its leucine-rich repeat receptor-like serine/threonine kinase CLAVATA 1 (CLV1) to control expression of WUS transcription factor (Ha et al., 2010).
The vascular meristem has also its own loop involving TDIF/TDR/WOX4 set (TRACHEARY ELEMENT DIFFERENTIATION INHIBITORY FACTORS / TDIF RECEPTOR / WOX4) (Furuta et al., 2014b). TDIF are CLAVATA3/EMBRYO SURROUNDING REGION-related peptides (CLE41/CLE42/CLE44) that induce cell proliferation and inhibit xylem differentiation (Schuetz et al., 2013). From a screen to find an analogous module to CLV3/CLV1, the *phloem intercalated with xylem* (*pxy*) mutant was isolated as insensitive to CLE41 TDIF treatments but also displays a disorganized xylem/phloem pattern (Fisher and Turner, 2007; Etchells and Turner, 2010). PXY encodes a CLV1 like protein suggesting that PXY is CLE41 receptor.

Surprisingly, *PXY* is expressed in procambium cells whereas a CLE41 signal comes from phloem cells. This signaling polarity was shown to be important to maintain the radial organization of vascular tissues and could regulate periclinal division in cambium. Thus, xylem/phloem ratio is early controlled during cell proliferation.

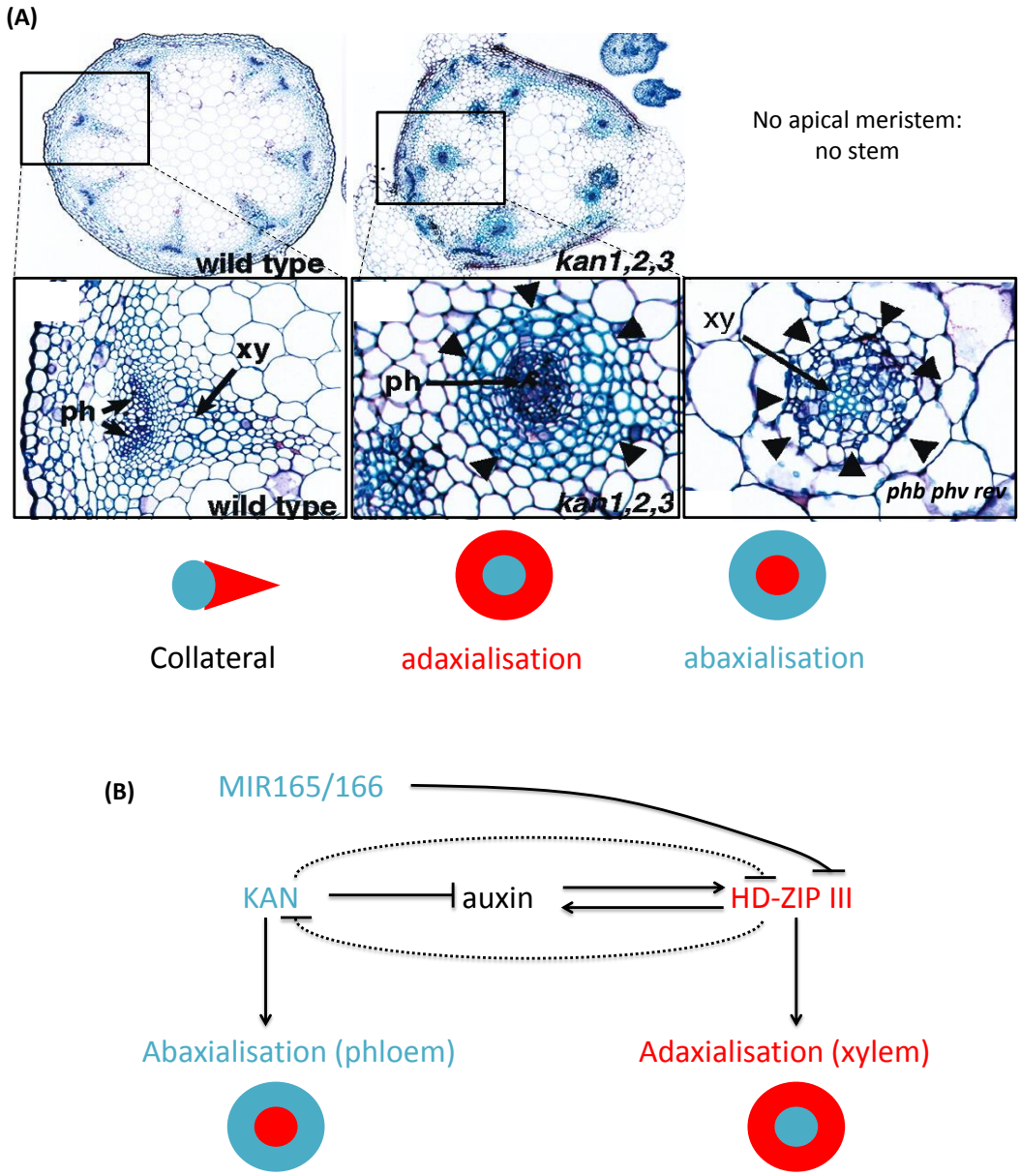

Figure 1.13: Abaxial / adaxial patterning control
(A) Stem section in WT., *phv phb rev* triple mutant hypocotyl section: vascular bundles are amphicribal: xylem surrounded by phloem. *kan* triple mutant stem section. Vascular bundles are amphivasal. Xylem surrounds phloem. Adapted from (Emery et al., 2003). **(B)** Model of adaxial / abaxial pattern control. *MIR165/166* and *KAN* are expressed in phloem and abaxial domains. *HD-ZIP III* are expressed in xylem and abaxial domains. In blue: phloem; Red: xylem

KANADI genes (*KAN* (Kerstetter et al., 2001)) encode transcription factors which are expressed in abaxial domains and in phloem. The *kan* triple mutant displays an amphivasal pattern (normally collateral in WT) where xylem surrounds phloem: there is an adaxialisation of vascular tissues (Figure 1.13A) (Furuta et al., 2014b).
On the contrary, phloem surrounds xylem in the *phavoluta/phabulosa/revoluta* triple loss of function mutant (*phv/phb/rev)* (Figure 1.13A). The pattern is named as amphicribal. Indeed there is an abaxialisation of vascular tissue (McConnell et al., 2001; Emery et al., 2003). *PHB/PHV/REV* encode class III DNA-binding homeodomain leucine-zipper (HD-ZIP III) transcription factors and are expressed in complementary domains of *KANADI* genes: adaxial and xylem domains (Emery et al., 2003).

Interestingly in *kan* triple mutant, one can observed an expansion of *HD-ZIP III* expression domains an when *KAN* is overexpressed, *HD-ZIP III* are repressed (Emery et al., 2003). In gain of function alleles of *PHB* or *PHV HD-ZIP III,* the expression domain of *YABBY* (another abaxial gene (Siegfried et al., 1999)) is limited (Emery et al., 2003). These data suggest an antagonistic regulation between *KAN* gene and *HD-ZIP III* genes to control abaxialisation and adaxialisaion of vascular tissues (Figure 1.13B). Despite this reciprocal action, *KAN* and *HD-ZIP III* were never shown to directly interact but it was clearly shown that they interact through auxin. *KAN* repress auxin signaling and transport when *HD-ZIP III* trigger auxin signaling (Schuetz et al., 2013).

In addition to auxin action on vascular patterning, HD-ZIP III mRNA stability is modulated by *MIR165* and *MIR166* microRNA. *MIR165* and *MIR166* expression domains overlap with *KAN* genes and over expression of *MIR165* and *MIR166* leads to the same abaxialisation phenotype observed in *phv/phb/rev* triple mutant (Schuetz et al., 2013).

In conclusion, balance between expression levels of *KAN, HD-ZIP III and MIR165/166* controls adaxialisation/abaxialisation of vascular pattern (Figure 1.13B). Together, these examples show how xylem can control phloem differentiation (and reciprocally) and how adaxialisation/abaxialisation is finely determinate.

1.3 Phloem tissues ontogenesis

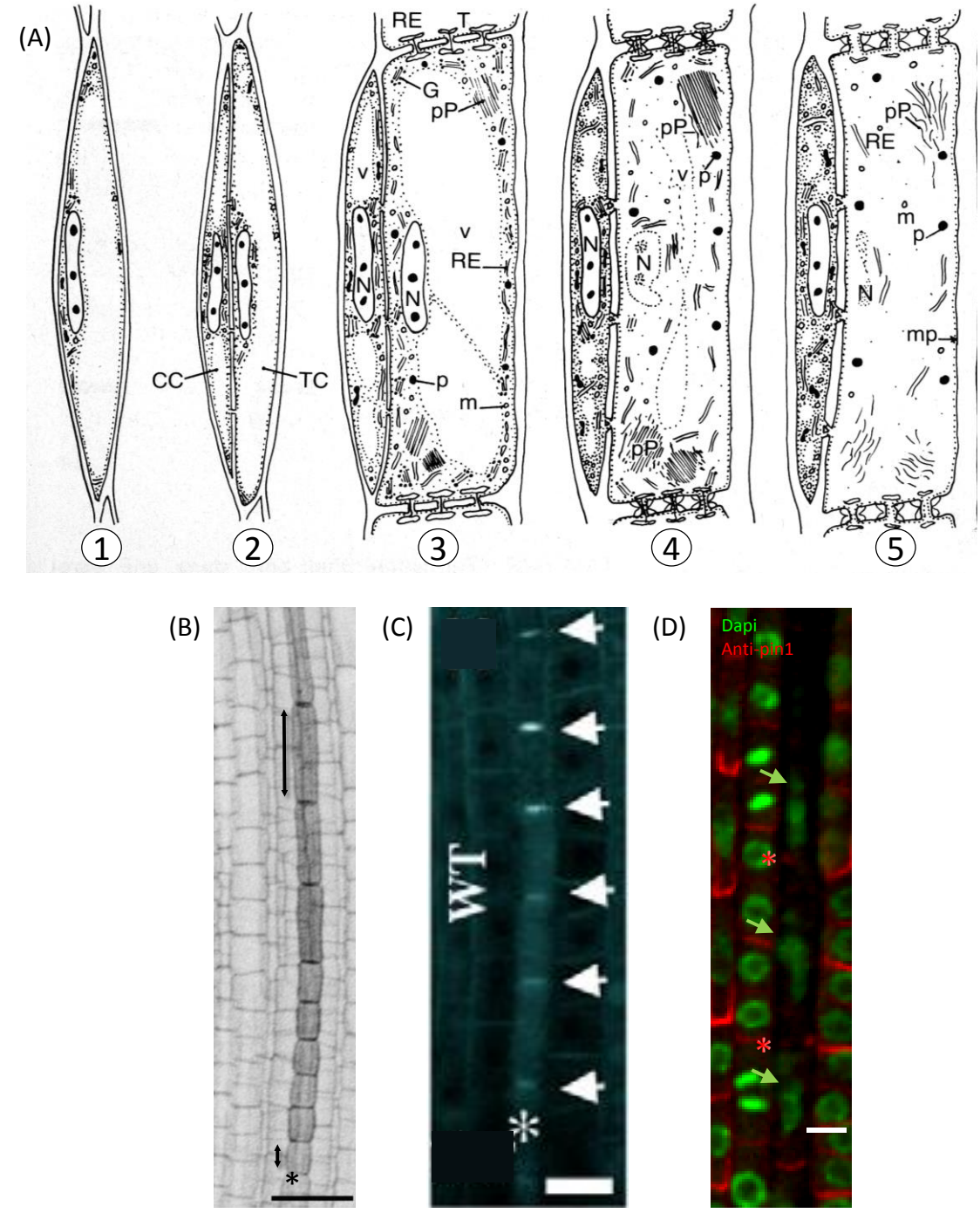

Figure 1.14: Cytological steps of phloem differentiation in root
(A) Schematic of cytological steps. 1: Phloem precursor cell; 2: Division of phloem precursor cell in companion cell (CC) and sieve element (SE); 3: Sieve element shape acquisition; 4: Degeneration of nuclei (N), vacuole (V), endoplasmic reticulum (ER), Golgi apparatus (G), mitochondria (M). Deposite of callose in plasmodesmata, drawing future sieve plate; 5: Sieve plate are formed, plasma membrane (mp) is still present, presence of P proteins (pP). From (Camefort, 1977)**(B)** Propidium iodide staining allow to visualize cell elongation (compare black arrows size) and cell wall thinckening (compare cell wall intensity along the cell file) . Star: phloem file; bar = 20µm. **(C)** Progressive deposite of callose (white arrow). Star: phloem file; scale bar: 20µm. From (Truernit et al., 2012). **(D)** Progressive disappearence (red star and green arrow) of PIN1 from the plasma membrane (visualized by anti-pin1 immunolocalization in red) and of nuclei (stained with DAPI: green).

Periclinal division of precursor of phloem cells is the first step of phloem differentiation. It produces sieve element on the one hand, companion cells on the other hand (Figures 1.3; 1.14A). In root, those divisions take place close to quiescent center. In leaf, periclinal divisions of phloem precursor cells occur at the end of vascular bundle and progressively form new phloem tubes (Lucas et al., 2013). During the phloem differentiation process, cells elongate (Figure 1.14B). Concomitantly, one can observe a progressive thickening of cell wall (Figure 1.14B), presumably to withstand high pressure caused by sap movements (Esau, 1969). To ease sap movements, plasmodesmata located at the ends of cells are modified with an increased diameter of the pores to form sieve plate pores. During phloem formation, a large amount of callose (β 1,3 glucane polymere) is deposited in the cell wall which will close the pores of plasmodesmata (Figures 1.14A,C) (Esau, 1969). Cell walls (middle lamella, cellulosic cell wall and callose plates) surrounding plasmodesmata are hydrolysed leaving an open pore and corresponding to sieve plate pores. The size of plasmodesmata aperture is controlled by the balance between callose synthase and callose degradation by β 1,3 glucanase activity (Levy et al., 2007) to allow intercellular communication and hence a correct development. The pore of plasmodesmata is occupied by a membranous cylinder: plasmotubule that communicates with endoplasmic reticulum. After complete perforation, endoplasmic reticulum disappears.

As described before, sieve elements are living cells that have lost most of their cellular components (Figure 1.14A). Indeed, nuclei, vacuole, endoplasmic reticulum and Golgi are degraded during phloem differentiation. Only some modified mitochondria remain and localize along cell wall (Figure 1.14A). The degradation of almost organelles permits to let free the lumen of the phloem tube to enhance the sap flow (Sjolund, 1997).

Organelles degradation can be parted in three steps (Furuta et al., 2014a):

(1) Modification of the structure of nuclei: from a smooth sphere to irregular shape (Figure 1.14D);

(2) Nuclei contracts and other organelles are deformed, NUCLEAR PORE PROTEIN1 (NUP1) and histone H2B are sprayed in cytoplasm suggesting a disorganization of nuclei (Figure 1.18B)

(3) Complete enucleation with persistent fragments of nuclear envelop and decrease of cytoplasm density. Mitochondria changed of shape and small lytic vacuoles form

perinuclear clusters. Lack of big central vacuole is a marker of programmed cell death.

Although description of cytological steps of phloem differentiation was well characterized, discovery of the molecular basis of phloem differentiation began recently. Several strategies were developed to identify genes involved during phloem differentiation. Reverse genetic permitted to describe callose involvement in this process (Xie et al., 2011). Oppositely, forward genetic screens, based on short root phenotypes, determined new mutants involved in phloem patterning (*apl, brx*) (Bonke et al., 2003; Mouchel et al., 2004). Indeed, an affected vascular transport leads to a shortening of root length. Gene trapping permitted to identify genes specifically expressed in phloem that also display short roots (*brx, ops*) (Nagawa et al., 2006; Bauby et al., 2007; Mouchel et al., 2004; Truernit et al., 2012). Finally suppressor screens of yet identified phloem mutants progressively decrypted the framework of phloem differentiation (Depuydt et al., 2013; Rodriguez-Villalon et al., 2014).

1.3.1 Identification of specific phloem marker genes

Originally, the *ALTERED PHLOEM DEVELOPMENT* (*APL*) gene was identified from a short root screen and was the first gene isolated to control phloem identity. *APL* encodes a MYB transcription factor that induces asymmetric cell division in protophloem (Bonke et al., 2003). *APL* is expressed in protophloem, companion cell and in sieve element and is largely used in other studies as phloem marker (Vatén et al., 2011; Scacchi et al., 2010; Depuydt et al., 2013) . The *apl* mutant presents a total absence of phloem cells but cells with xylem identity are present in phloem poles (Figure 1.15). On contrary, ectopic expression of *APL* inhibits xylem formation. These data suggest that APL control phloem specification and inhibits xylem formation in phloem poles.

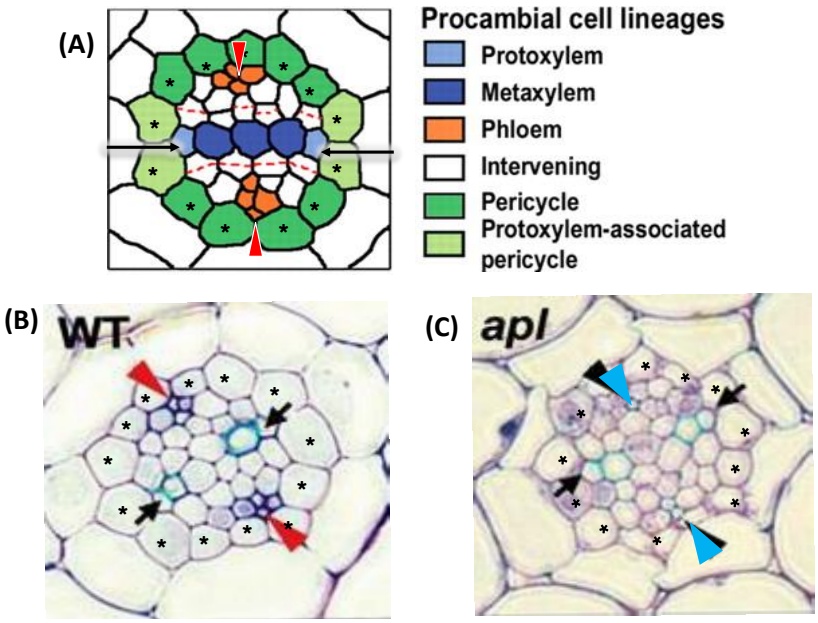

Figure 1.15: Phenotypes of phloem differentiation mutants
(A) Schematic representation of vasculature in the stele of *Arabidopsis* root (transverse section). Adapted from (Mähönen et al., 2006). **(B-C)** Transversal root section of WT **(B)** and *apl* mutant **(C)**. Adapted from(Bonke et al., 2003). Stars: pericycle; Red arrow: protophloem; Black arrow: protoxylem; Blue arrow: protoxylem in protophloem pole.

One of the successful strategies is the use gene-trapping screen to identify vascular genes (Nagawa et al., 2006; Bauby et al., 2007).

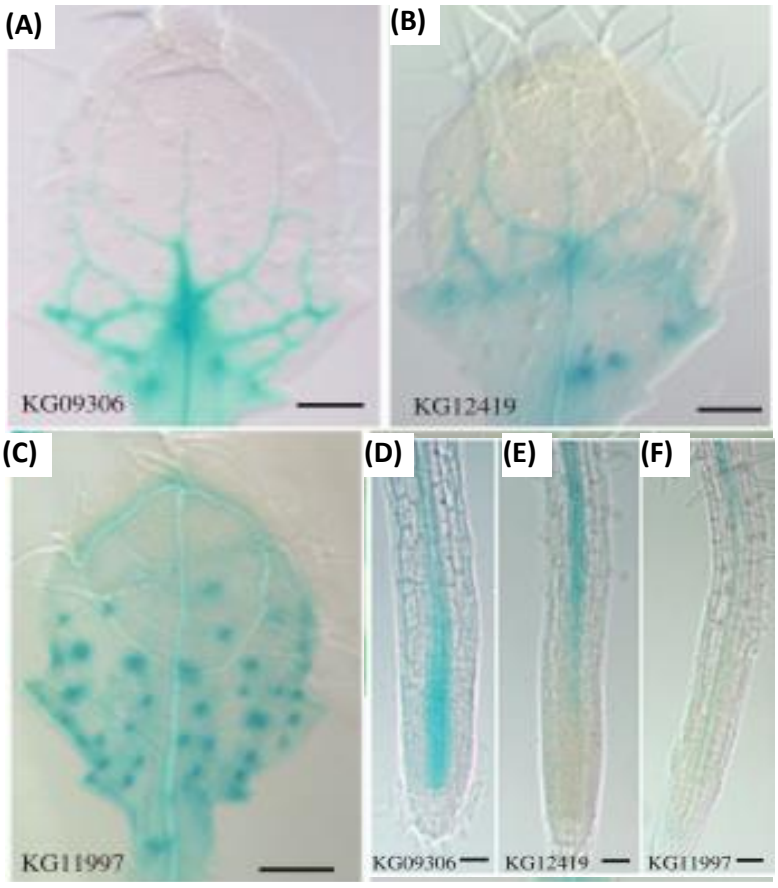

Figure 1.16: Phloem makers of Nagawa et al. study
Gene trap lines exhibiting GUS staining in the procambium. **(A-C)** GUS staining pattern of a young rossette leaf of **(A)** KG09306 (PINHEAD), **(B)** KG12419 (KTN), **(C)** KG11997 (OCTOPUS) **(D-F)** GUS staining pattern of a root of **(D)** KG09306 (PINHEAD), **(E)** KG12419 KTN, **(F)** KG11997 (OCTOPUS). Scale bars in **(A-C)** 25 mm; **(D-F)** 12,5 mm. From (Nagawa et al., 2006)

The first study (Nagawa et al., 2006) identified *PINHEAD*, *a KATANIN (KTN)* gene and a gene of unknown function (Atg3g09070), later identified as *OCTOPUS,* to be specifically expressed in procambium cells (Figure 1.16). *PINHEAD* is an *ARGONAUTE* gene family member, involved in gene silencing. *PINHEAD* could maintain cells proliferation in apical meristems and in procambium. *KTN* has a microtubule-severing activity. The *ktn* mutant is smaller and the vasculature appears discontinuous. *KTN* is involved in continuous vascular bundles formation and cell elongation.

The second study isolated five *PROTOPHLOEM DIFFERENTIATION* markers (*PD1-PD5* markers), early expressed in phloem (Table 1.1) (Bauby et al., 2007). *PD1* and *PD3* are annotated to encode proteins linked to the membrane (GPI-anchored and PIP-4,5 kinase respectively). *PD4* is *BREVIS RADIX* (see below) and *PD5* encodes a protein of unknown function: OCTOPUS (also previously identified in Nagawa et al. gene trapping screen (Nagawa et al., 2006)). Those PD markers are temporally expressed at different moments of development (Figure 1.17). All PD markers, except PD1, are expressed in mature embryo. *PD1-PD4* are expressed in protophloem precussor cells, *PD5* is expressed in both protophloem and metaphloem cells. *PD1* and *PD3* are expressed during protophloem differentiation. *PD4* and *PD5* defined pre-patterning of future vascular bundles at procambial stage.

Table 1.1: Description of protophloem differentiation markers

Marker	Accession	Phenotype of corresponding mutant	Fonction
PD1	At3g01950	-	GPI-like protein
PD2	At3g49680	-	BCAT3
PD3	At1g10900	-	PIP2-kinase
PD4	At1g31880	Short primary root	BREVIS RADIX
PD5	At3g09070	Short primary root	OCTOPUS

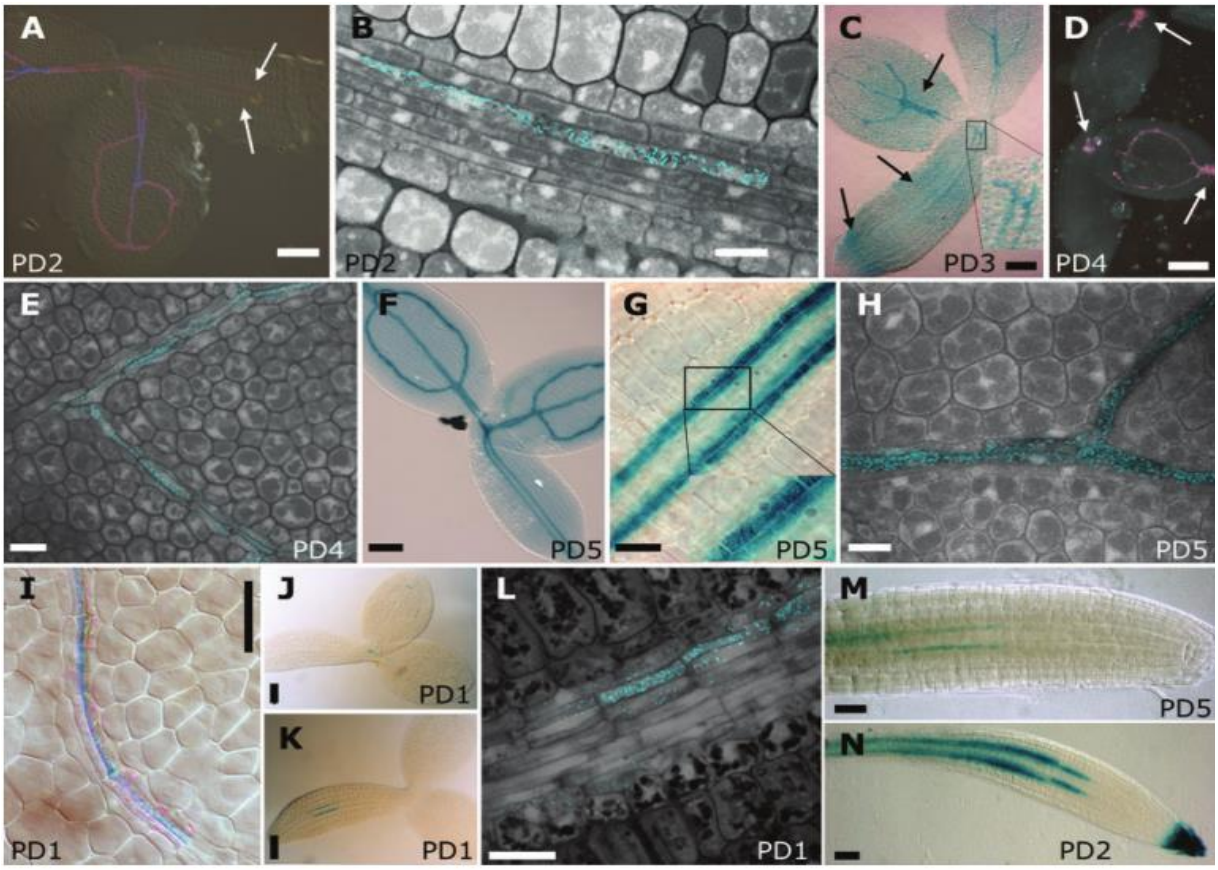

Figure 1.17: Identification of *PROTOPHLOEM DIFFERENTIATION* markers by Bauby et al. (2007)
Early GUS expression patterns of the PD markers. **(A)** Mature embryo PD2 marker expression in dark field showing the branching of phloem cell files in the cotyledonary node and the absence of expression in the lower part of the hypocotyl (white arrows). **(B)** Confocal image of the upper part of the hypocotyl of an AB- and GUS-stained mature embryo with PD2 marker expression showing protophloem precursor specificity. **(C)** PD3 marker expression in a mature embryo. PD3 GUS expression is also present in the epidermis (black arrows). **(D)** PD4 marker expression in a mature embryo (dark field). PD4 GUS expression is restricted to the hydathodes and cotyledon veins, and to two poles at the cotyledonary node in the sagittal plane (white arrows). **(E)** Confocal section of an AB- and GUS-stained mature embryo with PD4 marker expression pattern showing protophloem precursor specificity. **(F, G)** PD5 marker expression in mature embryos. **(G)** Magnification of the phloem poles in the hypocotyl, showing the expression of the PD5 marker in protophloem precursors and metaphloem initials. **(H)** Confocal section of an AB- and GUS-stained embryonic cotyledon with PD5 marker expression in protophloem precursors and metaphloem initials. **(I, J, K, L)** PD1 marker, 24- **(I, J)** and 36-h- **(K)** old seedlings. **(L)** Section of an AB- and GUS-stained 36-h-old embryo, PD1 marker expression pattern showing the protophloem precursor specificity. The PD1 marker is expressed only 24– 36 h after germination. **(M, N)** Primary root expression pattern of a 5 DAG seedling of PD5 and PD2 marker lines. Note that PD2 is also expressed in the columella. Scale bars¼100mm **(A, C, D, F, J, K)**, 10 mm **(B, H)**, 20 mm **(E, G, I)**. From (Bauby et al., 2007)

1.3.2 Reverse genetic permitted to describe some cytological steps of phloem differentiation

1.3.2.1 Enucleation marker

As all transcription factors, APL tunes expression of target genes. To identify genes downstream of APL, phloem cells of WT plant and *apl* mutant are used in a transcriptomic analysis. The results permitted to identify two transcription factors *NAC45* and *NAC86* (Furuta et al., 2014a) expressed in sieve elements before the initiation of the enucleation program.

In *nac45 nac86* double mutant, there is no more mature phloem, whereas other tissues appear normal suggesting a phloem specificity of *NAC45* and *NAC86*. It results on defect of phloem transport and a short root. In *nac45/86* phloem cells, enucleation and cytoplasm degradation do not occur (Figure 1.18). However, sieve plates, development of mitochondria and lytic vacuoles are normal. By their study, Furuta et al. (Furuta et al., 2014a) showed that NAC45/86 control the enucleation, organelles clustering and cytoplasm degradation in phloem. However, some processes necessary to phloem differentiation (for instance, the thickening of cell wall and callose deposition) are not controlled by NAC45/NAC86.

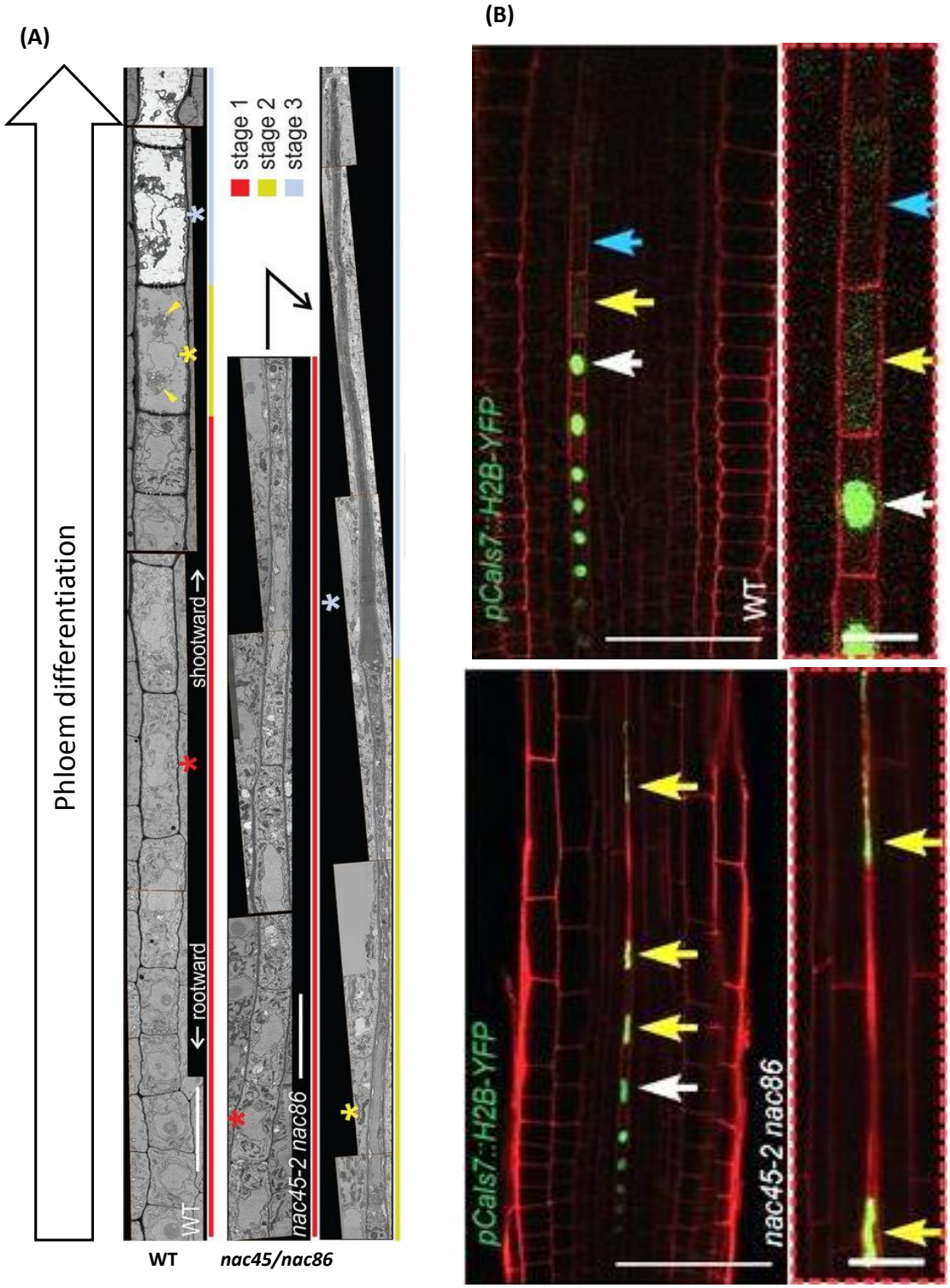

Figure 1.18: Control of callose deposition is necessary for normal phloem development
(A) Overview of sieve elements differentiation in WT that shows a decrease in cytoplasm density whereas it does not occur in *nac45 nac86* mutant. **(B)** During phloem differentiation, the H2B-YFP protein spreads in the cytoplasm of WT cells but stays localized in the cell nucleus of *nac45 nac86* double mutant. (A-B) From (Furuta et al., 2014a).

1.3.2.2 Callose deposition

Callose deposition plays a crucial role in wounding, pathogens attacks, for the growth of pollen tube during pollination but also in sieve plates formation (Xie et al., 2011). Amounts of callose in the cell wall impact cell communications. For instance increased callose degradation during sieve plates formation enhances molecules movements without size restriction and increased callose deposition decreases trafficking (Xie et al., 2011; Vatén et al., 2011). In *Arabidopsis*, among twelve genes involved in callose biosynthesis, *CALLOSE SYNTHASE 3 (CalS3)* and *CALLOSE SYNTHASE 7 (CalS7)* genes are responsible for phloem sieve plates formation (Xie et al., 2011; Vatén et al., 2011).

CalS7 is expressed in phloem and the corresponding protein accumulates in sieve plate. The *callose synthase 7* loss of function mutant (*cs7*) displays defects in sieve plates formation (absence of callose in vascular tissues, loss of characteristic structure in tooth and decrease of the number of plasmodesmata) (Figure 1.19A). In addition to be involved in callose biosynthesis, CalS7 is also essential for sieve plates shape (Xie et al., 2011).

CalS3 is expressed in phloem of the stele as well the protein is located in plasmodesmata (Figure 1.19B). The gain of function mutant for the *CalS3* gene (*cals3d)* presents a shorter root and many defects in phloem establishment. In *cals3d*, transient excessive accumulation of callose in phloem plasmodesmata influences cell communication in early stages of development. It results difficulties in phloem transport as attested by pAtSUC2::GFP marker (Figure 1.19C) (Vatén et al., 2011).

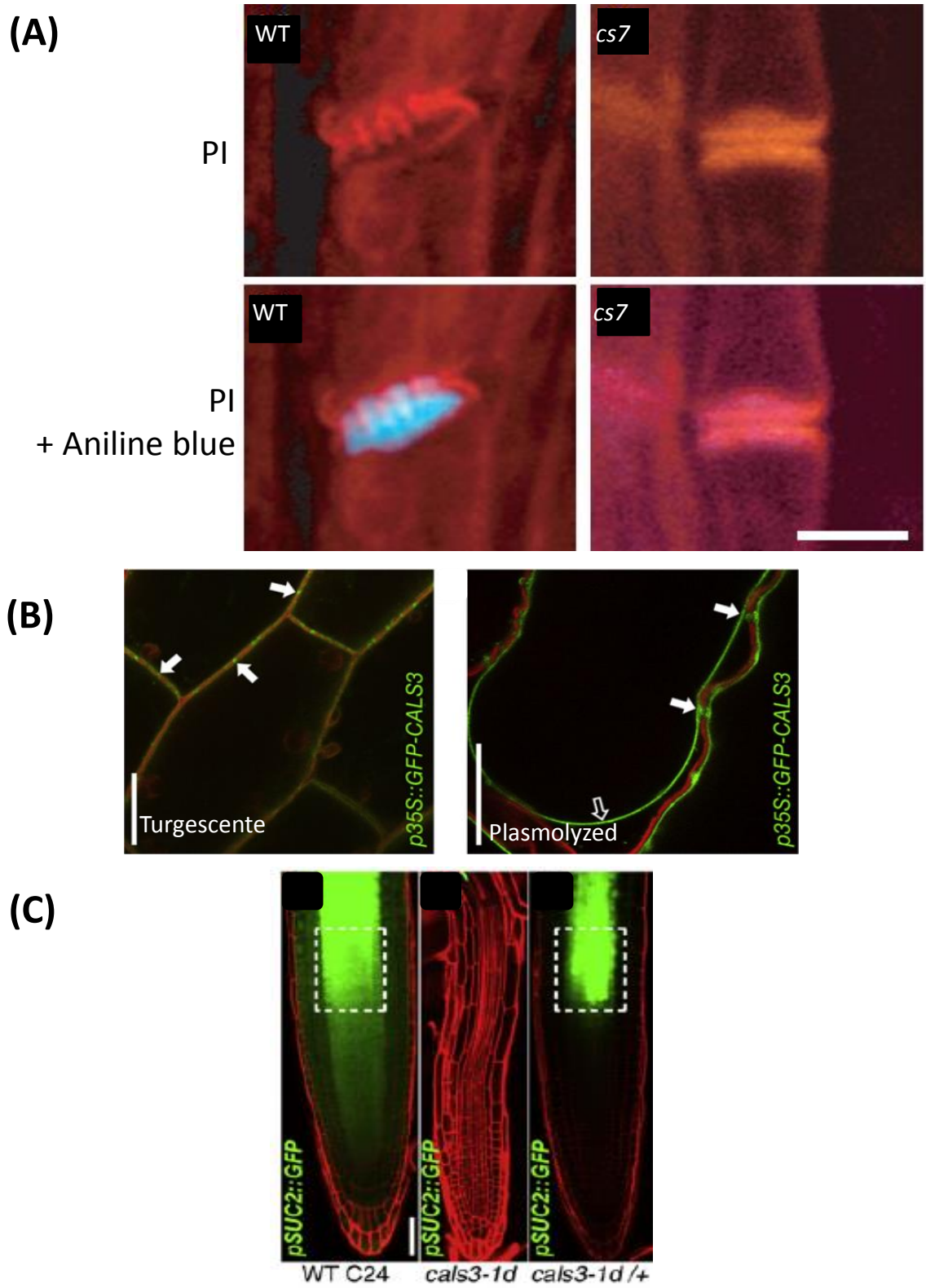

Figure 1.19: Callose synthases involved in callose deposition during phloem development
(A) The cs7 mutant displays sieve plate defects. Propidium iodide (PI) and aniline blue dyes in WT and *cs7* mutant. Bar = 5µm. Adapted from (Xie et al., 2011). **(B)** CALS3 is a membrane protein presents in sieve pores. Subcellular localization of CALS3 in plasmodesmata of cotyledon before and after plasmolysis. bar = 25µm; White arrows: plasmodesmatal localization. **(C)** pAtSUC2::GFP in WT, *cals3-1d* and *cals3-id (+/-)* mutants. (B-C) From (Vatén et al., 2011)

1.3.3 Forward genetic: isolation of *BREVIS RADIX* (*BRX*)

BRX was isolated from the Umkirch-1 (Uk-1) accession which displays a short root caused by a defect in cell elongation and a decrease of cell production (Mouchel et al., 2004). The introgressed line in Sav-0 allowed to identify the causal allele BRX^{S} (BREVIS RADIX). BRX belongs to a multigenic family composed of five members which are only found in multicellular plants. The BRX family genes encode proteins with highly conserved domains forming α-helical domain that are characteristic to transcription factor (Mouchel et al., 2004; Luscombe et al., 2000). Indeed, BRX is a transcription factor that is originally localized at the plasma membrane in a polar fashion before been translocated to the nucleus to control transcription of its target (Mouchel et al., 2004; Scacchi et al., 2009).

brx mutants also display short root and defects in phloem formation as evidence by propidium iodide staining that reveals short isolated cells with "gap" identity suggesting defects in phloem differentiation (Figure 1.20A). Gaps correspond to short cells present within normal elongated cells and that do not acquire the thickening of wall. However, the phloem marker *APL* is still expressed in *brx* mutant but its expression is not continuous along *brx* phloem lines (Figure 1.20B) suggesting that phloem differentiation occurs in *brx* mutants but some cells escape to this program (Scacchi et al., 2010). One of the most important steps of phloem establishment is asymmetric division of phloem precursor cell that occurs very early during phloem development. Gaps observed in *brx* mutant result in defects of essential periclinal division of phloem precursor cells (Rodriguez-Villalon et al., 2014).

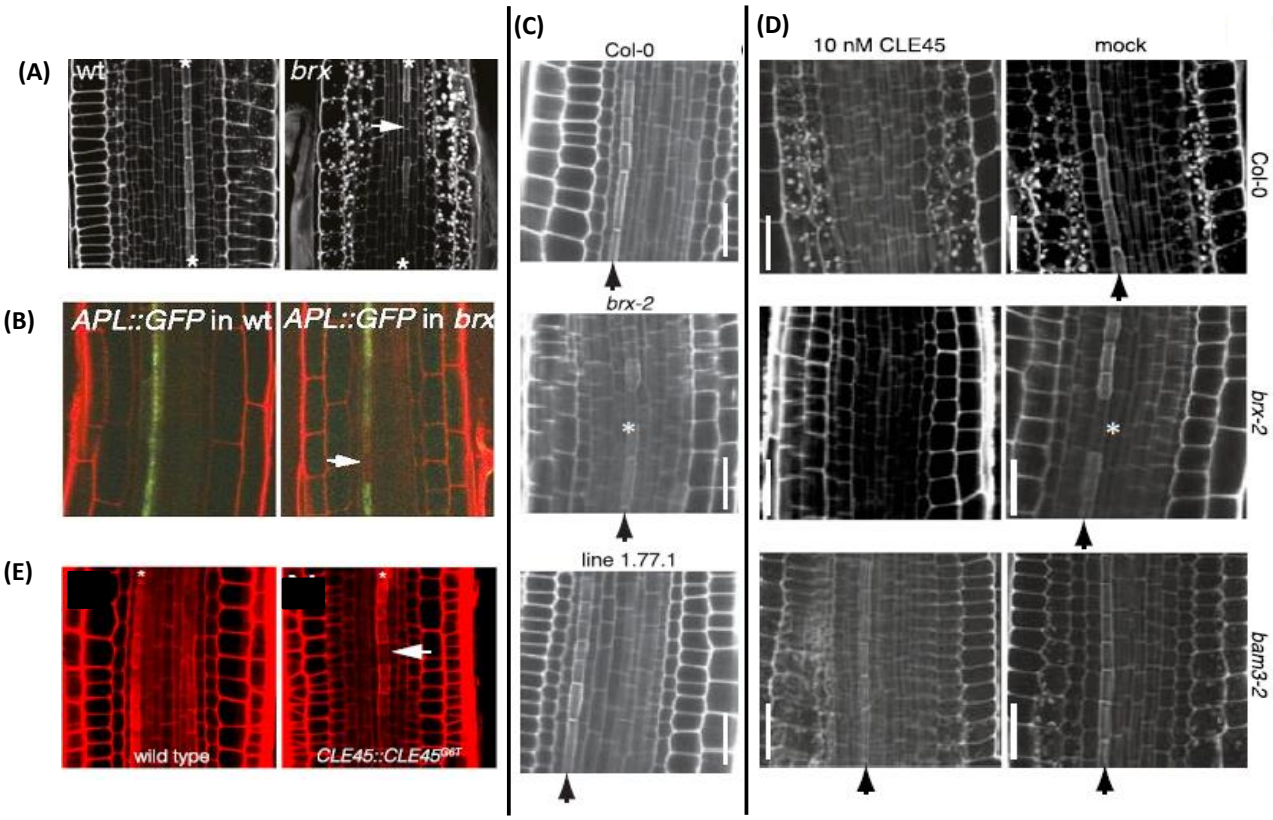

Figure 1.20: Control of phloem differentiation by the BRX/BAM3/CLE45 signaling module
(A) The *brx* mutant presents « gap » inside the phloem file. Gaps correspond to shorter with a thiner cell wall that have escaped the cell differentiation process. Propidium iodide staining on 5 days old seedlings. Arrowhead indicates gap in *brx,* star phloem file. **(B)** Expression of APL::GFP in WTand *brx* at 5 dag. Arrowhead indicates a gap in expression. (A-B) From (Scacchi et al., 2010). **(C)** Isolation of BAM3 as a suppressor of *brx*. Rescue of differentiation gaps in the *brx-2* mutants (asterisk) in line 1.77.1 (*bam3*) as revealed by propidium iodide staining. Arrowheads indicate protophloem cell files. (C-D) From (Depuydt et al., 2013) **(D)** Inhibition of protophloem differentiation by CLE45 treatment as revealed by propidium iodide staining. Arrowheads indicate protophloem cell file; star: gap. **(E)** Occurrence of gaps (arrowhead) in the phloem of CLE45::CLE45G6T (right), but not wild type plants (left). (D-E) From (Rodriguez-Villalon et al., 2014)

Many studies tried to characterise *BRX* function and revealed *BRX* as a junction between several hormonal pathways: BRX is involved in auxin and cytokinin (Cf §1.2.4) signaling pathway but also operate in brassinosteroid pathway.

Indeed, in *brx* mutant, the transcript level of *CONSTITUTIVE PHOTOMORPHOGENESIS AND DWARF (CPD* (Szekeres et al., 1996)) is downregulated (Mouchel et al., 2006). CPD is involved in brassinosteroids biosynthesis suggesting that BRX could also act on this pathway. Interestingly, *brx* meristem size and cell elongation defects can be rescued by brassinosteroids treatment during embryogenesis. Even more striking brassinosteroid treatments on *brx* permitted to restore expression of numerous genes including all genes

involved in auxin transport. This suggests a crosstalk between brassinosteroids and auxin through *BRX* (Mouchel et al., 2006).

It is worth noting that *BRX* expression is induced by auxin and is repressed by brassinosteroids and cytokinin. This study shows interactions between different hormones with a common point: *BRX* is required for optimal phloem development both during embryogenesis and seedling development.

1.3.4 Additional actors: toward a genetic framework controlling phloem differentiation

A suppressor screen on *bxr* isolated two genes: *BAM3* (*BARELY ANY MERISTEM 3*) a receptor like kinase (Figure 1.20C) and *OCTOPUS* (*OPS*) an unknown function gene (Depuydt et al., 2013; Rodriguez-Villalon et al., 2014).

BAM3 is a CLAVATA1-related receptor like kinase (DeYoung et al., 2006). To identify BAM3 ligand, *bam3* mutant was treated with different CLE (CLAVATA3/ENDOSPERM SURROUNDING REGION) peptides influencing root growth. *bam3* is partially insensitive to CLE45, suggesting that CLE45 could be BAM3's ligand (Figure 1.20D) (Depuydt et al., 2013). In WT, there is a gradual expression level of *BRX, CLE45* and *BAM3* that progressively overlap along the root (Depuydt et al., 2013; Rodriguez-Villalon et al., 2014):

- *BRX* is first expressed in meristematic zone
- then *CLE45* expression starts to be expressed with *BRX*
- *BAM3* later on phloem differentiating cell file

In *brx*, BAM3 is strongly induced with an ectopic pattern suggesting that *BRX* limits *BAM3* expression domain (Depuydt et al., 2013). One could conclude that *brx* defects would results from *BAM3* deregulation leading to a stochastic phloem differentiation.

Interestingly, CLE45 treatments modify phloem differentiation: cells do not present anymore thickening of wall (Figure 1.20D) and *APL* expression is totally abolished suggesting that BAM3/CLE45 block phloem differentiation. These phenotypes are an aggravated version of *brx* defects that affect only some cells of the phloem file. To elucidate CLE45 function on phloem differentiation, transient treatment of CLE45 were applied. Study showed that CLE45

blocks phloem differentiation acting on cell that have not started their differentiation yet. Indeed, CLE45 blocks periclinal division in protophloem cells, essential for sieve elements formation (Rodriguez-Villalon et al., 2014).

To obtain transgenic line overexpressing CLE45 and because CLE45 effect is very strong, a mutated weak version of CLE45 is done: *cle45*^{G6T}. The CLE45:: *cle45*^{G6T} line lead to the lack of periclinal division confirming functionality of *cle45*^{G6T} as active CLE45 peptide. The CLE45:: *cle45*^{G6T} recapitulates phenotypes observed in *brx* mutant (Figure 1.20E). These data suggest that gaps present in *brx* are the result of a stochastic deregulation of threshold activity of the CLE45-BAM3 pathway (Rodriguez-Villalon et al., 2014). In conclusion, BAM3/CLE45 is required for proper protophloem differentiation inhibiting periclinal cell division in provascular cells.

The second allele isolated from suppressor screen of *brx* mutant corresponds to a gain-of function mutation in *OPS* gene (OPS^{E319K} = *ops-D*) suggesting that *OPS* acts downstream of *BRX* (Rodriguez-Villalon et al., 2014). The *ops* loss-of-function mutant shares several common phenotypes with *brx* mutant including stochastic phloem differentiation in root (Mouchel et al., 2004; Scacchi et al., 2010; Truernit et al., 2012). Thus *BRX* and *OPS* induce phloem differentiation in root. When introduced in extra-copy, the pOPS::OPS-GFP construct confers a resistance to CLE45 treatment (Rodriguez-Villalon et al., 2014). Moreover, study of phloem defects in root reveal that *bam3* mutation is able to rescue both *brx* and *ops* defect. All together, these results indicate an opposite activity between BRX/OPS and CLE45/BAM3 during phloem differentiation depending of the threshold of CLE45 amount that inhibits phloem differentiation (Figure 1.20D CLE45 treatment compared to Figure 1.20E) (Rodriguez-Villalon et al., 2014). Interestingly, a similar regulation to CLE45/BAM3 is found during xylem differentiation and is controlled by the TDIF/TDR module CLE41/PXY (Cf § 1.1.5). This module recruits a GLYCOGEN SYNTHASE KINASE 3 (GSK3) of the brassinosteroid signaling pathway to inhibit xylem differentiation (Cf §3.3) (Kondo et al., 2014).
BRX and OPS activities are linked to induce phloem differentiation, OPS acting downstream of BRX (Figure 1.21). However, the exact pathway downstream of OPS remains elusive. Seeing that BRX runs into auxin, cytokinin and brassinosteroid signaling pathway, one can expect that OPS acts at least in one of these three pathways.

During my thesis, I identified OPS as a positive regulator of the brassinosteroid signaling to induce phloem differentiation. I will therefore develop next current knowledge on brassinosteroid hormones: their signaling pathway and the developmental processes they are involved in.

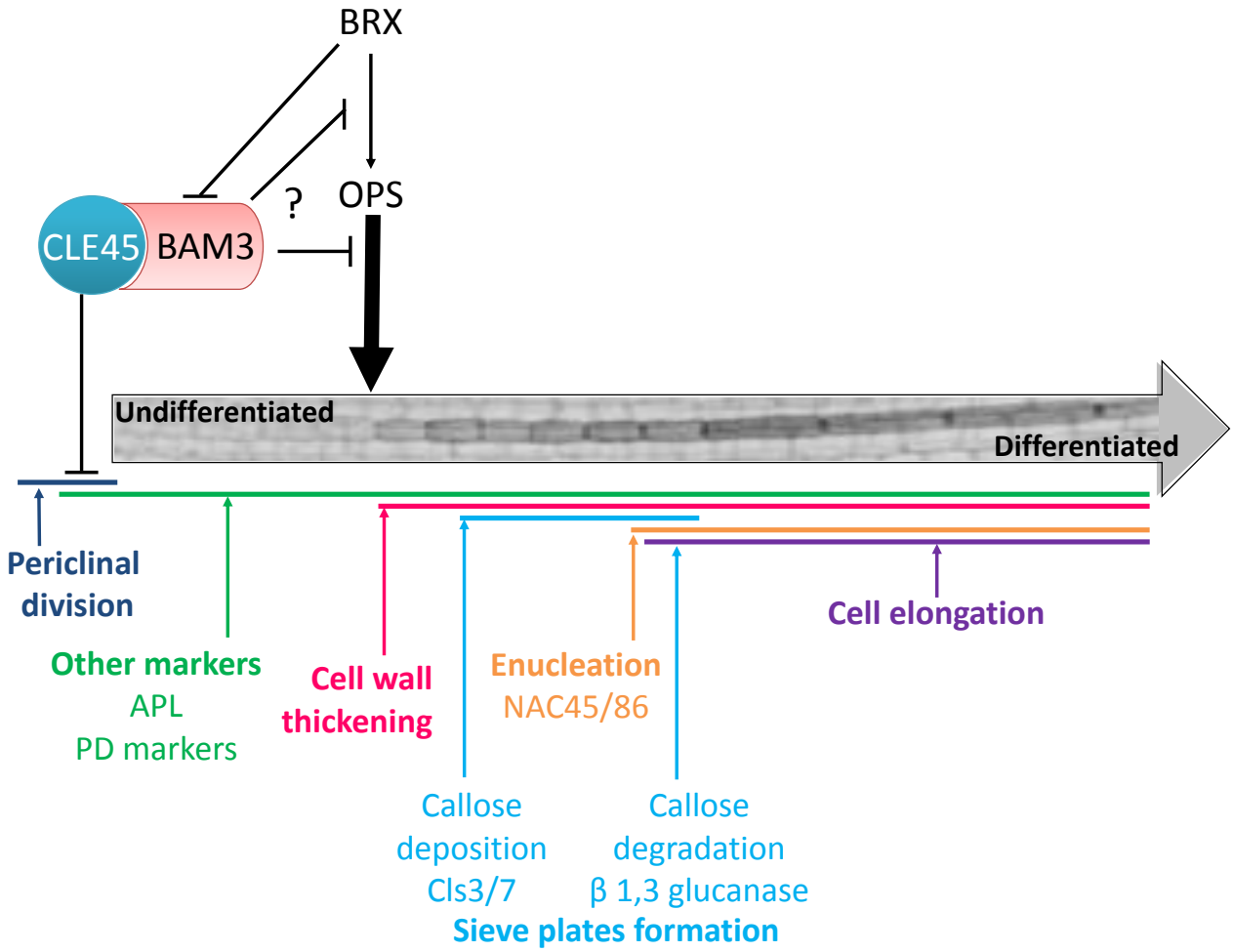

Figure 1.21: Framework of phloem differentiation along the root

2 Brassinosteroid hormones

Brassinosteroids are steroid phytohormones present in a wide range of taxonomic groups from the algae to the Angiosperm group (Bajguz and Tretyn, 2003).

Phytohormones, or plant hormones, are chemical products carrying information. They are signaling molecules acting on themselves or on cells different from those in which they were produced. Hormones (auxin, ethylene, jasmonic acid…) are involved in multiple developmental and defense-related processes and their action can be tissue- or concentration-dependent.

Brassinosteroids have only been discovered fairly recently: they are known for less than 50 years (compared to auxin that is known since Darwin (Darwin, 1880) and Went (Went, 1927) works). However, the brassinosteroid signaling pathway is the best described of the known hormones with an exhaustively described signal transduction cascade from receptors to transcription factors.

2.1 History of brassinosteroids and presentation of mutant phenotypes

2.1.1 The discovery of the "Brassins"

riginally, Mitchell et al. (Mitchell et al., 1970; Mitchell and Gregory, 1972) were the first to mention brassinosteroids. Actually, they named it "brassins". They identified this new hormone from an extract of rape pollen (*Brassica napus L.*) that induces internodes elongation when applied on a young bean internode (Figure 2.1). Chromatography and UV light assays defined the fatty nature of this compound.

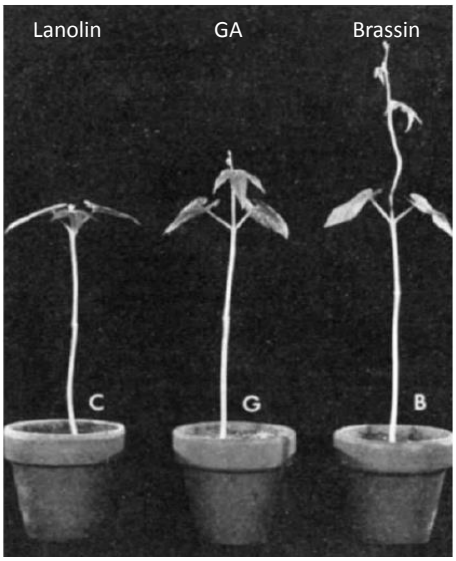

Figure 2.1: The discovery of Brassins
Elongation of bean plants treated at their second internode with lanolin (fatty substance); 0,001µg of giberillic acid or 10µg of Brassins during 4 days. Adapted from (Mitchell et al., 1970)

Only 9 years later through the work of Grove et al. (Grove et al., 1979) was isolated the active molecule. They crystalized 4 mg of brassinolide (BL) thanks to extraction of 40 kg of pollen and established the structure of brassinolide by X-ray crystallography: brassinolide was determined as a steroid phytohormone very close to ecdysone, an insect steroid hormone whose structure is the most similar to brassinolide.

Since the isolation of brassinolide by Grove et al. (Grove et al., 1979), a lot of brassinolide analogs were identified and referred to with the generic term "brassinosteroids" (Fujioka and Sakurai, 1997). Although many natural brassinosteroids have now been identified and their global effect on plant described, brassinosteroid biosynthesis, metabolism and molecular effects remain unclear.

2.1.2 *det2*, the first brassinosteroid mutant in *Arabidopsis thaliana*

The *det2* mutant of *Arabidopsis thaliana* (Chory et al., 1991) was isolated for its de-etiolated characteristics when grown in darkness (short hypocotyl, developed and opened cotyledons, accumulation of anthocyanins) (Figure 2.2A). Moreover, the *det2* mutant displays a dwarfed appearance in light condition, dark green leaves and reduced male fertility. It is affected in light response with an induction of light-regulated gene in darkness, delayed senescence and an elongated vegetative phase. Thus, DET2 could be involved in a developmental pathway regulated by light. Mapping of the *det2* mutation and gene sequence analysis of DET2 (Li et al., 1996) revealed homology to steroid 5α-reductase enzymes of mammals. This suggests that DET2 could catalyze similar enzyme reaction as found in mammals: the reduction of steroids. Many steroids are known in plant but only brassinosteroids affect growth. Thus, DET2 may catalyze a reduction of steroid intermediate during brassinosteroid biosynthesis. Supporting this hypothesis, treatment with BL rescued the *det2* phenotype (Figure 2.2B). DET2 implication in the brassinosteroid pathway was later confirmed by a chemical study: the *det2* mutant does not accumulate brassinosteroids but accumulates higher concentrations of intermediate metabolic products of brassinosteroid biosynthesis compared to WT (Noguchi et al., 1999).

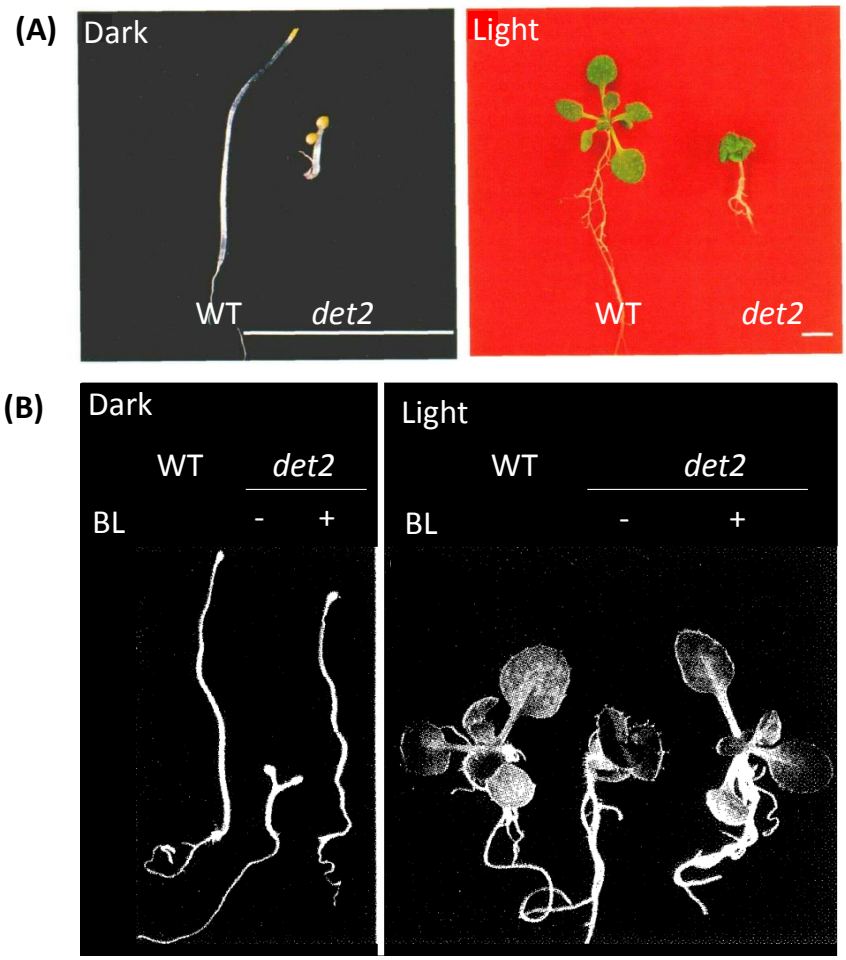

Figure 2.2: *det2*, the first brassinosteroids mutant
(A) Phenotype of 7 days-old dark-grown *det2* seedling (left) and 12 days-old light-grown seedling (right) compared to wild-type plants. bar = 1cm. Adapted from Chory et al., 1991. **(B)** *det2* growth defects are rescued by exogenous brassinolide application. 10 days-old dark-grown seedlings (left), 12 days-old light-grown seedlings (right). Adapted from (Li et al., 1996)

2.1.3 Overview of the methods used to isolate brassinosteroid mutants

It's only 20 years after the identification of brassins in 1970 and brassinolide in 1979 (BL, the most active form of brassinosteroid) (Mitchell et al., 1970; Mitchell and Gregory, 1972; Grove et al., 1979) that the first biosynthesis and perception mutants of Arabidopsis have been identified. Adoption of *Arabidopsis thaliana* as a model species in plant biology and the beginning of the genomic area permitted a quick building of brassinosteroid knowledge and identification of numerous mutants involved in each step of brassinosteroid pathway (from biosynthesis to molecular response).

To determine the involvement of genes in biosynthesis or signaling pathway, or just place them along the pathway, it is possible to use different approaches:

- Quantify chemical intermediate products of the pathway and identify which one are accumulated, which ones are defectives. This approach links protein activity to a biosynthetic step.
- Use physiologic method by brassinolide or brassinazole treatments (brassinosteroid biosynthesis inhibitor, (Asami et al., 2000)). For instance, brassinolide treatments rescue mutant affected in biosynthesis whereas a mutant which has its signaling pathway constitutively activated will be hypersensitive. Oppositely constitutive brassinosteroid signaling mutants will be insensitive to brassinazole.
- Practice a genetic approach to establish epistasic relationship between genes. Well, cross a dominant (or semi dominant) br^a-*D* mutant that constitutively induce the brassinosteroid pathway with a recessive defective mutant (br^b mutant, deficient mutant unable to produce brassinosteroids or a mutant affected in signaling) and describe the offspring. In the simplest case, if offspring phenotype looks like br^a-*D* mutant, then BR^a gene is downstream to the BR^b one.

As described before, *det2* was the first isolated brassinosteroid mutant and was a fortuitous discovery as attested by its name “de-etiolated-2”(Chory et al., 1991; Li et al., 1996). *det2* was isolated from a screen of defective light response mutants. Similarly, *cpd* (*constitutive photomorphogenesis and dwarfism*) was isolated for defects in root and hypocotyl elongation in darkness (Szekeres et al., 1996). From a screen for dwarf phenotypes, *dwarf4* was isolated in 1998 (Azpiroz et al., 1998; Choe et al., 1998). These three mutants accumulate chemical intermediate of brassinosteroid biosynthesis indicating their involvement in this process.

Pharmacological progress such as the isolation of brassinolide (Grove et al., 1979), as well as the identification of the brassinosteroid biosynthesis inhibitor brassinazole (BRZ) (Asami et al., 2000) permitted to develop new screens to isolate brassinosteroid related mutants. Indeed, *bri1* (*brassinosteroid insensitive 1=bin1)* (Clouse et al., 1996; Li and Chory, 1997) and *bin2-1D* (*brassinosteroid insensitive 2*) (Li et al., 2001) were isolated as mutants insensitive to brassinolide treatments. Brassinazole treatment permitted to identify the *bzr1-1D* mutant (*brassinazole resistant 1*,(Wang et al., 2002)), a constitutive brassinosteroid response mutant insensitive to BRZ treatments.

To gain insight into brassinosteroid signaling, one strategy was to find, by a genetic approach, suppressors of the *brassinosteroid insensitive 1* mutant (*bri1*). A classical mutagenesis method using ethylmethansulfonat (EMS) revealed BES1 (*bri1 EMS suppressor 1*, (Yin et al., 2002)) as the first *bri1* suppressor. In parallel to EMS mutagenesis, insertion mutagenesis by T-DNA is a powerful tool to identify genes, but genetic and functional redundancies are real brakes in the loss-of-function method. To overcome this limitation, an alternative gain of function approach, activation tagging, can also be used to reveal gene function. Thus, *BAK1* (*bri1-associated receptor kinase1-1dominant* (Li et al., 2002)) and BSU1 (*bri1 suppressor 1* (Mora-García et al., 2004)) were isolated by activation tagging as dominant suppressors of *bri1*, whereas *CDG1* (*CONSTITUTIVE DIFFERENTIAL GROWTH 1*) was isolated for its elongated hypocotyl in light when it is overexpressed (Muto et al., 2004).
Two hybrid screens and physical protein-protein interaction methods isolated BKI1 (BRI1 KINASE INHIBITOR 1, (Wang and Chory, 2006)) as an interactor with BRI1 and numerous 14-3-3λ proteins as interactors with BZR1 (Gampala et al., 2007).
Proteomic study of early brassinosteroid responsive membrane proteins by two-dimensional difference gel electrophoresis (2D-DIGE) identified the three BSK homologous (BRASSINOSTEROID SIGNALING KINASE (Tang et al., 2008)) as rapidly phosphorylated protein upon BL treatment.

Interestingly, molecular gain-of-function, caused by a dominant (or semi-dominant mutation) is not necessarily responsible of an activation of the pathway and a loss-of-function mutation does not necessarily interrupt the pathway. Indeed, the gain-of-function *bin2-1D* mutant represses the pathway whereas recessive mutations in the triple loss-of-function mutant *bin2-3 bil1 bil2* induce the pathway. This points the notion of positive regulator and negative regulator of the pathway. To shed light on the plethora of mutants, I propose here to classify them into categories based on their phenotype: the brassinosteroid defective mutants that interrupt the pathway and the constitutive brassinosteroid mutants that constitutively induce the pathway (Table 2.1 and Figure 2.3).

Table2.1 : Identification of brassinosteroid mutants

Kind of mutant	Pathway	Names	Screen	Kind of mutation	Reference	Ecotype
Brassinosteroid defective mutants	Biosynthesis	*det2-1*	Photomorphogenesis	EMS	Chory et al., 1989	Col
		cpd	Photomorphogenesis	t-DNA	Szekeres et al., 1996	Col
		dwarf4-2	dwarfism	t-DNA	Azpiroz et al., 1998/Choe et al., 1998	WS
	Signaling	*bri1-5*	BL insensitive (weak allele)	EMS	Li et al., 2002 (Clouse et al.,1996)	WS
		bri1-116	BL insensitive (strong allele)	EMS	Li and Chory, 1997 (Clouse et al., 1996)	Col
		bki-flag	BRI1 partner	Over-expressor	Wang et al., 2013	Col
		cdg1-2 / cdl1-1	Reverse genetic	t-DNA	Muto et al., 2004 / Kim et al., 2011	Col
		bsk	Rapidly phosphorylated in response to BL treatment	t-DNA	Tang et al., 2008	
		bin2-1D	BL insensitive	EMS	Li et al., 2001	Col
Brassinosteroid constitutive mutants	Signaling	*bak1-1D*	supressor of *bri1-5*	Activation tagging	Li et al., 2002	WS
		bki	BRI1 partner	Rnai	Wang et al., 2013	Col
		cdg1-D	Elongated hypocotyl	Activation tagging	Muto et al., 2004	Col
		bsu1-1D	supressor of bri1-5	Activation tagging	Mora-Garcia et al., 2004	WS
		triple gsk3	Reverse genetic	t-DNA	Yan et al., 2009	WS
		bzr1-1D	BRZ resistant	EMS	Wang et al., 2002	Col
		bes1-D	supressor of *bri1-119*	EMS	Yin et al., 2002	En

In red: gain-of-function mutant; in green: loss-of-function mutant0

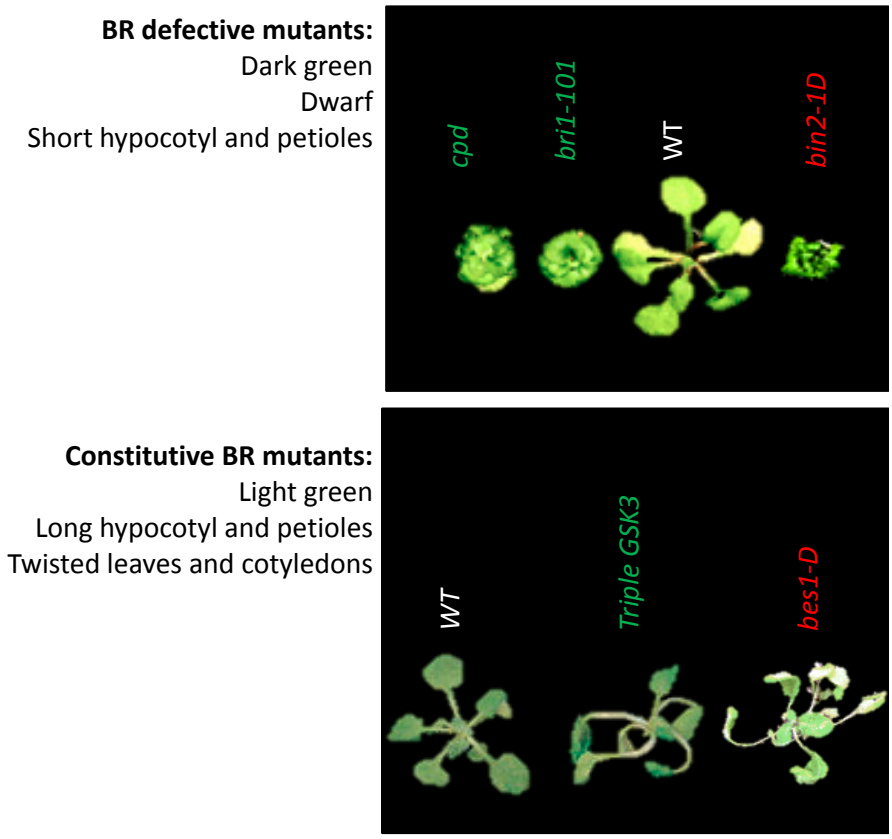

Figure 2.3: Growth phenotypes of BR defective and consitutive BR mutants
In green: loss-of-function mutant; in red gain-of-function mutant
Adapted from (Vert and Chory, 2006; Li et al., 2001; Yin et al., 2002)

Initially, brassinosteroid mutants were known as dwarf, with round and green darker leaves, short petiole and hypocotyl and correspond to brassinosteroid defective mutant (Figure 2.3). A brassinosteroid defective phenotype can either be produced by (1) loss-of-function mutations in biosynthetic enzymes (e.g. *det2*, (Chory et al., 1991)) and rescue by exogenous BL application(Szekeres et al., 1996), (2) by loss-of-function mutations in positive signaling component of the response pathway (e.g. *bri1* (Li and Chory, 1997)) or (3) by a gain-of-function mutation in a negative regulator of the signaling pathway (e.g. *bin2-1D* (Li et al., 2001)).

Similarly the constitutive brassinosteroid mutants can either originate from loss-of-function of negative regulator of the pathway (e.g. *bin2-3 bil1 bil2*, (Yan et al., 2009)) or gain-of-function of positive regulator of the pathway (e.g *bes1-D*, (Yin et al., 2002)). Constitutive brassinosteroid mutants are characterized by long petioles and hypocotyls, curly cotyledons and leaves and a light green color.

2.2 From brassinosteroids production to cellular response: description of brassinosteroid pathway

2.2.1 Biosynthesis of brassinosteroids

Brassinosteroids are molecules derived from steroids (Figure 2.4A). Steroids are a large group of lipids including sterols (Figure 2.4B) present in a wide range of organisms (bacteria, yeast, fungi, insects, mammals and plants). The most well-known form of animal sterol is cholesterol, an essential component of cellular membranes and the precursor of various compounds, especially hormones. Plant sterols are sisterol (C29), campesterol (C28) and sigmasterol (C29) commonly called phytosterols (Vanmierlo et al., 2013).

Brassinosteroids are produced from a reticulated biosynthetic pathway starting from squalene fatty acid, a linear C30 molecule that is cyclized in the major brassinosteroids precursor campesterol (Figure 2.4B). Originally, brassinosteroid biosynthesis was elucidated in Madagascar periwinkle (*Catharanthus roseus*) (Fujioka and Sakurai, 1997) and then confirmed by the analysis of brassinosteroid mutants in *Arabidopsis thaliana* (Noguchi et al., 1999; Choe et al., 1998). Recent reviews nicely resume brassinosteroid biosynthesis in Arabidopsis (Chung and Choe, 2013; Vriet et al., 2013).

The brassinosteroid biosynthesis is not linear (Figure 2.4B): several enzymes are able to act at different steps of the biosynthesis pathway, on different substrates. Thus, campesterol can be modified by two enzymes: either hydroxylated by DWARF4 (DWF4) or dehydrogenated by CONSTITUTIVE PHOTOMORPHOGENESIS and DWARF (CPD). It seems that the order of the reaction is determined by the availability of substrates and enzymes.

DWF4 can metabolize many substrates (campesterol, (24R)-ergost-4-en-3-one, (24R)-5α-ergostan-3one, campestanol and 6-oxocampestanol). Similarly, CPD can act on campesterol, (22S)-22-hydroxy-campesterol, (22S)-22, and 23-dihydroxy-campesterol.

Likewise, the DET2 protein acts as a steroid 5α-reductase on three substrates. ROT3 and CYP90D1 have a redundant C-23 hydroxylase action on the pathway. CYP85A1 and CYP85A2 catalyze the C-6 oxidation reaction, converting the 6-deoxo-typhasterol and the 6-deoxo-castasterone in the oxygenated forms typhasterol and castasterone.

However, the last step of the pathway corresponds to the catalysis of castasterone into brassinolide by CYP85A2. The presence of a saturated methyl or ethyl groups on C24 confers

the biological activity to brassinosteroids. However, the most important forms of brassinosteroids are brassinolide and castasterone because they are widely distributed and most biologically active (Bajguz and Tretyn, 2003).

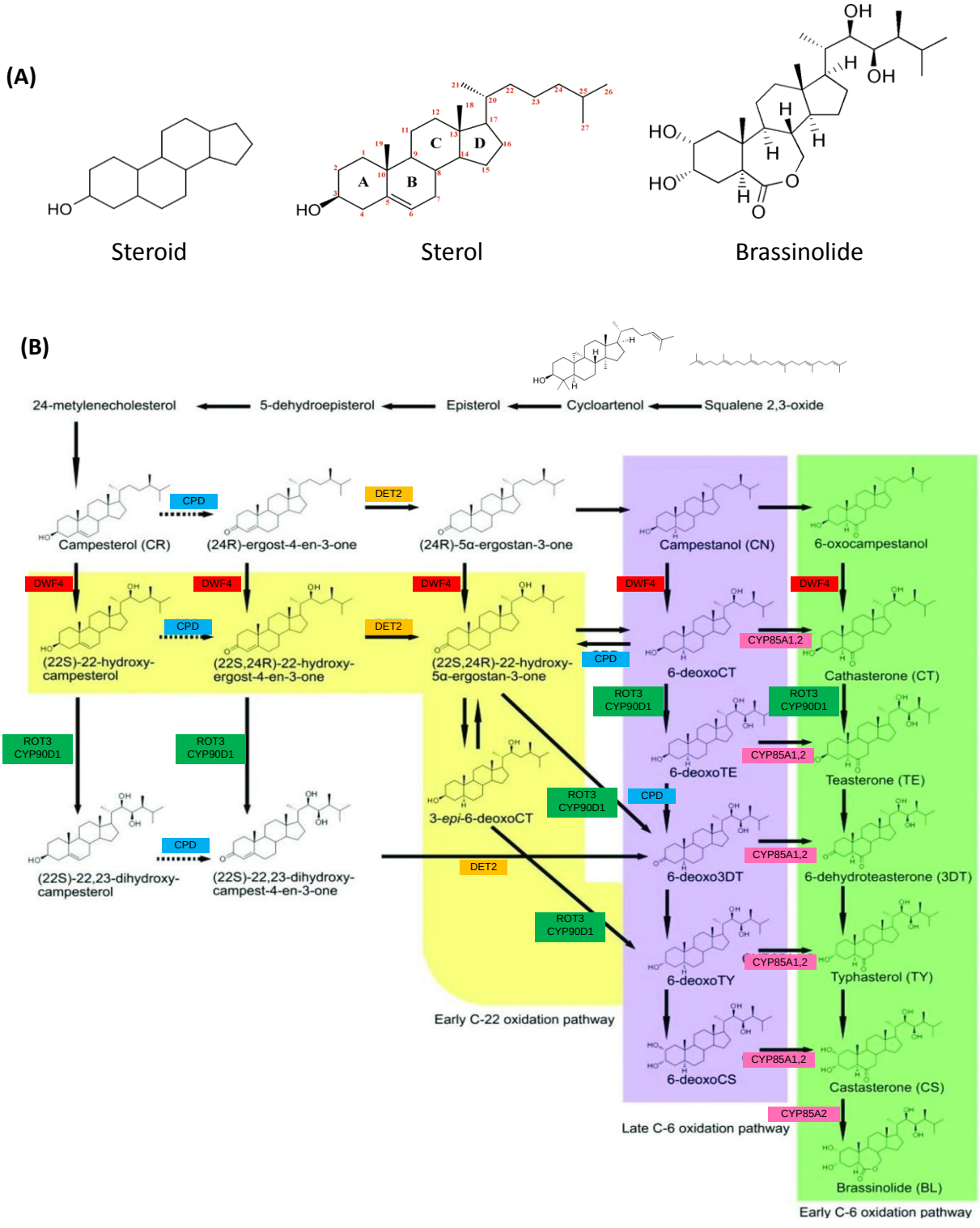

Figure 2.4: Brassinosteroids biosynthesis
(A) Chemical structure of diverse steroid molecules. **(B)** Campesterol pathway of BRs biosynthesis. Adapted from (Chung and Choe, 2013)

2.2.2 Transport of brassinosteroids

Contrary to auxin that is synthesized mainly in only a few locations such as meristems and young developing organs, brassinosteroids are synthesized in all parts of the plant. The expression of the *YUCCA* and *DET2* genes, representative for auxin and brassinosteroids biosynthesis, respectively, illustrate this difference (Figure 2.5). It is well known that auxin is transported at long distances thanks to the phloem (Petrásek and Friml, 2009). However, the situation for brassinosteroids is much less clear.

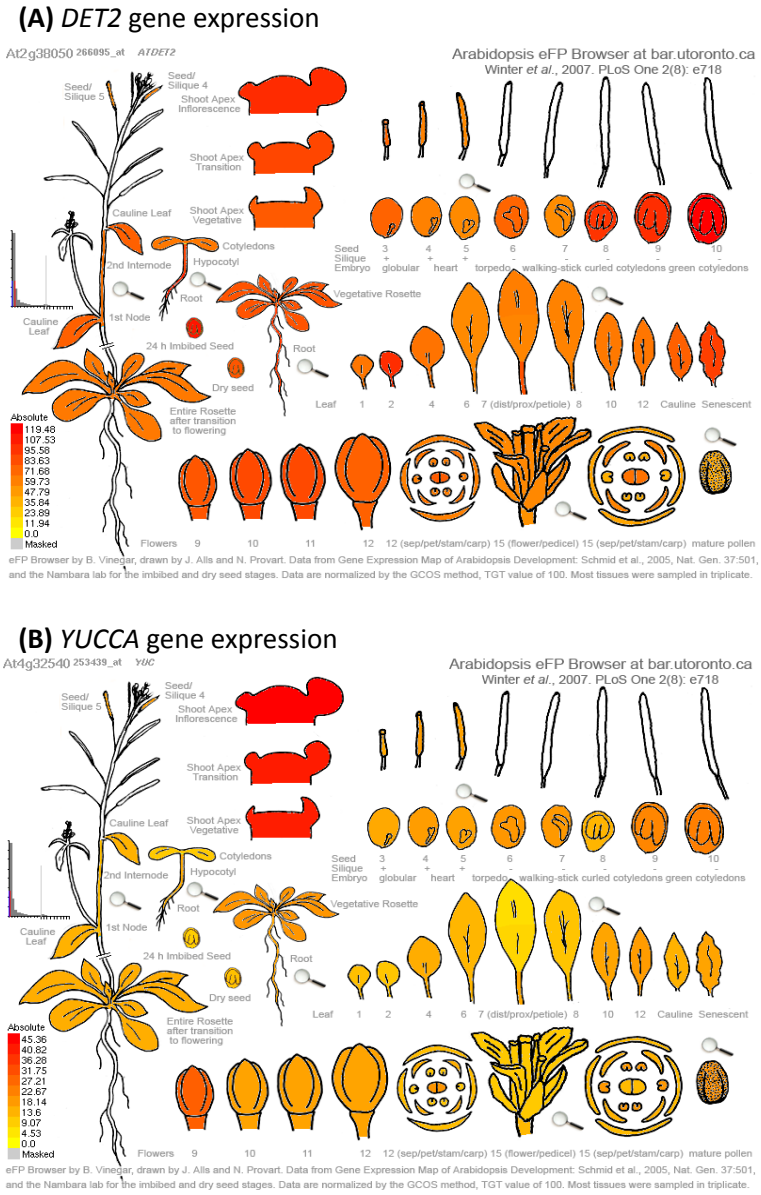

Figure 2.5: Location of brassinostroids and auxin biosynthesis
(A) The expression pattern of DET2 illustrates the wide area of brassinosteroids biosynthesis in Arabidopsis. **(B)** The expression pattern of YUCCA illustrates the specific place of auxin production in meristematic zone of Arabidopsis. From Arabidopsis eFP Browser http://bar.utoronto.ca/efp/cgi-bin/efpWeb.cgi

Long distance transport of brassinosteroids was tested in pea (Symons and Reid, 2004) and in tomato (Montoya et al., 2005) (Figure 2.6A) using grafting experiments that provide no evidence for long distance transport.

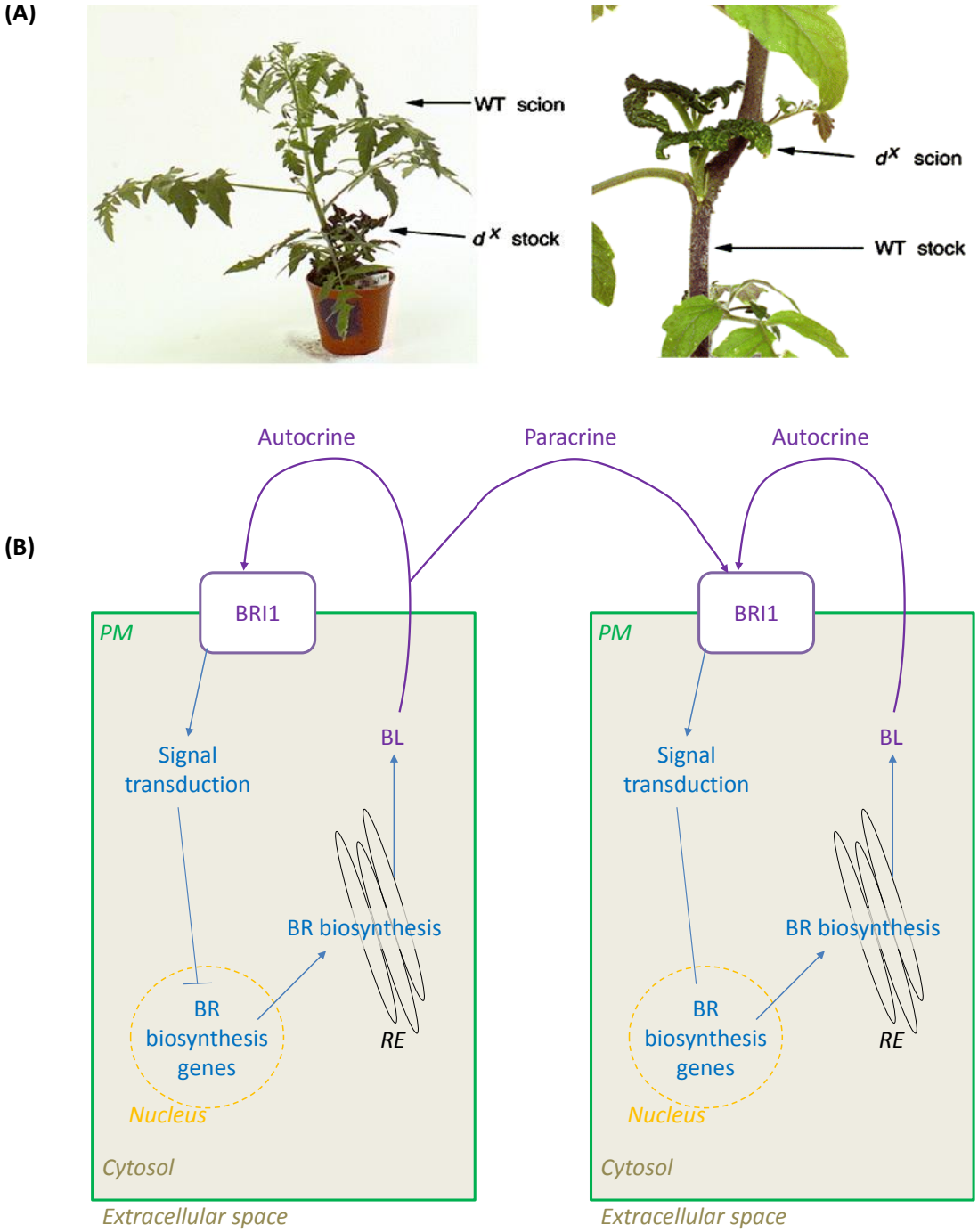

Figure 2.6: Brassinosteroids transport
(A) There is no long distance transport of brassinosteroids in tomato plants. Reciprocal grafting assays between a WT and brassinosteroids deficient tomato mutant (d^x) do not rescue the dwarf phenotype. From (Montoya et al., 2005). **(B)** Brassinosteroids perception at the plasma membrane suggests secretion of brassinosteroids outside of the cell and its autocrine and paracrine action for a short distance transport.

Brassinosteroid short-range mobility is also arguable. Because brassinosteroid signal is perceived at the plasma membrane (He et al., 2000; Wang et al., 2001; Vert et al., 2005), it is likely that they are secreted outside of the cell where they are produced. In agreement with this hypothesis, brassinosteroids are detected in the medium of *Zinnia elegans* cell culture (Yamamoto et al., 1997). Brassinosteroids are synthetized in endoplasmic reticulum, move into cytoplasm and are secreted outside of the cell where they could be perceived by surrounding cells (paracrine mode) or the same cell (autocrine mode) (Figure 2.6B) (Symons et al., 2008).

However, Savaldi-Goldstein et al. (Savaldi-Goldstein et al., 2007) study provides cues showing contrary. Here, expression of a biosynthesis gene in meristem epidermis (L1) of a biosynthesis mutant (*cpd*, ML1::CPD-YFP) permits to rescue development defects of *cpd* mutant. Similarly, expression of BRI1 in L1 layer cells of shoot apical meristem in a *bri1* mutant rescues the WT phenotype. These data suggests that proper brassinosteroid signaling in meristem epidermis is essential for plant development. On the contrary, expression of a catabolic enzyme of brassinosteroids in L1 layer of WT plant leads to smaller plants compared to WT suggesting that brassinosteroids have a limited mobility between layers in meristem and supporting hypothesis of no short distance transport (Savaldi-Goldstein et al., 2007).

To conclude, it remains unclear if brassinosteroid transport outside of the cell is passive or active, but some transporters facilitating secretion of steroid molecules out of animal cells have been identified (Young and Fielding, 1999) and one of the many transporters that have still to be characterized in plants may play a similar role in brassinosteroid export.

2.2.3 The brassinosteroid signaling pathway

The brassinosteroid signaling pathway can be separated in two parts: perception at the plasma membrane by a receptor like kinase (RLK) and transduction of the brassinosteroid signal from the cytoplasm to the nucleus by intracellular phosphorylation-mediated signaling cascades.

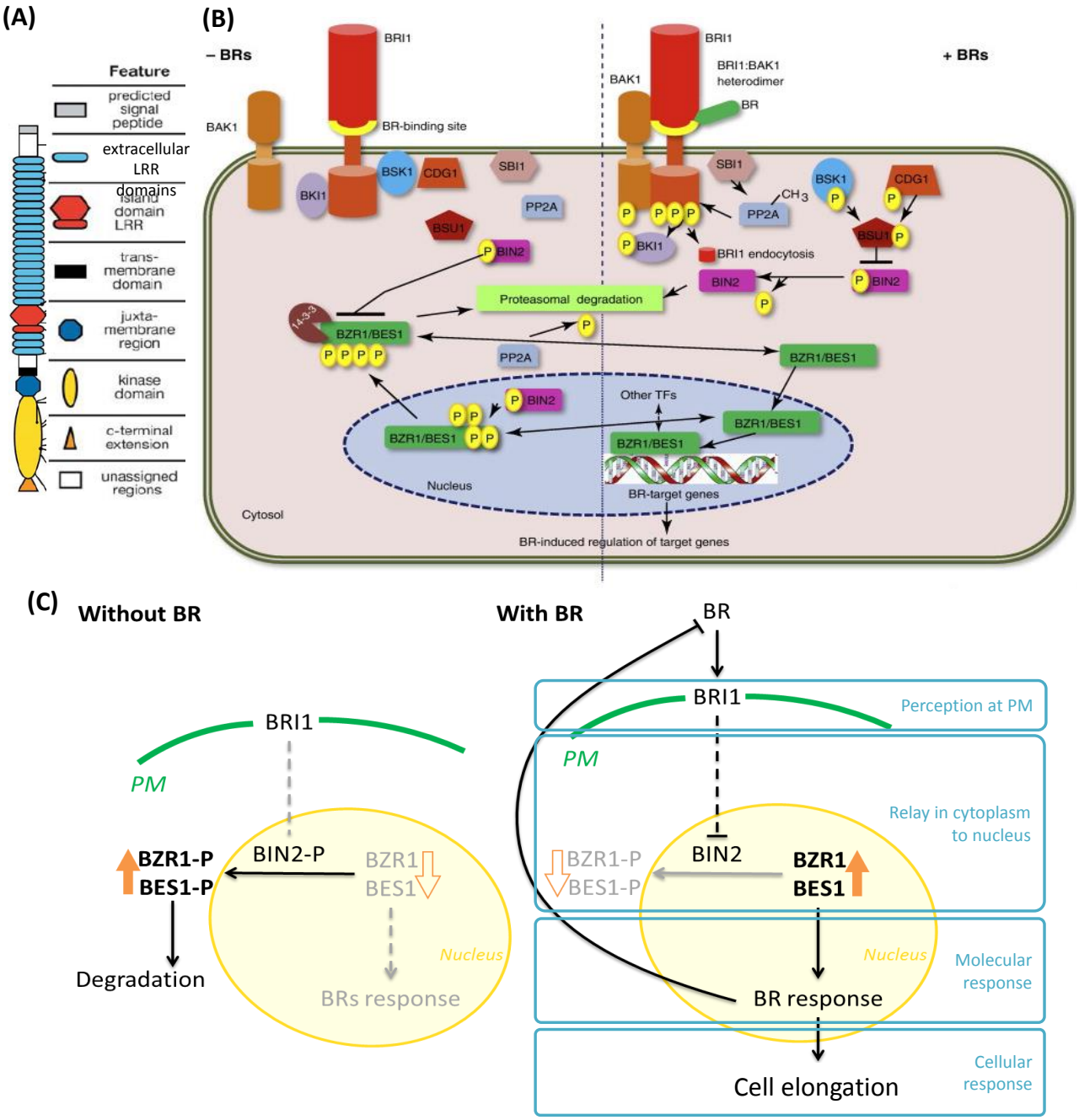

Figure 2.7: Brassinosteroids signaling pathway: a phosphorylation-mediated cascade from plasma membrane to nucleus

(A) Structure of BRI1 receptor. From (Vert et al., 2005) **(B)** Detailed brassinosteroids signaling pathway. From (Choudhary et al., 2012). **(C)** Simplified pathway. In absence of brassisnosteroids (left), BIN2 kinase is active and phosphorylates the two transcription factors BZR1 and BES1 that are unable to bind their target genes in the nucleus. (Right) Brassinosteroids are perceived at the plasma membrane (PM) by the membrane receptor-kinase BRI1. Several steps later, It leads to an inactivation of BIN2 by dephosphorylation allowing accumulation of unphosphorylated BES1 and BZR1 able to induce the brassinosteroids cellular response such as increased cell elongation or the inhibition of brassinosteroids biosynthesis by a negative feedback.

2.2.3.1 Sensing of the brassinosteroid signal at the plasma membrane by BRI1/BAK1 heterodimer

Brassinosteroid signal is perceived at the surface of cell by BRASSINOSTEROID INSENSITIVE 1 receptor (BRI1 (Clouse et al., 1996; Li and Chory, 1997; He et al., 2000; Wang et al., 2001)) (Figure 2.7). BRI1 is a transmembrane protein composed of a 20 leucine rich repeat (LRR) domains interrupted by a stretch of amino acids termed as island domain, a single transmembrane membrane helix and a cytoplasmic serine/threonine kinase domain (RLK) (FIGURE 2.7A) (Vert et al., 2005). BRI1 works in tandem with its co-receptor BAK1 (BRI1-ASSOCIATED RECEPTOR KINASE 1 (Li et al., 2002)) a small LRR-RLK also known as SERK1. In absence of brassinosteroids, BRI1 is auto-inactivated (Wang et al., 2005) and associated with BRI1 KINASE INHIBITOR 1 (BKI1 (Wang and Chory, 2006; Jaillais et al., 2011)). BKI1 interacts with the cytoplasmic kinase domain of BRI1 preventing the activation of BRI1 and inhibiting BRI1/BAK1 heterodimer formation.

Binding of brassinosteroids by island domain of BRI1 causes a conformational change in the receptor that induces autophosphorylation of BRI1 (a phosphorylation of BRI1 by itself) and phosphorylation of BKI1, thus releasing BKI1 from BRI1 at the plasma membrane into the cytosol and formation of BRI1/BAK1 heterodimer (Jaillais et al., 2011). BRI1/BAK1 interaction provokes a sequential and reciprocal transphoshorylation of BRI1 and BAK1 (exchange of phosphate group between BRI1 and BAK1 and reciprocally) which is necessary for full BRI1 activity (Wang et al., 2008).

Subsequently, activated BRI1 phosphorylates CDG1 (Kim et al., 2011) and/or BSK kinases (Tang et al., 2008) two membrane-associated proteins.

2.2.3.2 Relay of brassinosteroid information in cytoplasm to the nucleus by a phosphorylation-mediated cascade

Once CDG1 and BSKs are activated, they are able to phosphorylate BRI1 SUPPRESSOR 1 (BSU1) (Mora-García et al., 2004; Kim et al., 2011, 2009) a nucleo-cytoplasmic phosphatase that dephosphorylates BRASSINOSTEROID INSENSITIVE 2 (BIN2 (Li et al., 2001; Mora-García et al., 2004; Kim et al., 2011)) on its conserved tyrosine 200 residue to inhibit BIN2 activity (Kim et al., 2009). BIN2 belongs to the GLYCOGEN SYNTHASE KINASE 3 family (GSK3 (Yan et al., 2009)) and is the key inhibitor of the brassinosteroid signaling pathway when activated

by autophosphorylation (Kim et al., 2009). Active phosphorylated BIN2 directly phosphorylates the two homologous transcription factors BRI1 EMS SUPPRESSOR 1 (BES1/BZR2 (Yin et al., 2002)) and BRASSINAZOLE RESISTANT 1 (BZR1 (Wang et al., 2002)) to repress their action in the nucleus (Peng et al., 2010). Phosphorylation destabilizes BES1 and BZR1 preventing their accumulation (Yin et al., 2002; Wang et al., 2002). BES1 is a nuclear protein (Vert and Chory, 2006), but BZR1 localization could be subject to dynamic regulation: the phosphorylated forms of BZR1 accumulate in the cytoplasm, presumably retained by a member of the phosphopeptide binding 14-3-3λ proteins family(Gampala et al., 2007; Ryu et al., 2007).

In presence of brassinosteroids, BIN2 is inactivated and degraded by the proteasome preventing its effect on the transcription factors (Peng et al., 2008). Additionally, upon dephosphorylation by phosphatase PP2A B' (Tang et al., 2011) BES1 and BZR1 transcription factors accumulate in the nucleus where they bind their target genes to regulate genes expression and induce the brassinosteroid response. The switch of BES1 phosphorylation in response to brassinosteroid signaling activation can be followed in western-blotting and can be used as a proxy of active brassinosteroid signaling (Figure 2.8a) (Yin et al., 2002).

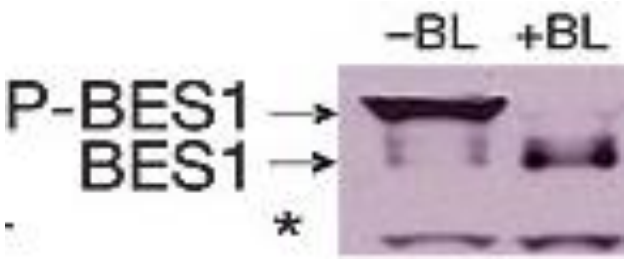

Figure 2.8: Molecular response of induced brassinosteroid pathway
BES1 western blotting on WT plants treated or not with brassinolide (BL). In presence of BL, the pathway is induced, there is a strong accumulation of unphosphorylated from of BES1. Actually phosphate charges of the phosphorylated form of BES1 (BES1-P) decrease binding capacity of sodium dodecyl sulfate (SDS) on BES1 protein. BES1-P migrates more slowly compared to the unphosphorylated one (BES1) because it is less negatively charged (Lee et al., 2013). From (Vert and Chory, 2006).

BES1 and BZR1 are homologous basic helix loop helix DNA binding transcription factors and have different identified DNA binding specificities. It has been shown that BZR1 binds brassinosteroid response elements (BRRE) (CGTG(T/C)G) (He et al., 2005), BES1 binds E-box

(CANNTG) and BRRE motifs (Yin et al., 2005; Yu et al., 2011). Both BES1 and BZR1 control more than 1000 genes involved in numerous cellular, metabolic and developmental processes (Sun et al., 2010). Cell wall modification and cellular transport are major cellular functions regulated by brassinosteroids, consistent with their effects on cell elongation. Several BZR1 targets are transcription factors and components of other signaling pathways such as the light or auxin pathways (Sun et al., 2010), illustrating the inter interplay between different signaling pathways.

2.2.4 Regulation of the brassinosteroid pathway

A negative feedback on brassinosteroid biosynthesis, controlled by BES1 and BZR1, is one of the first brassinosteroid responses, resulting in a decreased transcription of brassinosteroid biosynthesis genes. Thus, the steady-state level of brassinosteroids is highly regulated by d*e novo* biosynthesis and inactivation of brassinosteroids ratio. Glycosylation, esterification, hydroxylation, methylation or sulfation on key brassinolide carbons are sufficient to reduce levels of bioactive brassinosteroids (Vriet et al., 2013).

In addition, the amounts of binding-competent receptor molecules can also be controlled. BRI1 and BAK1 are mainly localized at the plasma membrane but also undergo clathrin-dependant endocytosis and cycle between the endosome and plasma membrane (Geldner et al., 2007; Irani et al., 2012; Di Rubbo et al., 2013). However the biological function of BRI1 endocytosis is largely discussed.

Geldner et al. (Geldner et al., 2007) argued that BRI1 endocytosis acts as a mechanism inducing the brassinosteroid pathway. The dwelling time of BRI1 at the plasma membrane would be restricted to ligand binding and activation, while signaling would be assigned to endosomal compartements (Geldner et al., 2007). On the other hand, blocking BRI1 endocytosis enhances brassinosteroid signaling, suggesting that endocytosis could mediate brassinosteroid signal attenuation (Irani et al., 2012; Di Rubbo et al., 2013).

2.2.5 How modulate the brassinosteroid pathway experimentally?

The brassinosteroid pathway can be artificially controlled by exogenous treatment (Figure 2.9).

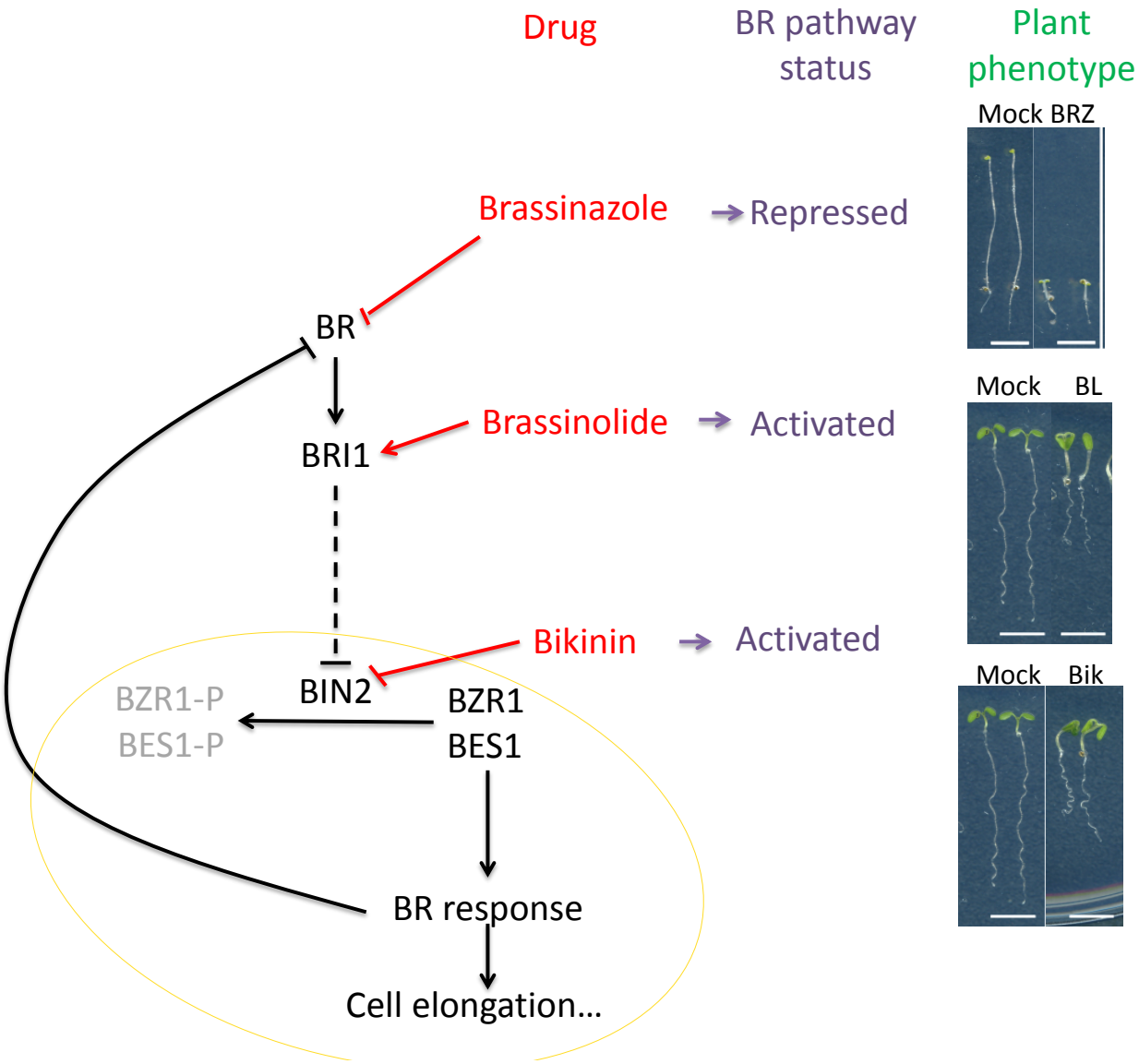

Figure 2.9: How to experimentally modulate brassinosteroid pathway?
Scheme presenting the action of various drugs on the BR pathway and their effect on plant development. Brassinazole (BRZ) (Asami et al., 2000) represses BR biosynthesis and invokes a dwarf phenotype. Brassinolide (BL) (Grove et al., 1979) and bikinin (Bik) (De Rybel et al., 2009) induces the pathway and provokes constitutive brassinosteroid phenotypes with elongated hypocotyl and curly cotyledons. Brassinolide is the most active form of brassinosteroids and is bound by the BRI1 receptor. Bikinin represses the GSK3 kinases including BIN2.

The pathway can be induced at two different steps of the signaling pathway. First, addition of brassinolide (Grove et al., 1979), which is the most active form of brassinosteroids, at micromolar concentration strongly induces the pathway by stimulating directly BRI1 receptor. Alternatively, the addition of bikinin, a GSK3-inhibitor (De Rybel et al., 2009), activate the signaling pathway by blocking the constitutive repression of BIN2 on the pathway. Bikinin reduces the kinase activity of seven GSK3 (including BIN2 and its relative

BIL1 and BIL2) on BES1 and BZR1 transcription factors. Induction of brassinosteroid pathway by brassinolide or bikinin provokes elongated hypocotyl and petioles and curly cotyledons phenotypes (Figure 2.9) and a typical molecular response as described for constitutive brassinosteroids mutants (accumulation of BES1 and BZR1 unphosphorylated forms and gene expression modulation).

Conversely, the brassinosteroid pathway can be repressed by the addition of brassinazole (BRZ, (Asami et al., 2000)). This compound directly acts at the biosynthesis level by inhibiting CPD enzyme, reducing the level of active form of brassinosteroids. Plants treated with BZR have growth defects and display photomorphogenesis in darkness as described for brassinosteroids defective mutants (Figure 2.9).

3 Roles of brassinosteroids in plant development

Like observed with other hormones, brassinosteroid signaling activity needs to be at an optimal rate to ensure proper plant development. Indeed, too high concentrations of brassinosteroids are as deleterious as are too low brassinosteroids concentrations. Here, I will develop brassinosteroid implications at multi scales in plants, from division to its implication on global shape control and try to give an overview of brassinosteroid involvement in different developmental processes.

3.1 Subcellular scale: brassinosteroids impact on cell wall and vice-versa

Growth of wall-enclosed plant cells is driven by turgor pressure and controlled by the extensibility of the cell wall. The cell wall is a complex matrix composed of polysaccharides (cellulose, hemicellulose, pectin) and lignin forming a hydrated gel network pervaded by proteins. The cell wall structure gives resistance to cell in an opposite principle to cell expansion and cell differentiation. During cell elongation, cell wall has to be modified: loosening of the primary cell wall occurs, water is taken up, the wall swells and new components are synthesized (Wolf et al., 2012a). Many proteins have been identified to participate in cell wall modification during cell expansion: glucanases, expansins, xyloglucan endotransglycosylases (XET) and pectinases (Cosgrove, 1997). Cell expansion is regulated by several hormone signaling pathways including brassinosteroids, auxin, ethylene, gibberellic acid and cytokinins (Vanstraelen and Benková, 2012). Here, only aspects concerning brassinosteroids are described.

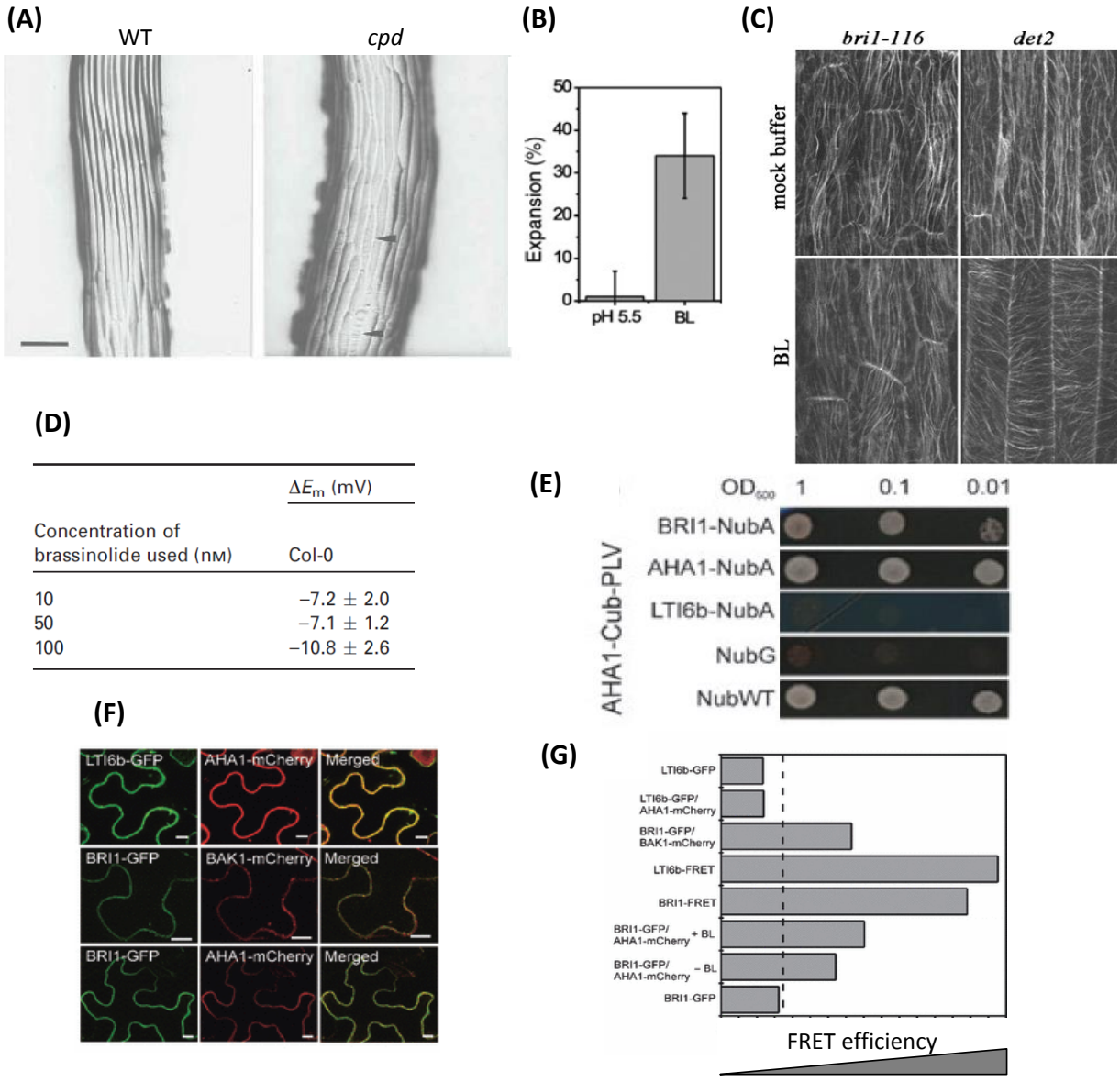

Figure 3.1: Brassinosteroids induce cell elongation

(A) The length of etiolated hypocotyl epidermal cells is shorter in *cpd* mutant compared to WT. From (Szekeres et al., 1996). **(B)** Brassinosteroids induce cell elongation. Quantitative comparison of cell wall expansion in plant treated with brassinolide (BL) compared to the WT, 30 minutes after treatment with BL. **(C)** YFP-tubulin signal in etiolated epidermal cells of *bri1-116* and *det2.* In mock condition microtubules display an oblique and longitudinal orientation. When treated with 1µM of brassinolide (BL) for 60 minutes they adopt a transversal orientation permitting cell elongation and reflecting reorientation of cellulose microfibrils. From (Wang et al., 2012). **(D)** BRs induce membrane hyperpolarization in root epidermal cells. Values indicates electric potential changes before and after 20 minutes of BL application. **(E)** Split-ubiquitin assays in yeast showing interaction between BRI1 and the H^+-ATPase AHA1. NubWT is the positive control, NubG the negative control. **(F)** BRI1 and AHA1 present the same membrane localization and could interact at the plasma membrane. Transcient transformation of tobacco epidermal cells coexpression the indicated mCherry or GFP fusion. **(G)** Protein-protein interaction showed by FRET. Lti6B /AHA1is used as a negative control, BRI1/BAK1 as a positive control. Individually transformed FRET fusions of BRI1 and LTI6b served as positive controls. The fusion protein are expressed transiently in tobacco epidermal cells. More FRET efficiency is high, more strong is the interaction between the proteins. (B,D-G) Adapted from (Caesar et al., 2011).

Brassinosteroids are well known to induce hypocotyl, stem, epicotyl, and coleoptile elongations by cell elongation (Figure 3.1A,B) (Szekeres et al., 1996; Clouse and Sasse, 1998). Furthermore, in brassinosteroid defective mutants grown in darkness (*det2* and *bri1-116*) microtubules present oblique and longitudinal orientations in epidermal cells, whereas in WT their orientation is mostly transversal (Figure 3.1C) (Wang et al., 2012). After a brassinosteroid treatment, microtubules are reoriented in a transversal plan in *det2* mutant, but not in *bri1-116* suggesting a BRI1 dependent-mechanism. Brassinosteroids contribute to reorientation of microtubules through BRI1, which then controls orientation of the cellulose microfibrils, to promote cell elongation in hypocotyl (Wang et al., 2012; Gutierrez et al., 2009) .

Whereas both brassinosteroids and auxin promote cell elongation, their dynamics appear different. Auxin action is a short-term effect (30 minutes) whereas the maximum elongation rate continues to increase for several hours in brassinosteroid treatment (Clouse and Sasse, 1998). This difference can also be observed in gene expression of *TCH4*. *TCH4* encodes a XET, the expression of which is more rapidly induced by auxin than brassinosteroids treatment (Xu et al., 1995).

Auxin induces growth via a mechanism called acid growth. Auxin enhances protons excretion by P-ATPase into the apoplast to initiate wall loosening by two modes of actions: (1) enhancement of P-ATPases vesicle secretion into the plasma membrane; (2) stimulation of P-ATPases activity. This acidification of the apoplast in turn leads to wall loosening which intiates cell growth (Rayle and Cleland, 1992). Brassinosteroids may induce growth by a similar mechanism. Indeed, brassinosteroid treatments induce a quick hyperpolarization of the plasma membrane (Figure 3.1D) provoked by a secretion of protons in apoplast. It is possible to record BRI1-GFP signal by fluorescence lifetime technique (FLT) (Caesar et al., 2011). Protonation/deprotonation of GFP chormophore is caused by enviromnent pH which influences the GFP fluorescence that is less fluorescent in acidic condition (Campbell and Choy, 2001). During cell expansion, there is a modification in BRI1-GFP signal, suggesting an alteration of BRI1-GFP environment: local hyperpolarization of the membrane. Protein interaction analysis show that BRI1 directly interacts with P-ATPase (Figure 3.1E) at the

plasma membrane (Figure 3.1F) and that the kinase domain of BRI1 is necessary to regulate the P-ATPase activity (Caesar et al., 2011).

Consistent with impact of brassinosteroids on loosening of cell wall by acidification, studies on PECTIN METHYLESTERASE (PME) showed involvement of brassinosteroids in cell wall homeostasis. PME promotes formation of Ca^{2+} bonds in the pectin matrix necessary for the rigidity of wall. Overexpression of a PME inhibitor (PMEIox) confers loosening of wall and promotes cell expansion. A suppressor screen on *PMEIox* identified first *BRI1* as potential regulator of cell wall integrity (Wolf et al., 2012b), then the *RECEPTOR LIKE PROTEIN 44 (RLP44)* whose corresponding protein interacts with BAK1 to induce brassinosteroid pathway independently to brassinosteroid ligand (Wolf et al., 2014). Thus in response to pectins changes in cell wall composition, RLP44 provides a lateral input modulating brassinosteroid signaling. Interestingly, brassinosteroid pathway control cell wall through many aspects (loosening, genes expression control (Caesar et al., 2011; Sun et al., 2010)) but a feedback loop from cell wall permits to divert brassinosteroid pathway for its advantage.

All those studies demonstrate the importance of brassinosteroids in coordinating cell elongation with cell wall synthesis and cytoskeleton organization.

3.2 Cellular scale: brassinosteroids inhibit differentiation in epidermis

3.2.1 Stomatal development is inhibited by brassinosteroids

In leaves, some cells diverge from the puzzle-like pattern created by pavement cells: stomata composed of two guard cells delimiting pore and that control plant–atmosphere gas exchanges. Acquisition of stomatal identity is regulated by a signaling pathway including the ERECTA family receptor-like kinase and MAPK complex involving the *YODA* gene that represses stomata formation (Figure 3.2C) (Wengier and Bergmann, 2012). Brassinosteroid defective mutants (e.g. *bri1-116* or *bsu-q*) display an excess of stomata while activation of the brassinosteroid pathway by bikinin or in the *triple gsk3* mutant (*bin2 bil1 bil2*) results in a decrease of stomata number (Figure 3.2A,B) (Kim et al., 2012). Those data suggest that brassinosteroids inhibit stomata formation.

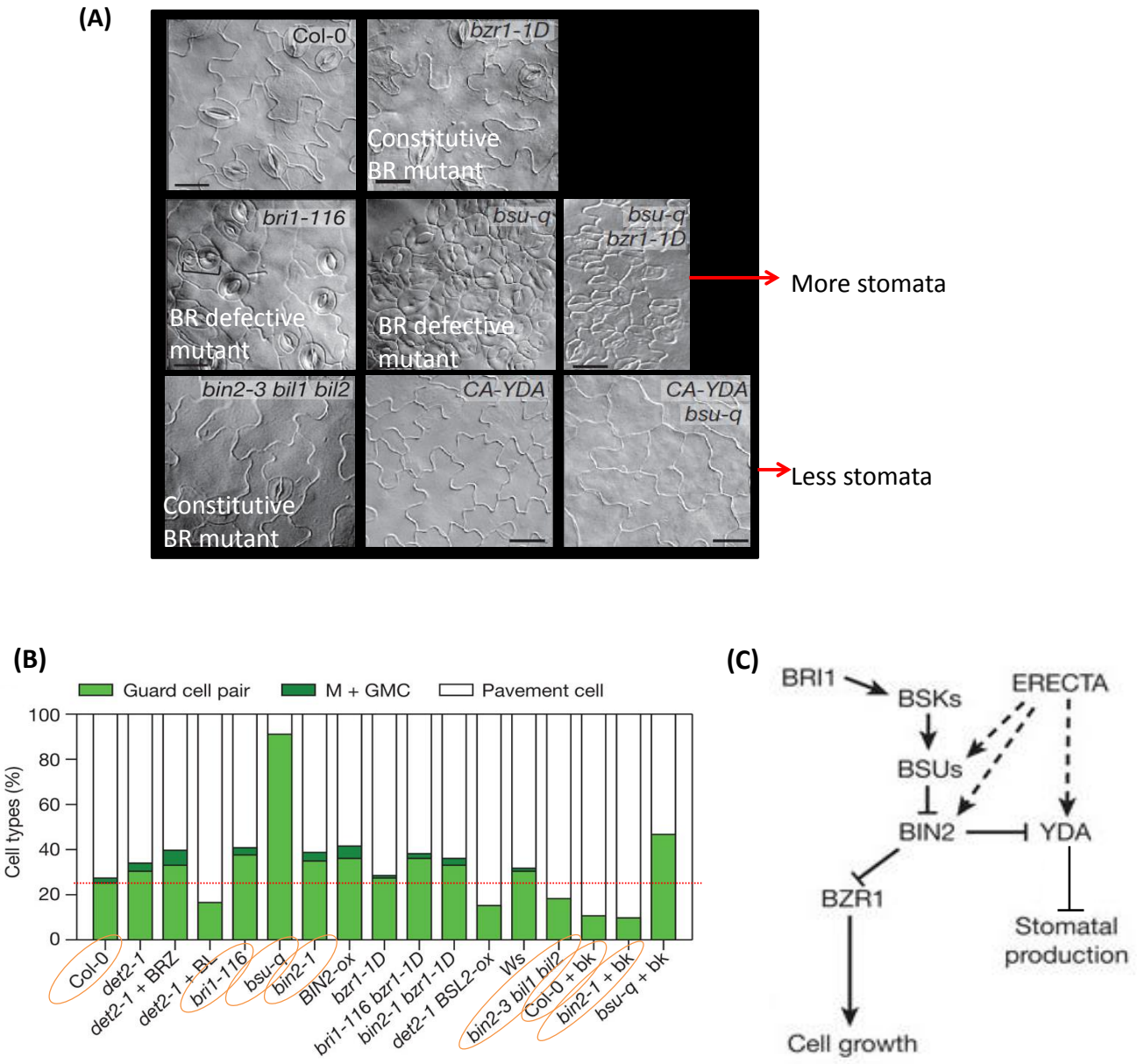

Figure 3.2 Brassinosteroids inhibit stomata development through regulation of BIN2 activity on the MAPKKK YODA

(A) Brassinosteroid defective mutants display higher density of stomata, while constitutive brassinosteroids mutant present less stomata compared to WT. Differential interference contrast microscopy (DIC) of abaxial cotyledons epidermis of 8 days old seedlings. Bar = 50µm. **(B)** Quantification of epidermal cell types of 8 days old seedlings, expressed as percentage of total cells. GMC: guard mother cell, M: meristemoids. **(C)** Model of stomatal development regulation by the BR pthway. When BIN2 is active, it phosphorylates YODA (YDA) to inhibit stomatal development. Adapted from (Kim et al., 2012)

Interestingly, the excess stomata number in *bsu-q* can be suppressed by the expression of a constitutively active YODA (CA-YDA) but not by the gain of function mutant *bzr1-D* whose stomata number appears normal (Figure 3.2A,B) suggesting that the stomata formation is independent to *BZR1* activity. Moreover, BIN and YODA interact *in vitro* and *in vivo* indicating a direct repression of YODA activity by BIN2 to induce stomata formation. To summarize, the brassinosteroid pathway inhibits stomata development through the direct regulation of the MAPKKK YODA by BIN2, another example of brassinosteroid pathway hijack (Kim et al., 2012) (Figure 3.2C).

3.2.2 Root hair formation is inhibited by brassinosteroids

Root hair formation can be predicted even before hair formation. Hair cells (H), or trichoblast cells, are adjacent to two cortical cells while non-hair cells (NH), atrichoblast cells, lie over a single cortex cell. The cell fate is thus determinated by positional cues involving non-autonomous cell signals (Grierson et al., 2014).

In molecular point of view, epidermal cell fate is dependent to a non-cell-autonomous regulatory system involving transcription factors able to move from N cell to NH cell (and reciprocally). NH or H identity is mainly dependent to *GLABRA2 (GL2*) gene expression that is induced by the transcription factors complex WER-GL3-TTG1 (respectively corresponding to WEREWOLF, GLABRA3, TRANSPARENT TESTA GLABRA1) (Figure 3.3). *GL2* is expressed in NH cell to confer a hairless cell fate. In absence of GL2, by default, cells acquire H cell fate (Figure 3.3A and 3.4) (Ishida et al., 2008; Grierson et al., 2014).

Actually, H cell fate is induced by CAPRICE (CPC). *CPC* is expressed in NH cell and moves to H cell to compete with WER forming a CPC-EGL3-TTG1 complex in H cell and inhibit GL2 expression (Figure 3.3). EGL3 is a GL3 homologous protein: ENHANCER OF GLABRA3. Although GL3 accumulate in the N position, both *GL3* and *EGL3* genes are preferentially transcribed in H position suggesting a migration of GL3 from H to NH cells (Grierson et al., 2014).

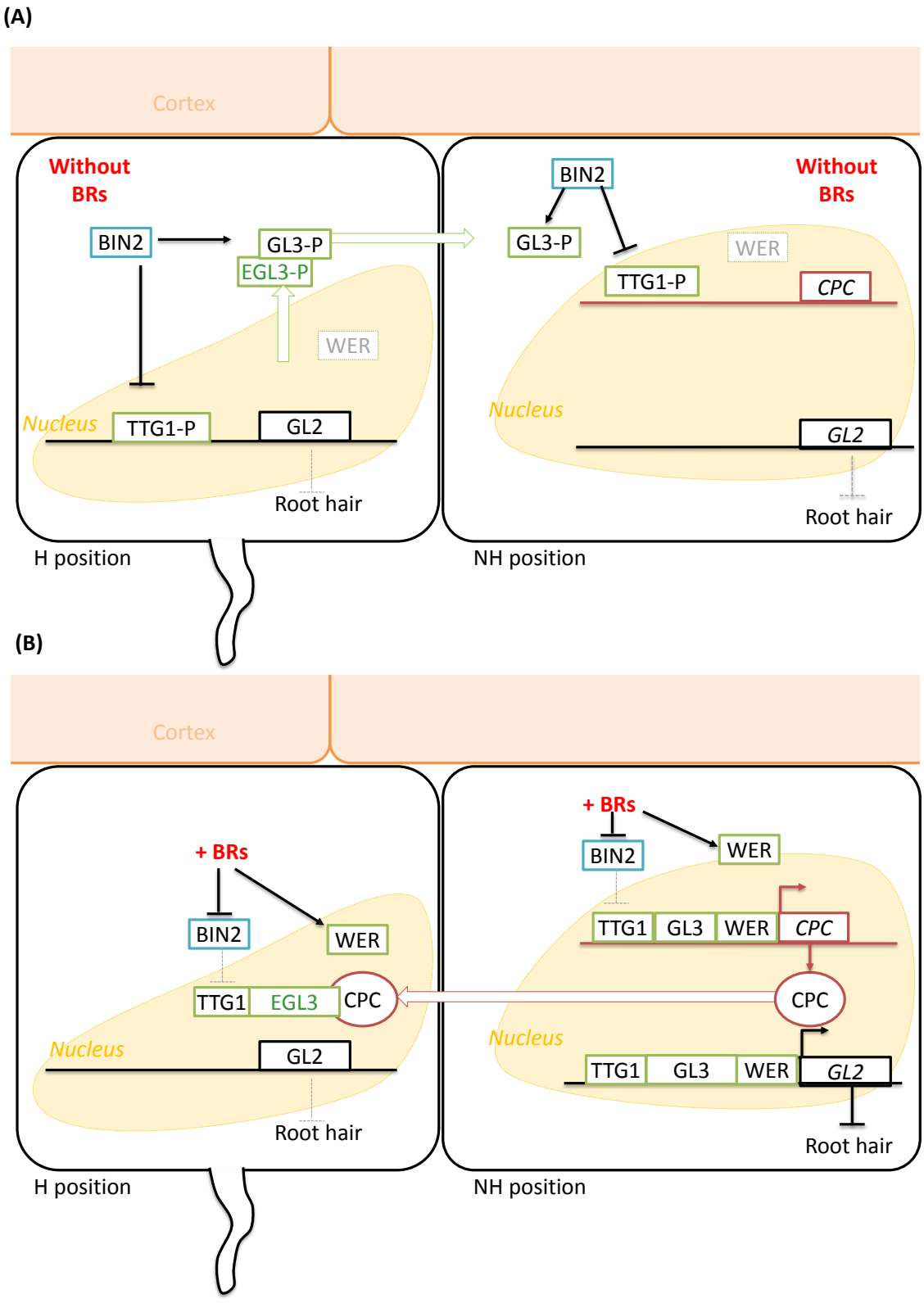

Figure 3.3: Model presenting the brassinosteroid control on cell fate determination in root epidermis
(A) In absence of brassinosteroids, BIN2 is active and represses the pathway through phosphorylation of TTG1. **(B)** In presence of brassinosteroids, BIN2 is inactivated allowing the formation of the TTG1/GL3/WER complex in NH cells to induce the transcription of *CPC* and *GL2* which inhibit root hair formation. Movement CPC proteins to H cells creates a compete with WER and repress the formation of TTG1/EGL3/WER complex blocking the expression of GL2 allowing root-hair formation. Dotted grey line: event does not occur. Black continuous line: event occurs. Thick arrow: protein movement.

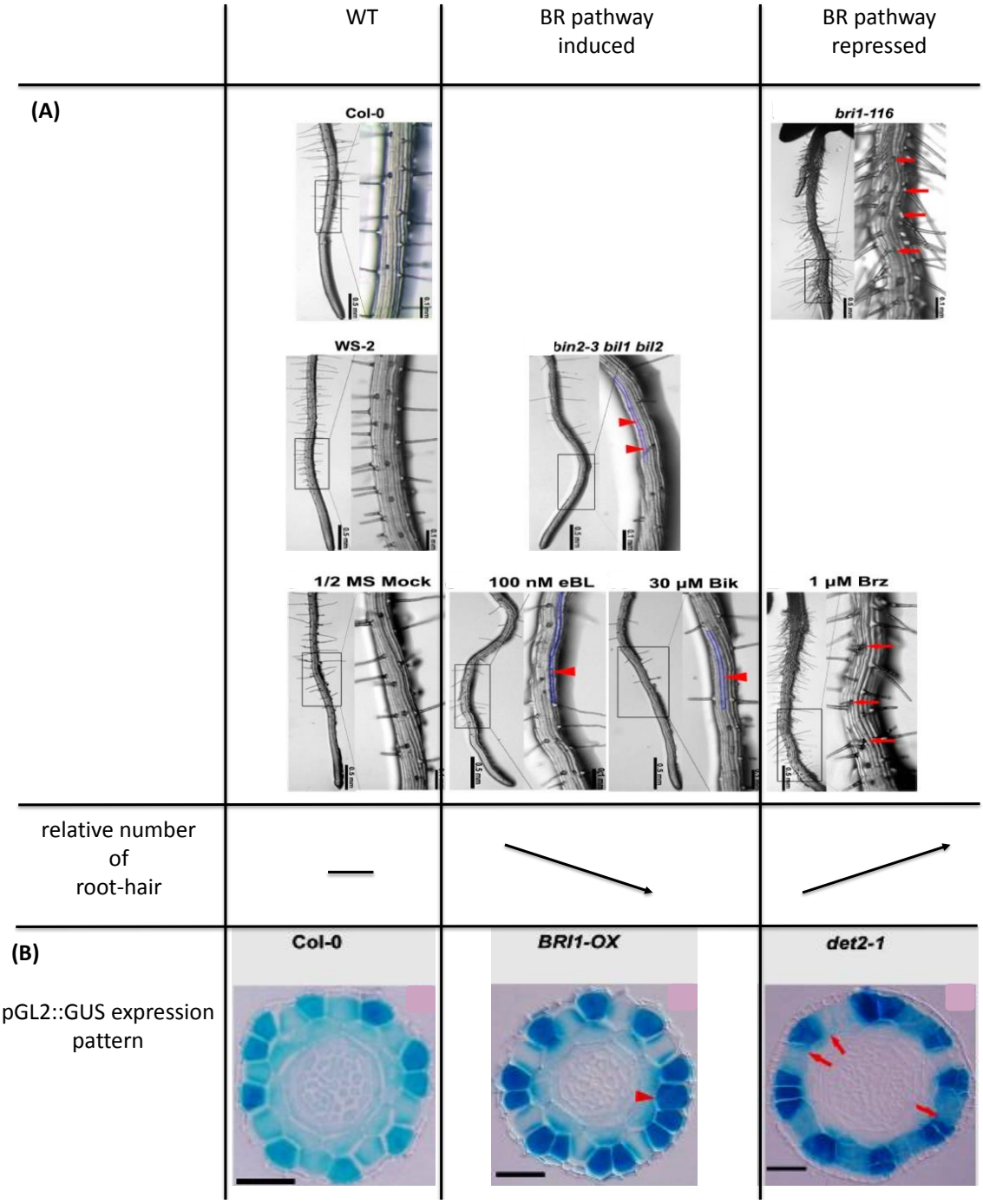

Figure 3.4: Brassinosteroids inhibit root-hair formation
(A) Root hair phenotypes in WT, BR defective mutants, BR constitutive mutants and in response to pharmacological treatments. Right images are the magnified areas shown in the left picture. Arrows: ectopic root-hairs and arrowheads: ectopic non-hairs cells. **(B)** pGL2::GUS expression pattern in BR-defective det2-1 and BR-constitutive BRI-OX transversal section of root meristem. Bar = 25µm. Red arrows: NH cells without pGL2::GUS; Arrowheads: H cell with ectopic pGL2::GUS. Adapted from (Cheng et al., 2014)

It has been shown that phytohormones control epidermal cell fates in the root. Abscissic acid inhibit hair root formation whereas ethylene and auxin promotes their formation (Ishida et al., 2008).

In brassinosteroid defective mutants such as *bri1-116*, *det2* or *cpd*, the number of H cells is increased, correlating with a decrease of GL2 expression in those mutants (Figure 3.4) (Cheng et al., 2014). On the contrary, constitutive brassinosteroid response mutants, such as *BRI1 overexpressor* or *triple GSK3 mutant,* display less H cells, consistent with the ectopic expression of GL2 in H position (in WT GL2 is restricted to NH cells). Those data suggest that brassinosteroids could induce NH cell fate and inhibits H cell fate (Cheng et al., 2014). Genetic analysis proposes that the early brassinosteroid signaling pathway acts upstream to the transcription factor complexes (WER-GL3-TTG1 and CPC-EGL3-TTG1) (Figure 3.3). Furthermore, proteins interaction coupled to phosphorylation analysis show that GSK3s are able to interact with EGL3 and TTG1 to phosphorylate them. GSK3 also interacts with WER but cannot phosphorylate it. Finally, GSK3 do not interact with CPC. EGL3 phosphorylation by GSK3 promotes EGL3 movement from nucleus of H cell to their cytosol. Phosphorylation of TTG1 by GSK3 suppresses WER-GL3-TTG1 activity (Cheng et al., 2014).

To summarize, in absence of brassinosteroids (Figure 3.4A), BIN2 is active, WER expression decreases. EGL3 and GL3 are phosphorylated and accumulate in the cytosol. TTG1 phosphorylation inhibits its activity. Thus, there is less formed WER-GL3/EGL3-TTG1 complex and their activities are reduced. In the presence of brassinosteroids (Figure 3.4B), BIN2 is repressed, EGL3 movement is inhibited, and WER expression is induced. WER-GL3-TTG1 activity is promoted, inducing GL2 and CPC expressions in NH position. CPC moves to H position, where it accumulates to form CPC-EGL3-TTG1 complex, unable to induce GL2 expression and by default giving an H fate.

3.3 Tissue scale: vascular tissues patterning

Brassinosteroid involvement in vascular tissues formation was first revealed on *Zinnia* explants, more particularly on the differentiation of tracheary elements (Iwasaki and Shibaoka, 1991). Effects of brassinolide and uniconazole (a steroid inhibitor (Iwasaki and

Shibaoka, 1991)) were evaluated by the number of differentiated cells after 54h of treatments (Figure 3.5A). Uniconazole treatment inhibits treachery cells differentiation but is counteracted by brassinolide (Figure 3.5A). Then, measurements of xylem differentiation markers confirmed the earlier study and permitted to conclude on the positive effect of brassinosteroids during xylem differentiation (Yamamoto et al., 1997). Several studies revealed vascular tissues defects in brassinosteroid mutants (Figure 3.5B), but no one defined the roles of brassinosteroid in vascular development (Szekeres et al., 1996; Li et al., 1996; Mora-García et al., 2004).

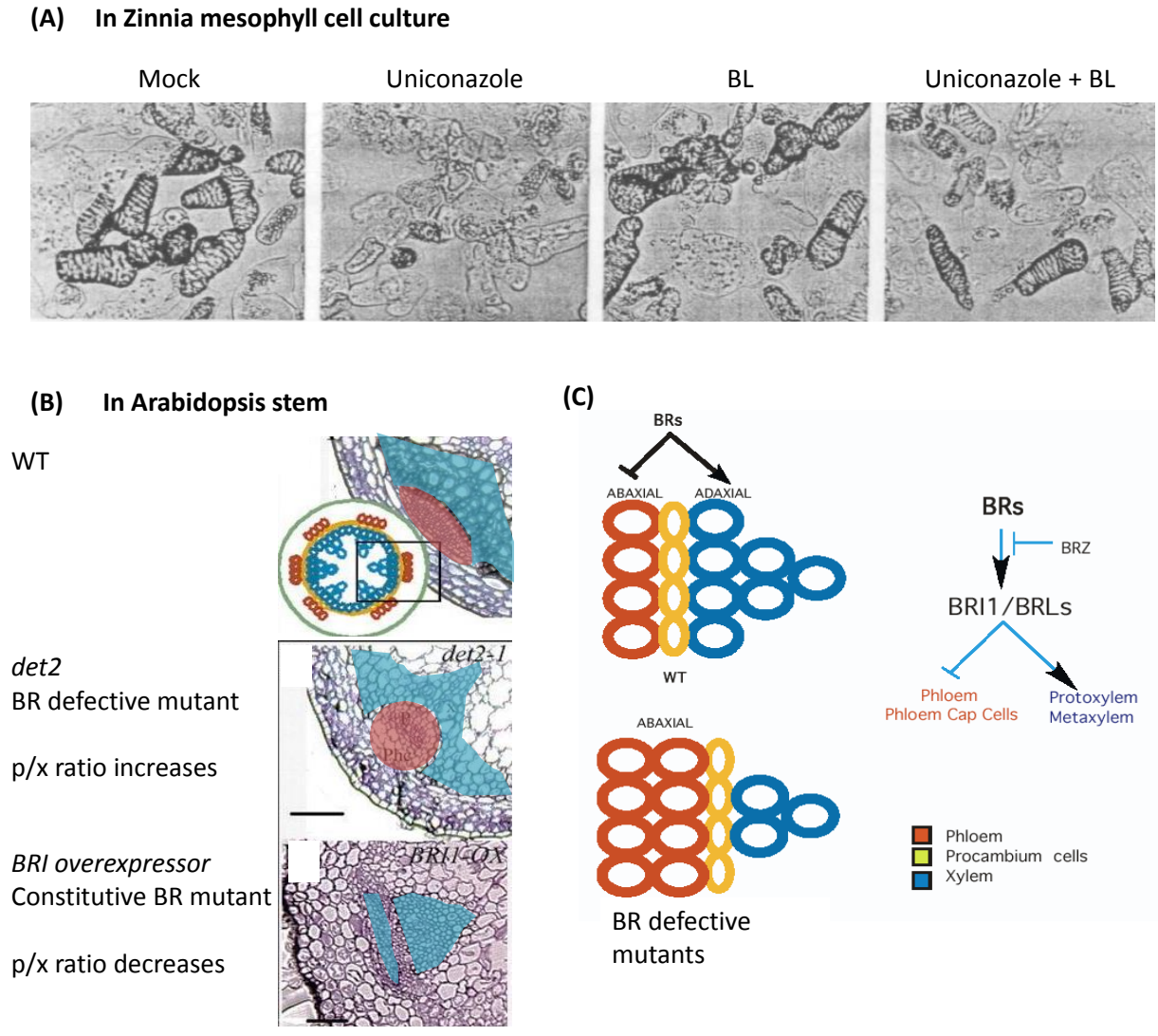

Figure 3.5: Brassinosteroids involvement during vascular differentiation
(A) Brassinosteroids induce xylem differentiation in *Zinnia elegans* mesophyll cell culture. Cells are treated with or without 3,4µM uniconazole (a synthetic plant growth retardant) and 2µM brassinolide. Adapted from (Iwasaki and Shibaoka, 1991) **(B)** Examples of brassinosteroids mutants affected in vascular patterning. p/x: phloem/xylem ratio; red: phloem; Blue: xylem; bar = 20µm. **(C)** Brassinosteroids modify xylem/phloem ratio in favor to xylem. Model of brassinosteroids effects on vascular patterning in Arabidopsis stem.
(B and C) Adapted from (Caño-Delgado et al., 2004)

In their study, Caño-Delgado et al. (Caño-Delgado et al., 2004) identified three *BRI1* homologous: *BRL1, BRL2* and *BRL3* and described their involvement during vascular differentiation. Contrary to *BRI1* that is expressed in the whole plant, *BRL1* and *BRL3* expression patterns are restricted to vascular tissues. Compared to wild type*, brl1* mutant shows an increase of phloem and a decrease of xylem proportions suggesting that *brl1* is involved in xylem/phloem differentiation (Caño-Delgado et al., 2004). These data are consistent with the known brassinosteroid-defective mutant *det2* that also exhibits a reduced xylem and an enlarged phloem (Figure 3.5B) (Li et al., 1996). In addition, *brl1 bri1-5 double mutant* displays strongest alterations in phloem compared to single mutant *brl1* and *bri1-5,* suggesting that the *BRL* and *BRI1* genes could function redundantly in phloem differentiation. In agreement with this hypothesis, *BRL1* and *BRL3* complement *bri1* mutant, BRL1 and BRL3 receptors bind brassinolide with high affinity and co-immunoprecipitation of BAK1/BRL3 showing that BRLs are also able to interact with BAK1 (Caño-Delgado et al., 2004; Fàbregas et al., 2013). Thus BRL1 and BRL3 were capable to induce brassinosteroid pathway in response to brassinosteroid signal.

In contrast to what is observed in *brl* mutant plants, *BRI overexpression* results in an increase of the xylem to phloem ratio (Figure 3.5B). Moreover, brassinosteroids could promote divisions of the procambial cells as observed in the stems of *BRI1 overexpressor* plants, where procambial tissue appeared to be enhanced compared with the wild type (Caño-Delgado et al., 2004).

By the way, collateral xylem/phloem ratio is controlled by the TRACHEARY ELEMENT DIFFERENTIATION INHIBITORY FACTOR / TDIF RECEPTOR (TDIF/TDR) complex that inhibits xylem differentiation and promotes meristematic activity of cambial cell (Cf §1.1.5). A recent study provides evidence for GSK3 involvement in this regulation (Kondo et al., 2014). Here, TDR interacts with GSK3 to deflect brassinosteroid pathway in favor to the repression of xylem differentiation inhibition.

In conclusion, collateral xylem/phloem pattern organization implies LRR-RLK leucine rich repeat receptor like kinase (BRI1, BRL1, BRL3 and TDR) to control the balance between xylem differentiation or cell proliferation. Activation of brassinosteroids signaling pathway

leads xylem differentiation whereas its inhibition through TDIF/TDR/GSK3 induces cell proliferation principally by inhibiting xylem cell differentiation.

3.4 Organ scale: brassinosteroids induce both division and differentiation in Root Apical Meristem

In their study, González-García et al. (González-García et al., 2011) observed a decrease of the root size in both brassinosteroid defective and constitutive mutants (Figure 3.6A). Enhanced brassinosteroid signaling through treatment with 4 nM brassinolide induces a reduction of root length compared to wild type (Figure 3.6B). Only very low amounts of brassinolide have a positive effect on growth. Root length seems to be brassinolide dose-dependent. This increased root growth could result from a combined increase in cell number and cell elongation.

Brassinosteroids were described to promote cell elongation as evidence by cell length measurement of brassinosteroid defective mutant and constitutive brassinosteroid mutants. Indeed, *bri1-116*, affected in the pathway displays short cells whereas *bes1-D* presents longer cells compared to WT (Szekeres et al., 1996; González-García et al., 2011). However, only few amount of brassinolide has a positive effect on root growth. A strong induction of the brassinosteroid pathway (as observed in *bes1-D* or with 4nM of brassinolide treatments) leads to a reduction of root length compared to WT. This suggests that cell elongation is not the solely responsible factor of root growth. Effectively, mitotic activity also permits to induce root growth by increase of cell number. Interestingly, both *bri1-116* and *bes1-D* are affected in cell division in division zone of the tip root as evidence by the mitotic activity marker KNOLLE (Völker et al., 2001; González-García et al., 2011).

In root, mitotic activity is controlled by quiescent center that is described as a zone with low mitotic activity inducing cell division in adjacent stem cells (Bennett and Scheres, 2010). pWUSCHEL-RELATED HOMEOBOX 5 (WOX5):GFP is used as quiescent center cells marker. In *bri1-116* expression of pWOX5::GFP decreases whereas it is enlarged when brassinosteroid signaling pathway is induced (Figure 3.6D,E). This suggests that WOX5 expression is induced by the brassinosteroids signaling pathway, downstream of BRI1. Thus brassinosteroids positively control mitotic activity but also induces differentiation promoting cell elongation (Figure 3.6F) (González-García et al., 2011).

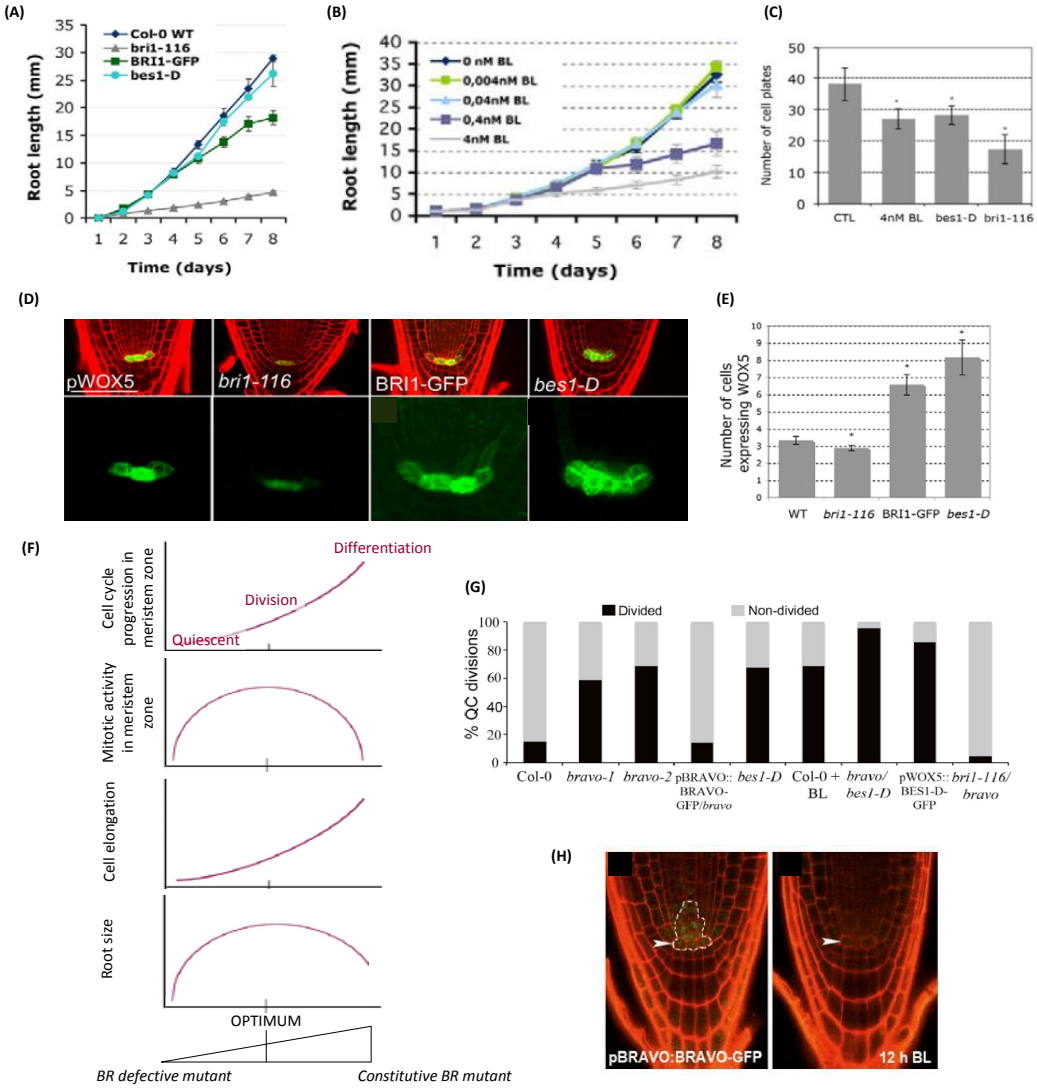

Figure 3.6: Brassinosteroids maintain meristem size through its interaction with BRAVO

(A) Modification in BR signaling alters root growth in both BR defective and constitutive BR mutants. Root-length of BR defective mutant *bri1-116*, and constitutive BR mutants *BRI1-GFP* and *bes1-D* seedlings compared with the wild type. Values represent the mean of 80 measurements of 6 days old seedlings ±s.d . **(B)** Root length of 6 days-old Col seedlings grown in increasing BL concentrations (from 0nM to 4nM). Values represent the mean of 30 measurements ±s.d. Concentrations of at least 0,4 nM BL were found to be sufficient to repress root growth. **(C)** Reduced cell plates number in roots treated with 4 nM BL treated Col-0 ($P<0.01$), and in *bes1-D* ($P<0.05$) and *bri1-116* mutants($P<0.001$). Asterisks indicate a statistically significant difference from the untreated Col-0 control. Values represent the mean of 10 measurements of number plates identified with KNOLLE immunolocalisation ±s.d. **(D)** Longitudinal view of 6-day-old root meristems counterstained with propidium iodide (top) and expressing the quiescent center marker pWOX5::GFP in different mutant backgrounds (bottom :green signal). Bar = 50µm. **(E)** Number of cells expressing pWOX5::GFP in different mutant backgrounds. Values represent the mean of 12 measurements ±s.d. **(F)** Graphical representation summarizing the dose-dependent effects of BR in root development at four levels:: cell cycle progression in meristem zone; mitotic activity in meristem zone; cell elongation; global phenotype resulting on the tree previous parameters. **(G)** Quantification of the QC divisions in 6-day-old roots expressed in percentage, (n > 50 seedlings for each genotype, (H) BRAVO is a nuclear transcription factor repressed after BL application. Six-day-old seedlings counterstained with propidium iodide. Bar = 25µm. (A-F) From (González-García et al., 2011). (G and H) From (Vilarrasa-Blasi et al., 2014)

The BRAVO gene could control this balance (Vilarrasa-Blasi et al., 2014). BRAVO is a R2R3-MYB transcription factor. It has been identified as a BES1 and BZR1 target enriched in the vascular initials and quiescent centers. In the *bravo* mutant, the division rate in the quiescent center is increased, as observed in the brassinosteroid constitutive mutant *bes1-D* (Figure 3.6G). In the *bri1-116 bravo* double mutant, there is no more cell division, whereas there is a stronger mitotic activity in the *bravo bes1-D* double mutant than in the simple mutants. Interestingly, an ectopic expression of *BRAVO* induces a shortening of the root and a decrease of the cell cycle activity in quiescent center (Figure 3.6G). These data suggest that BRAVO is a negative regulator of quiescent center mitotic activity upstream of BRI1 and counteracts the brassinosteroid effect that induces quiescent center division.

While *BRAVO* and *BES1* are expressed in the same cell they regulate antagonist effect to control meristem optimum activity: quiescent center divisions are repressed by *BRAVO* but are induced by *BES1.* At first, BES1 regulates the E-box of BRAVO promoter to repress BRAVO activity as confirmed by brassinolide treatment that reduces BRAVO gene activity (Figure 3.6H). Therefore, a feedback loop between division, BRAVO and brassinosteroids action has been proposed. On the other hand, overexpression of BRAVO in a *bes1-D* background suppresses the division phenotype of *bes1-D* mutant*;* BRAVO interacts in nucleus with the dephosphorylated (and active) form of BES1 mutant. All together these data provides cues for a negative repression of BRAVO on active BES1 (Vilarrasa-Blasi et al., 2014).

To conclude, the shortness of brassinosteroid defective mutant is a consequence of a decrease of cell elongation coupled to an altered mitotic activity caused by a diminution of quiescent center size. In the quiescent center, the brassinosteroids induce cell division but this activity is repressed by BRAVO to restrict quiescent center size to a few cells. In *bes1-D* mutant, the size of quiescent center is enhanced suggesting a modification of the BES1/BRAVO balance. However, the mitotic activity in division zone of *bes1-D* mutant is decreased. Brassinosteroids have an ambivalent behavior: they promote division in quiescent center and induce differentiation of distal cells that quickly exit from cell cycle explaining the duality in *bes1-D* mutant. Brassinosteroids regulate the division/differentiation balance in meristem to maintain an optimum meristem size for root growth: a struggle between renewal and differentiation.

4 *OCTOPUS* gene and thesis objectives

The *OCTOPUS* (*OPS*) gene has been isolated from a promoter trap screen (Bauby 2007) to identify new component involved in protophloem formation. Thus, five protophloem differentiation (PD) markers were isolated, including OPS (PD5) (Bauby et al., 2007).

OPS is initially expressed in provascular cells, then restricted to phloem initial cells and later to sieve elements (Figure 4.1A). The gene encodes a protein of unknown function. It belongs to a multigenic family of five members that all share a same domain of unknown function the DUF740 domain. OPS is a polar membrane associated protein accumulating at the apical pole of the cells (Nagawa et al., 2006; Bauby et al., 2007; Truernit et al., 2012; Benschop et al., 2007).

The *ops* mutant displays a short root (Figure 4.1B) and numerous phloem development defects resulting on stochastic phloem differentiation in root and difficulties in establishment of vascular pattern in cotyledons characterized by a reduction of the number of vascular loops (Figure 4.1C) (Truernit et al., 2012). In *ops* root phloem, some cells escape the phloem differentiation process and have reduced elongation, no thickening of wall (Figure 4.1C), callose deposit and nuclei persistence (Figure 4.1D). In these cells, we can also notify absence of expression of PD1, another protophloem marker (Figure 4.1E). Moreover, in *ops* mutant phloem transport is affected as evidence by pAtSUC2::GFP marker producing a soluble GFP under the control of a companion cells specific promoter (Truernit et al., 2012). Indeed, in *ops* mutant, the GFP signal seems to have difficulties to be transported.

Furthermore, overexpresion of *OPS* leads to an opposite phenotype to the one observed in *ops* mutant (Figure 4.1C). *OPS* overexpression induces to a more complex vascular pattern in cotyledons, with an increase in the number of vascular loops and late phloem differentiation in root. These data suggest that *OPS* could control phloem differentiation (Truernit et al., 2012).

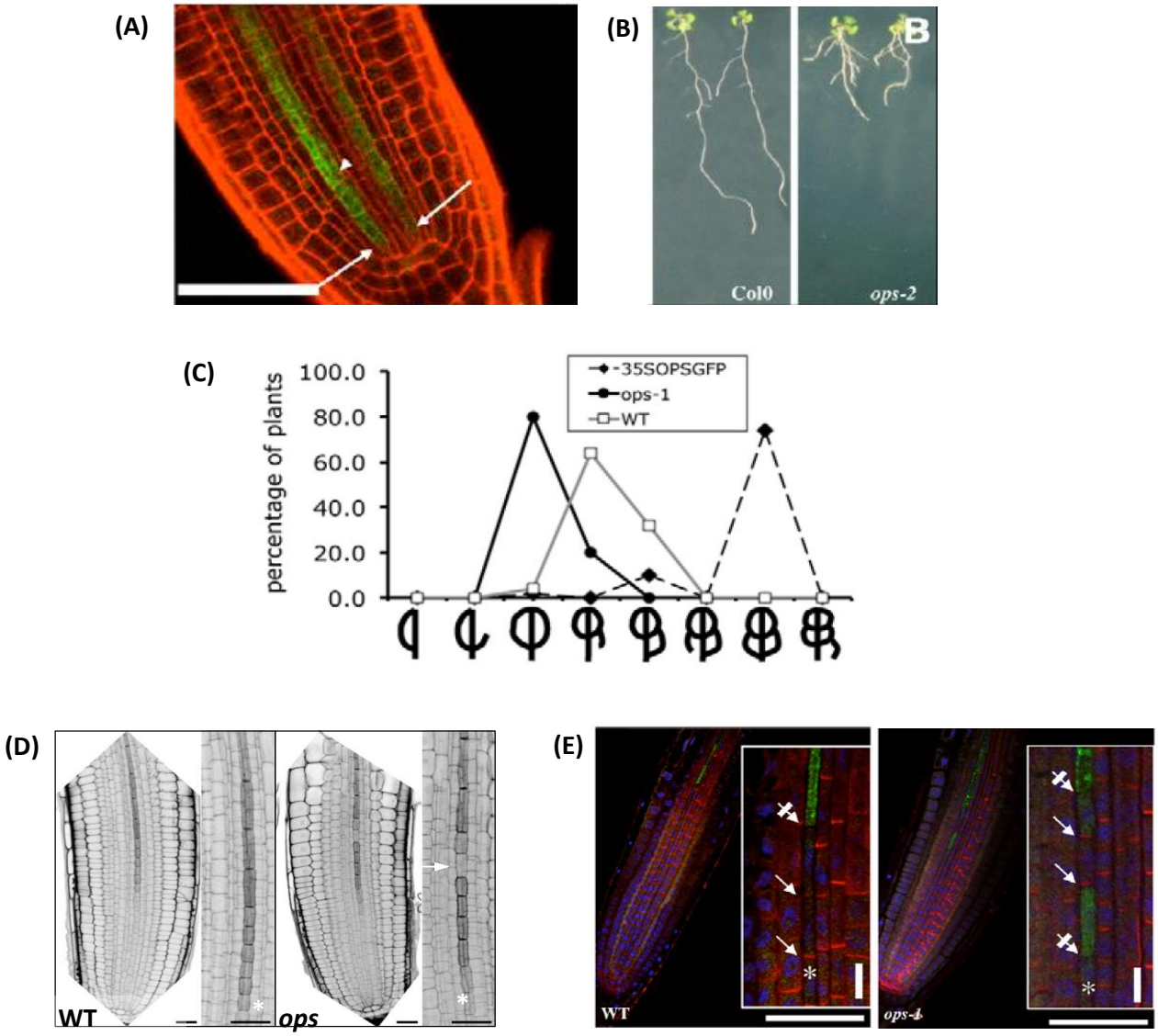

Figure 4.1: *OCTOPUS* gene and its corresponding mutant presentations
(A) Expression of pOPS:OPS-GFP$_{ER}$ in phloem cell files of 5-days-old root seedling. Arrows: phloem initials; arrow head: asymmetric division of provascular cells. Bar = 10µm. **(B)** *ops* mutant displays a short root compared to WT. (10 days-old light-grown seedlings). **(C)** *ops* and OPS overexpressor display opposite phenotype. Percentage of cotyledons of mature embryo displaying the indicated phenotype. N=50. **(D)** Identification of gap (white arrow) within the phloem cell file (star). Propidium iodide staining of 7 days-old seedlings. Bar = 20µm. **(E)** *ops* mutant display stochastic phloem differentiation in 5 days-old root compared to WT. Red: immunolocalisation of PIN1; green: pPD1::GFP$_{ER}$ marker; blue: DAPI staining; asterisk: phloem file; arrow: PIN1; crossed arrow: disappearance of PIN1. bar = 100µm; 20µm for insets. (A-C, E) From (Truernit et al., 2012)

To summarize, we know few things about OPS. It is an associated membrane protein that is accumulated at the apical pole of early differentiating phloem precursor cells. OPS is implicated in vascular patterning and induces phloem differentiation.

Recent data on suppressor screen of *brx* mutant isolated *ops* gain-of-function allele suggesting that OPS acts downstream to BRX. The set OPS/BRX that induces phloem differentiation is counteracted by CLE45/BAM3 module that inhibits phloem differentiation by inhibition of essential periclinal division for phloem differentiation (Figure 4.2) (Rodriguez-Villalon et al., 2014).

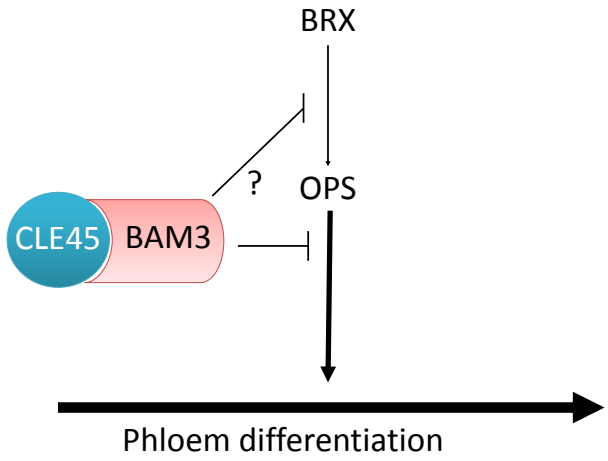

Figure 4.2: OPS involvement in phloem differentiation framework

However, many questions remain to be elucidated:

What is the molecular function of OPS and its DUF740 domain?

How and why is OPS protein targeted to the membrane? And why is it polar?

What is the biological role of the OPS-LIKE *proteins? Are they functionally redundant with OPS?*

In this context, the goal of my thesis was to better understand the molecular function of OCTOPUS-related proteins. I focused my work on the clade of three genes composed of *OPS, OPSL1 and OPSL2*. Using pharmacological, genetic, molecular, biochemical and cytological approaches, I characterized *OPS* as a positive regulator of the brassinosteroid signaling pathway. The study of *OPSL1* and *OPSL2* suggest that those OPS-related proteins may serve similar function in different cell types.

RESULTATS

PARTIE 1:

OCTOPUS UN NOUVEAU MEMBRE DE LA VOIE DES BRASSINOSTEROIDES

1 OCTOPUS positively regulates brassinosteroid signaling pathway to control phloem differentiation in *Arabidopsis thaliana*

ANNE Pauline, AZZOPARDI Marianne, BEAUBIAT Sébastien, GISSOT Lionel, (FAURE Jean-Denis), HEMATY Kian & PALAUQUI Jean-Christophe

INRA, Institut Jean-Pierre Bourgin, UMR 1318, ERL CNRS3559, Saclay Plant Sciences, RD10, F-78026 Versailles, France

AgroParisTech, Institut Jean-Pierre Bourgin, UMR 1318, ERL CNRS3559, Saclay Plant Sciences, RD10, F-78026 Versailles, France

This work will be submitted to Current biology, for a report format.

1.1 Summary

The OCTOPUS (OPS) protein is a polar membrane associated protein, expressed in provascular cells and then restricted to phloem. The *ops* mutant displays a short root, an altered vascular network in cotyledons and an intermittent phloem differentiation in root. Here, we present OPS as a positive regulator of the brassinosteroid (BR) pathway. OPS overexpressing lines show phenotypes reminiscent of constitutive BR mutants (elongated petioles and hypocotyl, twisted cotyledons). Moreover, OPS-OE lines are insensitive to both brassinolide and brassinazole treatments suggesting OPS acts at the signaling level. Analysis of BR molecular responses confirms that BR signaling is induced upon OPS overexpression. Genetic analysis reveals epistatic relationship between OPS and BR signaling components suggesting a role for OPS in BR signaling downstream of BRI1 and upstream of BZR1 and BES1. Directed protein interactions between OPS and known BR signaling components identified BIN2 as a potential partner of OPS. Finally we provide evidence that BR signaling is required for correct phloem differentiation. Together our results suggest a role for *OPS* as a new positive regulator of BR signaling pathway necessary for phloem differentiation.

Key words: OPS, phloem, BIN2, Arabidopsis thaliana, Brassinosteroids

1.2 Results

OPS-OE transgenic lines display phenotypes of brassinosteroid constitutive response

OPS is involved in phloem differentiation (Bauby et al., 2007; Truernit et al., 2012), however its exact role in this process remains unclear. To gain insight into its function, we overexpressed OPS-GFP in *Arabidopsis thaliana* Columbia plants. Most of the lines carrying p35S::OPS-GFP construct displayed elongated hypocotyls and petioles and curly cotyledons and leaves together with GFP expression (Figure 1A). Among them, we selected a monolocus transgenic line that displayed a reproducible phenotype during the first two weeks of growth for further investigation and called it OPS-OE in this manuscript. These phenotypes were reminiscent of those observed in mutants with strong constitutive BR response such as *bes1-D* plants (Yin et al., 2002, 2005) (Figure S1A). Furthermore, OPS-OE phenotype could be mimicked in WT seedlings grown on Arabidopsis medium containing 1 µM of brassinolide (BL), the most active form of BRs (Mitchell et al., 1970; Mitchell and Gregory, 1972; Grove et al., 1979) (Figure 1A,B) or 50 µM bikinin, a GSK3 specific inhibitor that constitutively induce BR signaling pathway (De Rybel et al., 2009) (Figure S1B,C). These results suggest that the OPS-OE line could constitutively activate the BR pathway.

In order to investigate the BR signaling level in the OPS-OE lines, we checked the phosphorylation status of BES1 protein, a key transcription factor involved in the transcriptional response of BR (Yin et al., 2002, 2005).

BRs are perceived at the plasma membrane by the BRI1 receptor kinase (BR INSENSITIVE 1, (Li and Chory, 1997; He et al., 2000)). In absence of BRs, the pathway is repressed by BIN2 (BR INSENSITIVE 2) a glycogen synthase kinase 3 (GSK3, (Li et al., 2001; Li and Nam, 2002)) that phosphorylates BES1 (BRI1-EMS-SUPPRESSOR 1) and BZR1 (BRASSINAZOLE-RESISTANT 1) transcription factors to induce their degradation and prevent their accumulation in the nucleus (Figure 1D) (Yin et al., 2002; Wang et al., 2002; He et al., 2002) In the presence of BRs this repressive mechanism is released through the inactivation of BIN2 by the phosphatase BSU1 (Mora-García et al., 2004; Kim et al., 2011, 2009). The active unphosphorylated forms of BES1 and BZR1 accumulate in the nucleus and bind their target genes to induce the BR cellular response such as cell elongation or a negative feedback on BR biosynthesis.

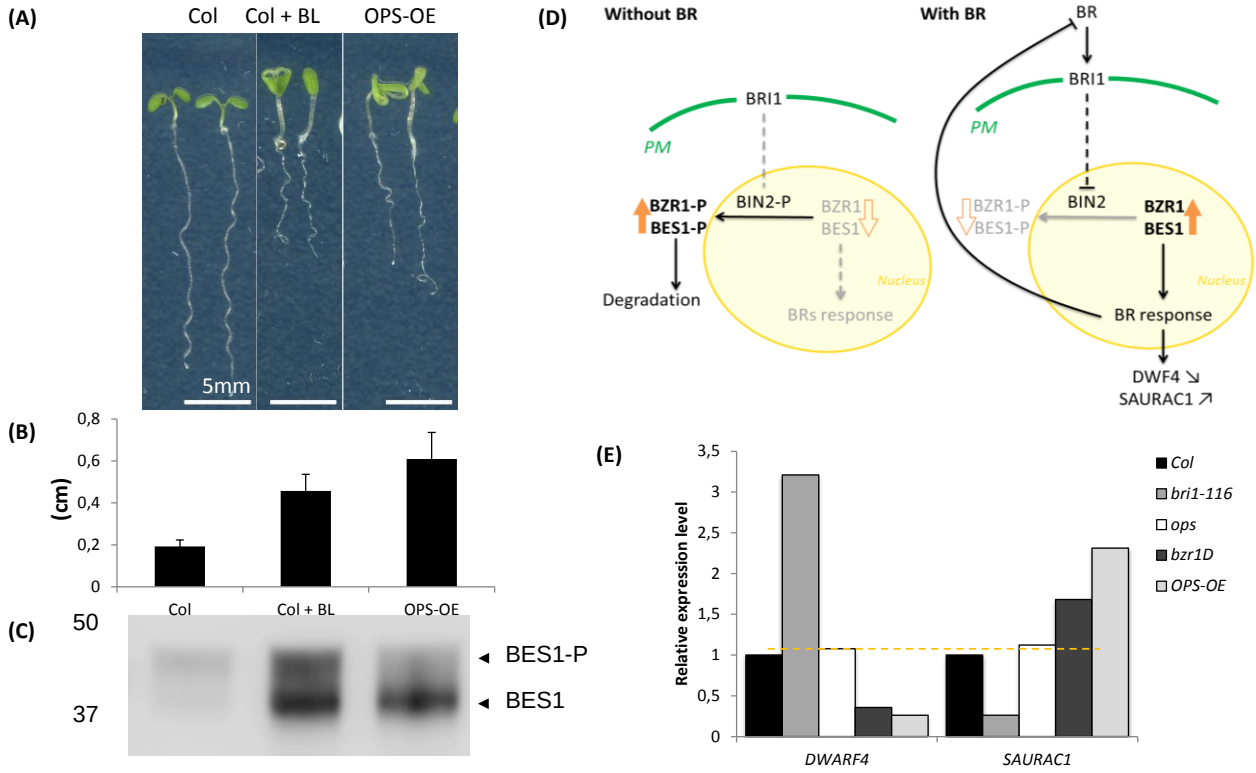

Figure 1: OPS-OE plants display a constitutive BR response.
(A-C) 7 days-old light-grown seedlings on arabidopsis medium 1% sucrose supplemented with or without 1 µM BL **(A)** OPS-OE phenotype is mimicked by BL treatment of WT seedlings. bar = 5 mm **(B)** Hypocotyl length of seedlings shown in (A) ; error bars represent SD, 30<n<40. **(C)** OPS-OE accumulates unphosphorylated BES1 protein as shown by Anti-BES1 western blot. **(D)** Simplified scheme of the BR pathway in absence (left) or presence (right) of BRs. In absence of BRs, BIN2 kinase is active and phosphorylates the two transcription factors BES1 and BZR1 that are unable to induce BR response. BRs are perceived by BRI1 receptor kinase at the plasma membrane and the signal is transduced inside the cell by a phosphorylation-cascade ultimately inhibiting the repressor BIN2. The subsequent accumulation of unphosphorylated forms of BES1 and BZR1 induces the BR response such as the negative feedback on the BR biosynthesis gene DWARF4 or the induction of cell elongation (correlated to SAUR-AC1 induction). **(E)** Transcripts level of *DWARF4* and *SAURAC1*, measured by RT-q-PCR on 7 days old seedlings of BR defective (bri1-116) or BR constitutive (bzr1-D) mutants compared to WT (Col)**.**

In WT plants, both phosphorylated and unphosphorylated forms of BES1 are detected by western blot (Figure 1C) indicating the versatile nature of this switch during development. When the pathway is activated by addition of BL in growth medium, WT plants mainly accumulate the unphosphorylated form of BES1 (Figure 1C). Similarly, the OPS-OE plants display an accumulation of the unphosphorylated form of BES1, even in absence of BL treatment, indicating a constitutive induction of BR signaling pathway in OPS-OE plants (Figure 1C).

To further assess the BR response in OPS-OE plants, we analyzed the expression level transcripts of DWARF4 *(DWF4)*, and of *SAURAC1* both regulated by BES1 and BZR1 (He et al., 2005; Yin et al., 2005; Vert and Chory, 2006). In BR defective mutants such as *bri1-116* (Li and Chory, 1997), *SAURAC1* is repressed whereas *DWF4* is strongly induced (Figure 1E). These genes are regulated in an opposite manner in constitutive BR mutant such as *bzr1-D* (Wang et al., 2002) (Figure 1E). In OPS-OE plants the level of BR transcriptional response is even stronger than in the constitutive mutant *bzr1-D*. In *ops* mutant, the transcript levels of *SAURAC1* and *DWF*4 were similar to WT plants (Figure 1E). *OPS* gene expression being restricted to the phloem, it is likely that *ops* mutation effect could have very little effect on global *SAURAC1* and *DWF*4 expression levels. Altogether, these results indicate that OPS-OE plants behave as constitutive BR mutants and activate BR-induced molecular and cellular responses.

OPS induces the brassinosteroid signaling pathway

The constitutive BR signaling observed in OPS-OE can either be the consequence of an increased BR biosynthesis or an activated BR signaling pathway. To discriminate between those two hypotheses, we conducted a pharmacological analysis of OPS-OE treated with BL or brassinazole (BRZ, a specific BR biosynthesis inhibitor, (Asami et al., 2000)). For this purpose, the OPS-OE line was compared to the *bzr1-D* mutant and WT plants.

In the presence of 2 µM BRZ in darkness, the hypocotyl length of WT plants is strongly reduced (almost 90% compared to non-treated plants, Figure 2A,B) while *bzr1-D* mutant is less sensitive to the treatment with a hypocotyl length that decreases only by 60%, a result which had led to the isolation of this mutant (*brassinazole resistant 1*, (Wang et al., 2002)). OPS-OE plants are almost insensitive to BRZ treatments with only 15% of growth reduction compared to non-treated plants (Figure 2A,B). In light conditions, WT plants treated with 1 µm BRZ exhibit a strong reduction of growth (Figure 2C) and a strong accumulation of the phosphorylated form of BES1 (Figure2D), whereas OPS-OE still display its BR-constitutive phenotype and mainly accumulates the BES1 unphophorylated form (Figure 2C,D).

In the presence of BL, WT plants display an increased hypocotyl elongation in light-grown seedlings (Figure 2C, S1D,E) whereas OPS-OE plants have a very slight increase suggesting that they are insensitive to BL treatment. Because OPS-OE is insensitive to both treatments, we conclude that OPS is a positive regulator of the BR signaling pathway.

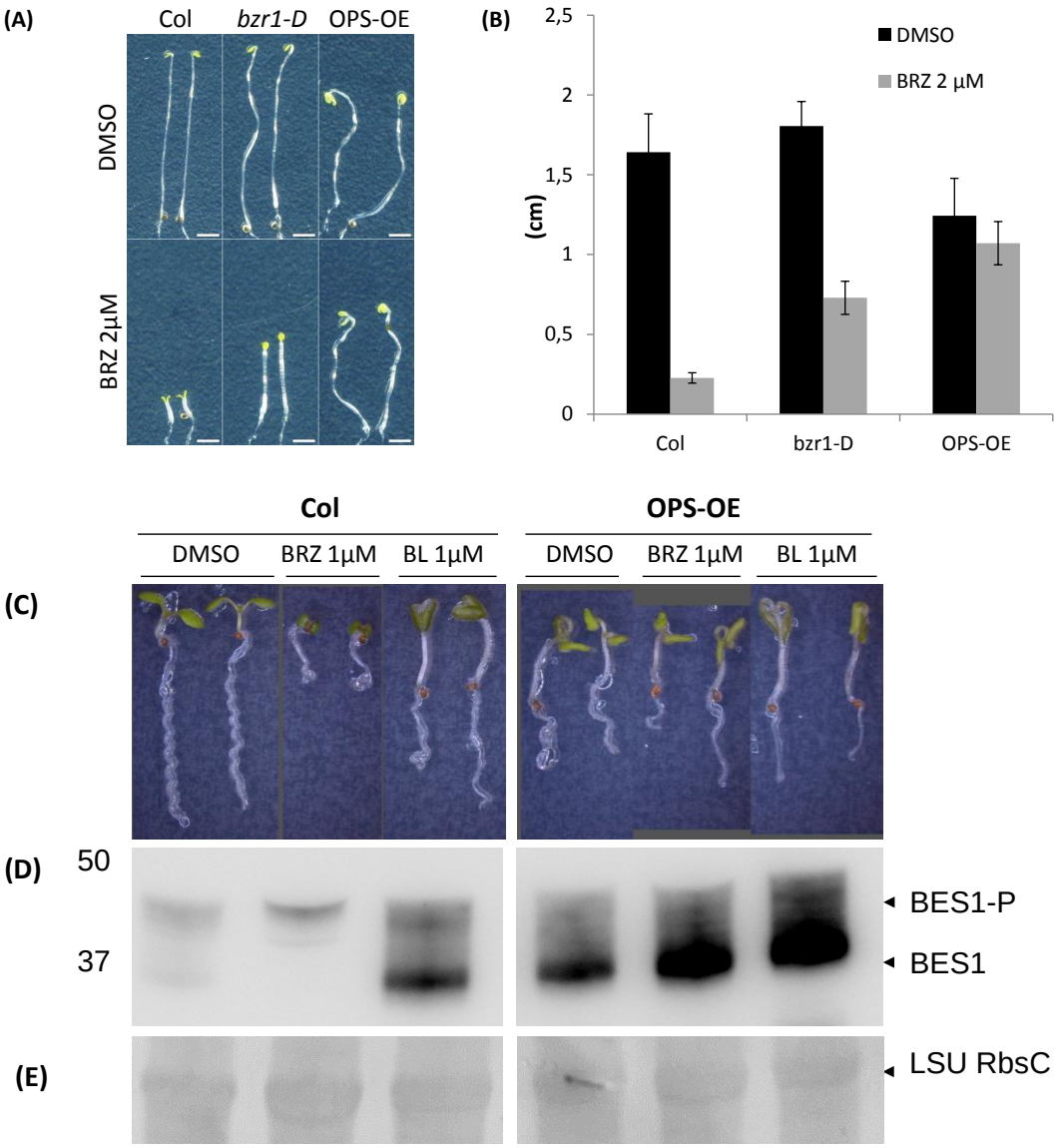

Figure 2 : OPS activates at the BR pathway at the signaling level
(A-B) 7 days-old dark-grown seedlings on arabidopsis medium without sucrose with or without 2µM BRZ **(A)** BRZ treatment inhibits hypocotyl elongation in darkness. OPS-OE is even less sensitive to BRZ treatment than *brzr1-D*. bar = 2mm **(B)** Corresponding hypocotyl length **(C)** 7 days old seedlings grown on arabidopsis medium supplemented with DMSO, 1% sucrose with or without 1µM BRZ/1µM BL **(D-E)** corresponding western blotting using **(D)** BES1 antibody **(E)** Coomassie staining as loading control (Large subunit Rubisco band)

OPS is epistatic to *BRI1* and *BIN2*

In order to specify *OPS* involvement in the BR signaling cascade, we analyzed the genetic interactions of *OPS* with genes of BR signaling components. Thus we crossed the OPS-OE plant into the BR insensitive mutants *bri1-116* (a strong loss-of-function allele, (Li and Chory, 1997)) and *bin2-1D* (a gain-of-function allele, (Li et al., 2001)). Those two mutants display typical phenotypes of BR defective mutants: short petioles and hypocotyl, dark-green round cotyledons and leaves (Figure 3A,B). Overexpression of *OPS* suppressed the dwarf seedling phenotype of *bri1-116* and *bin2-1D* restoring the elongation of petioles and hypocotyl (Figure 3A,B). This was confirmed by BES1 phosphorylation status, normally hyperphosphorylated in *bri1-116* and *bin2-1D* mutants, but becoming mainly unphosphorylated upon OPS overexpression (Figure 3C). These data suggest that OPS function is epistatic to these two components.

OPS interacts with BIN2 at the plasma membrane

These results would suggest that *OPS* is a positive regulator of the BR signaling pathway acting downstream of BRI1 and BIN2. However, BIN2 directly phosphorylates BES1 and BZR1 (Yin et al., 2002; He et al., 2002) and OPS-OE modifies the phosphorylation status of BES1 in *bin2-1D* suggesting OPS could directly inhibit BIN2 activity. To test this hypothesis, we studied a directed interaction between OPS and BIN2. Because OPS is an membrane associated protein, a yeast two-hybrid assay by split ubiquitin system (Stagljar et al., 1998) was performed to test OPS-BIN2 interaction which shown that OPS interacts with BIN2 in yeast (Figure 3E). Furthermore, Bimolecular Fluorescence Complementation (BiFC, (Desprez et al., 2007)) assays in *Nicotiana benthamiana* epidermal cells transiently co-expressing OPS fused to the N-terminal half of YFP (nYFP-OPS) and BIN2 fused to the C-terminal half of YFP (cYFP-BIN2) revealed an OPS/BIN2 interaction at the plasma membrane (Figure 3F). However, neither pavement cells co-expressing nYFP-OPS and BRI1-cYFP, nor BAK1-cYFP and OPS-cYFP showed any fluorescence signal (Figure 3F, S2).

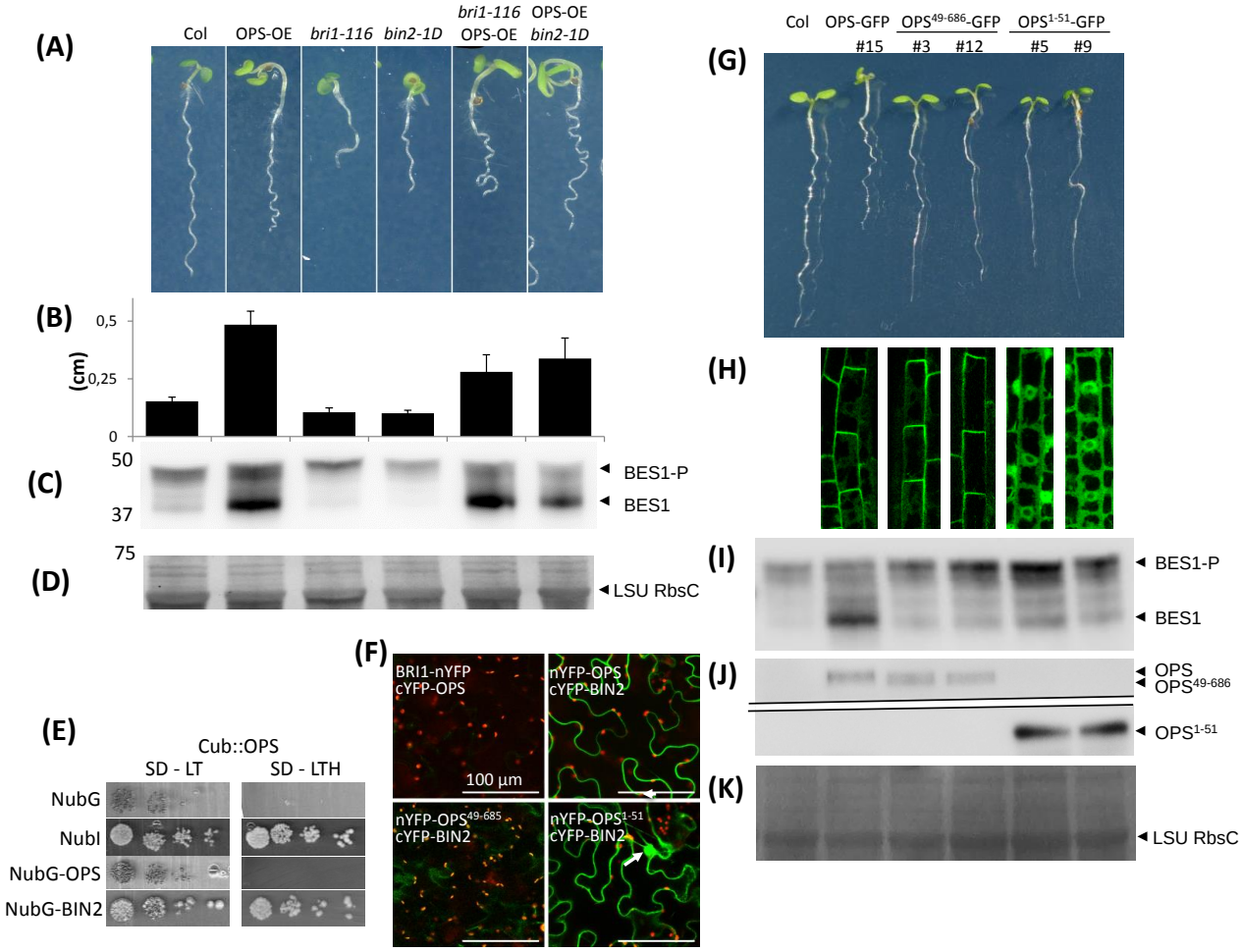

Figure 3: *OPS* is epistatic to *BRI1* & *BIN2* to control BR response

(A-D) OPS-OE suppresses *bri1-116* and *bin2-1D phenotypes* in 7 days old seedlings grown on arabidopsis medium 1% sucrose.**(A)** OPS-OE suppresses bri1-116 and bin2-1 growth defects **(B)** Hypocotyl length measurement of seedlings shown in (A) ; error bars represent SD, 20<n<30 .**(C)** Anti-BES1 western blotting OPS-OE restores accumulation of unphosphorylated BES1 in bri1-116 and bin2-1 **(D)** Coomassie staining of the blotted membrane is used as a loading control **(E-F)** OPS interaction with BIN2 in yeast and tobacco epidermal cells **(E)** OPS interacts with BIN2 in split-ubiquitin system in yeast. NubG and NubI are used as negative and positive control respectively. (SD-LTH + 25mM 3AT medium) **(F)** OPS and BIN2 interact at the plasma membrane. The 51 first amino acids of OPS interacts with BIN2 in the cytosol and in the nucleus (marked by an arrowhead and an arrow respectively). Interaction is visualized in split-YFP assay by confocal microscopy in epidermal cells of transiently transformed Nicotiana benthamiana epidermal cells. Green: YFP signal; red: autofluorescence; bar = 100µm. **(G-K)** Expression of truncated OPS protein able to bind BIN2 or the plasma membrane do not display the OPS-OE phenotype. **(G)** Phenotype of 7 days-old light-grown transgenic lines on arabidopsis medium 1%. **(H)** Subcellular localisation of GFP-fusions. **(I)** Phosphorylation status of BES1 in the corresponding transgenic lines monitored bi anti-BES1 western blotting **(J)** and expression level of GFP-fusion monitored by anti-GFP western blotting **(K)** Coomassie staining of the membrane is used as loading control.

Interaction with BIN2 and plasma membrane localization are required for OPS to positively regulate BR signaling

The interaction of OPS and BIN2 at the plasma membrane is contrasting to the biological activity of BIN2 which has been described as occuring mostly in the nucleus (Vert and Chory, 2006). What could be the biological function of OPS/BIN2 interaction at the plasma membrane?

It still remains unclear which mechanism is involved in OPS targeting to the plasma membrane as the protein does not possess any predicted transmembrane domains or GPI anchors. Nevertheless, bioinformatic analysis (CSSPalm, (Ren et al., 2008)) predicts palmitoylation sites in the OPS sequence at residues Cys31 (score: 0.435) and Cys46 (score: 0.898) (Figure S3A). Palmitoylation corresponds to the linkage of palmitate (a 16 carbon long fatty acid) on cysteine residues. Palmitoylation is involved in protein interactions, enzymatic activity regulation and in membrane protein targeting (Hemsley, 2014) and has been shown essential for membrane targeting of CDG1 (Kim et al., 2011). To verify a possible role of those cysteines in OPS targeting, truncated version of OPS were performed in fusion to the GFP (Figure S3B). The N-terminal domain containing the predicted palmytoylated cysteines has been fused to the GFP protein (OPS^{1-51}-GFP) or deleted from the full length protein (OPS^{49-685}-GFP) and overexpressed in wild type plants.

OPS^{1-51}-GFP is found soluble in both the cytosol and nucleus of plant cells (Figure 3H) while OPS^{49-685}-GFP is still present at the plasma membrane in a polar fashion like full length OPS-GFP. This suggests that the predicted palmitoylated cysteines are not necessary for OPS targeting and polarity at the plasma membrane. However, unlike OPS-GFP, OPS^{49-685}-GFP lines did not display the constitutive BR phenotype (Figure 3G,I) suggesting that the N-terminal domain of OPS is essential for its function. This deletion of the N-terminal domain could either alter the correct folding of OPS^{49-685} protein or its interaction with BIN2 preventing the activation of the signaling pathway. Indeed unlike OPS^{49-685}, the first 51 amino acids of OPS are sufficient to interact with BIN2 in a BiFC assay (nYFP-OPS1-51 + cYFP-BIN2, Figure 3F). The reconstitution of the YFP fluorescence reveals a nuclear and cytosolic interaction between OPS N-terminal domain and BIN2.

Similarly, transgenic lines overexpressing the soluble OPS^{1-51}-GFP do not display neither the subcellular localization nor the constitutive BR phenotype of OPS-GFP plants (Figure 3G-I),

suggesting that OPS targeting to the plasma membrane is also essential for OPS function. Altogether these results suggest that both the interaction with BIN2 and the plasma membrane localization are required for OPS to exert its positive effect on BR signaling.

Brassinosteroid signaling is involved in phloem differentiation

To investigate the possible role of OPS-mediated inhibition of BIN2 repression during phloem differentiation, BIN2 activity has been inhibited by bikinin treatment in *ops* mutants. The *ops* mutant displays a short root phenotype, less complex vascular pattern in cotyledons and defects in phloem differentiation in the root (Truernit et al., 2012).

In root, phloem differentiation can be detected with the progressive thickening of the cell wall concomitant with cell elongation (Figure 4A). While most of the WT plants did not display defects (80% on Arabidopsis medium supplemented with DMSO), in *ops* mutant two alterations with variable proportions can be found together representing 50% of altered roots: (1) 45% of phloem "gap" corresponding to an island of undifferentiated cells inside a differentiated phloem file, (2) 5% "overlap" corresponding to an unaligned phloem differentiated cell file (Figure 4A,B). Treatment of *ops* mutant with 25 µM of bikinin rescued *ops* phloem defects confirming that inhibition of BIN2 activity is necessary for correct phloem differentiation.

Beside its repression of the BR signaling pathway, BIN2 is known to regulate several signaling pathways including auxin or MAP Kinase signaling (Galvan-Ampudia and Vernoux, 2014). We wondered whether involvement of the BR pathway downstream of BIN2 is necessary for phloem differentiation. To verify this, *ops* was crossed with *bzr1-D* and *bes1-D* mutants activating BR responses downstream of BIN2.

Unlike *ops bes1-D, ops bzr1-D* double mutants rescued *ops* root growth defects suggesting that either only BZR1 transcriptional response is required for vascular differentiation or that the *bes1-D* genetic background (Enkheim-2) could somehow impact root growth (Figure 4C,D).

We assessed phloem defects rescue in *ops bzr1-D* and *ops bes1-D* roots. Both *bzr1-D* and *bes1-D* mutations permit to reestablish correct phloem differentiation in *ops* mutant (Figure 4E), supporting positive effect of BRs on phloem differentiation. However the number of vascular loops in *ops bes1-D* and *ops bzr1-D* mutants was similar to *ops* mutant, while WT,

bes1-D and *brz1-D* vascular loops were comparable indicating that this embryonic phenotype was not rescued (Figure S4). Taken together, these observations indicate a role for BR signaling through regulation of BIN2 activity on the transcription factors BES1 and BZR1 for the phloem differentiation process in the root.

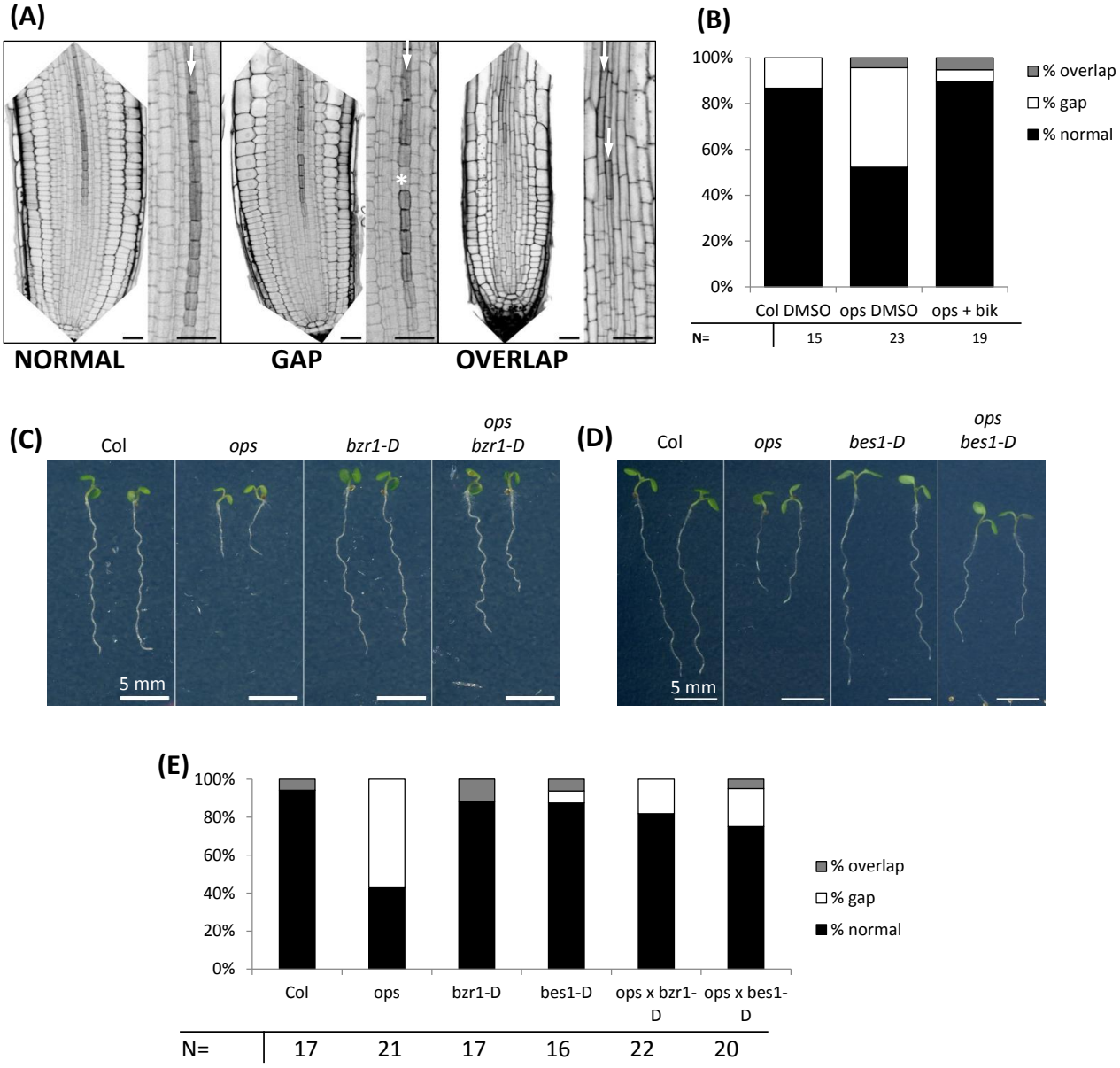

Figure 4 : Constitutive BR signaling restores *ops* phloem defects in root
(A) typical phloem phenotypes observed by confocal imaging with propidium iodide staining. Normal: a gradual thickening of the cell wall is observed with increased PI staining along the phloem cells file (arrow). Gap : undifferentiated cells identified by non-thickening of the cell-wall (asterisk). Overlap : phloem cells differentiation switches between adjacent cell files along the root. Bar = 20µm. **(B)** Bikinin treatment restores ops phloem defects. Percentage of roots presenting the phenotypes described in (A) in at least one of the two phloem cell files observed in roots of 7 days-old light-grown seedlings with or without 25 µM bikinin. N: number of roots observed. **(C)** *bzr1-D* restores *ops* root length of 7 days-old light-grown seedlings **(D)** but not *bes1-D*. bar= 5mm. **(E)** *bzr1-D* and *bes1-D* rescue ops phloem defects in roots. Quantification of phloem defects performed as described in (A-B).

1.3 Discussion

Current knowledge of BR signaling pathway reveals a complex integration of various signals regulating the BR signaling pathway (Zhu et al., 2013; Wolf et al., 2014). From the hormone perception by BRI1 at the plasma membrane to the nuclear response mediated by the transcription factors BES1 and BZR1, many proteins are involved in signal transduction. Among them BIN2 stands out as a key regulator integrating various signals (Galvan-Ampudia and Vernoux, 2014)..

Here we present, genetic, physiological and biochemical evidences for the involvement of OPS in the BR signaling pathway by contributing to the regulation of BIN2, a signal integration hub repressing the BR signaling pathway. Based on OPS-OE lines studies, we provide phenotypical and molecular support for its role in inducing BR responses such as BES1 dephosphorylation. Furthermore, physiological and genetic analyses placed OPS into the BR signaling pathway as a positive regulator causing the accumulation of unphosphorylated form of BES1. OPS interacts with BIN2 in yeast and *in planta* through its N-terminal domain. Taken together, our results suggest that OPS may inhibit BIN2 repression to induce BR signaling.

BIN2 has been described as a nucleo-cytoplasmic protein that occasionally can be detected at the plasma membrane (Vert and Chory, 2006; Kim et al., 2009), however its proper localization and detection is still a matter of debate (Peng et al., 2008; Vert and Chory, 2006). Studies have pointed out the important role played by the compartmentalization of BIN2 in regulating this pathway (Vert and Chory, 2006). Thus, *bin2-1* gain-of-function mutation accumulates inside the nucleus and a plant expressing BIN2 protein fused to a NLS have been shown to enhance the dwarf phenotype compared to plant expressing BIN2 alone or deprived of its functional NLS (Vert and Chory, 2006). Given these data, the activity of BIN2 is highly dependent upon its subcellular localization. Similar mechanisms are described in animals in which Wnt signaling pathway plays an important role in development, stem cell and cancers. The Wnt pathway involved GSK3 proteins that mediate β-catenin degradation by phosphorylation. In presence to Wnt, GSK3 is incorporated into multivesicular endosomes, sequestered from its cytosolic substrates and leading to an inhibition by compartmentalization (Taelman et al., 2010).

Here, we provide evidence that OPS interacts with BIN2 at the plasma membrane and that the location of this interaction is important for the BR response to occur. We thus suggest

that OPS interacts with BIN2 at the plasma membrane to repress its action on BES1 and BZR1 in the nucleus. In such a scenario, upon the binding of BR to BRI1, OPS may hold BIN2 at the plasma membrane, away from its substrates BES1 and BZR1. Consistent with our hypothesis of BIN2 relocalization, the fact that OPS-OE can counteract the *bin2-1D* mutant suggest that, under the action of OPS, bin2-1D mutant protein is not able to exert its repressive activity onto nuclear BES1 and BZR1. However, this BIN2 relocalization hypothesis remains to be confirmed.

OPS has been involved in vascular differentiation since 1) its expression coincides with the site of cell fate decision during early vascular development (preprocambial cells, (Bauby et al., 2007)) and phloem differentiation (phloem initials) 2) vascular loops and phloem differentiation defects have been detected in *ops* mutant (Truernit et al., 2012). In the light of the implication of *OPS* in the BR signaling pathway, we show that *bzr1-D* and to a lesser extent *bes1-D* can partially rescue some phenotypes of *ops*. However, the vascular loops defects in *ops* cotyledons were not restored by neither *bes1-D* nor *bzr1-D*. Because vascular loops in cotyledons are established during embryogenesis (Bauby et al., 2007), it is possible that *BES1* and *BZR1* expression was not sufficient during embryogenesis to circumvent *ops* defects. BES1 and BZR1 do not share the same target and can impact differently on *ops* mutants. Moreover other targets of GSK3 such as BES1/BZR1 homologs BEH1-4 may also be affected in *ops* mutants. Interestingly, BEH1 and BEH2 are expressed preferentially in the apical part of the embryo at heart stage (Figure S5), the location of the future vascular loops. Additional experiments will be required to address a possible role of *BEH1/BEH2* in *OPS*-mediated embryonic vascular differentiation.

1.4 Supplemental data

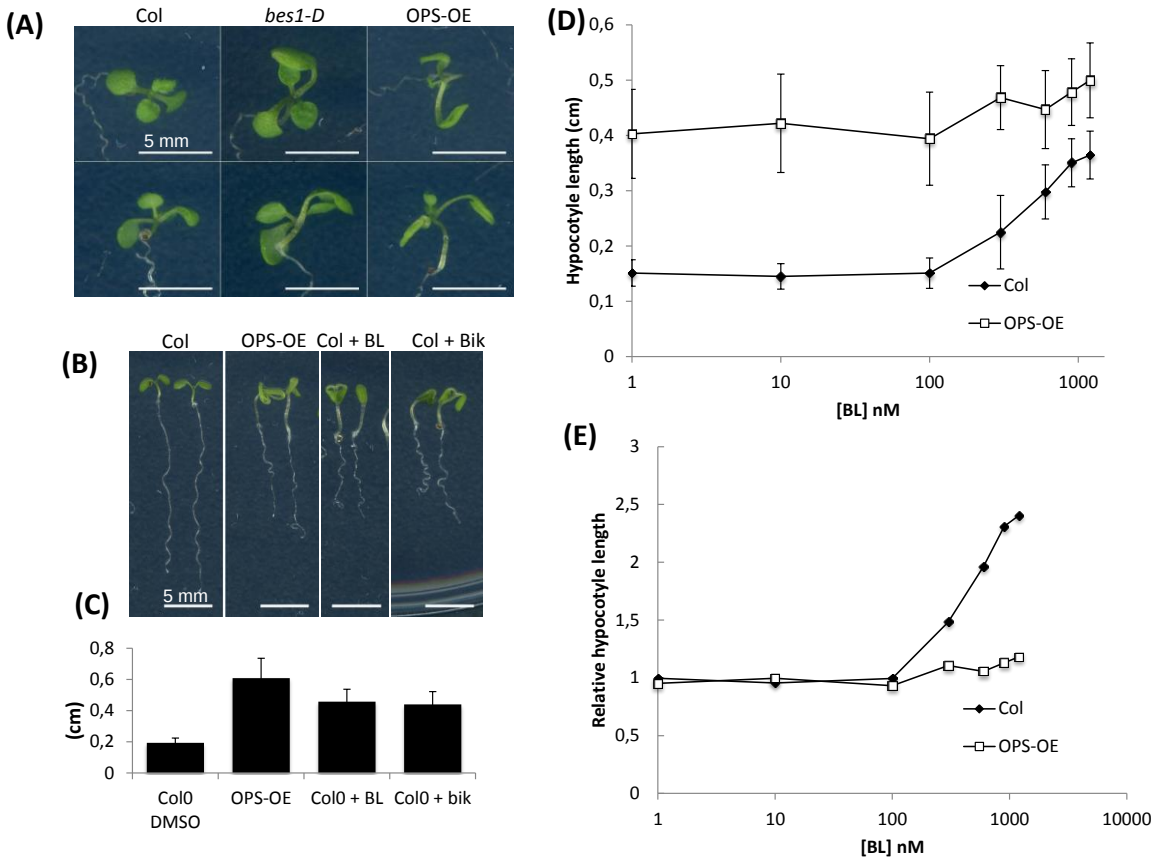

Figure S1 : OPS-OE display growth phenotypes of plants with constitutive BR responses
(A) OPS-OE light-grown phenotype is reminiscent of BR constitutive mutants such as *bes1-D*. 15 days-old seedlings light-grown on Arabidopsis medium with 1% sucrose. **(B-C)** OPS-OE phenotype can be mimicked by both 1 µM BL or 50 µM bikinin treatments. **(B)** 7 days-old seedlings grown on Arabidopsis medium with 1% sucrose. bar: 5 mm **(C)** Corresponding hypocotyl length **(D-E)** OPS-OE is insensitive to BL treatment (0-1,2µM). **(D)** Hypocotyle length of 7 days-old light-grown seedlings on Arabidopsis medium with 1% sucrose +/- BL **(E)** Relative hypocotyle length compared to non-treated plants (DMSO+0µM BL).

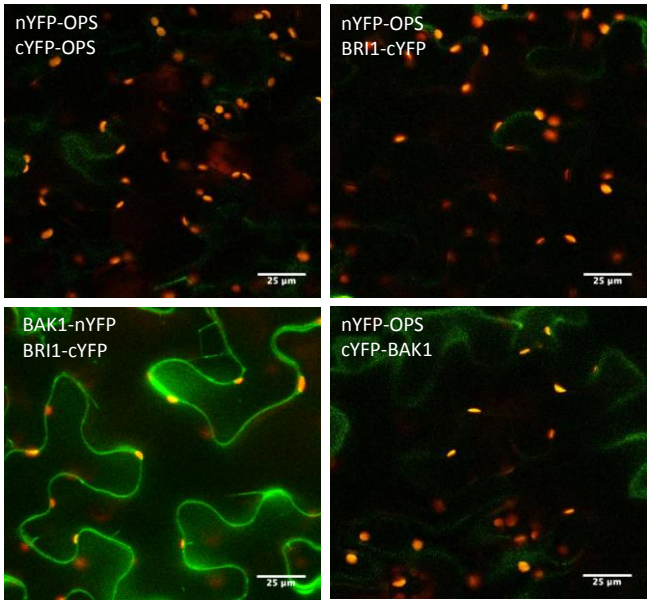

Figure S2: OPS does not homodimerize and does not interact with BRI1 and BAK1 by BiFC (split-YFP)
Protein-Protein interaction visualized by split-YFP in tobacco leaf epidermis observed by confocal microscopy. Transient expression of the indicated proteins fused to nYFP or cYFP is performed by agrobacterium-mediated leaf transformation of 3 weeks old *Nicotiana Benthamiana* plants. bar = 25 µm; green: YFP signal; red: autofluorescence

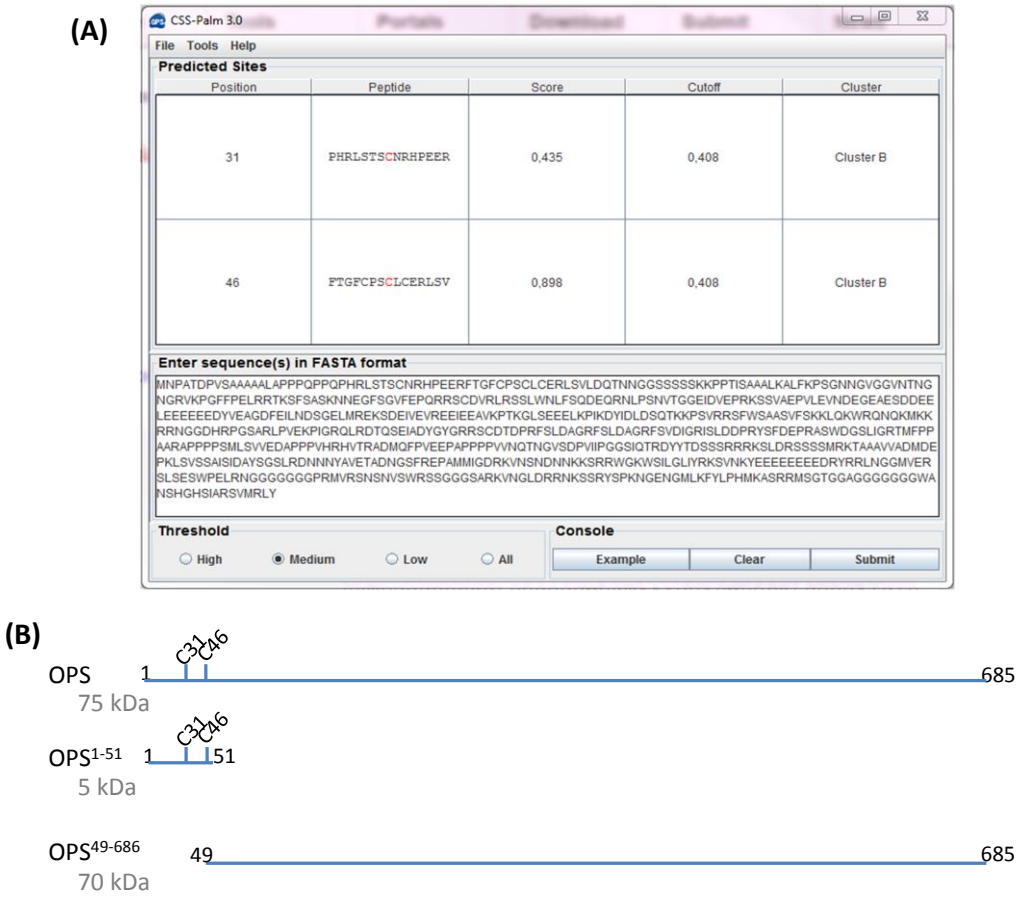

Figure S3: Prediction of putative palmitoylation sites in OPS and truncated OPS protein sequences
(A) Bioinformatic prediction of palmitoylation in OPS protein sequence idientifies Cys31 and Cys46 as putative palmitoylation sites (CSS-palm 3.0, (Ren et al., 2008)) **(B)** Schematic representation of truncated version of OPS protein and their predicted molecular weight.

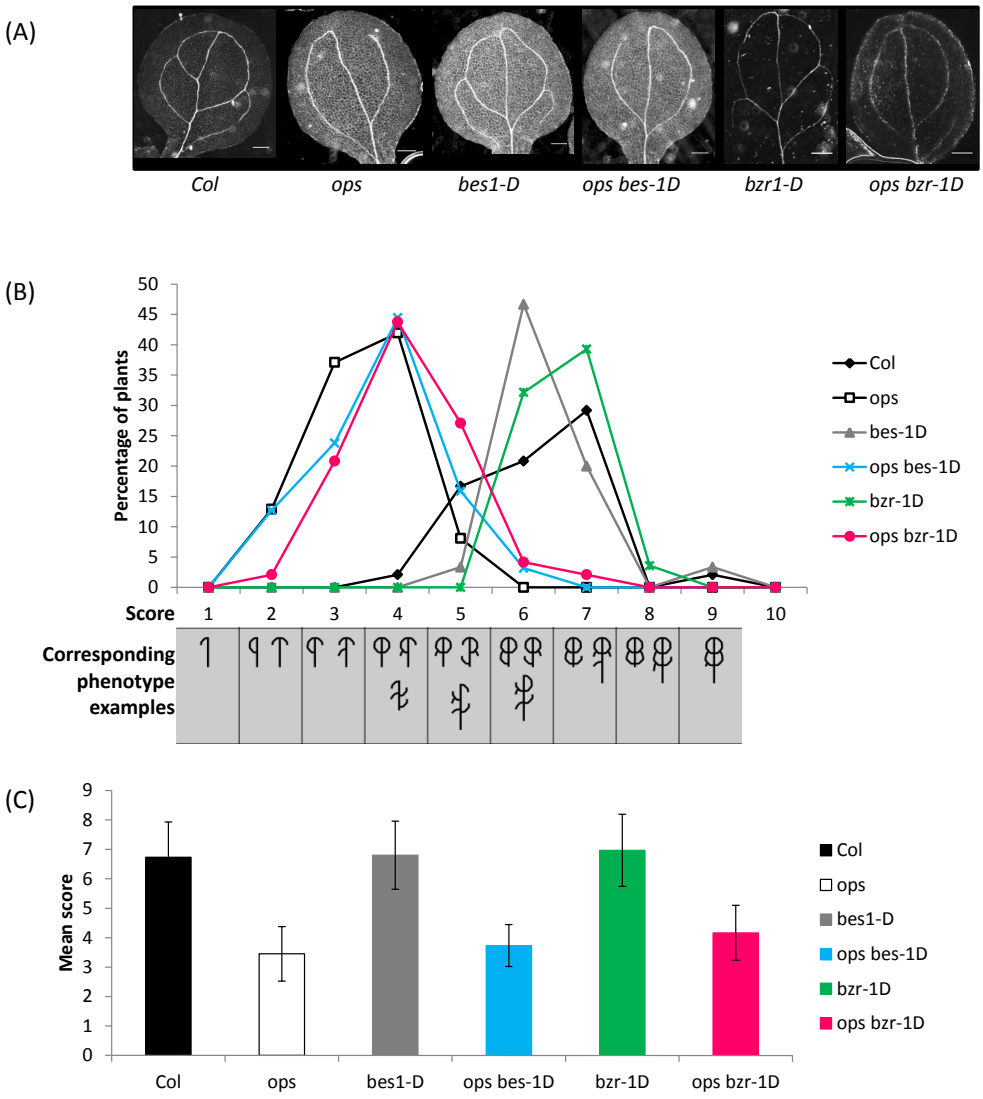

Figure S4: *bes1-D* and *bzr1-D* mutations do not rescue vasculature defects in *ops* cotyledons
(A) Phenotype of vascular loops in cotyledons of 7 days old seedlings. Bar= 200 µm **(B)** Percentage of plants presenting the described vascular complexity score. Complexity score includes number of initiated vascular loops and number of closed vascular loops. Scheme below descrbies the phenotypes scored in 7 days-old light-grown seedlings of the different genotypes. (n=20) **(C)** Mean score for each genotype (n=20).

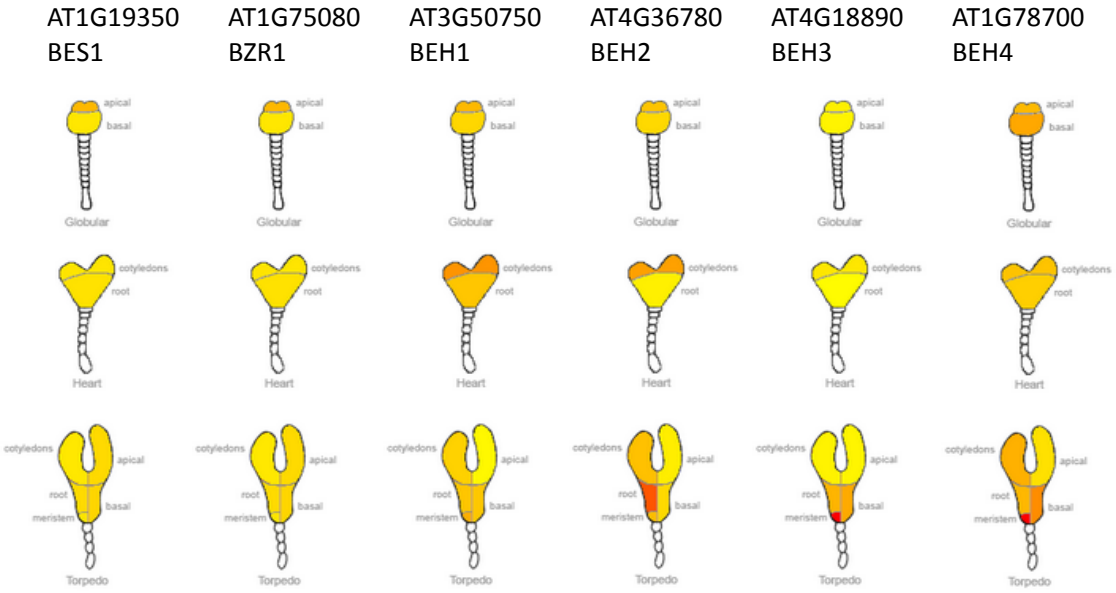

Figure S5 : Expression of BZR1, BES1 and their homologous gene expression during embryogenesis as described in published microarray datasets.
From Arabidopsis eFP Browser (http://bar.utoronto.ca/efp/cgi-bin/efpWeb.cgi)

1.5 Experimental procedures

Plants material and growth conditions

Arabidopsis thaliana ecotype Columbia (Col) was used as a wild-type control for phenotypic comparison. All plants used are in Col ecotype background excepted the *bes1-D* mutant in the ecotype Enkheim-2 (Yin et al., 2002). Seeds were sown on Arabidopsis medium (Duchefa, as describe by Estelle and Somerville (Estelle and Somerville, 1987)) supplemented with 1% sucrose for light-grown condition. brassinazole (BRZ, TCI), 24 epi-brassinolide (BL, Sigma-Aldrich), or bikinin (Bik, Sigma-Aldrich) were added at the indicated concentrations dissolved in DMSO, equivalent concentrations of DMSO are added in control conditions. After 48h at 4°C in darkness, plants were grown under long day conditions in Petri Dishes (16h light/8h dark cycle, 60% humidity, 18°C day and night). For seedling grown in dark conditions, a flash of light was made during 6 hours to induce germination before wrapping Petri Dishes into 2 foils of aluminum and place them at 18°C.

Cloning and transgenic plants

cDNA were successively cloned by Gateway cloning technology (Invitrogen) in a pDONR207 using BP clonase, sequenced, then transferred in the different pDEST using LR clonase: pBiFC(1-4) for the BiFC experimentation (Desprez et al., 2007) or pMDC83 (Curtis and Grossniklaus, 2003) for overexpression fused to GFP. BIN2 was amplified by RT-PCR from Col cRNA template using a high-fidelity DNA-polymerase (Phusion, Finnzyme). cDNAs of *BRI1* and *BAK1* were provided by S. Wolf (Wolf et al., 2014) in a pDONR207 vector. OPS cDNA in pDONR207 comes from Truernit et al 2012. For primer sequences see table 1. *Arabidopsis thaliana* plants were transformed with Agrobacterium by floral dipping method (Clough and Bent, 1998) and homozygous lines carring pMDC83 vector were selected on hygromycin (30µg/ml) selection medium.

Protein-Protein Interaction Analysis

Concerning transient transformations for BiFC, leaves of 3 weeks old plants of *Nicotiana benthamiana* were transformed by co-infiltration of agrobacterium strains carrying the appropriate pBIFC vectors according to (Voinnet et al., 2003). Fluorescence was detected 3 days after infiltration by confocal microscopy.

Regarding the interaction in yeast, we used the two-hybrid split-ubiquitin system from Dualsystem Biotech for protein-protein interaction assays of membrane proteins. cDNA were amplified by RT-PCR from Col cDNAs template with Phusion polymerase (Finnzyme) and cloned them at the SfiI restriction sites in in pPR3N/pBT3N (Dualsystem Biotech). Plasmids were selected on kanamycin or carbenicilin depending on vector resistance. NMY51 (Dualsystem Biotech) yeast strand was transformed by thermic shock and selected on SD-LT medium and then transfered on SD-LTH supplemented with an increasing concentration of 3AT.

Plant cytology and imaging

Acquisitions weres performed on a Leica SP5 II AOBS tandem HyD confocal laser-scanning microscope equipped with a x40 oil immersion objective (REF with NA) used for imaging of propidium iodide stained Arabidopsis roots and x63 water immersion objective (REF with NA) used for imaging of benthamiana leaf segment BiFC. Propidium iodide staining was performed as described by Truernit (Truernit et al., 2008). Excitation wave lengths were 488

nm for GFP, 514 nm for YFP, 488-561 nm for propidium iodide staining. Fluorescence was recorded between 530 and 600 nm for YFP, between 490 and 525 nm for GFP, between 570 and 700 nm for propidium iodide staining. FM4-64 fluorescence was recorded between 600 nm and 720 nm. To study venation patterns, cotyledons were fixed in a ethanol/ acetic anhydride/water solution (v/v/v 50/10/40) and cleared in a chloral hydrate/glycerol solution. For roots and hypocotyl length analysis, plants were grown on petri dishes placed vertically that were were directly scanned at a 600dpi resolution with a scanner. Images were analyzed with ImageJ64 version 1.48 software (Abràmoff et al., 2004) and manuscript figures were prepared using the FigureJ plugin (Mutterer and Zinck, 2013) and Powerpoint.

Expression analysis

Total RNA were extracted with the RNeasy Plant mini kit (Qiagen) and cDNA were produced by reverse transcription (REF Invitrogen). Real Time quantitative-PCR were performed on a CFX real-time thermocycler (Bio-Rad) using sybergreen (Eurogentec) according to manufacturer instructions. We used a synthetic gene reference corresponding to the average between three genes APT1 (At1g27450), PP2A-A3 (At1g13320), SAND (At2g28390) as described in (Masclaux 2014?).

Gel electrophoresis and western blotting

Harvested 10-d-old Arabidopsis seedlings were ground in SDS sample buffer without bromphenol blue (62.5 mM Tris-HCl, pH 6.8, 2% (w/v) SDS, 10% (v/v) glycerol, 5% (v/v) β-mercaptoethanol). Total extracts were denaturated by heating at 95°C for 10 min. Cell debris were then pelleted by centrifugation at 6,000g for 10 min, protein concentrations in the supernatant were determined using the RCDC protein assay kit (Bio-Rad). 20 µg of protein were loaded and separated on precast 10% acrylamide gel (Mini-Protean or Criterion TGX gels, Bio-Rad). For immunodetection the proteins were transferred onto PVDF membranes (Bio-Rad) using a Trans-Blot Turbo Transfer System (Bio-Rad). The membranes were blocked with 5% (wt/vol) non-fat dry milk in Tris-buffered saline (TBS)/Tween 20. Subsequently the membranes were probed overnight at 4°C with a rabbit anti-BES1 antibody (gift of (Yin et al., 2002)) or anti-GFP antibody (Roche , ref#11814460001). After washing, the membranes were incubated with anti-rabbit (for BES1) or anti-mouse (for GFP) secondary antibody conjugated to HRP (Santa Cruz Biotechnology). Protein bands were developed using Clarity

ECL substracte (Bio-Rad) and visualized using an LAS-4000 system (Fujifilm). The same membranes were stained with PageBlue Protein Staining Solution (Thermo Scientific) to verify equal loading of protein samples.

Primers sequences in the 5' to 3' orientation

Table 1:

OPS pBT3-N or pPR3-N SfiI	F	ATTAACAAG GCC ATT ACG GCCATGAATCCAGCTACTGACCCAGTCTCCGCC
	R	AACTGATTGGCCGAGGCGGCCTCAATACAGCCTCATTACACTCCTCGCTATAGAATGCCCG
OPS CDS gtw	F	GGGGACAAGTTTGTACAAAAAAGCAGGCTCCATGAATCCAGCTACTGACCCA
	R wo stop	GGGGACCACTTTGTACAAGAAAGCTGGGTCTTAAGTTCCAGATTGATTCAAGAAGC
	R STOP	GGGGACCACTTTGTACAAGAAAGCTGGGTCTCAATACAGCCTCATTACACTCCTCGC
BIN2 CDS gtw	F	GGGGACAAGTTTGTACAAAAAAGCAGGCTCCATGGCTGATGATAAGGAGATGCCTGC
	R wo stop	GGGGACCACTTTGTACAAGAAAGCTGGGTCAGTTCCAGATTGATTCAAGAAGC
	R STOP	GGGGACCACTTTGTACAAGAAAGCTGGGTCTTAAGTTCCAGATTGATTCAAGAAGC
BIN2 pPR3N SfiI	F	ATTAACAAGGCCATTACGGCCATGGCTGATGATAAGGAGATGCCTGCTGCTG
	R	AACTGATTGGCCGAGGCGGCCTTAAGTTCCAGATTGATTCAAGAAGCTTAGACCC
DWF4 qPCR	F	AGGGAATCATCGTCGACACC
	R	GGCTGAGATCACCGGTAACA
SAURAC1 qPCR	F	AGGGAATCATCGTCGACACC
	R	TGGTATTGTTAAGCCGCCCA
qPCR reference genes	F SAND	AAC TCT ATG CAG CAT TTG ATC CAC T
	R SAND	TGA TTG CAT ATC TTT ATC GCC ATC
	F APT1	CGGGGATTTTAAGTGGAACA
	R APT1	GAGACATTTTGCGTGGGATT
	F PP2A-A3	GCAATCTCTCATTCCGATAGTC
	R PP2A-A3	ATACCGAACATCAACATCTGG
OPS CDS^{49-685} gtw	F	GGGGACAAGTTTGTACAAAAAAGCAGGCTCCATGGAACGTCTCTCAGTCTTAGATCAG
	R wo stop	GGGGACCACTTTGTACAAGAAAGCTGGGTCTTAAGTTCCAGATTGATTCAAGAAGC
OPS CDS^{1-51} gtw	F	GGGGACAAGTTTGTACAAAAAAGCAGGCTCCATGAATCCAGCTACTGACCCA
	R wo stop	GGGGACCACTTTGTACAAGAAAGCTGGGTCGAGACGTTCACAGAGACAAGA
ops-2 genotyping	F1 WT allele	CAA CGA AAC CTT CCA AGC AAT G
	R1 WT allele	GGC GTC AAG AGA GAA TCT TC
	F2 mutant allele	AAA AGC CTC CGA CCA TCT CTG C
bri1-116 sequencing	F	GATTCCGAAATGGATTGGCCG
	R	GGCGAAGTGTGACCTCCATA
bin2-1D sequencing	F	GTTGCTGGAGTTTGTCACAGAG
	R	GCGCTGTGCATCTTAGACTTGG
bes1-D sequencing	F	TCCCGAGTCCTTCTCGAGTT
	R	GACAATTGCTGTGGTGCAGG
bzr1-D sequencing	F	CGCCGACTTCTAAGAACCCG
	R	CCACGAGCCTTCCCATTTCC
Salk mutants genotyping	LbB1.3	ATTTTGCCGATTTCGGAAC

1.6 Acknowledgments

We thank our former colleague and friend S. Wolf for providing the *bin 2-1*, *bes1-D* and *bzr1-D* mutants and BRI, BAK1 cDNA in the pDONR207 vector used in this study. We are very grateful to Y. Yin for the kind gift of the anti-BES1 antibody. We would like to thank G. Vert, O. Hamant, S. Mongrand, N. Arnaud, S. Wolf and N. Geldner for stimulating discussions and K. Belcram and O. Grandjean for their useful technical advices. P.A. is a recipient of a PhD fellowship from the french "Ministère de la Recherche".

1.7 Bibliography

Abràmoff, M.D., Magalhães, P.J., and Ram, S.J. (2004). Image Processing with ImageJ. Biophotonics Int. **11**: 36–42.

Asami, T., Min, Y.K., Nagata, N., Yamagishi, K., Takatsuto, S., Fujioka, S., Murofushi, N., Yamaguchi, I., and Yoshida, S. (2000). Characterization of brassinazole, a triazole-type brassinosteroid biosynthesis inhibitor. Plant Physiol. **123**: 93–100.

Bauby, H., Divol, F., Truernit, E., Grandjean, O., and Palauqui, J.-C. (2007). Protophloem differentiation in early Arabidopsis thaliana development. Plant Cell Physiol. **48**: 97–109.

Clough, S.J. and Bent, A.F. (1998). Floral dip : a simplified method for Agrobacterium-mediated transformation of Arabidopsis thaliana. Plant J. **16**: 735–743.

Curtis, M.D. and Grossniklaus, U. (2003). A Gateway Cloning Vector Set for High-Throughput Functional Analysis of Genes in Planta. Plant Physiol. **133**: 462–469.

Desprez, T., Juraniec, M., Crowell, E.F., Jouy, H., Pochylova, Z., Parcy, F., Höfte, H., Gonneau, M., and Vernhettes, S. (2007). Organization of cellulose synthase complexes involved in primary cell wall synthesis in Arabidopsis thaliana. Proc. Natl. Acad. Sci. U. S. A. **104**: 15572–7.

Estelle, M.A. and Somerville, C. (1987). Auxin-resistant mutants of Arabidopsis thMiana with an altered morphology. Mol Gen Genet **206**: 200–206.

Galvan-Ampudia, C.S. and Vernoux, T. (2014). Signal integration by GSK3 kinases in the root. Nat. Cell Biol. **16**: 21–3.

Grove, M.D., Spencer, G.F., and Rohwedder, W.K. (1979). Brassinolide, a plant growth-promoting steroid isolated from Brassica napus pollen. Nature **281**.

He, J.-X., Gendron, J.M., Sun, Y., Gampala, S.S.L., Gendron, N., Sun, C.Q., and Wang, Z.-Y. (2005). BZR1 is a transcriptional repressor with dual roles in brassinosteroid homeostasis and growth responses. Science **307**: 1634–8.

He, J.-X., Gendron, J.M., Yang, Y., Li, J., and Wang, Z.-Y. (2002). The GSK3-like kinase BIN2 phosphorylates and destabilizes BZR1, a positive regulator of the brassinosteroid signaling pathway in Arabidopsis. Proc. Natl. Acad. Sci. U. S. A. **99**: 10185–90.

He, Z., Wang, Z.Y., Li, J., Zhu, Q., Lamb, C., and Chory, J. (2000). Perception of Brassinosteroids by the Extracellular Domain of the Receptor Kinase BRI1. Science (80-.). **288**: 2360–2363.

Hemsley, P.A. (2014). The importance of lipid modified proteins in plants. New Phytol.

Kim, T.-W., Guan, S., Burlingame, A.L., and Wang, Z.-Y. (2011). The CDG1 kinase mediates brassinosteroid signal transduction from BRI1 receptor kinase to BSU1 phosphatase and GSK3-like kinase BIN2. Mol. Cell **43**: 561–71.

Kim, T.-W., Guan, S., Sun, Y., Deng, Z., Tang, W., Shang, J.-X., Sun, Y., Burlingame, A.L., and Wang, Z.-Y. (2009). Brassinosteroid signal transduction from cell-surface receptor kinases to nuclear transcription factors. Nat. Cell Biol. **11**: 1254–60.

Li, J. and Chory, J. (1997). A putative leucine-rich repeat receptor kinase involved in brassinosteroid signal transduction. Cell **90**: 929–38.

Li, J. and Nam, K.H. (2002). Regulation of brassinosteroid signaling by a GSK3/SHAGGY-like kinase. Science **295**: 1299–301.

Li, J., Nam, K.H., Vafeados, D., and Chory, J. (2001). BIN2, a new brassinosteroid-insensitive locus in Arabidopsis. Plant Physiol. **127**: 14–22.

Mitchell, J.W. and Gregory, L.E. (1972). Enhancement of Overall Plant Growth, a New Response to Brassins. Nature **239**: 253–254.

Mitchell, J.W., Mandava, N., Worley, J.F., Plimmer, J.R., and Smith, M. V. (1970). Brassins - a New Family of Plant Hormones from Rape Pollen. Nature **225**: 1065–1066.

Mora-García, S., Vert, G., Yin, Y., Caño-Delgado, A., Cheong, H., and Chory, J. (2004). Nuclear protein phosphatases with Kelch-repeat domains modulate the response to brassinosteroids in Arabidopsis. Genes Dev. **18**: 448–60.

Mutterer, J. and Zinck, E. (2013). Quick-and-clean article figures with FigureJ. J. Microsc. **252**: 89–91.

Peng, P., Yan, Z., Zhu, Y., and Li, J. (2008). Regulation of the Arabidopsis GSK3-like kinase BRASSINOSTEROID-INSENSITIVE 2 through proteasome-mediated protein degradation. Mol. Plant **1**: 338–46.

Ren, J., Wen, L., Gao, X., Jin, C., Xue, Y., and Yao, X. (2008). CSS-Palm 2.0: an updated software for palmitoylation sites prediction. Protein Eng. Des. Sel. **21**: 639–44.

De Rybel, B. et al. (2009). Chemical inhibition of a subset of Arabidopsis thaliana GSK3-like kinases activates brassinosteroid signaling. Chem. Biol. **16**: 594–604.

Stagljar, I., Korostensky, C., Johnsson, N., and Heensen, S.H. (1998). A genetic system based on split-ubiquitin for the analysis of interactions between membrane proteins in vivo. Proc. Natl. Acad. Sci. U. S. A. **95**: 5187–5192.

Taelman, V.F., Dobrowolski, R., Plouhinec, J.-L., Fuentealba, L.C., Vorwald, P.P., Gumper, I., Sabatini, D.D., and De Robertis, E.M. (2010). Wnt signaling requires sequestration of glycogen synthase kinase 3 inside multivesicular endosomes. Cell **143**: 1136–48.

Truernit, E., Bauby, H., Belcram, K., Barthélémy, J., and Palauqui, J.-C. (2012). OCTOPUS, a polarly localised membrane-associated protein, regulates phloem differentiation entry in Arabidopsis thaliana. Development **139**: 1306–15.

Truernit, E., Bauby, H., Dubreucq, B., Grandjean, O., Runions, J., Barthélémy, J., and Palauqui, J.-C. (2008). High-resolution whole-mount imaging of three-dimensional tissue organization and gene expression enables the study of Phloem development and structure in Arabidopsis. Plant Cell **20**: 1494–503.

Vert, G. and Chory, J. (2006). Downstream nuclear events in brassinosteroid signalling. Nature **441**: 96–100.

Voinnet, O., Rivas, S., Mestre, P., and Baulcombe, D. (2003). An enhanced transient expression system in plants based on suppression of gene silencing by the p19 protein of tomato bushy stunt virus. Plant J. **33**: 949–956.

Wang, Z.Y., Nakano, T., Gendron, J., He, J., Chen, M., Vafeados, D., Yang, Y., Fujioka, S., Yoshida, S., Asami, T., and Chory, J. (2002). Nuclear-localized BZR1 mediates brassinosteroid-induced growth and feedback suppression of brassinosteroid biosynthesis. Dev. Cell **2**: 505–13.

Wolf, S. et al. (2014). A receptor-like protein mediates the response to pectin modification by activating brassinosteroid signaling. Proc. Natl. Acad. Sci.

Yin, Y., Vafeados, D., Tao, Y., Yoshida, S., Asami, T., and Chory, J. (2005). A new class of transcription factors mediates brassinosteroid-regulated gene expression in Arabidopsis. Cell **120**: 249–59.

Yin, Y., Wang, Z.Y., Mora-Garcia, S., Li, J., Yoshida, S., Asami, T., and Chory, J. (2002). BES1 accumulates in the nucleus in response to brassinosteroids to regulate gene expression and promote stem elongation. Cell **109**: 181–91.

Zhu, J.-Y., Sae-Seaw, J., and Wang, Z.-Y. (2013). Brassinosteroid signalling. Development **140**: 1615–20.

2 Résultats complémentaires

2.1 Relocalisation de BIN2 à la membrane par OCTOPUS

Nous venons de voir que les protéines OPS et BIN2 interagissent à la membrane. Nous proposons un modèle de régulation dans lequel OPS pourrait séquestrer BIN2 à la membrane bloquant ainsi son activité inhibitrice sur la voie des brassinostéroïdes (Vert and Chory, 2006). Selon ce modèle lorsque la voie des brassinostéroïdes est activée, OPS retiendrait BIN2 à la membrane afin d'empêcher son action sur les facteurs de transcription BES1 et BZR1. Chez les animaux, un modèle semblable est décrit mettant en action des GSK3s dont l'activité serait inhibée par séquestration à l'intérieur de corps multi-vésiculaires. Les GSK3s, étant séparées de leurs substrats, ne peuvent plus réprimer la voie (Taelman et al., 2010).

Afin de tester ce modèle, nous avons étudié la localisation de BIN2 en présence ou non d'OPS.

Des plantes transgéniques contenant les constructions 35S::BIN2-mRFP1 (pH7RWG2, (Karimi et al., 2002)) ont été utilisées. En T1, certains transformants présentaient un phénotype fort avec un hypocotyle court, des feuilles rondes et vert foncé et un nanisme. Ces plantes étaient pour la plupart stériles. Cependant, nous avons sélectionné deux lignées indépendantes pour réaliser des croisements avec la plante OPS-OE (portant la construction 35S::OPS-GFP). La descendance a été analysée par microscopie confocale mais ne montrait pas de signal fluorescent évident.

Parallèlement à cette étude et afin de s'affranchir du phénotype trop fort des lignées stables 35S::BIN2-mRFP, nous avons étudié la localisation de la construction 35S ::HA-mCherry-BIN2 (pEG106,(Gutierrez et al., 2009)) seule ou en combinaison avec la construction 35S ::OPS-GFP en expression transitoire dans des feuilles de Nicotiana benthamiana. Les échantillons sont observés 3 jours plus tard par microscopie confocale. Comme décrit par Vert et Chory (Vert and Chory, 2006) dans des cellules d'Arabidopsis exprimant BIN2 de façon stable, BIN2 se localise à la membrane, dans le cytoplasme et majoritairement dans le noyau (Figure 5.1A). En présence d'OPS-GFP, la localisation de HA-mCherry-BIN2 semble être légèrement modifiée puisque le signal nucléaire est plus faible (Figure 5.1A).

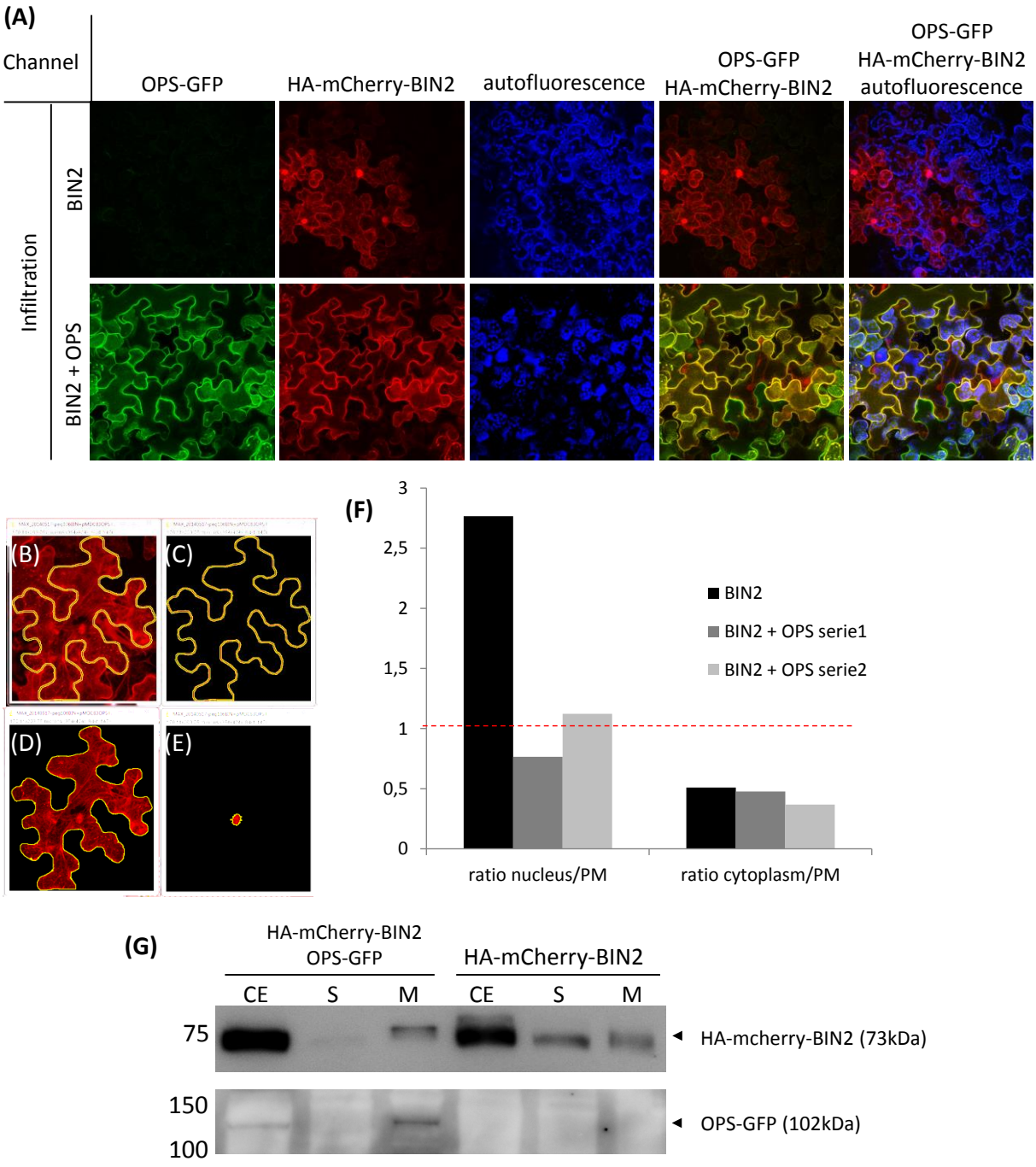

Figure 5.1 : Localisation subcellulaire de BIN2 en présence d'OPS-GFP

(A) Transformations transitoires de feuilles de tabac par HA-mCherry-BIN2 (signal rouge) en présence ou non d'OPS-GFP (signal vert). En bleue: l'autofluorescence. **(B)** Projection de 69 coupes (mode max intensity) d'un pas de 0,42µm (épaisseur totale 28,5µm). La projection incorpore le noyau entier et des portions de cytoplasme et membrane. **(C)** Extraction de la membrane plasmique de la cellule de la figure (B). **(D)** Extraction du cytoplasme de la cellule de la figure B. **(E)** Extraction du noyau de la cellule de la figure (B). **(F)** Ratio d'intensité moyenne du signal mCHerry-BIN2 entre les différents compartiments cellulaires extraits en (C/D/E). Mesures faites sur l'intensité de signal BIN2 sur des cellules exprimant BIN2 en présence ou non d'OPS-GFP. La cellule (B) est découpée en zones (C-E) et le « mean gray value » est mesuré pour chacune d'entre elle sur ImageJ (Abràmoff et al., 2004). **(G)** Western-blot sur fractionnement cellulaire de feuilles de tabac transformées par HA-mCHerry-BIN2 en présence ou non d'OPS-GFP. Un anticorps anti-HA et un anti-corps anti-GFP révèlent respectivement HA-mCherry-BIN2 et OPS-GFP.

Afin de quantifier ces différences, des ratios d'intensité de fluorescence ont été calculés pour chacune des conditions. Les piles d'images composant une série de coupes de 0,42µm sont projetées en 2D (mode max intensity) sur ImageJ (Abràmoff et al., 2004) (Figure 5.1B). Ces séries incorporent un noyau entier, une portion de cytoplasme et une portion membranaire. De cette projection d'images est extraite l'intensité de fluorescence moyenne des pixels en périphérie des cellules (considérée comme la membrane), au cytoplasme et au noyau (Figure 5.1C-E). Les valeurs obtenues sont alors utilisées pour mesurer les ratios noyau/membrane plasmique (N/PM) et cytoplasme/membrane plasmique (C/PM) (Figure 5.1F) permettant ainsi de comparer la répartition subcellulaire de BIN2 entre les différents compartiments indépendamment du niveau d'expression des différentes cellules analysées. Un ratio N/PM de 1 reflète une quantité égale de BIN2 à la membrane et au noyau. Si la valeur est supérieure à 1, la quantité de BIN2 dans le noyau est supérieure à celle présente au niveau de la membrane plasmique.

Le ratio N/PM est de 2,5 lorsque HA-mCherry-BIN2 est la seule construction présente dans les feuilles de tabac alors qu'elle équivaut à 1 en présence d'OPS (Figure 5.1F). Il semblerait donc que la proportion de BIN2 nucléaire soit plus importante en absence d'OPS-GFP qu'en présence d'OPS-GFP. En revanche le ratio C/PM reste inchangé dans les deux conditions (Figure 5.1F) suggérant que la localisation de HA-mCherry-BIN2 en présence d'OPS-GFP n'affecte pas la répartition de BIN2 entre la membrane et le reste de la cellule (cytoplasme = cytosol + noyau). Plusieurs hypothèses peuvent expliquer ces résultats :

(1) La répartition entre le cytosol et noyau pourrait être affectée (à mesurer). En présence d'OPS-GFP, une partie de la fraction nucléaire de HA-mCherry-BIN2 serait allouée à la membrane ou sinon bloquée dans cytosol.

(2) La fraction nucléaire de la protéine peut être dégradée plus vite en présence d'OPS ou au contraire la fraction membranaire peut-être stabilisée.

Cependant ces mesures ont été réalisées sur un nombre très limité de cellules et doivent être reproduite à plus grande échelle afin de confirmer ces valeurs suggérant une localisation différente de BIN2 sous l'influence d'OPS.

Afin de préciser ces résultats, nous avons tenté de détecter ces protéines dans les différents compartiments cellulaires biochimiquement par fractionnement cellulaire. A partir des mêmes feuilles de tabac infiltrées par des constructions 35S::HA-mCherry-BIN2 et 35S::OPS-GFP, un extrait total des protéines a été séparé des débris du broyat par centrifugation à

basse vitesse (10min à 6 000 rpm) puis les fractions microsomale et soluble ont été séparées par ultra-centrifugation (1h à 100 000 rpm). Les différentes fractions cellulaires (extrait total : CE ; fraction soluble : S et fraction membranaire : M) ont été analysées par western-blot (Figure 5.1G). La présence de BIN2 et d'OPS dans chacune d'entre elles est révélée par un anticorps anti-HA et anti-GFP respectivement. Confirmant nos observations microscopiques, HA-mCherry-BIN2 est présent dans la fraction soluble et dans la fraction membranaire. En présence d'OPS-GFP, la quantité de HA-mCherry-BIN2 dans la phase soluble semble être diminuée en faveur de la fraction microsomale suggérant une relocalisation de BIN2 à la membrane. Cependant, il semblerait qu'une partie du matériel ait été perdu au cours de l'expérimentation puisque la phase membranaire n'est pas enrichie malgré la diminution de l'intensité de la fraction soluble dans la condition HA-mCherry-BIN2 + OPS-GFP. Par ailleurs, nous avons pu observer un fort taux de clivage des étiquettes HA-mCherry et GFP perturbant les conclusions du fractionnement. La dégradation des protéines de fusion peut provenir des conditions d'extractions (pourtant réalisée à 4°C et avec un cocktail d'inhibiteurs de protéases) ou bien d'une possible dégradation in planta de BIN2. En effet, il a été reporté que BIN2 pourrait être ubiquitinylée et dégradée par le protéasome lorsque la voie de signalisation des brassinostéroïdes est activée (Peng et al., 2008). Cette expérience sera renouvelée en ajoutant du MG132 au tampon d'infiltration afin d'inhiber cette dégradation protéique.

2.2 Interaction d'OPS et CDG1 à la membrane.

L'un des objectifs de ma thèse était de comprendre quels sont les mécanismes permettant d'adresser la protéine OPS à la membrane. Nous avons précédemment montré que, contrairement à CDG1 (Kim et al., 2011), OPS n'est pas adressé à la membrane par palmitoylation au niveau des résidus cystéine du domaine N-terminale. Comme nous savons qu'OPS est impliquée dans la voie des BR, l'un des mécanismes d'adressage d'OPS à la membrane pourrait être son interaction avec des membres de la voie eux même localisés au niveau de la membrane plasmique.

Pour répondre à cette question, différentes protéines membranaires de la voie de signalisation des brassinostéroïdes ont été testées en interaction dirigées *in vivo* avec la protéine OPS. Le système choisi est le split-YFP (BiFC,(Desprez et al., 2007)) dans des cellules

épidermiques de *Nicotiana benthamiana*. La protéine OPS est fusionnée à la partie N-terminal de la protéine YFP (nYFP-OPS) et infiltrée dans les cellules épidermiques de tabac en présence de BRI1 (Li and Chory, 1997), BAK1 (Li et al., 2002), CDG1 (Kim et al., 2011) fusionnées à la partie C-terminale de la protéine YFP (BRI1-cYFP, BAK1-cYFP, cYFP-CDG1). Par cette approche, nous n'avons pas pu mettre en évidence d'interactions entre OPS et BRI1, ni entre OPS et BAK1 (Figure S2). En revanche, l'interaction nYFP-OPS et cYFP-CDG1 révèle un signal proche de la membrane plasmique (Figure 5.3A). Nous n'avons pas observé de signaux au niveau des travées cytoplasmiques caractéristiques d'une localisation cytoplasmique. Ceci suggère qu'OPS et CDG1 interagissent *in vivo* au niveau de la membrane. La protéine CDG1 étant localisée au niveau de la membrane (Kim et al., 2011), elle pourrait être responsable de l'adressage d'OPS à la membrane.

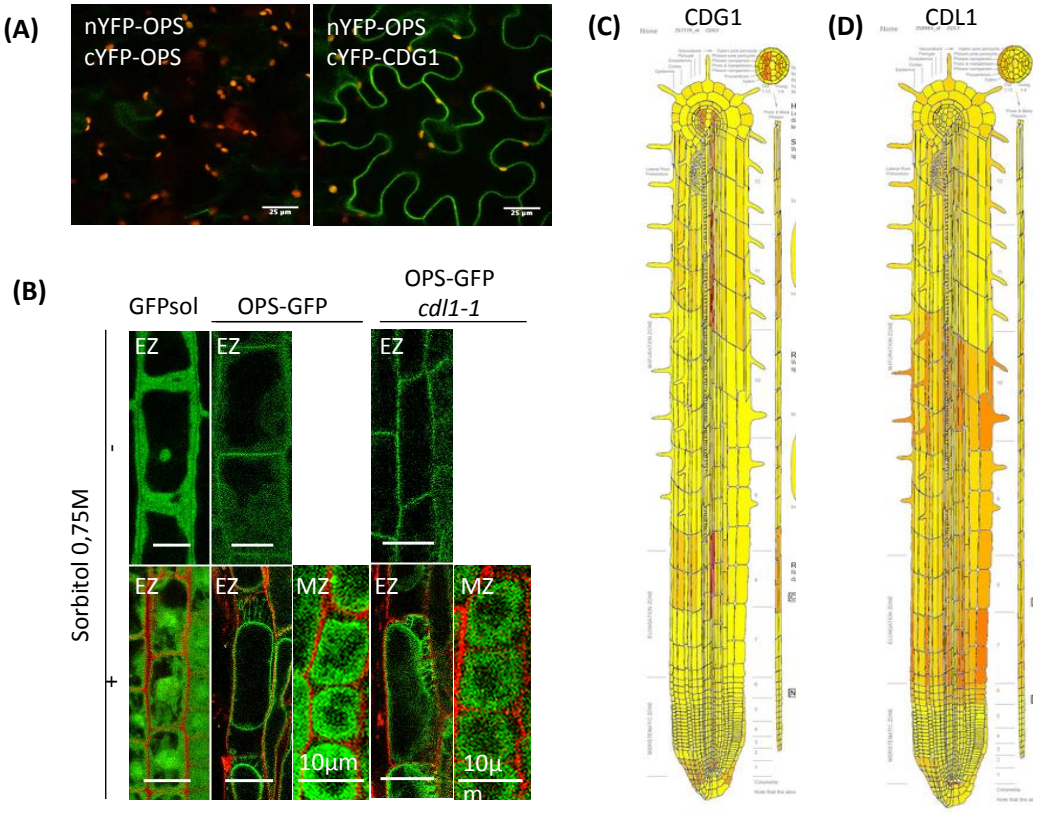

Figure 5.2 : Localisation d'OPS-GFP dans un fond mutant cdl1-1
(A) CDG1 et OPS interagissent ensemble à la membrane par split-YFP. Transformation transitoire de feuille de tabac. **(B)** Localisation subcellulaire d'OPS-GFP dans un contexte *cdl1* mutant au niveau de la zone d'élongation (EZ) ou dans la pointe racinaire (MZ). Plantes âgées de 7 jours, traitées ou non avec 0,75M de sorbitol. GFP-sol est utilisée comme contrôle de protéine soluble. Echelle: 20µm sauf si précisée. **(C)** Patron d'expression de CDG1 dans la racine. **(D)** Patron d'expression de CDL1 dans la racine. (C-D) Analyse eFP browser http://bar.utoronto.ca/efp/cgi-bin/efpWeb.cgi, consulté le 10/10/2014.

Afin de vérifier cette hypothèse, la localisation d'OPS-GFP a été analysée dans des contextes mutants : pour le gène *CDG1* (*cdg1-2* un allèle « knockout » du gène,(Muto et al., 2004)) ; pour le gène *CDL1 (CGD1 LIKE 1)* un gène homologue à *CDG1* ; (*cdl1-1*, Salk_114130 un allèle « knockout »,(Kim et al., 2011)) et dans le double mutant *cdl1 cdg1-2*. Le but de cette expérience est d'identifier ou non une délocalisation d'OPS-GFP vers le cytosol. Le gène *CDG1* étant peu exprimé dans la partie végétative des plantules (Kim et al., 2011), j'ai commencé l'analyse de la localisation de la protéine OPS-GFP dans le contexte *cdl1-1* (*CDL1* étant exprimé de manière ubiquiste dans les partie végétatives,(Kim et al., 2011)). Des plantes homozygotes pour *cdl1-1* exprimant la GFP (OPS-GFP) ont été observées par microscopie confocale en présence ou non de 0,75M de sorbitol.

Une lignée transgénique contenant la construction 35S::GFP (GFP-soluble) est utilisée comme marqueur cytosolique. Afin de repérer la paroi, une coloration à l'iodure de propidium est couplée à l'observation de la GFP. Dans la racine, la protéine OPS ::GFP est principalement localisée à la membrane plasmique comme en témoignent les expériences de plasmolyse en présence de sorbitol (Figure 5.3B). Cependant, une fraction cytosolique est également détectable, particulièrement dans les cellules méristématiques peu vacuolisées. Dans un contexte *cdl1-1* mutant, la localisation de la protéine OPS-GFP ne semble pas être modifiée par rapport aux plantes « contrôle ». Cependant, le gène *CDG1* est peut être également exprimé dans la partie racinaire de la plante comme le prédit « the Arabidopsis eFP Browser » (Figure 5.3C). Il faudra attendre l'analyse des lignées *cdg1-2 cdl1-1* OPS-OE avant de conclure définitivement sur l'implication de CDG1 dans l'adressage d'OPS à la membrane. Par ailleurs, cette hypothèse n'est peut-être pas la bonne, d'autres mécanismes (ou interaction avec d'autres protéines) peuvent être responsables de l'adressage d'OPS à la membrane.

2.3 Analyse des interactions entre VCC et OPS

Au cours de ma thèse, nous avons été contactés par H. Roschzttardtz, post-doc dans le laboratoire de Marisa Otegui (Univ. Madison) pour étudier les interactions génétiques entre le gène OPS et le gène *VASCULAR CONNECTIVITY COTYLEDON* (*VCC*, At2g32280). Ce gène code une protéine contenant un domaine de fonction inconnue DUF1218. *VCC* appartient à une famille multigénique de 15 gènes présentant 4 domaines transmembranaires ayant une

topologie proches des tetraspanines. Chez les animaux, les tetraspanines interviennent comme centres organisateurs des membranes plasmiques agissant comme des protéines de recrutement pour l'ancrage de plusieurs protéines à la membrane. Chez Arabidopsis, on dénombre 17 tetraspanines préférentiellement localisées à la membrane parfois de manière polaire (ex. appareil filiforme des synergides,(Boavida et al., 2013)). Curieusement, l'un des membres de la famille DUF1218 a été décrit pour interagir avec la protéine BRL2 afin de contrôler la mise en place des tissus vasculaires dans la feuille (Ceserani et al., 2009).

Le mutant *vcc* présente une diminution de la complexité du patron vasculaire dans les cotylédons. Inversement, la surexpression de *VCC* a conduit à une complexification du réseau avec une augmentation du nombre de boucles vasculaires formées dans les cotylédons. Ces phénotypes étant très similaires à ceux observés chez le mutant *ops* et dans les lignées surexprimant *OPS* (Truernit et al., 2012), les lignées WT, *ops*, vcc et *ops vvc* ont été soumises à une analyse phénotypique comparative. Nous avons pu montrer que la complexité du réseau vasculaire du double mutant *ops vcc* était aggravée comparée aux simples mutants suggérant un effet additif de ces deux mutations ((Roschzttardtz et al., 2014) ; ANNEXE 1). Par ailleurs, l'interaction physique entre OPS et VCC a été testée dans un système double hybride par split-ubiquitine. Nous avons pu montrer que ces deux protéines sont capables d'interagir *in vivo* dans la levure. Cette interaction a été confirmée par BiFC dans des protoplastes d'Arabidopsis.

D'après une analyse bio-informatique, la famille de protéines DUF1218 pourrait contenir quatre domaines transmembranaires. Certains de ces membres présentent une localisation membranaire démontrée (AT1G68220 ; AT3G15480,(Benschop et al., 2007)) ce qui fait de VCC une protéine candidate potentielle permettant d'ancrer OPS à la membrane.

Afin de confirmer ou d'infirmer cette hypothèse des plantes transgéniques portants la construction 35S::OPS-GFP ont été croisées avec le mutant *vcc*. Le but de cette expérience sera de regarder une éventuelle délocalisation d'OPS sous l'effet de la perte d'interaction avec la protéine VCC fonctionnelle. Ce résultat préciserait l'interaction physique et génétique observée entre OPS et VCC : le phénotype du mutant vcc pouvant être le résultat d'un défaut d'adressage d'OPS (ou de l'un des membre de la famille *OPS*).

3 Discussion

Au cours de cette étude, nous venons d'attribuer une fonction moléculaire à la protéine OPS. Différentes preuves appuient l'implication d'*OPS* dans la voie de signalisation des brassinostéroïdes. L'expression d'*OPS* sous le contrôle d'un promoteur fort induit de manière constitutive la voie des BR. Cette réponse se traduit tant au niveau du phénotype de croissance (élongation de l'hypocotyle et des pétioles, cotylédons enroulés) qu'au niveau moléculaire (régulation traductionnelle de BES1, régulation transcriptionnelle). De plus, des données physiologiques et génétiques indiquent qu'OPS intervient de manière positive sur la voie de signalisation en aval de BRI1 et en amont de BES1 et BZR1. Des tests d'interactions dirigées montrent également qu'OPS interagit physiquement avec BIN2 à la membrane suggèrant qu'OPS pourrait intervenir dans la voie en tant que répresseur de BIN2.

Nous proposons un modèle selon lequel l'activation de la voie par OPS résulterait de la rétention de BIN2 à la membrane. Cette répression correspondrait à une inhibition spatiale, éloignant BIN2 de ces substrats. Cependant, l'analyse de la localisation de BIN2 en présence ou non d'OPS dans *Nicotiana benthamiana* présente ses limites. Le tabac est un système hétérologue dans lequel on force l'expression des gènes *BIN2* et *OPS*. De plus, le gène *OPS* est conservé chez les plantes supérieures. Lors d'une simple infiltration mCherry-*BIN2*, la localisation de la protéine BIN2 est influencée par la présence possible de protéines OPS-LIKE endogène au tabac. Il est donc difficile de montrer l'envergure de l'influence d'OPS sur la localisation de BIN2 dans ce système. Il serait préférable d'observer la localisation de BIN2 dans les cellules initiales du phloème dans un contexte mutant *ops* chez Arabidopsis. Idéalement une combinaison de mutant *opsl* ou une lignée RNAi réprimant directement le clade de trois gènes *OPS, OPSL1* et *OPSL2* ou toute la famille *OPS* permettrait de démontrer ce modèle.

Par ailleurs, OPS interagit avec un autre membre de la voie de signalisation : CDG1. Cette interaction pourrait à la fois être indispensable à la voie de signalisation des brassinostéroïdes (OPS interviendrait comme intermédiaire moléculaire ou relais de l'information) ou pourrait simplement être responsable de la localisation membranaire d'OPS. L'étude de la localisation d'OPS dans un fond CDG1 mutant permettra de répondre à cette question.

La protéine OPS est une protéine polaire mais aucun membre de la voie n'a encore été décrit comme tel. L'étude de la localisation subcellulaire de CDG1 et de BIN2 dans le phloème est à envisager. De plus, BSL1 et BSK1-3 sont d'autres protéines de la voie localisées à la membrane. L'interaction entre OPS et ces protéines reste à tester.

En outre, OPS interagit avec VCC à la membrane. La structure protéique de VCC étant proche de celle des tétraspanines, VCC pourrait agir comme organisateur membranaire. Afin de comprendre le rôle de l'interaction OPS/VCC, la localisation d'OPS-GFP dans un fond *vcc* mutant mérite d'être étudiée. La protéine VCC est-elle impliquée dans la voie de signalisation des brassinostéroïdes? Interagit-elle avec les partenaires membranaires de la voie en tant que chef organisateur permettant de rapprocher physiquement les partenaires dans une zone restreinte de la membrane plasmique? L'interaction entre VCC et les différents acteurs membranaires de la voie sera testée.

PARTIE 2 :

ANALYSE DE LA FAMILLE *OCTOPUS*

Au cours du chapitre précédent, nous avons montré le rôle d'OCTOPUS (OPS) en tant que régulateur positif de la voie de signalisation des brassinostéroïdes. Ces conclusions étaient majoritairement basées sur l'étude d'une lignée surexprimant *OPS* (OPS-OE), aucun phénotype classique relié aux brassinostéroïdes (nanisme, photomorphogénèse à l'obscurité) n'ayant pu être mis en évidence chez le simple mutant *ops*. Cependant certains arguments suggèrent que la voie de signalisation des brassinostéroïdes est affectée chez ce mutant : (1) le mutant est partiellement restauré par un traitement à la bikinine, (2) l'allèle gain de fonction *bzr1-D* restaure également la longueur de la racine dans ce mutant.
Le gène *OPS* code une protéine conservée chez les angiospermes possédant un domaine de fonction inconnue DUF740 (Figure 6.1B). Il appartient à la famille multigénique pfam05340 composée de cinq gènes chez Arabidopsis qui partagent tous ce domaine (Figure 6.1A-C). *OPS* appartient plus particulièrement au clade de trois gènes composés d'*OPS* (At3g09070), *OCTOPUS-LIKE 1* (*OPSL1*, At5g01170) et *OCTOPUS-LIKE 2* (*OPSL2*, At2g38070) avec qui il partage 50% d'homologie de séquence protéique (Figure 6.1A, C). Les gènes *OPS, OPSL1, OPSL2* seront désignés sous le terme générique *OPS-LIKE* (*OPSL*).

Afin de préciser le rôle des autres membres de la famille *OPS* sur le développement des plantes et plus particulièrement sur la voie des brassinostéroïdes, nous avons développé une approche génétique pour répondre à ces questions. L'étude génétique utilisant les simples mutants d'une famille multigénique n'est pas toujours suffisante pour révéler un phénotype du fait de la redondance qui peut exister au sein d'une famille. La redondance fonctionnelle peut être définie comme la capacité pour un gène (ou le produit d'un gène) à compenser au moins partiellement la perte de l'activité d'un autre gène non allélique. Dans le cadre d'une redondance fonctionnelle, il est alors nécessaire de travailler avec des combinaisons de mutants pour révéler la fonction d'une famille de gènes.

Au sein de la famille OCTOPUS, existe-il une redondance fonctionnelle impliquée dans la voie de signalisation des brassinostéroïdes ?

Afin de préciser le rôle des autres membres de la famille *OPS*, j'ai étudié le clade *OPS, OPSL1* et *OPSL2*. Dans un premier temps j'ai analysé les lignées surexprimant les gènes *OPSL*, puis

les profils d'expression des gènes *OPSL1* et *OPSL2*. J'ai ensuite caractérisé les mutants correspondants et les différentes combinaisons de mutants.

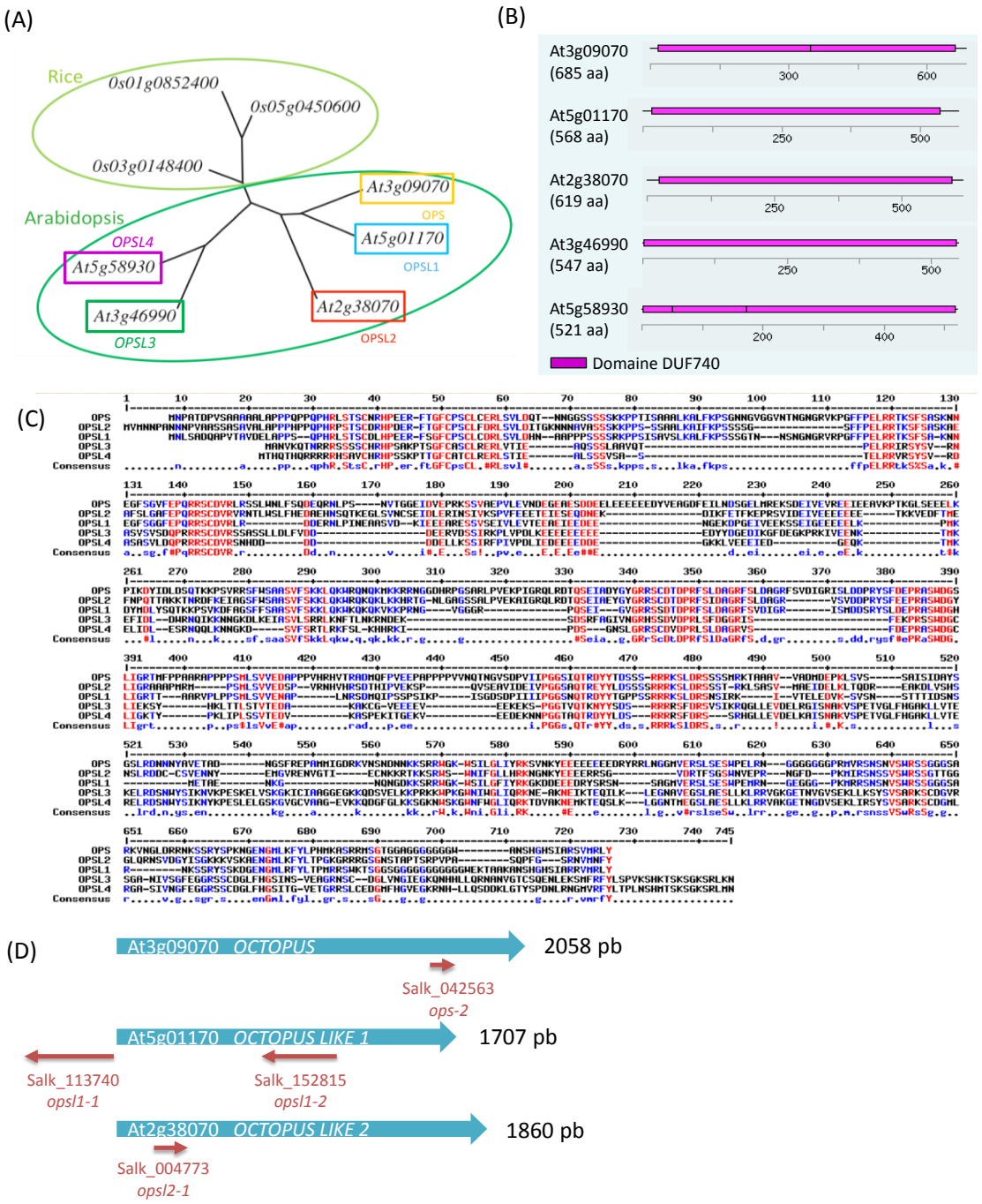

Figure 6.1: Portrait de la famille *OCTOPUS*

(A) Arbre phylogénétique de la famille *OPS-LIKE*. Adapté de Nagawa et al., 2006 **(B)** Le domaine DUF740 occupe toute la longueur des protéines de la famille OPCTOPUS. aa: acides aminées. Adapté de http://aramemnon.uni-koeln.de/index.ep **(C)** Alignement de séquence des protéines OPS-LIKE http://multalin.toulouse.inra.fr/multalin/ **(D)** Les gènes *OPS-LIKE*, longueur de leur CDS et allèles des mutants Salk

1 Etude des lignées surexprimant des *OCTOPUS-LIKE*.

Les gènes *OPS-LIKE* ont été exprimés sous le contrôle d'un promoteur constitutif (35S) et fusionnés à la GFP. Ces lignées seront désignées par la suite par OPS-LIKE-OE. Le but était de voir si la surexpression les gènes *OPSL1* et *OPSL2* conduisait aux mêmes phénotypes, de préciser la localisation subcellulaire des OPS-LIKE et de mettre en évidence une fonction commune aux *OPS-LIKE*.

1.1 Etude du phénotype des lignées surexprimant des *OPS-LIKE*

A partir des constructions décrites plus hautes, des plantes transgéniques d'*Arabidopsis thaliana* ont été obtenues. Les lignées OPSL1-OE et OPSL2-OE présentent des phénotypes similaires aux lignées OPS-OE (Figure 6.2A,B,D). L'hypocotyle est plus long, les pétioles sont allongés et les cotylédons sont enroulés.

Ce phénotype est très visible en T1 mais peu stable comme le montre la lignée OPSL2-OE. Au sein d'une même lignée homozygote, certaines plantules présentent le phénotype, d'autres pas. Le phénotype de réponse constitutive de la lignée OPSL2-OE est très hétérogène (Figure 6.2A,B,D). Néanmoins, ce phénotype caractéristique des mutants présentant une réponse constitutive aux brassinostéroïdes est observé dès l'instant où les gènes OPSL sont surexprimés. Ceci suggère fortement une fonction similaire pour les trois gènes *OPS, OPSL1 et OPSL2*.

Afin de tester cette hypothèse, nous avons évalué le statut de phosphorylation de BES1 dans les lignées OPS-LIKE-OE (Figure 6.2F). Comme pour la lignée OPS-OE, la lignée OPS-L1-OE accumule de manière préférentielle la forme non phosphorylée de BES1 suggérant que la voie des brassinostéroïdes est induite dans ces lignées. Cette expérience mérite d'être répétée sur une lignée OPSL2-OE homogène. Cependant, nos données suggèrent que les gènes *OPS-L1* et *OPS-L2* seraient également impliqués dans la voie des brassinostéroïdes qu'ils réguleraient positivement.

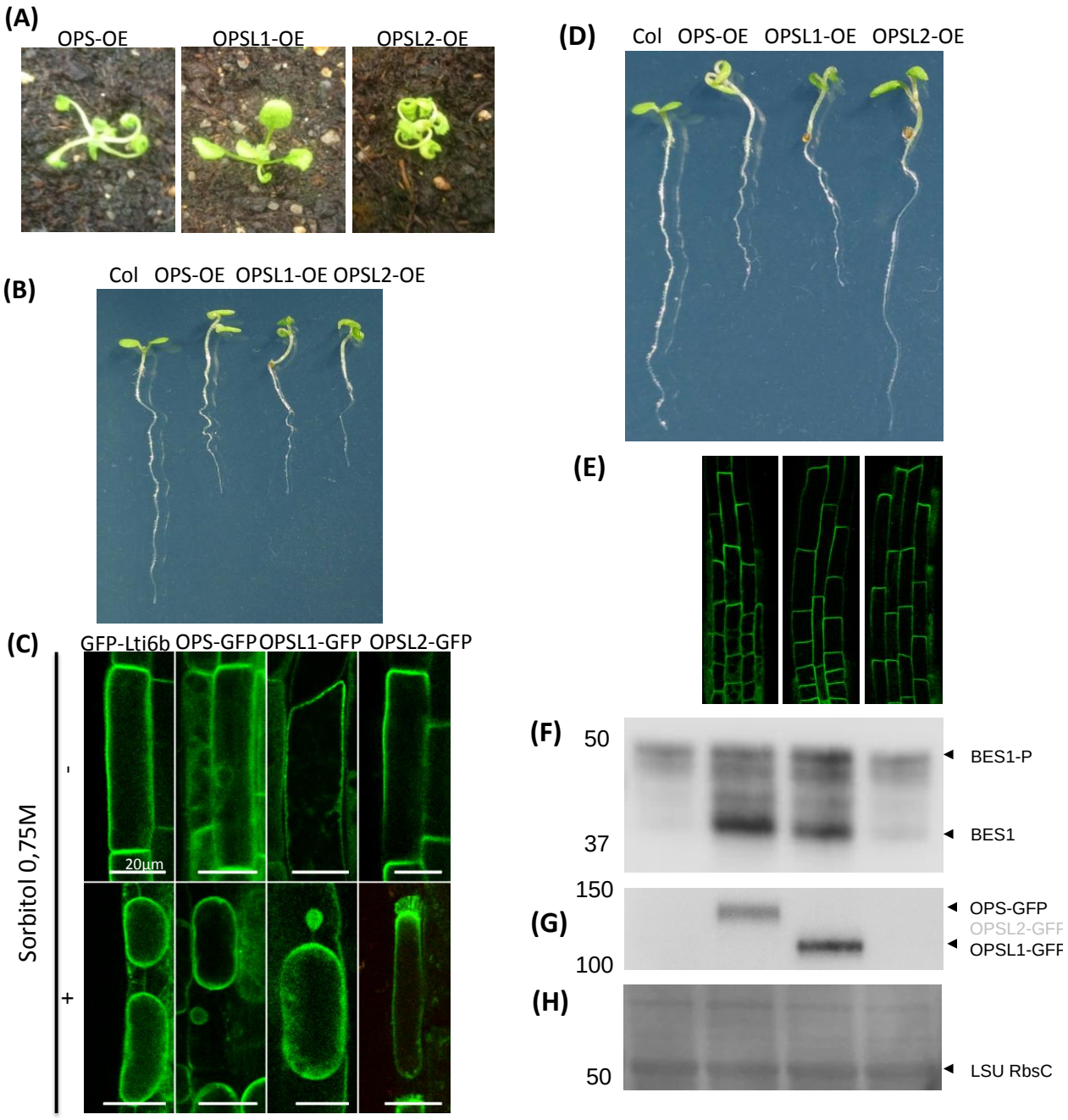

Figure 6.2 : Les lignées transgéniques surexprimant des *OPS-LIKE* ont un phénotype similaire à la lignée transgénique OPS-OE et induisent la voie des brassinostéroïdes

(A-B) Phénotypes des lignées transgéniques OPS-LIKE-OE. **(A)** plantes T1 âgées de 3 semaines ayant poussées en serre **(B)** plantules T2 âgées de 7 jours ayant poussé in vitro. (NB les lignées OPSL2-OE présentaient un fort taux de « silencing » du transgène et seule une minorité des plantules de cette lignée présentent ce phénotype) **(C)** Localisation subcellulaire des protéines OPS-LIKE-GFP et Lti6B-GFP exprimées sous le contrôle d'un promoteur 35S, traitées ou non avec du sorbitol à 0,75M et observées par microscopie confocale. Les protéines OPSL-GFP sont localisées à la membrane dans la racine Echelle : 20µm **(D-H)** Plantules agées de 7 jours ayant poussé sur milieu Arabidopsis **(D)** Phénotype des plantules. OPSL2-OE revertant (la majorité des plantules de cette lignée présentent ce phénotype) **(E)** Localisation subcelulaire des OPSL-GFP (polaire et apicale) **(F)** Western-blot anti-BES1 correspondant **(G)** Western blot anti-GFP controlant l'expression le niveau d'expression des proteines OPSL-GFP **(H)** Coloration Coomassie. LSU RbsC: large sous unité de la RUBISCO

1.2 Complémentation du phénotype *ops* par OPS-L1-OE et OPS-L2-OE

Afin de tester si les gènes *OPS-LIKE* assurent la même fonction qu'OPS, nous avons surexprimé *OPSL1* et *OPSL2,* fusionnés à la GFP dans un fond génétique *ops* par transformation d'Arabidopsis.

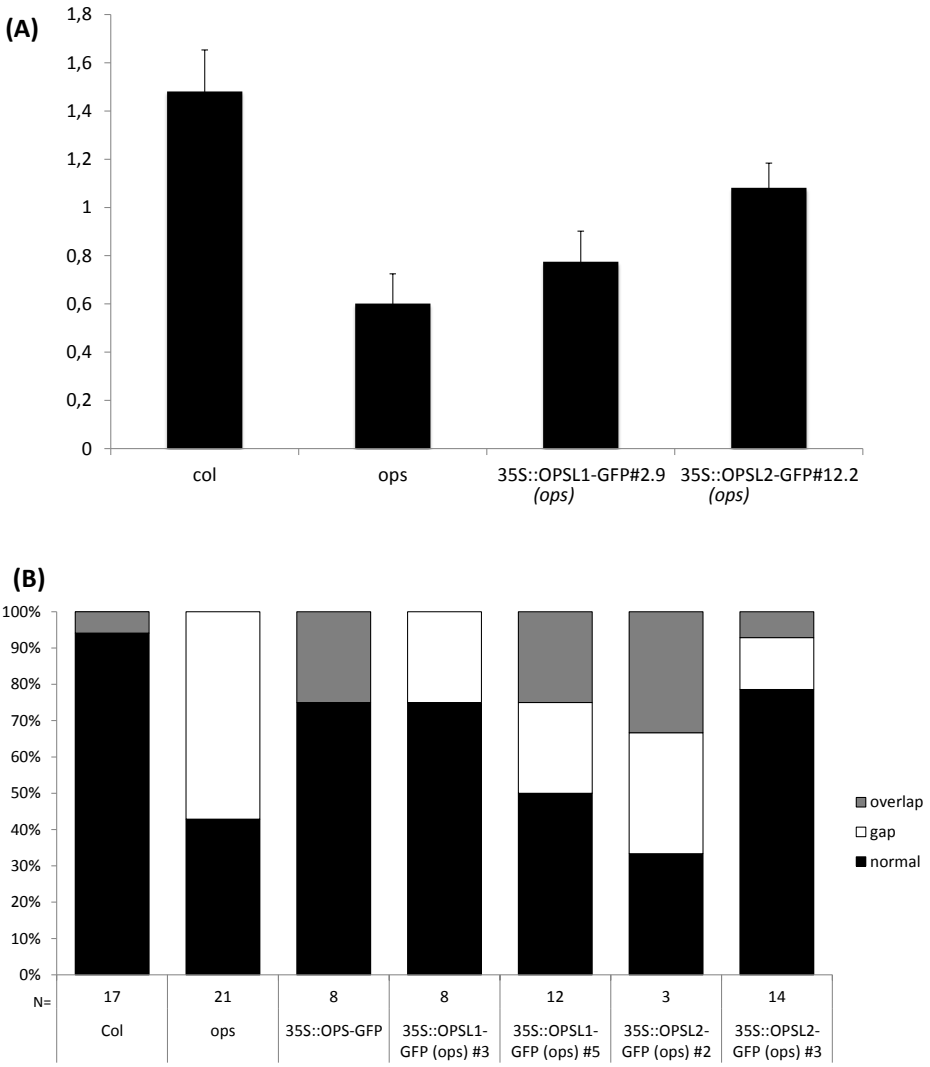

Figure 6.3 : Complémentation partielle d'*ops* par les lignées surexprimant des *OPS-LIKE*
(A) Longueur de racines du mutant *ops* dans un fond génétique surexprimant ou non des *OPS-LIKE*. Plantules âgées de 7 jours ayant poussées sur milieu Arabidopsis à 1% de saccharose à la lumière. **(B)** Phénotype phloèmien racinaire chez le mutant *ops* dans un fond génétique surexprimant ou non des *OPS-LIKE*. Plantules 7 jours ayant poussées sur milieu Arabidopsis à 1% de saccharose à la lumière, colorées à l'iodure de propidium et analysées par microscopie confocale.

Nous avons suivi le développement racinaire ainsi que la différenciation du phloème dans les différents contextes génétiques. Alors que le mutant *ops* présente une racine atrophiée, la sur-expression des gènes *OPSL1* et *OPSL2* dans ce contexte conduit à une restauration partielle de cette racine (Figure 6.3A). Cependant, la surexpression des *OPS-LIKE dans* un

contexte Col conduit également à une atrophie de la racine (Figure 6.2B). Il semble donc difficile pour ces lignées de restaurer parfaitement un défaut de croissance racinaire.

Le mutant *ops* présente également plus de 50% de racines affectées dans la différenciation du phloème alors que la lignée *ops* 35S::OPS-L2-GFP#3 ne présente que 20% de défauts (Figure 6.3B). Cette complémentation du phénotype d'*ops* par la surexpression des gènes OPS-LIKE ne se vérifie pas pour les autres lignées surexprimant les gènes *OPS-LIKE* dans un fond *ops*. Il semblerait qu'il y ait qu'une complémentation partielle du phénotype phloèmien au niveau de la racine par les lignées OPS-LIKE-OE. Pourtant, ce résultat est en accord avec les résultats trouvés au laboratoire (Truernit et al., 2012) montrant que la complémentation du mutant *ops* par une construction 35S::OPS-GFP n'était que partielle.

Afin de vérifier la complémentarité des *OPS-LIKE*, leur interchangeabilité et de s'affranchir de l'effet délétère de la surexpression des gènes *OPS-LIKE*, il est envisagé de complémenter le mutant *ops* par une stratégie d'échange de promoteur de type pOPS::OPSL1 et/ou pOPS::OPSL2. D'autre part, OPS-OE permet de restaurer les mutants *bri1-116* et *bin2-1D*. Afin de confirmer la redondance fonctionnelle des gènes *OPSL*, des croisements entre OPSL-OE et ces deux mutants seront à prévoir.

1.3 Etude de la localisation subcellulaire des protéines OPS-LIKE

Nous avons utilisé les lignées surexprimant les *OPS-LIKE* pour étudier la localisation subcellulaire des protéines OPS-LIKE.

Des plantules contenant les constructions 35S::OPS-GFP, 35S::OPSL1-GFP, 35S ::OPSL2-GFP et 35S ::Lti6b-GFP ont été cultivées pendant 7 jours et observées par microscopie confocale. Lti6B est une protéine membranaire utilisée comme témoin. On remarque que les protéines OPS-LIKE présentent une localisation comparable à celle de Lti6B, à la différence près que les OPS-LIKE semblent s'accumuler préférentiellement au pôle apical des cellules (Figure 6.2C,E). Afin de s'assurer que le signal observé correspond effectivement à un signal membranaire et non pariétal, les plantules ont été traitées au sorbitol. Le sorbitol a pour but de plasmolyser les cellules et de décoller les membranes plasmiques des parois cellulaires. Les signaux OPSL-GFP suivent le mouvement de rétraction de la cellule, comme Lti6B-GFP (Figure 6.2C). D'après ces observations, les protéines OPS-LIKE sont des protéines associées à la membrane qui s'accumulent au pôle apical des cellules.

2 Etude des profils d'expression des gènes *OCTOPUS-LIKE*

Les travaux de Nagawa et al. et Bauby et al. (Nagawa et al., 2006; Bauby et al., 2007) ont permis d'identifier le gène *OPS* sur la base d'un crible de piégeage de promoteur spécifiquement exprimé dans les tissus vasculaires. Dans ce cadre, l'insertion du gène rapporteur *UidA,* codant pour la glucuronidase*,* en aval du promoteur *OPS* conduit à l'expression du gène *UidA* dont l'activité est ensuite révélée par un test d'activité glucuronidase. Le gène *OPS* s'exprime très tôt au cours du développement comme en atteste son expression dès le stade globulaire de l'embryon (Truernit et al., 2012). Peu à peu son expression se restreint au procambium dans l'embryon mature où elle préfigure les futurs tissus vasculaires pour se limiter ensuite uniquement au phloème dans la racine (Bauby et al., 2007). Nagawa et al. (Nagawa et al., 2006) ont également étudié les profils d'expression des gènes les plus proches d'*OPS* (*OPSL1* et *OPSL2*) dans des lignées transgéniques contenant le gène *UidA* exprimé sous le contrôle des promoteurs *OPSL1* et *OPSL2.*

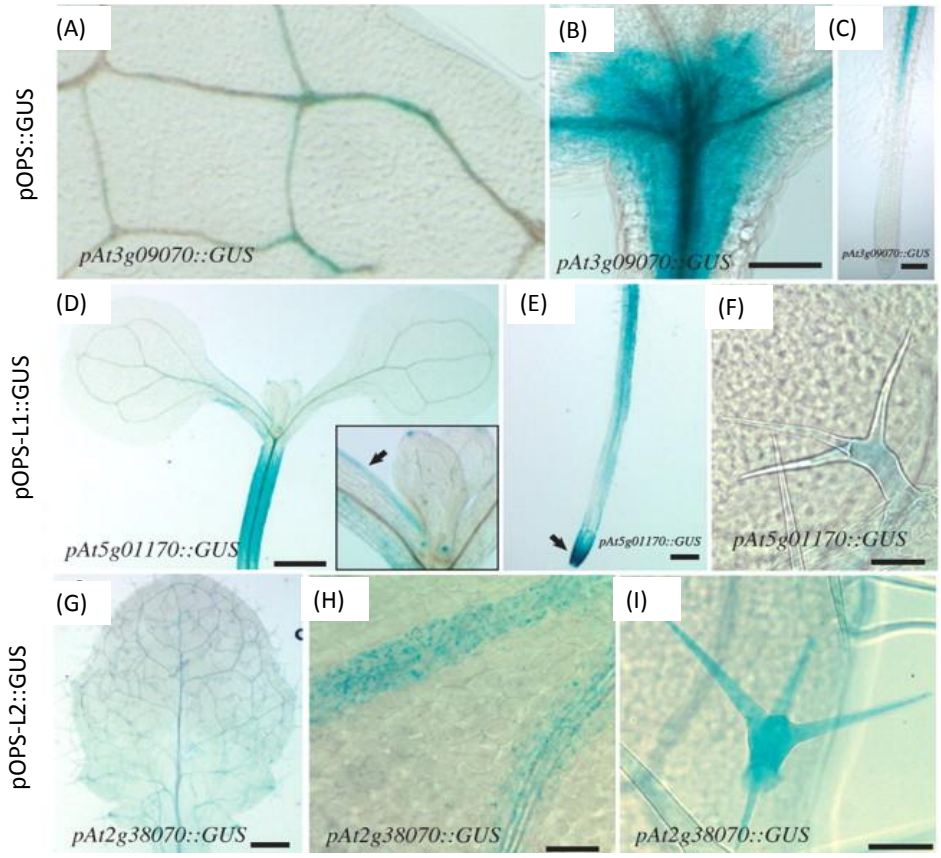

Figure 6.4: Profil d'expression des gènes de la famille *OPS-LIKE* par Nagawa et al.
(A-C) Coloration GUS de plante transgénique pOPS::GUS. La coloration GUS est détectée dans les tissus vasculaires des feuilles de rosette**(A)** et des racines **(C)**. La région du méristème apical caulinaire est aussi colorée **(B)**. **(D-F)** Coloration GUS de plante transgénique pOPS-L1::GUS La coloration GUS est détectée dans les tissus vasculaires et dans l'épiderme des organes aérien **(D)** et racinaires **(E)**. La pointe racinaire (flèche en E) et les trichomes **(F)** sont aussi colorés. La flèche dans l'encart **(D)** pointe la coloration GUS dans l'épiderme de pétiole d'un cotylédon **(G-I)** Coloration GUS de plante transgénique pOPS-L2::GUS. La coloration GUS est détectée dans le procambium des feuilles de rosette **(G et H)**. Les trichomes sont également colorés **(I)**. Echelle en **(A-C), (E)** et **(G)** = 100 µm; **(D)** = 200 µm; **(F), (H), (I)** = 20 µm. Adapté de (Nagawa et al., 2006)

2.1 Etude de l'expression du gène *OCTOPUS-LIKE1*

Nagawa et al. ont pu montrer que le gène *OPSL1* est exprimé dans les tissus vasculaires des cotylédons, de l'hypocotyle et de la racine (Figure 6.4D) (Nagawa et al., 2006). Cette expression n'est pas restreinte aux tissus vasculaires puisque l'activité glucuronidase est également détectée au niveau de l'épiderme (Figure 6.4D), des trichomes (Figure 6.4F) et de la pointe de la racine (Figure 6.4E).

Afin de préciser l'expression du gène *OPSL1* au sein du tissu vasculaire nous avons étudié cette lignée transgénique au cours du développement. L'étude a été menée à différents stades au cours de l'embryogenèse et sur des plantules cultivées in vitro âgées de 7 jours. Le test cyto-enzymologique de l'activité glucuronidase a été réalisé avec des concentrations variables en ferricyanure et ferrocyanure.

En condition de faibles concentrations en ferrcyanure-ferrocyanure (entre 0 et 1mM), je n'ai pas mis en évidence d'expression du gène *OPSL1* au cours de l'embryogénèse (Figure 6.5H-K). En revanche, *OPSL1* est exprimé dans l'épiderme à des stades post-embryonnaires dans les parties racinaire (Figure 6.5L) et aérienne (Figure 6.5M, N). Au niveau de l'épiderme racinaire, *OPSL1* n'est pas exprimé dans toutes les files cellulaires, suggérant une expression préférentielle pour un type cellulaire (soit les trichoblastes ou atrichoblastes). Des colorations GUS en condition de forte concentration en ferricyanure-ferrocyanure (10mM) couplées à une coloration à l'iodure de propidium (IP) qui colore les parois cellulaires ont permis de préciser la localisation cellulaire de l'expression. A l'aide d'un microscope confocal, une série de coupes optiques longitudinales de la racine a été effectuée, préservant le signal de fluorescence de la paroi (IP) et la réflexion des cristaux issus des produits de l'activité glucuronidase. La reconstitution d'une coupe transversale virtuelle de la racine a permis de montrer que le gène *OPSL1* s'exprime dans les cellules atrichoblastiques de la racine (Figure 6.5V).

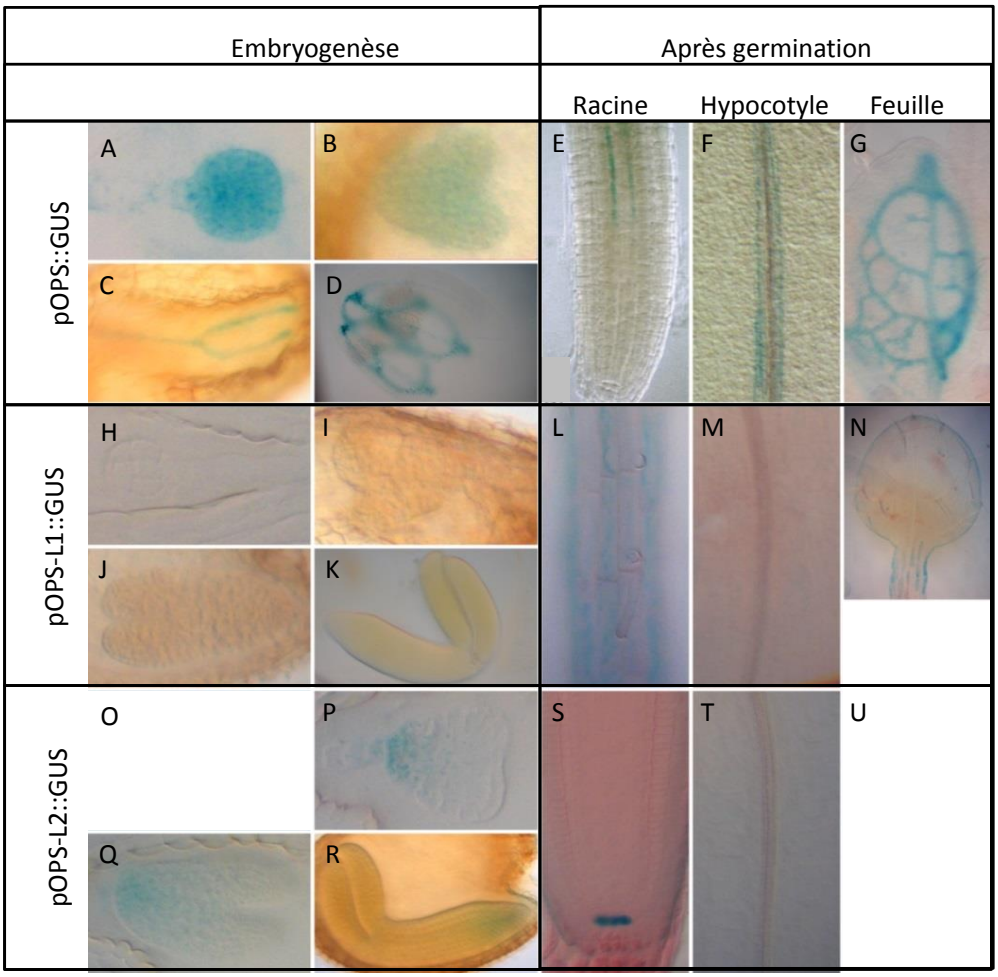

(V)

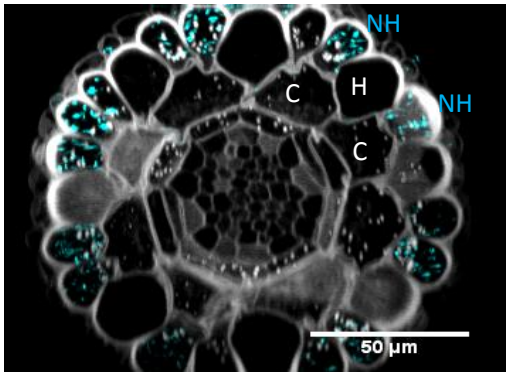

Figure 6.5: Profil d'expression des gènes *OPS-LIKE* au cours du développement
(A-G) Coloration GUS d'une plante transgénique pOPS::GUS. **(H-N)** Coloration GUS d'une plante transgénique pOPS-L1::GUS **(O-U)** Coloration GUS d'une plante transgénique pOPS-L2::GUS
Profil d'expression au cours de l'embryogenèse: **(A,H,O)** Stade globulaire ; **(B,I,P)** Stade cœur ; **(C,J,Q)** Stade torpedo; **(D,K,R)** Embryon mature
Profil d'expression après germination: **(E,L,S)** dans la racine; **(F,M,T)** dans hypocotyle ; **(G,N,U)** dans la feuille.
(V) *OPS-L1* est exprimé dans les atrichoblastes. Analyse confocal d'une coloration GUS de plante transgénique pOPS-L1::GUS couplée à une coloration à l'iodure de propidium. Echelle: 50µm; C: cortex ; H: trichoblaste; NH: atrichoblastes
Concentration en ferricyanure-ferrocyanure: (A,B,H-K) 0mM ; (C,D) 2mM; (P-R) 1mM; (E-G,L-N,V) 10mM de ferricyanure ferrocyanure (S,T) 7,5mM

Par ailleurs, *OPSL1* s'exprime également au niveau de la marge foliaire et à la base du pétiole de la feuille dans une file cellulaire sur deux (Figure 6.5N). Ce profil préférentiel pour un type cellulaire semble être conservé dans l'ensemble de la plante.

De manière surprenante, je n'ai pas réussi à reproduire les résultats de Nagawa et al. concernant l'expression d'*OPSL1* au niveau du procambium ni à mettre en évidence de redondance d'expression entre *OPS* et *OPSL1*. Pour répondre à cette question et afin d'étudier la localisation subcellulaire de chacune des protéines OPS-LIKE, j'ai cloné un fragment génomique d'*OPSL1* sous le contrôle de son propre promoteur (2Kb) en fusion traductionnelle dans des vecteurs exprimant soit la GFP ou la RFP (pGWB4 et pGW553 respectivement (Nakagawa et al., 2007)). Malheureusement, parmi 12 lignées transgéniques analysées, aucune n'exprimait suffisamment fortement le signal fluorescent pour être capable d'identifier la localisation tissulaire et subcellulaire d'OPSL1-XFP.

2.2 Etude de l'expression du gène *OCTOPUS-LIKE2*

Nagawa et al. (Nagawa et al., 2006) ont pu montrer que le gène *OPSL2* est exprimé dans le procambium des feuilles et dans les trichomes (Figure 6.4G-I). Afin de préciser l'expression du gène *OPSL2* au sein du tissu vasculaire nous avons étudié cette lignée transgénique au cours des mêmes stades de développement que pour *OPSL1*.

Au cours de l'embryogenèse, le gène *OPSL2* s'exprime à la base de l'embryon dès le stade cœur (Figure 6.5P-R). Son domaine d'expression se précise après germination pour se restreindre aux seules cellules du centre quiescent (Figure 6.5S). De même que pour *OPSL1*, je n'ai pas réussi à reproduire les observations de Nagawa et al. (Nagawa et al., 2006) concernant les domaines d'expressions d'*OPSL2*.

Par la suite j'ai voulu étudier la localisation tissulaire et subcellulaire d'OPSL2. Je voulais également exprimer de manière conjointe les *OPS-LIKE* et mettre en évidence une éventuelle redondance d'expression, c'est pourquoi j'ai effectué des clonages pour exprimer *OPSL2* en fusion transcriptionnelles et traductionnelles d'*OPSL2*. Malheureusement, je n'ai pas pu obtenir de lignées transgéniques présentant un niveau d'expression satisfaisant me permettant de répondre à ces questions.

D'après mes données d'expression GUS, les gènes *OPS-LIKE* ne sont pas redondants car leurs profils d'expression ne se recoupent pas. Pour compléter l'étude d'expression des *OPS-LIKE*, il faudrait cribler plus de lignées transgéniques pOPSL::XFP et pOPSL::OPSL-XFP permettant ainsi d'isoler des lignées exprimant suffisamment fortement le signal fluorescent ou réaliser des hybridations *in situ*.

3 Etude génétique des simples mutants et des combinaisons de mutants *octopus-like*

Avant mon arrivée au laboratoire, des lignées mutantes *ops*, *opsl1* et *opsl2* avait déjà été isolées et des combinaisons de mutants étaient disponibles. J'ai donc consacré ma première année de thèse à l'étude de ces mutants et de leurs combinaisons. Ces premières combinaisons de mutants, disponibles avant mon arrivée et utilisant l'allèle *opsl1-1* (Salk_113740*)* (Figure 6.1D)*,* présentaient un phénotype non lié au locus *OPSL1* et ont fortement retardé l'avancée de ce projet. Nous avons alors isolé un deuxième allèle (*opsl1-2*, Salk_152815) (Figure 6.1D) et reproduit les croisements pour obtenir les combinaisons de mutants. C'est pourquoi la caractérisation de ces mutants multiples est encore peu aboutie.

3.1 Obtention des mutants et combinaisons de mutants

Afin de réaliser une étude génétique sur le clade *OPS-LIKE*, nous avons utilisé plusieurs mutants insertionels relatifs à *OPS*, *OPSL1* et *OPSL2*. Les mutants *ops-like* sont des mutants d'insertion ADN-T dans l'écotype Columbia. Le mutant *ops-2* avait déjà été décrit (Truernit et al., 2012) et correspond à la lignée (Salk_042563) (Figure 6.1D). Nous disposions d'un allèle *opsl2-1* pour le gène *OPSL2* (Salk_004773) et deux allèles pour le gène *OPSL1 : opsl1-1 et opsl1-2* (Salk_113740 et Salk_152815) (Figure 6.1D).

Avant mon arrivée au laboratoire, des analyses génétiques avaient permis d'isoler des lignées homozygotes pour *opsl1-1* et *opsl2-1* ainsi que deux combinaisons de sesqui-mutants (trois des quatre copies mutées) pour les combinaisons *opsl1-1 opsl2-1* et *ops opsl1-1*. Ces

deux combinaisons présentaient des phénotypes développementaux similaires à savoir une hypertrophie du méristème apical caulinaire. Nous étions donc partis en premier lieu sur l'étude et la caractérisation du phénotype méristématique de ces combinaisons de mutants. Cependant, au cours de cette analyse, je me suis aperçue que le matériel génétique n'était pas homogène et que le phénotype sur lequel nous travaillions n'était pas lié au locus, mais qu'il s'agissait d'une mutation parasite issue de la lignée d'insertion *opsl1-1*. Nous avons décidé de repartir d'un nouvel allèle *opsl1* : le Salk_152815, *opsl1-2*. Après avoir vérifié le matériel génétique, j'ai généré les différentes combinaisons de mutants par croisements.

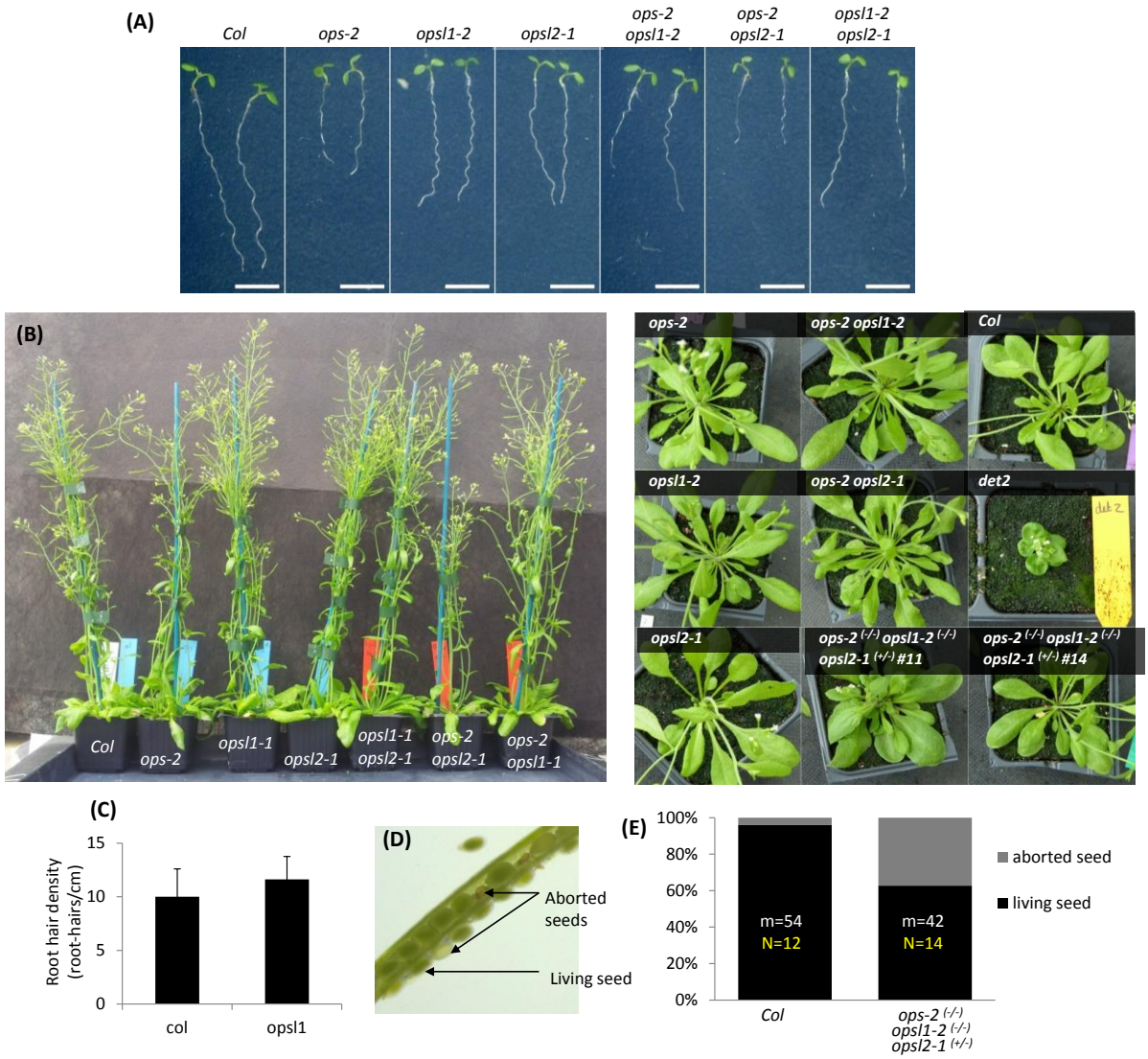

Figure 6.6: Phénotypes des mutants *ops et ops-like, seuls ou en* combinaison
(A) Plantules de 7 jours ayant poussée sur milieu Arabidopsis à la lumière **(B)** Plantes âgées de 8 semaines poussées en serre (vue de face). Plantes âgées de 5 semaines poussées en serre (vue de dessus) **(C)** Densité de poils absorbants chez le mutant *opsl1-2* comparée au sauvage (N=10) **(D)** Dissection de silique et phénotype des graines (vivante ou avortée) **(E)** Pourcentage des graines vivantes et avortées issues d'une plante sauvage et d'une combinaison de mutants *ops-2 (-/-) opsl1-2 (-/-) opsl2-1 (+/-)*. m: nombre moyen de graines par silique; N:nombre total de siliques disséquées.

3.2 Etude des simples mutants *octopus-like*

Le mutant *ops-2* décrit par Truernit et al. (Truernit et al., 2012), présente une racine courte (Figure 6.6A) et des défauts dans la mise en place des tissus vasculaires. Chez *ops-2*, il y a une perte de la complexité du réseau vasculaire avec une diminution du nombre de boucles vasculaires cotylédonaires (Figure 6.7A,B,D) .

Dans une moindre mesure, les mutants *opsl1-2* et *opsl2-1* semblent présenter comme *ops-2* des défauts de développement racinaire avec une racine plus courte que le sauvage (Figure 6.6A). Cependant, la quantification de cette altération doit être déterminée.

Aux vues du profil d'expression du gène *OPSL1*, j'ai tenté de caractériser plus finement d'éventuels défauts dans la mise en place des poils racinaires. Pour cela, j'ai effectué cette analyse sur des plantules âgées de 7 jours et ai déterminé la densité de poils absorbants sur les deux faces de la racine sur une section de 1 mm à partir du premier poil formé. Les résultats préliminaires suggèrent que la densité de poils racinaires est légèrement plus importante chez le mutant *opsl1-2* que chez la plante sauvage (Figure 6.6C). Cette expérience doit être répétée en augmentant le nombre d'échantillons.

A la lumière de l'étude de Gonzalez-Garcia et al. (González-García et al., 2011), l'étude à l'échelle microscopique du mutant *opsl2-1* pourrait être envisagé afin d'analyser l'impact d'*OPSL2* sur la maintenance du centre quiescent (activité mitotique, taille du méristème).

Par ailleurs, l'analyse macroscopique des mutants *ops-like* n'a pas permis pas de révéler un phénotype développemental évident en serre (Figure 6.6B).

3.3 Etude des combinaisons de mutants *octopus-like*

3.3.1 Etude du phénotype

Afin de révéler un phénotype et identifier l'implication des gènes *OPS-LIKE* dans le développement, les combinaisons de mutants d'*ops-like* ont été générées.

Au stade plantule, le phénotype « racine courte » visible dans le mutant *ops-2* est toujours présent dans les différentes combinaisons *ops-2 opsl1-2* et *ops-2 opsl2-1* et semble être aggravée dans la combinaison avec *opsl2-1* (Figure 6.6A).

La complexité des boucles vasculaires cotylédonaires a également été étudiée dans les mutants et combinaison de mutants. Un score de complexité est attribué au réseau vasculaires cotylédonaires de plantes âgées de 7 jours. Ce score prend en compte le nombre de boucles vasculaires initiées et le nombre de boucles fermées. Pour exemple, un cotylédon à deux boucles ouvertes et une boucle fermée se verra attribuer un score de 4 (3 boucles initiées dont une fermée : 3+1) (Figure 6.7C). Bien que les mutants *opsl1-2* et *opsl2-1* montrent une complexité comparable au sauvage (Figure 6.7A,B,D), les phénotypes des doubles mutants semblent être aggravés comparé au simple mutant *ops-2* (Figure 6.7A,B,D) suggérant une redondance fonctionnelle des gènes *OPSL* dans la mise en place des réseaux vasculaires cotylédonaires. De plus, ces données confirment l'étude de Nagawa et al. (Nagawa et al., 2006) stipulant que les gènes *OPSL* sont exprimés dans les tissus provasculaires.

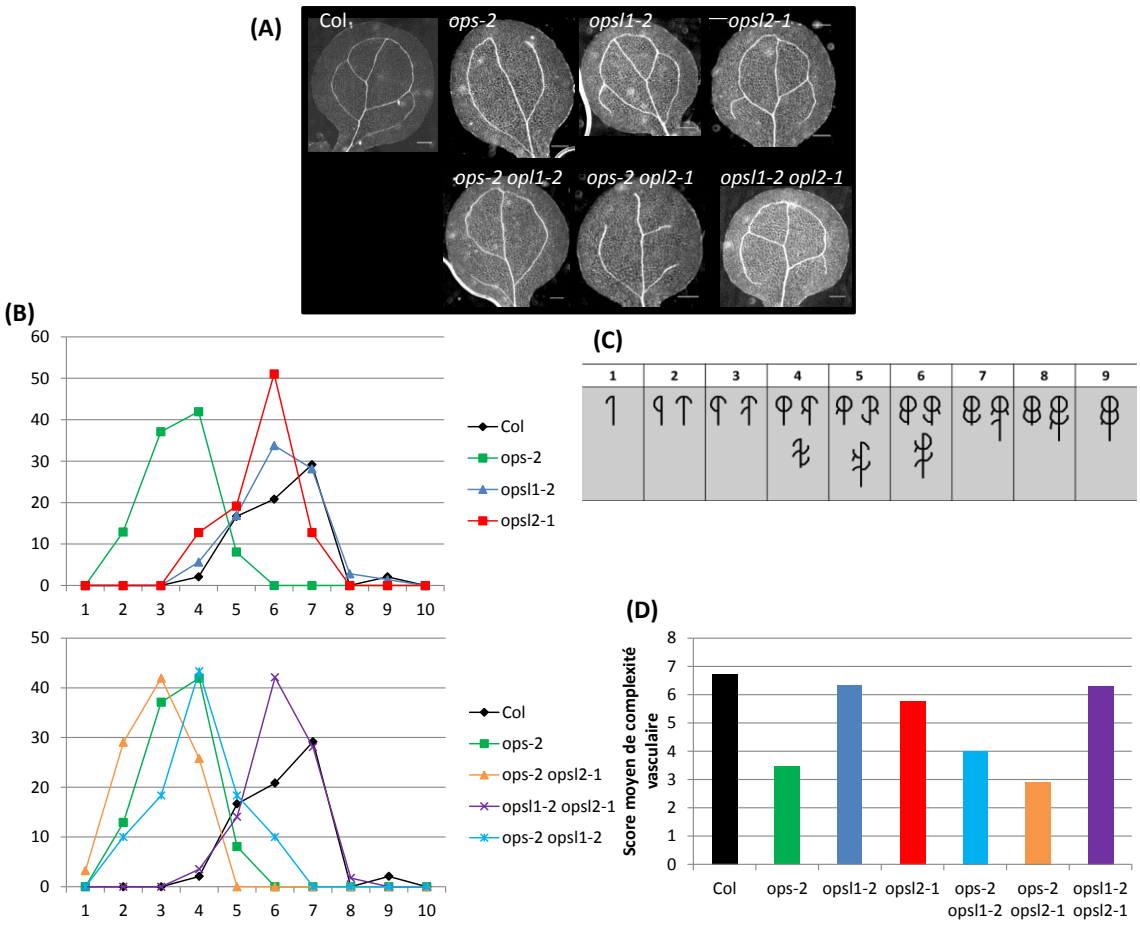

Figure 6.7: Une redondance dans le mise en place des patrons vasculaires cotylédonaires au sein de la famille *OPS*

(A) Phénotypes caractéristiques observés au niveau des boucles vasculaires cotylédonaires pour chacun des génotypes. Echelle: 200 µm **(B)** Pourcentage de plantes pour chaque score dans les génotype simple mutant (haut) et en combinaison de mutant (bas) **(C)** Phenotype correspondant à chaque score attribué **(D)**Score moyen de complexité pour chacun des génotypes

A des stades plus avancés, les plantes *ops-2 opsl2-1* ont des hampes florales d'une taille réduite comparées aux plantes sauvages (Figure 6.46D). La combinaison *opsl1-1 opsl2-1* quant à elle reste semblable au sauvage et la combinaison *ops opsl1-1* semblable à *ops*.

L'identification de plantes mutantes pour les trois loci, par génotypage des descendants F2 d'un croisement entre les double mutants ops-2 opsl2-1 et opsl1-2 opsl2-1 , n'a pas permis d'identifier de triples mutants homozygotes. Au mieux, j'ai identifié une plante de génotype *ops-2*$^{(-/-)}$ *opsl1-2* $^{(-/-)}$ *opsl2-1*$^{(+/-)}$. La descendance de cette plante n'a également pas permis d'identifier de triple mutants.

La difficulté à isoler un triple mutant suggère que cette combinaison n'est pas viable. Pour vérifier cette dernière hypothèse, des siliques d'une plante mère *ops-2*$^{(-/-)}$ *opsl1-2* $^{(-/-)}$ *opsl2-1*$^{(+/-)}$ ont été disséquées afin de mettre en évidence une éventuelle létalité embryonnaire. Nous avons pu constater que le pourcentage de graines non viables (avortement précoce, retard de développement) (Figure 6.6D) était supérieur à celui trouvé dans une plante sauvage (Figure 6.6E). Ces données suggèrent donc que l'obtention d'un triple mutant conduit à une létalité embryonnaire. Afin de caractériser au mieux la létalité embryonnaire chez le triple mutant, nous envisageons de caractériser le nombre d'embryons arrivant à terme dans les différents fonds mutants (simple et double mutants). On peut se demander quelle étape du développement est affectée dans la combinaison triple mutant. Est-ce au moment de la fécondation ou après fécondation que le développement est stoppé ? Une étude fine du développement embryonnaire permettra de définir à quel stade ces plantes sont affectées. Afin de contourner la létalité embryonnaire du triple mutant et de pouvoir étudier le rôle de ces trois gènes sur le développement post-embryonaire, il est envisagé de construire des lignées RNAi inductibles permettant de cibler les trois gènes.

Par ailleurs, il semblerait que la combinaison *ops-2*(-/-) *opsl1-2*(-/-) *opsl2-1*(+/-) ait une tendance au nanisme comme le montre les plantes en serre (Figure 6.6B). Cependant, d'une plante à l'autre, le phénotype apparait variable (feuilles plus ou moins rondes et compactes). La caractérisation phénotypique de cette combinaison reste donc à éclaircir.

3.3.2 Analyse de la réponse aux brassinostéroïdes chez les mutants *ops-like* et les combinaisons de mutants

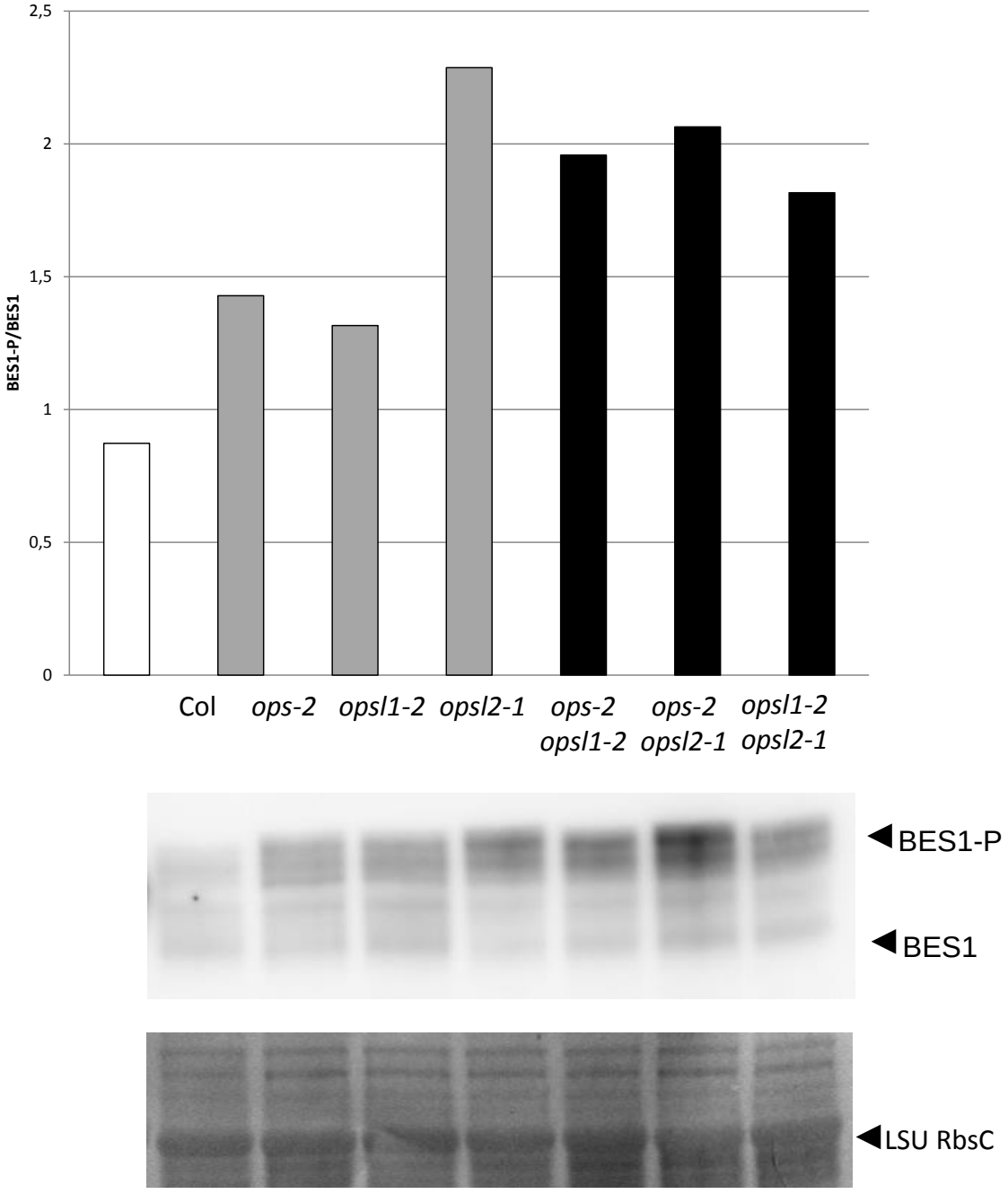

Figure 6.8: Les mutants *ops-like* et leurs combinaisons sont altérés au niveau de la voie des brassinostéroïdes **(A)** Ratio des intensités de signal des formes phosphorylées et non phosphorylées de BES1 dans les différents fond génétiques du Western-BLOT anti-BES1 prédenté en (B). Intensité de bande mesurées sur ImageJ **(B)** Western-blot anti-BES1 des simples mutants et des combinaisons de mutants *ops-like*. Plantules âgées de 7jours. **(C)** coloration coomassie de la membrane révélée en (B) servant de contrôle de chargement

Afin de préciser le rôle de la famille *OPS* dans la voie de signalisation des BR, nous avons contrôlé le statut de phosphorylation de BES1 dans les simples mutants et les différentes

combinaisons de mutants disponibles. Pour mettre en évidence des différences plus subtiles entre les contextes génétiques, nous avons mesuré le ratio BES1-P/BES1 qui correspond à la quantification de l'intensité des bandes non phosphorylées sur l'intensité des bandes phosphorylées (Figure 6.8A,B). Si le ratio est supérieur à 1, la forme phosphorylée est préférentiellement accumulée, symptôme d'une voie de signalisation de BR inhibée.

Les simples mutants *ops-2* et *opsl1-2* ont un ratio comparable au sauvage et semblent peu affectés dans la signalisation des brassinostéroïdes. Le mutant *opsl2-1*, en revanche, présente un effet plus prononcé sur la voie de signalisation comme en atteste son ratio BES1-P/BES1 supérieur à 2.

Les combinaisons de mutants sont aussi plus affectées que le sauvage et les simples mutants *ops-2* et *opsl1-2* mais reste comparable au mutant *opsl2-1.* Ces données suggèrent donc que la voie de signalisation des BR serait perturbée lorsque l'on accumule des mutations dans les gènes *OPS-LIKE*.

3.3.3 Une boucle de contrôle des brassinostéroïdes sur les gènes *OPSL*

Des analyses de transcriptome de mutants de la voie de signalisation des brassinostéroïdes ont révélé que *BRI1* est induit par la signalisation des brassinostéroïdes (Sun et al., 2010). Dans cette même étude, l'expression du gène *OPSL4* semble également contrôlée par la voie des brassinostéroïdes, mais de manière négative.

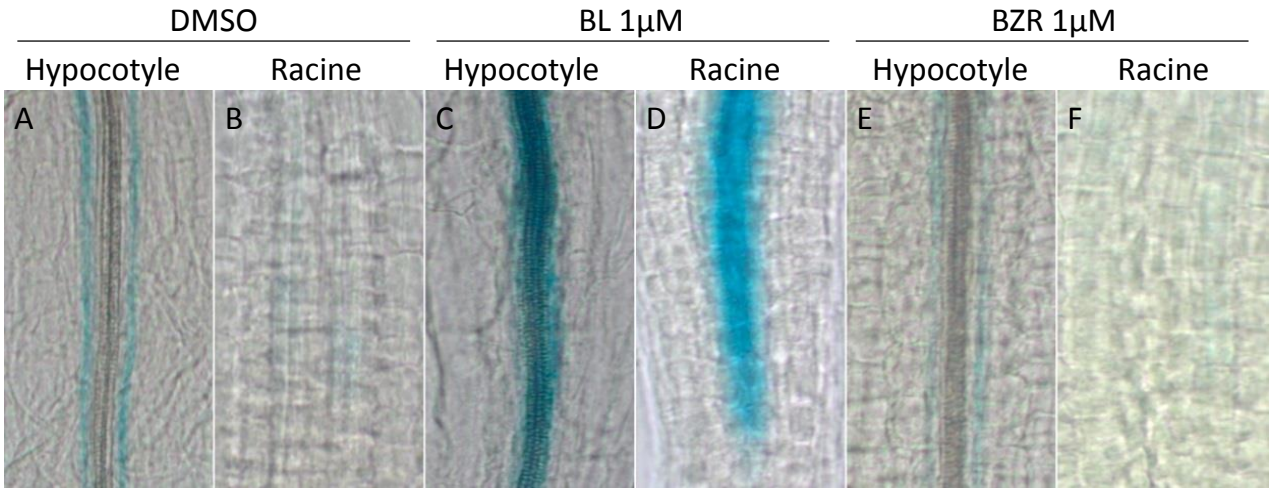

Figure 6.9: La expression du gène *OPS* peut être modulée par des traitements aux brassinostéroïdes
Coloration GUS (10mM de ferricyanure-ferrocyanure) de plantes transgéniques pOPS::GUS âgées de 7 jours 7 ayant poussé sur un milieu arabidopsis à 1% de saccharose avec ou sans 1µM BL / 1µM BZR.

Afin de confirmer le contrôle de l'expression des gènes *OPS* par la voie des brassinostéroïdes, des plantes transgéniques exprimant la construction pOPS ::UidA ont été cultivées *in vitro* en présence de 1µM de brassinolide ou 1µM de brassinazole. Une analyse qualitative de l'activité glucuronidase indique que l'expression de pOPS :UidA est induite par l'ajout de BL dans le milieu de croissance (Figure 6.9C-D comparé à 6.9A-B). L'effet du brassinazole est moins clair et nécessiterait une quantification plus précise (Figure 6.9E-F comparé à 6.9A-B).

Par ailleurs, des données de ChIP révèlent que le promoteur du gène *OPSL2* est reconnu par la protéine BZR1 (Sun et al., 2010). Les boites de fixation sur l'ADN des facteurs de transcription BZR1 et BES1 ont été caractérisées (He et al., 2005; Yin et al., 2005; Yu et al., 2011).

Une analyse de la séquence d'ADN des promoteurs *OPS-LIKE* révèle la présence de boites BRRE (CGTG(T/C)G) et E-box (CANNTG) pouvant être la cible des facteurs de transcription BZR1 et BES1 (Figure 6.10).

Ces éléments suggèrent qu'il pourrait exister un rétrocontrôle positif de la voie des brassinostéroïdes sur la transcription des gènes *OPS-LIKE*. Ces données seraient à confirmer par une analyse RT-q-PCR permettant de quantifier les taux de transcrit des gènes *OPS-LIKE* dans les différentes conditions hormonales.

(A)

(B)

(C)

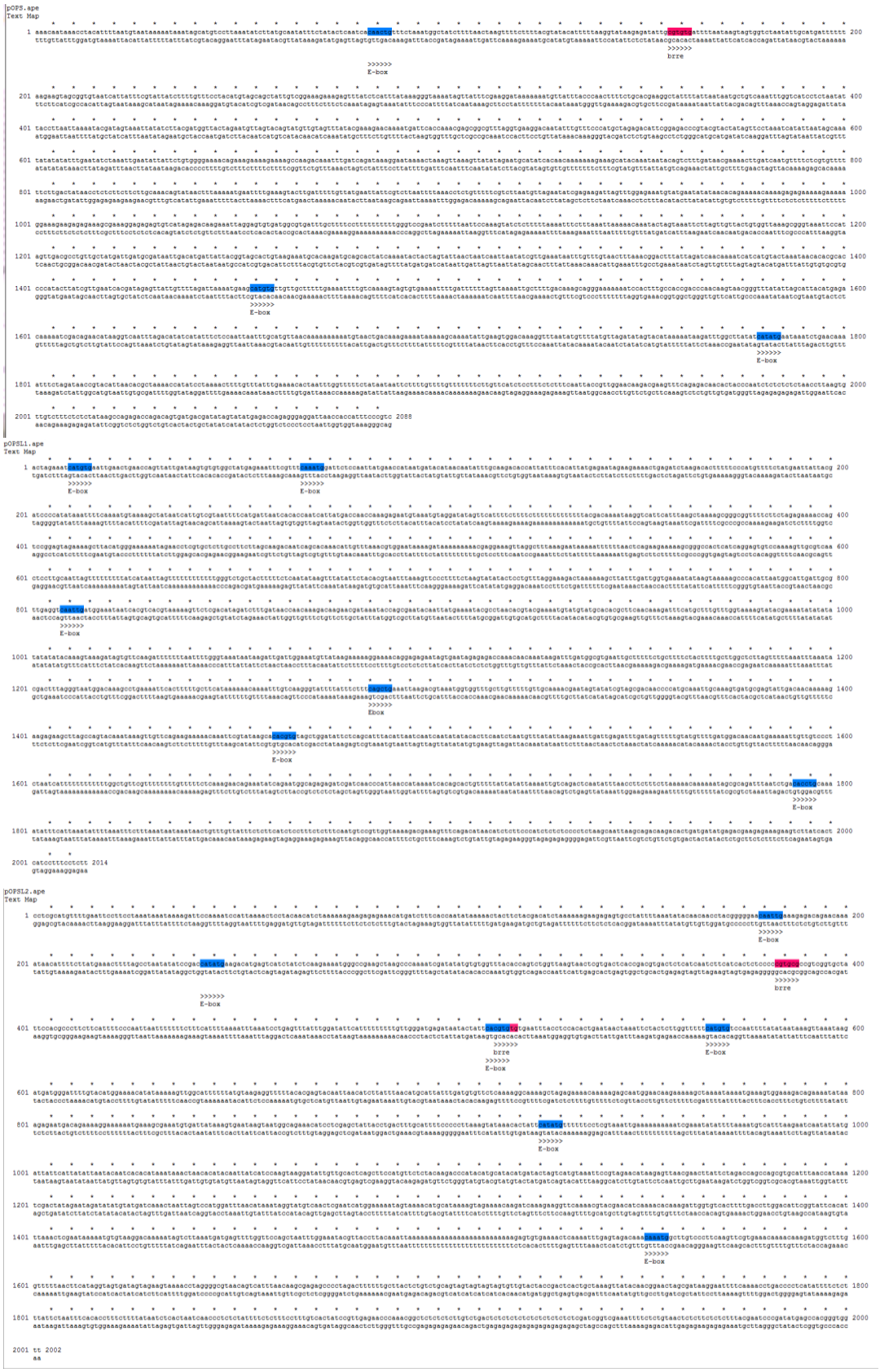

Figure 6.10: Les séquences des promoteurs *OPS-LIKE* contiennent par les motifs BRRE et E-box.
(A) Promoteur *OPS* 2kb en amont de l'ATG **(B)** Promoteur *OPSL1* 2kb en amont de l'ATG **(C)** Promoteur *OPSL2* 2kb en amont de l'ATG
En bleu : E-box (CANNTG); en rouge : BRRE (CGTG(T/C)G)

4 Discussion-conclusion

La surexpression des *OPS-LIKE* donne le même phénotype dans les différentes lignées OPS-LIKE-OE: allongement de l'hypocotyle, cotylédons enroulés. Ce phénotype, caractéristique des mutants induisant de manière constitutive la voie des brassinostéroïdes, est confirmé par l'accumulation préférentielle de la forme non phosphorylée de BES1 dans les OPS-OE et OPSL1-OE, mais reste à vérifier dans une lignée OPSL2-OE plus stable.
D'autre part, la localisation subcellulaire commune aux OPS-LIKE (membranaire et apicale) suggère que les protéines OPS-LIKE sont redondantes fonctionnellement. L'aggravation des phénotypes racinaire et vasculaires cotylédonaires d'*ops-2* en combinaison avec le mutant *opsl2-1*, ainsi que les difficultés à obtenir des plantes triples mutantes pourraient être des arguments supplémentaires de la redondance des gènes *OPS-LIKE* pendant l'embryogenèse et au cours du développement post-embryonnaire.

La caractérisation phénotypique fine des mutants *ops-like* et des combinaisons de mutants par une analyse microscopique des tissus est prévue. L'élongation de l'épiderme chez le mutant *opsl1-2* ou encore taux d'activité mitotique chez le mutant *opsl2-1* pourrait être des pistes d'études. Afin de compléter l'analyse des mutants *ops-like* dans la réponse aux brassinostéroïdes, il sera envisagé d'étudier les *ops-like* (et des différentes combinaisons de mutants) en réponse à des traitements hormonaux (brassinolide, bikinine et brassinazole) ainsi que leurs réponses transcriptionnelles (taux de transcrits des gènes *DWF4, SAURAC1*).

Contrairement à ce qui est décrit par Nagawa et al. (Nagawa et al., 2006), l'étude des profils d'expression des *OPS-LIKE* ne se recoupe pas : il n'y a pas de redondance d'expression. Il se pourrait qu'un phénomène de silencing du gène rapporteur GUS se produise dans ces lignées. Pourtant l'aggravation du phénotype cotylédonaire suggère que les gènes *OPSL* sont exprimés de manière conjointe dans le contrôle de la mise en place des boucles vasculaires au cours de l'embryogenèse. En effet, la difficulté à obtenir un triple mutant suggère que le gène *OPSL1* est exprimé au cours de l'embryogenèse alors que je n'étais pas en mesure de le montrer.

Cependant, le profil d'expression des *OPS-LIKE* semble être spécifique à chacun des gènes *OPS-LIKE*. Le gène *OPS* serait associé aux tissus vasculaires, *OPSL1* à l'épiderme, *OPSL2* au centre quiescent.

Nous avons pu montrer l'implication des gènes *OPS-LIKE* dans la voie des BR. De manière tout à fait intéressante, Kim et al. et Cheng et al. (Kim et al., 2012; Cheng et al., 2014) ont précisé l'implication de BIN2 et plus généralement des brassinostéroïdes dans la mise en place de l'identité cellulaire de l'épiderme (respectivement au cours de la différentiation des stomates et des trichoblastes). Le profil d'expression dans l'épiderme racinaire suggère que le gène *OPSL1* pourrait être impliqué dans la différentiation des cellules épidermiques par le biais des brassinostéroïdes. *OPSL1* pourrait participer à la mise en place de l'identité atrichoblastiques des cellules épidermiques de la racine en induisant la voie de signalisation des brassinostéroïdes (inhibant la formation de poils absorbant en position NH, Cf Introduction §3.2.2).

Par ailleurs, OPS interagit avec la protéine BIN2 par son extrémité N-terminale. Le domaine N-terminal semble très conservé dans les gènes *OPSL1* et *OPSL2,* mais s'avère plus court chez *OPSL3* et *OPSL4* (Figure 6.1B). La redondance se restreint elle au clade *OPS, OPSL1, OPSL2* ou s'étend-elle à toute la famille ? Les protéines de la famille OPSL induiraient-elles la voie des brassinostéroïdes en inhibant le répresseur BIN2 (et ses homologues) ?
Il semblerait que ce soit le cas pour *OPSL1* et *OPSL2* dont la surexpression conduit à un phénotype de réponse constitutive aux brassinostéroïdes (macroscopique et moléculaire). L'étude de la famille *OPSL* sera complétée par l'étude des deux autres membres de la famille *OPSL3* et *OPSL4*.
Nous pouvons également nous demander si tous les membres OPSL peuvent interagir avec BIN2 ou s'il existe une interaction spécifique OPSL1/BIL1 comme par exemple dans les interactions BSU1/CDG1 et BSL1/CDL1 (Kim et al., 2011) ? Une meilleure connaissance des patrons d'expression des différentes GSK3s pourraient nous éclairer sur cette question. Il serait envisageable de tester deux à deux les différentes interactions protéiques entre OPS, OPSL1, OPSL2 et BIN2, BIL1, BIL2.

DISCUSSION GENERALE

1 OCTOPUS un nouvel acteur de la voie de signalisation des brassinostéroïdes

L'orchestration du développement de la plante ne résulte pas de l'action d'une seule hormone mais d'un ensemble de facteurs intégrant les informations venant de la cellule, du tissu, de l'organe et de l'environnement global de la plante. Les brassinostéroïdes sont des hormones participant à cette régulation qui ont été majoritairement décrites pour leur action sur l'élongation cellulaire et dont la voie de signalisation a été largement explorée.

Au cours de notre étude, nous avons montré que la surexpression du gène OPS active de manière constitutive la voie des brassinostéroïdes comme le confirment les données biochimiques et moléculaires. Par une étude physiologique et génétique, *OPS* a pu être replacé au sein de la voie de signalisation en aval du récepteur BRI1. OPS interagit avec CDG1 une kinase membranaire et BIN2 une kinase nucléo-cytoplasmique. OPS pourrait agir de manière positive sur la voie en réprimant le répresseur BIN2. De nombreuses questions restent en suspens concernant le rôle de cette protéine dans cette voie de signalisation et son rôle dans la régulation des GSK3s.

Un rôle pour OPS dans la séquestration de BIN2 à la membrane ?

OPS : un séquestreur membranaire de BIN2 ?

Chez les animaux, la voie de signalisation des protéines Wnt joue un rôle majeur dans le développement et la maintenance de l'état totipotent des cellules.

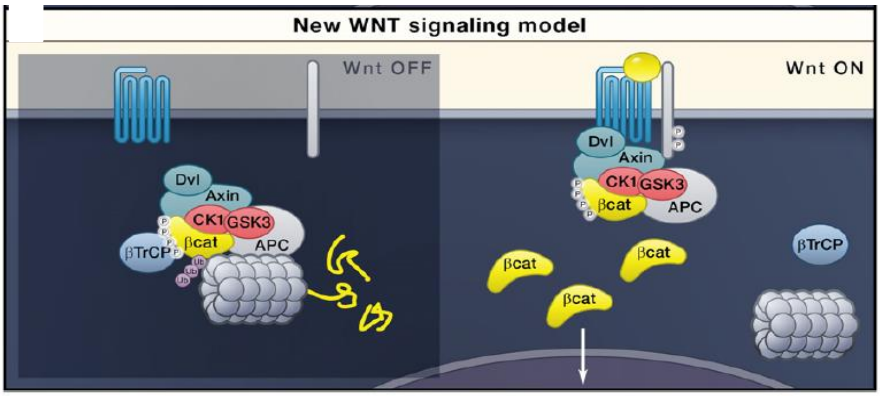

Figure 7.1 : Voie de signalisation Wnt
En abscence de Wnt, le complexe de destruction est localisé dans le cytoplasme où il interagit avec la fomre phosphorylée et ubiquitinylée de la b-catenine. Wnt induit l'association entre le complexe et LRP à la membrane. Après induction de la voie, la b-catenine est toujours phosphorylée, mais non ubiquitinilée et s'accumule alors.
De (Clevers and Nusse, 2012)

En absence de la glycoprotéine Wnt, la voie est inactive. Le complexe de destruction, dont les GSK3s font partie intégrante, se localise alors dans le cytoplasme où il phosphoryle les β-caténines pour induire leur dégradation et empêche ainsi leur activité de facteur de transcription dans le noyau (Figure 7.1). Lorsque la voie est activée par la fixation de Wnt sur son récepteur Frizzled (FZ) et son co-recepteur LRP6, la protéine Disheveled (DVL) est recrutée à la membrane. DVL induit l'agrégation du complexe de destruction cytosolique des β-caténines à la membrane éloignant les GSK3s de leur substrat (Clevers and Nusse, 2012). Récemment, Taelman et al. (Taelman et al., 2010) ont montré que la séquestration des GSK3s dans des corps vésiculaires de type MVB (Multivesicular Body) permet de séparer physiquement cette enzyme des β-caténines cytosoliques et d'augmenter ainsi leur temps de demi-vie. De manière analogue, la protéine OPS pourrait jouer le rôle de séquestreur de BIN2 en le retenant à la membrane. L'activité de BIN2 sur ses substrats nucléo-cytoplasmiques serait ainsi bloquée par une inhibition spatiale sous l'action d'OPS.

OPS : un intermédiaire moléculaire ?

OPS interagit à la fois avec CDG1 et avec BIN2 en système hétérologue (BiFC dans le tabac et split-ubiquitine dans la levure). Au cours de la cascade de signalisation, BSU1 une phosphatase nucléo-cytoplasmique est activée par CDG1 pour réprimer BIN2. OPS pourrait agir comme intermédiaire moléculaire pour favoriser le rapprochement physique entre les différents acteurs de la voie. L'interaction OPS/BSU reste donc une interaction physique primordiale à tester. De plus, l'analyse des protéines impliquées dans un complexe avec OPS permettrait en partie de répondre à cette question. A cette fin, nous collaborons avec l'équipe de D. Weijers pour analyser par Maldi-TOF les protéines complexées à la protéine OPS dans des plantes OPS-OE.

Le domaine N-terminal d'OPS indispensable à la séquestration de BIN2 pour l'activation de la voie des brassinostéroïdes ?

Nous avons montré qu'OPS interagit avec BIN2 par son extrémité N-terminale (OPS^{1-51}). De plus, les plantes exprimant de manière constitutive cette OPS^{1-51} ne présentent plus le phénotype caractéristique d'OPS-OE (hypocotyle allongé, cotylédons enroulés). Dans ces plantes, la protéine OPS^{1-51} marquée à l'aide de la GFP présente une localisation uniquement cytoplasmique ce qui pourrait expliquer l'absence de phénotype. Est-ce que la séquestration

de BIN2 à la membrane est le mécanisme inhibitoire de l'action de BIN2 sur ses substrats ? Pour tester cela il conviendrait de fusionner OPS$^{1-51}$ à un domaine d'ancrage à la membrane pour observer si cela induit la voie de la même façon que OPS-OE. Si la localisation de OPS$^{1-51}$ à la membrane permet de copier le phénotype d'OPS-OE, cela suggéra que l'hypothèse de séquestration de BIN2 à la membrane est indispensable à l'activation de la voie des brassinostéroïdes. Si ce n'est pas le cas, l'activation de la voie pourrait résulter de la formation d'un complexe plus général incluant OPS/BIN/CDG1 et probablement d'autres protéines tel que BSU1.

(A)

MNPATDPVSAAAAALAPPPQPPQPHRLSTSCNRHPEERFTGFCPSCLCERLSVLDQTNNGGSSSSSKKPPTISAAALK
ALFKPSGNNGVGGVNTNGNGRVKPGFFPELRRTKSFSASKNNEGFSGVFEPQRRSCDVRLRSSLWNLFSQDEQRNL
PSNVTGGEIDVEPRKSSVAEPVLEVNDEGEAESDDEELEEEEEEDYVEAGDFEILNDSGELMREKSDEIVEVREEIEEAV
KPTKGLSEEELKPIKDYIDLDSQTKKPSVRRSFWSAASVFSKKLQKWRQNQKMKKRRNGGDHRPGSARLPVEKPIGR
QLRDTQSEIADYGYGRRSCDTDPRFSLDAGRFSLDAGRFSVDIGRISLDDPRYSFDEPRASWDGSLIGRTMFPPAARAP
PPPSMLSVVEDAPPPVHRHVTRADMQFPVEEPAPPPPVVNQTNGVSDPVIIPGGSIQTRDYYTDSSSRRRKSLDRSSS
SMRKTAAAVVADMDEPKLSVSSAISIDAYSGSLRDNNNYAVETADNGSFREPAMMIGDRKVNSNDNNKKSRRWGK
WSILGLIYRKSVNKYEEEEEEEEDRYRRLNGGMVERSLSESWPELRNGGGGGGGPRMVRSNSNVSWRSSGGGSAR
KVNGLDRRNKSSRYSPKNGENGMLKFYLPHMKASRRMSGTGGAGGGGGGGWANSHGHSIARSVMRLY

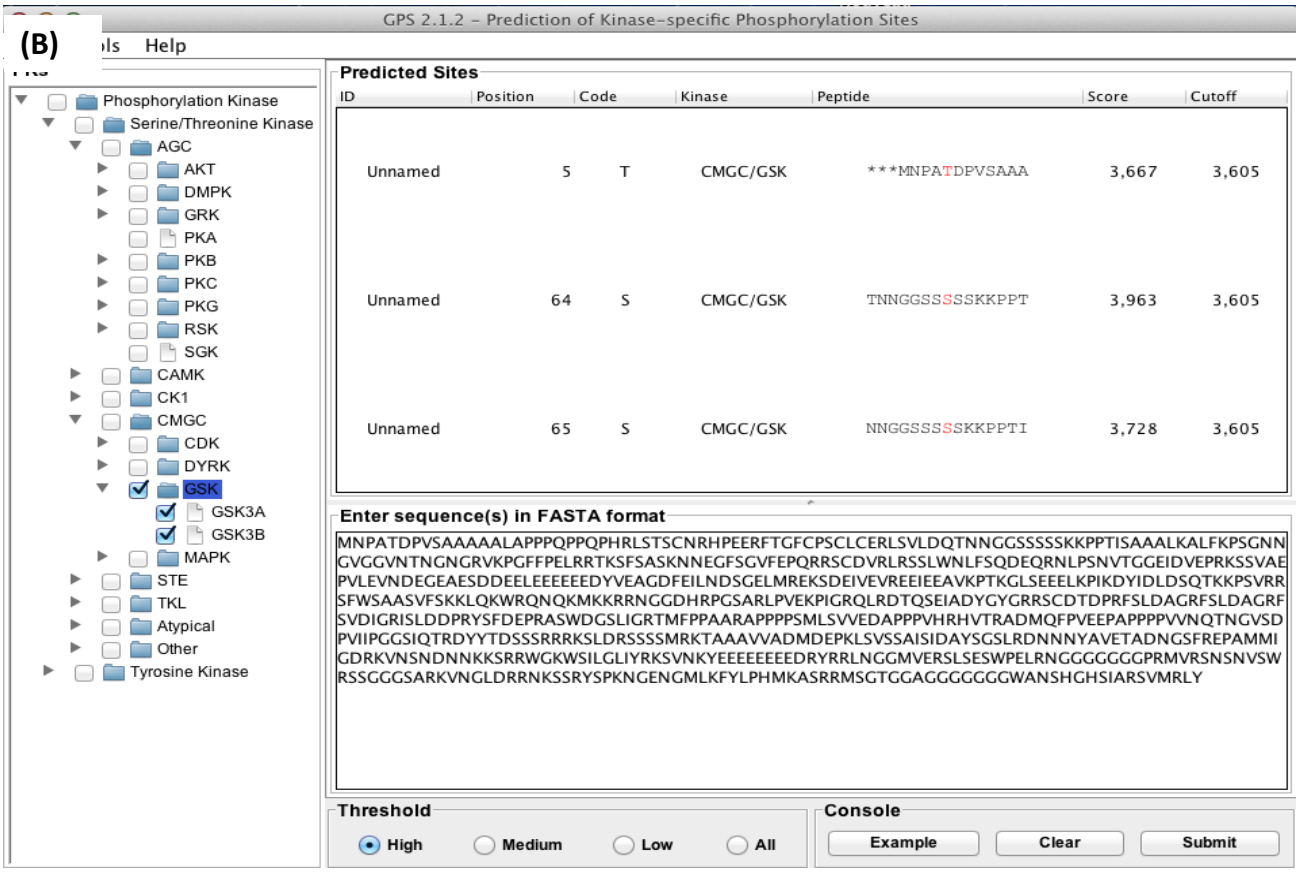

Figure 7.2 : OPS une cible putative des GSK3?
(A) Séquence protéique d'OPS contenant des motifs d'interaction GSK3 putatifs ((S/T)XXX(S/T), souligné dans la séquence). En rouge les résidus Ser/Thr prédit comme étant potentiellement des sites de phosphorylation (identifiés grâce à l'analyse (B)). **(B)** Analyse bioinformatique des sites putatifs de phosphorylation d'OPS par les GSK3 animales. (GSP 2.1.2; (Xue et al., 2011b)

Par ailleurs, l'analyse de la séquence protéique d'OPS révèle des motifs consensus de reconnaissance de BIN2 (S/T)XXX(S/T) (Peng et al., 2010) sur l'ensemble de la protéine OPS (Figure 7.2A). Une analyse bioinformatique de prédiction de phosphorylation par les GSK3s (GSP 2.1.2 (Xue et al., 2011a)) indique que deux de ces motifs pourraient être phosphorylés, dont l'un dans le domaine OPS^{1-51} (Figure 7.2). De plus, OPS a été identifiée dans un phosphoprotéome membranaire nous indiquant qu'OPS est une protéine phosphorylée (Benschop et al., 2007). Le rôle de BIN2 dans la phosphorylation d'OPS sera considéré.

Une redondance fonctionnelle à explorer

Le gène *OPS* a été initialement isolé comme impliqué dans la différenciation du phloème (Bauby et al., 2007; Truernit et al., 2012). Ce gène appartient à une famille multigénique composée de 5 gènes présentant tous un domaine de fonction inconnu DUF740. L'étude de l'expression des trois gènes *OPS, OPSL1* et *OPSL2,* appartenant au même clade, ne semble pas montrer de superposition entre patrons d'expressions contrairement à ce qu'ont pu montrer Nagawa et al. (Nagawa et al., 2006). Bien que seul le mutant *ops* présente un phénotype clair (racine courte, patrons vasculaires cotylédonaires moins complexes que chez le sauvage, différenciation du phloème racinaire stochastique), les combinaisons de mutants semblent aggraver le phénotype du simple mutant *ops* et présentent une plus forte diminution de la complexité du réseau vasculaire. Ces données suggèrent l'existence d'une redondance génétique et confirment l'étude de Nagawa et al. (Nagawa et al., 2006) qui présente les DUF740 comme des gènes spécifique du procambium. Cependant la caractérisation complète des mutants *opsl1-2* et *opsl2-1* ainsi que celle des combinaisons de mutants restent à terminer.

D'autre part, les plantes exprimant de manière constitutive le gène *OPS* fusionné à la GFP, ou l'un de ses homologues (*OPSL1, OPSL2*), arborent des phénotypes semblables (élongation de l'hypocotyle et des pétioles, cotylédons twistées, induction de la voie des brassinostéroïdes) et présentent des localisations subcellulaires similaires. Ces données suggèrent donc l'existence d'une redondance fonctionnelle. Cependant, l'étude de d'expression tissulaires de cette famille de gènes doit être approfondie soit en analysant de nouvelles lignées transgéniques contenant les constructions pOPSL ::OPSL-GFP, soit en

effectuant des hybridations *in situ* pour chacun des gènes de la famille. D'autre part, l'étude des deux autres membres de la famille (*OPSL3* et *OPSL4*) reste à explorer.

OPSL est-il un membre indispensable de la voie de signalisation des brassinostéroïdes ?

L'étude du triple mutant *opsl* semble indiquer la présence d'une létalité embryonnaire qui reste à confirmer. Ceci suggère que la fonction de ces gènes est indispensable au développement de la plante. Peu de données font état de phénotypes embryonnaires au sein de la voie des brassinostéroïdes. C'est probablement lié au fait que la majorité des acteurs de cette voie présente également une redondance fonctionnelle. L'équipe d'A. Cano-Delgado (Caño-Delgado et al., 2004) rapportent qu'un triple mutant *bri1.101 brl1 brl3* donne une plante pratiquement stérile, cependant l'allèle *bri1.101* est moins fort que *bri1.116* et les embryons n'ont pas été décrits dans ces mutants.

Etant donné nos difficultés à obtenir une combinaison de triples mutants, l'utilisation d'une lignée RNAi inductible, diminuant l'expression de l'ensemble des *OPSL* ou du clade *OPS,* serait un matériel précieux dans l'étude du gène *OPS* comme membre indispensable à la voie des brassinostéroïdes. Puisque notre étude est majoritairement basée sur la caractérisation de la lignée OPS-OE, l'objectif serait d'identifier un phénotype et une réponse moléculaire opposés à ceux observés dans la lignée OPS-OE. Si ce n'est pas le cas, cela signifierait donc qu'OPSL n'est pas indispensable à la signalisation des brassinostéroïdes bien qu'il permette l'activation de la voie. Dans ce deuxième cas, OPSL pourrait interagir ponctuellement avec BIN2 pour contrôler la mise en place des tissus dans lesquels ils sont exprimés. OPSL agirait alors comme un amplificateur transitoire de la voie créant une réponse hypersensible dans des tissus bien spécifiques.

Il ne faut cependant pas exclure le fait qu'une partie de la voie de signalisation des brassinostéroïdes peut être détournée vers d'autres fonctions biologiques (Kim et al., 2012; Kondo et al., 2014; Wolf et al., 2014). Dans leur étude, Wolf et al. (Wolf et al., 2014) montre que RLP44 interagit avec le complexe BRI1/BAK1 pour maintenir l'homéostasie de la paroi cellulaire au cours de l'expansion cellulaire. Ainsi RLP44 intègre un signal autre que la présence de brassinostéroïdes (une altération des pectines) pour induire la voie de signalisation via le complexe BRI1/BAK1. .

De même les GSK3s pourraient agir en tant que « hub » au niveau de plusieurs voies de signalisation (Galvan-Ampudia and Vernoux, 2014):

- Ainsi BIN2 est capable de connecter la signalisation des brassinostéroïdes avec la voie des MAPK dans la régulation du développement des stomates (Kim et al., 2012).
- BIN2 est également au carrefour de deux voies de signalisation celle des brassinostéroïdes et de l'auxine via la phosphorylation d'ARF2 par BIN2 (Vert et al., 2008; Cho et al., 2014).
- Le module TDIF-TDR-GSK3 est impliqué dans la balance entre maintenance du procambium et différenciation du xylème en modulant la phosphorylation de BES1 (Kondo et al., 2014).

Outre la réponse d'élongation cellulaire liée à l'activation constitutive des brassinostéroïdes, des régulations plus fines sont également présentes au niveau de la décision de la destinée cellulaire. C'est le cas pour le développement des stomates (Kim et al., 2012), la différenciation du xylème (Kondo et al., 2014), des cellules de la columelle (González-García et al., 2011; Vilarrasa-Blasi et al., 2014) et des atrichoblastes (Cheng et al., 2014).

Au vu de la spécificité d'expression d'*OPS* (procambium, phloème) nous pouvons supposer qu'OPS n'intervient pas au niveau de tous les types cellulaires dans le contrôle de la voie des brassinostéroïdes. Toutefois, l'analyse de l'expression d'*OPSL1* et d'*OPSL2* suggère que cette régulation puisse se produire au sein de certains types cellulaires. En effet, *OPSL1* est exprimé au niveau des cellules atrichoblastes et il a récemment été montré que les GSK3s et la voie des brassinostéroïdes jouent un rôle primordial dans l'établissement de cette identité cellulaire en affectant spécifiquement la phosphorylation de certains facteurs de transcription (Cheng et al., 2014). Il serait intéressant de comprendre le rôle du gène *OPSL1* la régulation de cette identité cellulaire. Pour cela la caractérisation phénotypique de la racine du mutant *opsl1* dans la zone pilifère ainsi que l'étude de l'expression de marqueurs moléculaires tels que GLABRA2 ::GUS dans un fond *opsl1* répondra en partie à cette question.

OPSL2 est exprimé dans les cellules du centre quiescent et deux articles ont révélés le rôle joué par les brassinostéroïdes sur le méristème racinaire (González-García et al., 2011; Vilarrasa-Blasi et al., 2014). L'étude plus fine du méristème racinaire chez le mutant *opsl2* est donc à considérer.

2 Quelles voies de signalisation dans la mise en place du phloème ?

Notre étude a également révélé l'implication de la voie de signalisation des BRs dans la mise en place du phloème. En effet, des traitements à la bikinine ainsi que l'introgression des mutations *bzr1-D* et *bes1-D* dans un fond *ops* permettent de restaurer partiellement le phénotype et de rétablir la continuité cellulaire au sein du phloème racinaire suggérant que les brassinostéroïdes agissent positivement sur la mise en place de ce tissu.

Cependant, cette implication doit être étendue. En effet, l'activation de la voie des brassinostéroïdes en aval d'*OPS* ne permet pas de rétablir le réseau vasculaire cotylédonaires dans le mutant *ops*. Les gènes *BES1* et *BZR1* ne sont probablement pas exprimés au cours de l'embryogenèse (Figure S5), or c'est à cette étape du développement que sont établis les tissus vasculaires dans les cotylédons (Bauby et al., 2007). Pour le moment, nous n'avons pas été en mesure de mettre en évidence des défauts vasculaires semblables à ceux observés chez *ops* dans les mutants affectés dans la voie des brassinostéroïdes. L'effet de ces mutants étant pléiotropes, il est difficile de déterminer dans quelle mesure le phloème racinaire est affecté. N'ayant basé l'étude de l'implication des brassinostéroïdes dans la mise en place du phloème que sur l'analyse du phloème racinaire, l'analyse des boucles vasculaires sera intégrée au phénotypage des différents mutants affectés dans la voie. L'utilisation de mutant spécifique du phloème tel que *brl1* ou *brl3* et de mutants faibles tels que *bri1-5* ou *cnu1* sera probablement l'une des stratégies à adopter.

Par ailleurs, la voie de signalisation des brassinostéroïdes est impliquée dans la différenciation du xylème. L'étude de A. Cano (Caño-Delgado et al., 2004) a confirmé que les récepteurs aux brassinostéroïdes agissent de façon redondante sur la division du cambium et la différenciation du xylème dans la hampe florale. Dans les simples mutants et combinaisons de mutants *brl*, la proportion de tissu xylèmien est réduite par rapport au phloème. Inversement la surexpression de *BRI1* conduit à une augmentation de la proportion de tissu xylèmien.

La mise en place de ces tissus (xylème et phloème) est sous la dépendance de plusieurs facteurs :

- la division du (pro)cambium (méristème vasculaire) qui assure la maintenance d'un groupe de cellules totipotentes controlée par le module TDIF/TDR (Tracheary element Differentiation Inhibitory Factor/ TDIF Receptor)
- les cellules qui s'engagent vers un programme de différenciation (en l'occurrence phloème et xylème)

Un défaut au sein de cette voie TDIF/TDR/WOX4 engendre une réduction de l'activité mitotique du cambium, et par conséquent un appauvrissement du nombre de cellules cambiales, et conduit les cellules vers la différenciation du xylème. En revanche, la fixation du ligand TDIF sur son récepteur TDR mène à l'activation et au relargage de BIN2 qui réprime alors l'action positive de BES1 sur la différenciation du xylème. Lorsqu'elle est activée, la voie TDR/BIN2/BES1 réprime la formation du xylème et induit la prolifération cellulaire grâce à l'activité de BIN2 (Kondo et al., 2014). Ces données complètent l'étude d'A. Cano-Delgado (Caño-Delgado et al., 2004) selon laquelle les brassinostéroïdes induisent la formation du xylème. Il existe donc une balance entre la voie BRI1/BIN2, qui induit la différenciation du xylème, et la voie TDR/BIN2 qui l'inhibe.

Récemment, le gène *OPS* a été isolé dans un crible suppresseur du mutant *brx* (Rodriguez-Villalon et al., 2014), présentant des phénotypes phloèmiens similaires à *ops,* à savoir une différenciation stochastique du phloème racinaire. La mutation dans le gène *OPS* conduit à un gain de fonction (*ops-D*) suggérant ainsi qu'*OPS* agirait en aval de *BRX*. *BRX* pourrait intervenir très en amont dans la voie des brassinostéroïdes. Une approche génétique couplée à l'étude de la réponse moléculaire de la voie des brassinostéroïdes approuvera l'implication de *BRX* dans cette voie de signalisation et mettra en lumière le rôle de BRX dans la voie des brassinostéroïdes. L'une des premières réponses à apporter serait de vérifier que les gènes les plus en aval de la voie restaurent le phénotype du mutant *brx* à savoir par l'étude des croisements *brx bzr1-D* et *brx bes1-D*. Par ailleurs, nous pouvons nous interroger sur l'impact qu'a la mutation *ops-D* sur la fonction d'OPS. De quelle manière cette mutation conduit à un gain de fonction ? La protéine OPS-D serait-elle plus stable que la protéine OPS ?

L'étude de Rodriguez et al. (Rodriguez-Villalon et al., 2014), montre que les lacunes phloèmiennes de mutants *ops* et *brx* résultent d'un défaut de division cellulaire, étape

indispensable au développement du phloème. L'acquisition de l'identité cellulaire phloèmienne est régulée par le niveau d'activité du module CLE45/BAM3 qui bloque la différenciation du phloème. *OPS* interviendrait comme un master régulateur de l'identité phloèmienne en induisant sa différenciation (Rodriguez-Villalon et al., 2014).

Le module CLE45/BAM3 est un système analogue au système TDIF/TDR qui inhibe la formation du xylème par l'intermédiaire de BIN2 (Kondo et al., 2014). Comme *OPS* intervient dans la voie *CLE45/BAM3* pour induire la différenciation du phloème, nous pourrions imaginer que *BIN2* intervienne dans cette voie pour bloquer la différenciation du phloème (Figure 7.3). Ainsi *OPS*, acteur positif de la voie des brassinostéroïdes, pourrait réprimer l'action de BIN2 pour induire la différenciation du phloème. L'introgression de la mutation *bin2-1D* sous le contrôle du promoteur BAM3 dans un fond *bam3* permettra de définir l'implication de *BIN2* dans cette voie ainsi que son influence sur la différenciation du phloème. Une étude pharmacologique sur les mutants *bin* (gain de fonction et perte de fonction) pourra être envisagée afin d'explorer la sensibilité de ces mutants à des traitements CLE45. Par analogie au système TDIF/TDR l'interaction physique entre BAM3 et BIN2 pourra être testée.

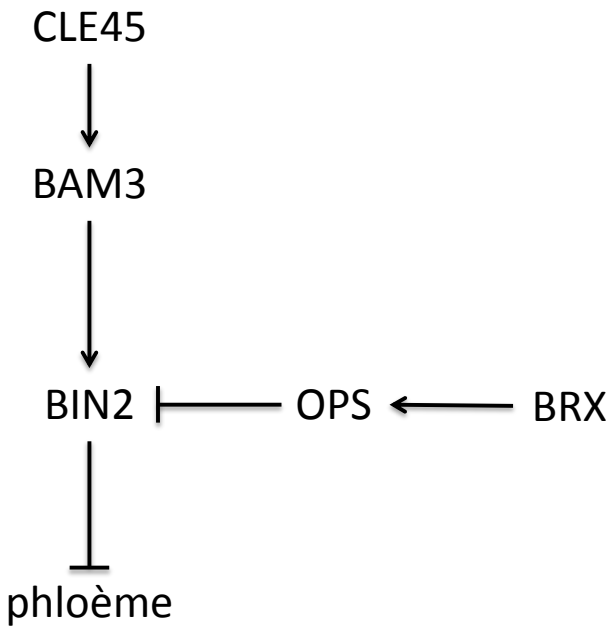

Figure 7.3 : Modèle hypothétique intégrant OPS et BIN2 au module CLE45/BAM3 dans le contrôle de la différentiation du phloème

3 OPS une protéine polaire et membranaire

Quel sous domaine protéique intervient dans la localisation d'OPS ?

La protéine tronquée OPS$^{49-686}$ est toujours adressée à la membrane de manière polaire. Ce qui suggère que les 48 premiers acides aminés ne sont pas essentiels à la localisation d'OPS. Cependant, l'analyse bio-informatique de la séquence d'OPS révèle deux domaines en super-hélices pouvant être responsable de son interaction avec d'autres protéines (Figure 7.4). Différentes versions tronquées découpant la protéine en sous-domaines permettraient d'identifier quelles séquences d'acides aminés pourraient être essentielles à la localisation membranaire d'OPS.

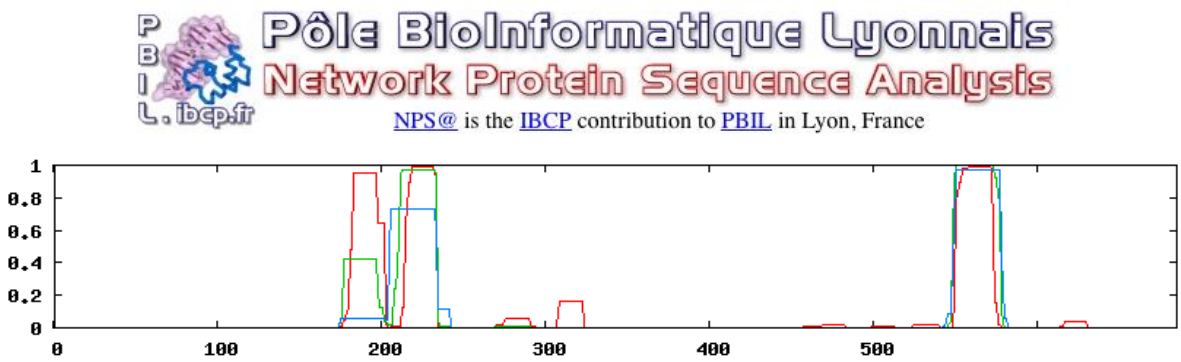

Figure 7.4 : Deux domaines en superhélices prédits dans la séquence d'OPS
http://npsa-pbil.ibcp.fr/cgi-bin/primanal_lupas.pl

Une interaction protéique responsable de la localisation d'OPS ?

CDG1, le premier candidat

Alternativement nous pouvons imaginer que la localisation d'OPS à la membrane se fasse par l'intermédiaire de son interaction avec une autre protéine membranaire. Une des pistes pouvant expliquer la localisation membranaire d'OPS serait son interaction avec la protéine membranaire CDG1. Cette protéine kinase et son homologue CDL1 sont adressés à la membrane grâce à une palmitoylation (Kim et al., 2011). En dépit des résultats négatifs obtenus au cours de l'étude de la localisation d'OPS dans un fond mutant *cdl1* (Figure 5.2), cette hypothèse n'est pas à écarter puisque l'étude de la localisation d'OPS dans les fonds *cdg1* et *cdg1 cdl1* est en cours. Etudier l'effet du 2-BromoPalmitate (inhibiteur de la

palmitoylation) sur la localisation d'OPS et de CDG1 permettrait également de répondre à cette question.

VCC, le deuxième candidat

Une autre piste à explorer concerne l'interaction entre OPS et VCC à la membrane (Roschzttardtz et al., 2014). VCC est une protéine à quatre domaines transmembranaires prédits et qui présente également des similarités avec des protéines de type tetraspanines (TET). Dans les cellules animales, les protéines TETs interagissent entre elles et avec d'autres protéines membranaires jouant le rôle d'organisateur pour former des micro-domaines impliqués dans des mécanismes de signalisation (Boavida et al., 2013). Des données biochimiques de fractionnements cellulaires ont permis de confirmer qu'OPS fait partie intégrante de la membrane et que cette protéine se retrouve dans des sous-domaines membranaires résistants aux détergents (Figure 7.5). A la différence de la Remorin (Raffaele et al., 2009) qui se localise au sein de micro-domaines discrets de la membrane, OPS se localise préférentiellement aux pôles apicaux des cellules mais de manière diffuse au sein de ce domaine membranaire. Il est donc tentant d'explorer la localisation subcellulaire fine de VCC et de tester l'influence de cette protéine sur la localisation et/ou la polarité d'OPS ou encore sa solubilité aux détergents.

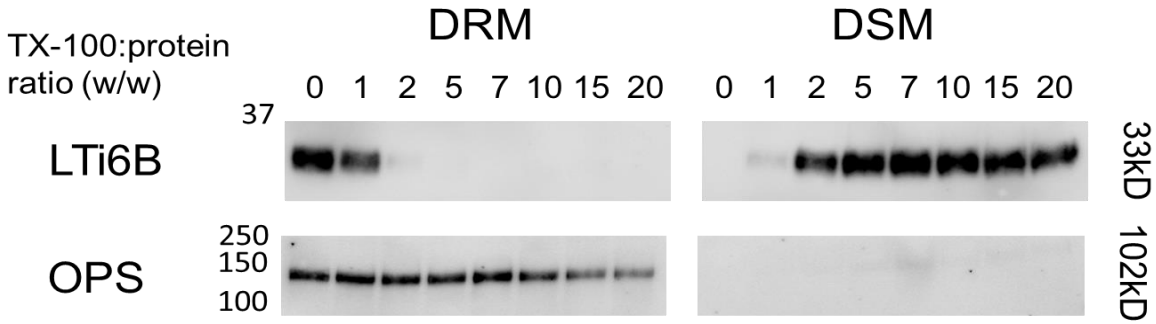

Figure 7.5 : OPS une protéine résistante aux détergents
Les membranes sont isolées de plantules âgées de 7 jours. Des aliquots correspondant à 20µg de protéines membranaires sont traités avec un détergent de 0:1 à 5:1 (Triton X-100 protein; w/w). Les proteines nonsolubilisées (DRM) et les protéines solubilisées (DSM) sont révélées par un anticorps anti-GFP (Chroomotek pour Lti6B, Roche pour OPS)

Pourquoi la protéine OPS est-elle polaire ?

Pour le moment, aucun acteur de la voie de signalisation des brassinostéroïdes n'a été décrit comme polaire. La localisation subcellulaire des membres de cette voie reste cependant mal caractérisée et décrite uniquement dans les tissus épidermiques (Vert and Chory, 2006; Di Rubbo et al., 2013). L'étude fine de la localisation subcellulaire des acteurs de la voie des brassinostéroïdes (en particulier CDG1 et BIN2), au sein de la file cellulaire phloèmienne pourrait être une piste intéressante à suivre.

Des traitements au brassinazole, brassinolide ou encore à la bikinine ne semblent pas impacter la localisation polaire et membranaire de la protéine OPS (données non présentées). Cependant, la polarité d'OPS dans les lignées OPS-OE n'est pas systématique, puisque dans les cellules de la feuille (excepté les tissus vasculaires) OPS ne semblent pas soumises à cette polarité. La protéine OPS intègre-t-elle un signal supplémentaire lui imposant une localisation apicale préférentielle au sein des membranes plasmiques de certains tissus?

Deux signaux polarisés sont connus pour être impliqués dans la mise en place des tissus vasculaires : l'auxine et les cytokinines (Cf Introduction §1.2). Une analyse pharmacologique complémentaire est envisagée afin de tester la localisation d'OPS en réponse à l'action de ces deux hormones et de leurs inhibiteurs respectifs.

BIBLIOGRAPHIE

Abràmoff, M.D., Magalhães, P.J., and Ram, S.J. (2004). Image Processing with ImageJ. Biophotonics Int. **11**: 36–42.

Asami, T., Min, Y.K., Nagata, N., Yamagishi, K., Takatsuto, S., Fujioka, S., Murofushi, N., Yamaguchi, I., and Yoshida, S. (2000). Characterization of brassinazole, a triazole-type brassinosteroid biosynthesis inhibitor. Plant Physiol. **123**: 93–100.

Azpiroz, R., Wu, Y., LoCascio, J.C., and Feldmann, K. a (1998). An Arabidopsis brassinosteroid-dependent mutant is blocked in cell elongation. Plant Cell **10**: 219–30.

Bajguz, A. and Tretyn, A. (2003). The chemical characteristic and distribution of brassinosteroids in plants. Phytochemistry **62**: 1027–1046.

Bauby, H., Divol, F., Truernit, E., Grandjean, O., and Palauqui, J.-C. (2007). Protophloem differentiation in early Arabidopsis thaliana development. Plant Cell Physiol. **48**: 97–109.

Van Bel, A.J.E. (1999). Evolution, polymorphology and multifunctionality of the phloem system. Perspect. Plant Ecol. Evol. Syst. **2**: 163–184.

Van Bel, A.J.E. (2003). The phloem , a miracle of ingenuity. Plant, Cell Environ. **26**: 125–149.

Bennett, T. and Scheres, B. (2010). Root development-two meristems for the price of one? Curr. Top. Dev. Biol. **91**: 67–102.

Benschop, J.J., Mohammed, S., O'Flaherty, M., Heck, A.J.R., Slijper, M., and Menke, F.L.H. (2007). Quantitative phosphoproteomics of early elicitor signaling in Arabidopsis. Mol. Cell. Proteomics **6**: 1198–214.

Berleth, T. and Jürgens, G. (1993). The role of the monopteros gene in organising the basal body region of the Arabidopsis embryo. Development **118**: 575–587.

Berleth, T., Mattsson, J., and Hardtke, C.S. (2000). Vascular continuity and auxin signals. Trends Plant Sci. **5**: 387–93.

Bishopp, A., Help, H., El-Showk, S., Weijers, D., Scheres, B., Friml, J., Benková, E., Mähönen, A.P., and Helariutta, Y. (2011). A mutually inhibitory interaction between auxin and cytokinin specifies vascular pattern in roots. Curr. Biol. **21**: 917–26.

Boavida, L.C., Qin, P., Broz, M., Becker, J.D., and McCormick, S. (2013). Arabidopsis tetraspanins are confined to discrete expression domains and cell types in reproductive tissues and form homo- and heterodimers when expressed in yeast. Plant Physiol. **163**: 696–712.

Bonke, M., Thitamadee, S., Mähönen, A.P., Hauser, M.-T., and Helariutta, Y. (2003). APL regulates vascular tissue identity in Arabidopsis. Nature **426**: 181–186.

Boyko, A., Hudson, D., Bhomkar, P., Kathiria, P., and Kovalchuk, I. (2006). Increase of homologous recombination frequency in vascular tissue of Arabidopsis plants exposed to salt stress. Plant Cell Physiol. **47**: 736–42.

Caesar, K., Elgass, K., Chen, Z., Huppenberger, P., Witthöft, J., Schleifenbaum, F., Blatt, M.R., Oecking, C., and Harter, K. (2011). A fast brassinolide-regulated response pathway in the plasma membrane of Arabidopsis thaliana. Plant J. **66**: 528–40.

Camefort (1977). Morphologie des végétaux vasculaires.

Campbell, N. and Reece, J. (2007). Biology Package, 7th edition (Pearson Eductaion Inc.).

Campbell, T.N. and Choy, F.Y.M. (2001). The Effect of pH on Green Fluorescent Protein : a Brief Review. Mol. Biol. Today **2**: 1–4.

Caño-Delgado, A., Lee, J.-Y., and Demura, T. (2010). Regulatory mechanisms for specification and patterning of plant vascular tissues. Annu. Rev. Cell Dev. Biol. **26**: 605–37.

Caño-Delgado, A., Yin, Y., Yu, C., Vafeados, D., Mora-García, S., Cheng, J.-C., Nam, K.H., Li, J., and Chory, J. (2004). BRL1 and BRL3 are novel brassinosteroid receptors that function in vascular differentiation in Arabidopsis. Development **131**: 5341–51.

Ceserani, T., Trofka, A., Gandotra, N., and Nelson, T. (2009). VH1/BRL2 receptor-like kinase interacts with vascular-specific adaptor proteins VIT and VIK to influence leaf venation. Plant J. **57**: 1000–14.

Cheng, Y., Zhu, W., Chen, Y., Ito, S., Asami, T., and Wang, X. (2014). Brassinosteroids control root epidermal cell fate via direct regulation of a MYB-bHLH-WD40 complex by GSK3-like kinases. Elife **3**: 1–17.

Cho, H. et al. (2014). A secreted peptide acts on BIN2-mediated phosphorylation of ARFs to potentiate auxin response during lateral root development. Nat. Cell Biol. **16**: 66–76.

Choe, S., Dilkes, B.P., Fujioka, S., Takatsuto, S., Sakurai, A., and Feldmann, K. a (1998). The DWF4 gene of Arabidopsis encodes a cytochrome P450 that mediates multiple 22alpha-hydroxylation steps in brassinosteroid biosynthesis. Plant Cell **10**: 231–43.

Chory, J., Nagpal, P., and Peto, C. a. (1991). Phenotypic and Genetic Analysis of det2, a New Mutant That Affects Light-Regulated Seedling Development in Arabidopsis. Plant Cell **3**: 445–459.

Choudhary, S.P., Yu, J.-Q., Yamaguchi-Shinozaki, K., Shinozaki, K., and Tran, L.-S.P. (2012). Benefits of brassinosteroid crosstalk. Trends Plant Sci. **17**: 594–605.

Chung, Y. and Choe, S. (2013). The Regulation of Brassinosteroid Biosynthesis in Arabidopsis. CRC. Crit. Rev. Plant Sci. **32**: 396–410.

Clevers, H. and Nusse, R. (2012). Wnt/β-catenin signaling and disease. Cell **149**: 1192–205.

Clough, S.J. and Bent, A.F. (1998). Floral dip : a simplified method for Agrobacterium-mediated transformation of Arabidopsis thaliana. Plant J. **16**: 735–743.

Clouse, S.D., Langford, M., and Mcmorris, T.C. (1996). A Brassinosteroid-lnsensitive Mutant in Arabidopsis thaliana Exhibits Multiple Defects in Growth and Development ’. Plant Physiol. **111**: 671–678.

Clouse, S.D. and Sasse, J.M. (1998). BRASSINOSTEROIDS: Essential Regulators of Plant Growth and Development. Annu. Rev. Plant Physiol. Plant Mol. Biol. **49**: 427–451.

Cosgrove, D.J. (1997). Relaxation in a high-stress environment: the molecular bases of extensible cell walls and cell enlargement. Plant Cell **9**: 1031–41.

Curtis, M.D. and Grossniklaus, U. (2003). A Gateway Cloning Vector Set for High-Throughput Functional Analysis of Genes in Planta. Plant Physiol. **133**: 462–469.

Darwin, C. (1880). The power of movement in plants.

Depuydt, S., Rodriguez-villalon, A., Santuari, L., Wyser-rmili, C., Ragni, L., and Hardtke, C.S. (2013). Suppression of Arabidopsis protophloem differentiation and root meristem growth by CLE45 requires the receptor-like kinase BAM3. PNAS **110**: 7074–7079.

Desprez, T., Juraniec, M., Crowell, E.F., Jouy, H., Pochylova, Z., Parcy, F., Höfte, H., Gonneau, M., and Vernhettes, S. (2007). Organization of cellulose synthase complexes involved in primary cell wall synthesis in Arabidopsis thaliana. Proc. Natl. Acad. Sci. U. S. A. **104**: 15572–7.

DeYoung, B.J., Bickle, K.L., Schrage, K.J., Muskett, P., Patel, K., and Clark, S.E. (2006). The CLAVATA1-related BAM1, BAM2 and BAM3 receptor kinase-like proteins are required for meristem function in Arabidopsis. Plant J. **45**: 1–16.

Emery, J.F., Floyd, S.K., Alvarez, J., Eshed, Y., Hawker, N.P., Izhaki, A., Baum, S.F., and Bowman, J.L. (2003). Radial Patterning of Arabidopsis Shoots by Class III HD-ZIP and KANADI Genes. Curr. Biol. **13**: 1768–1774.

Esau, K. (1969). The Phloem Encycloped. B. Born- taeger, ed.

Estelle, M.A. and Somerville, C. (1987). Auxin-resistant mutants of Arabidopsis thMiana with an altered morphology. Mol Gen Genet **206**: 200–206.

Etchells, J.P. and Turner, S.R. (2010). The PXY-CLE41 receptor ligand pair defines a multifunctional pathway that controls the rate and orientation of vascular cell division. Development **137**: 767–74.

Fàbregas, N., Li, N., Boeren, S., Nash, T.E., Goshe, M.B., Clouse, S.D., de Vries, S., and Caño-Delgado, A.I. (2013). The brassinosteroid insensitive1-like3 signalosome complex regulates Arabidopsis root development. Plant Cell **25**: 3377–88.

Fisher, K. and Turner, S. (2007). PXY, a receptor-like kinase essential for maintaining polarity during plant vascular-tissue development. Curr. Biol. **17**: 1061–6.

Froelich, D.R., Mullendore, D.L., Jensen, K.H., Ross-Elliott, T.J., Anstead, J. a, Thompson, G. a, Pélissier, H.C., and Knoblauch, M. (2011). Phloem ultrastructure and pressure flow: Sieve-Element-Occlusion-Related agglomerations do not affect translocation. Plant Cell **23**: 4428–45.

Fujioka, S. and Sakurai, A. (1997). Brassinosteroids. Nat. Prod. Rep. **14**: 1–10.

Furuta, K.M. et al. (2014a). Arabidopsis NAC45/86 direct sieve element morphogenesis culminating in enucleation. Science **933**.

Furuta, K.M., Hellmann, E., and Helariutta, Y. (2014b). Molecular control of cell specification and cell differentiation during procambial development. Annu. Rev. Plant Biol. **65**: 607–38.

Galvan-Ampudia, C.S. and Vernoux, T. (2014). Signal integration by GSK3 kinases in the root. Nat. Cell Biol. **16**: 21–3.

Gampala, S.S. et al. (2007). An Essential Role for 14-3-3 Proteins in Brassinosteroid Signal Transduction in Arabidopsis. Dev. Cell **13**: 177–189.

Geldner, N., Anders, N., Wolters, H., Keicher, J., Kornberger, W., Muller, P., Delbarre, A., Ueda, T., Nakano, A., and Jürgens, G. (2003). The Arabidopsis GNOM ARF-GEF mediates endosomal recycling, auxin transport, and auxin-dependent plant growth. Cell **112**: 219–30.

Geldner, N., Hyman, D.L., Wang, X., Schumacher, K., and Chory, J. (2007). Endosomal signaling of plant steroid receptor kinase BRI1. Genes Dev. **21**: 1598–602.

González-García, M.-P., Vilarrasa-Blasi, J., Zhiponova, M., Divol, F., Mora-García, S., Russinova, E., and Caño-Delgado, A.I. (2011). Brassinosteroids control meristem size by promoting cell cycle progression in Arabidopsis roots. Development **138**: 849–59.

Grierson, C., Nielsen, E., Ketelaarc, T., and Schiefelbein, J. (2014). Root hairs. Arabidopsis Book **12**: e0172.

Grove, M.D., Spencer, G.F., and Rohwedder, W.K. (1979). Brassinolide, a plant growth-promoting steroid isolated from Brassica napus pollen. Nature **281**.

Gutierrez, R., Lindeboom, J.J., Paredez, A.R., Emons, A.M.C., and Ehrhardt, D.W. (2009). Arabidopsis cortical microtubules position cellulose synthase delivery to the plasma membrane and interact with cellulose synthase trafficking compartments. Nat. Cell Biol. **11**: 797–806.

Ha, C.M., Jun, J.H., and Fletcher, J.C. (2010). Shoot apical meristem form and function. Curr. Top. Dev. Biol. **91**: 103–40.

Hardtke, C.S. and Berleth, T. (1998). The Arabidopsis gene MONOPTEROS encodes a transcription factor mediating embryo axis formation and vascular development. EMBO J. **17**: 1405–1411.

He, J.-X., Gendron, J.M., Sun, Y., Gampala, S.S.L., Gendron, N., Sun, C.Q., and Wang, Z.-Y. (2005). BZR1 is a transcriptional repressor with dual roles in brassinosteroid homeostasis and growth responses. Science **307**: 1634–8.

He, J.-X., Gendron, J.M., Yang, Y., Li, J., and Wang, Z.-Y. (2002). The GSK3-like kinase BIN2 phosphorylates and destabilizes BZR1, a positive regulator of the brassinosteroid signaling pathway in Arabidopsis. Proc. Natl. Acad. Sci. U. S. A. **99**: 10185–90.

He, Z., Wang, Z.Y., Li, J., Zhu, Q., Lamb, C., and Chory, J. (2000). Perception of Brassinosteroids by the Extracellular Domain of the Receptor Kinase BRI1. Science (80-.). **288**: 2360–2363.

Hemsley, P.A. (2014). The importance of lipid modified proteins in plants. New Phytol.

Inoue, T., Higuchi, M., Hashimoto, Y., Seki, M., Kobayashi, M., Kato, T., Tabat, S., Shinozaki, K., and Kakimoto, T. (2001). Identification of CRE1 as a cytokinin receptor from Arabidopsis. Nature **409**: 48–51.

Dello Ioio, R., Nakamura, K., Moubayidin, L., Perilli, S., Taniguchi, M., Morita, M.T., Aoyama, T., Costantino, P., and Sabatini, S. (2008). A genetic framework for the control of cell division and differentiation in the root meristem. Science **322**: 1380–4.

Irani, N.G. et al. (2012). Fluorescent castasterone reveals BRI1 signaling from the plasma membrane. Nat Chem Biol **8**: 583–589.

Ishida, T., Kurata, T., Okada, K., and Wada, T. (2008). A genetic regulatory network in the development of trichomes and root hairs. Annu. Rev. Plant Biol. **59**: 365–86.

Iwasaki, T. and Shibaoka, H. (1991). Brassinosteroids Act as Regulators of Tracheary-Element Differentiation in Isolated Zinnia Mesophyll Cells. Plant Cell Physiol. **32**: 1007–1014.

Jaillais, Y., Hothorn, M., Belkhadir, Y., Dabi, T., Nimchuk, Z.L., Meyerowitz, E.M., and Chory, J. (2011). Tyrosine phosphorylation controls brassinosteroid receptor activation by triggering membrane release of its kinase inhibitor. Genes Dev. **25**: 232–7.

Karimi, M., Inzé, D., and Depicker, A. (2002). GATEWAY^{TM} vectors for Agrobacterium-mediated plant transformation. Trends Plant Sci. **7**: 193–195.

Kerstetter, R. a, Bollman, K., Taylor, R. a, Bomblies, K., and Poethig, R.S. (2001). KANADI regulates organ polarity in Arabidopsis. Nature **411**: 706–9.

Kim, T.-W., Guan, S., Burlingame, A.L., and Wang, Z.-Y. (2011). The CDG1 kinase mediates brassinosteroid signal transduction from BRI1 receptor kinase to BSU1 phosphatase and GSK3-like kinase BIN2. Mol. Cell **43**: 561–71.

Kim, T.-W., Guan, S., Sun, Y., Deng, Z., Tang, W., Shang, J.-X., Sun, Y., Burlingame, A.L., and Wang, Z.-Y. (2009). Brassinosteroid signal transduction from cell-surface receptor kinases to nuclear transcription factors. Nat. Cell Biol. **11**: 1254–60.

Kim, T.-W., Michniewicz, M., Bergmann, D.C., and Wang, Z.-Y. (2012). Brassinosteroid regulates stomatal development by GSK3-mediated inhibition of a MAPK pathway. Nature **482**: 419–22.

Kondo, Y., Ito, T., Nakagami, H., Hirakawa, Y., Saito, M., Tamaki, T., Shirasu, K., and Fukuda, H. (2014). Plant GSK3 proteins regulate xylem cell differentiation downstream of TDIF-TDR signalling. Nat. Commun. **5**: 3504.

Lee, C.-R., Park, Y.-H., Kim, Y.-R., Peterkofsky, A., and Seok, Y.-J. (2013). Phosphorylation-Dependent Mobility Shift of Proteins on SDS-PAGE is Due to Decreased Binding of SDS. Bull. Korean Chem. Soc. **34**: 2063–2066.

Levy, A., Erlanger, M., Rosenthal, M., and Epel, B.L. (2007). A plasmodesmata-associated beta-1,3-glucanase in Arabidopsis. Plant J. **49**: 669–82.

Li, J. and Chory, J. (1997). A putative leucine-rich repeat receptor kinase involved in brassinosteroid signal transduction. Cell **90**: 929–38.

Li, J., Nagpal, P., Vitart, V., McMorris, T.C., and Chory, J. (1996). A Role for Brassinosteroids in Light-Dependent Developement of Arabidopsis. Science (80-.). **272**: 398–401.

Li, J. and Nam, K.H. (2002). Regulation of brassinosteroid signaling by a GSK3/SHAGGY-like kinase. Science **295**: 1299–301.

Li, J., Nam, K.H., Vafeados, D., and Chory, J. (2001). BIN2, a new brassinosteroid-insensitive locus in Arabidopsis. Plant Physiol. **127**: 14–22.

Li, J., Wen, J., Lease, K. a, Doke, J.T., Tax, F.E., and Walker, J.C. (2002). BAK1, an Arabidopsis LRR Receptor-like Protein Kinase, Interacts with BRI1 and Modulates Brassinosteroid Signaling. Cell **110**: 213–222.

Ligrone, R., Duckett, J.G., Renzaglia, K.S., Ambientali, S., Universita, S., and Caserta, I.- (2000). Conducting tissues and phyletic relationships of bryophytes. Philos. Trans. R. Soc. B Biol. Sci. **355**: 795–813.

Lucas, W.J. et al. (2013). The plant vascular system: evolution, development and functions. J. Integr. Plant Biol. **55**: 294–388.

Luscombe, N.M., Austin, S.E., Berman, H.M., and Thornton, J.M. (2000). An overview of the structures of protein-DNA complexes. Genome Biol. **1**: 1–37.

Mähönen, A.P., Bishopp, A., Higuchi, M., Nieminen, K.M., Kinoshita, K., Törmäkangas, K., Ikeda, Y., Oka, A., Kakimoto, T., and Helariutta, Y. (2006). Cytokinin Signaling and Its Inhibitor AHP6 Regulate Cell Fate During Vascular Development. Science **311**: 94–8.

Mähönen, A.P., Bonke, M., Kauppinen, L., Riikonen, M., Benfey, P.N., and Helariutta, Y. (2000). A novel two-component hybrid molecule regulates vascular morphogenesis of the Arabidopsis root. Genes Dev. **14**: 2938–2943.

Marcos, D. and Berleth, T. (2014). Dynamic auxin transport patterns preceding vein formation revealed by live-imaging of Arabidopsis leaf primordia. Front. Plant Sci. **5**: 235.

McConnell, J.R., Emery, J., Eshed, Y., Bao, N., Bowman, J., and Barton, M.K. (2001). Role of PHABULOSA and PHAVOLUTA in determining radial patterning in shoots. Nature **411**: 709–13.

Mitchell, J.W. and Gregory, L.E. (1972). Enhancement of Overall Plant Growth, a New Response to Brassins. Nature **239**: 253–254.

Mitchell, J.W., Mandava, N., Worley, J.F., Plimmer, J.R., and Smith, M. V. (1970). Brassins - a New Family of Plant Hormones from Rape Pollen. Nature **225**: 1065–1066.

Montoya, T., Nomura, T., Yokota, T., Farrar, K., Harrison, K., Jones, J.D.G., Jones, J.G.D., Kaneta, T., Kamiya, Y., Szekeres, M., and Bishop, G.J. (2005). Patterns of Dwarf expression and brassinosteroid accumulation in tomato reveal the importance of brassinosteroid synthesis during fruit development. Plant J. **42**: 262–9.

Mora-García, S., Vert, G., Yin, Y., Caño-Delgado, A., Cheong, H., and Chory, J. (2004). Nuclear protein phosphatases with Kelch-repeat domains modulate the response to brassinosteroids in Arabidopsis. Genes Dev. **18**: 448–60.

Mouchel, C.F., Briggs, G.C., and Hardtke, C.S. (2004). Natural genetic variation in Arabidopsis identifies BREVIS RADIX, a novel regulator of cell proliferation and elongation in the root. Genes Dev. **18**: 700–14.

Mouchel, C.F., Osmont, K.S., and Hardtke, C.S. (2006). BRX mediates feedback between brassinosteroid levels and auxin signalling in root growth. Nature **443**: 458–61.

Muto, H., Yabe, N., Asami, T., Hasunuma, K., and Yamamoto, K.T. (2004). Overexpression of Constitutive Differential Growth 1 Gene , Which Encodes a RLCKVII-Subfamily Protein Kinase , Causes Abnormal Differential and Elongation Growth after Organ Differentiation in Arabidopsis 1. Plant Physiol. **136**: 3124–3133.

Mutterer, J. and Zinck, E. (2013). Quick-and-clean article figures with FigureJ. J. Microsc. **252**: 89–91.

Nagawa, S., Sawa, S., Sato, S., Kato, T., Tabata, S., and Fukuda, H. (2006). Gene trapping in Arabidopsis reveals genes involved in vascular development. Plant Cell Physiol. **47**: 1394–405.

Nakagawa, T., Kurose, T., Hino, T., Tanaka, K., Kawamukai, M., Niwa, Y., Toyooka, K., Matsuoka, K., Jinbo, T., and Kimura, T. (2007). Development of series of gateway binary vectors, pGWBs, for realizing efficient construction of fusion genes for plant transformation. J. Biosci. Bioeng. **104**: 34–41.

Noguchi, T., Fujioka, S., Takatsuto, S., Sakurai, A., Yoshida, S., Li, J., and Chory, J. (1999). Arabidopsis det2 is defective in the conversion of (24R)-24-methylcholest-4-En-3-one to

(24R)-24-methyl-5alpha-cholestan-3-one in brassinosteroid biosynthesis. Plant Physiol. **120**: 833–40.

Peng, P., Yan, Z., Zhu, Y., and Li, J. (2008). Regulation of the Arabidopsis GSK3-like kinase BRASSINOSTEROID-INSENSITIVE 2 through proteasome-mediated protein degradation. Mol. Plant **1**: 338–46.

Peng, P., Zhao, J., Zhu, Y., Asami, T., and Li, J. (2010). A direct docking mechanism for a plant GSK3-like kinase to phosphorylate its substrates. J. Biol. Chem. **285**: 24646–53.

Petrásek, J. and Friml, J. (2009). Auxin transport routes in plant development. Development **136**: 2675–88.

Pittermann, J., Limm, E., Rico, C., and Christman, M. a (2011). Structure-function constraints of tracheid-based xylem: a comparison of conifers and ferns. New Phytol. **192**: 449–61.

Pittermann, J., Sperry, J.S., Hacke, U.G., Wheeler, J.K., and Sikkema, E.H. (2005). Torus-Margo Pits Help Conifers Compete with Angiosperms. Scie **310**: 2005.

Raffaele, S. et al. (2009). Remorin, a solanaceae protein resident in membrane rafts and plasmodesmata, impairs potato virus X movement. Plant Cell **21**: 1541–55.

Rayle, D.L. and Cleland, R.E. (1992). The Acid Growth Theory of auxin-induced cell elongation is alive and well. Plant Physiol. **99**: 1271–4.

Reed, J.W. (2001). Roles and activities of Aux/IAA proteins in Arabidopsis. Trends Plant Sci. **6**: 420–5.

Ren, J., Wen, L., Gao, X., Jin, C., Xue, Y., and Yao, X. (2008). CSS-Palm 2.0: an updated software for palmitoylation sites prediction. Protein Eng. Des. Sel. **21**: 639–44.

Rodriguez-Villalon, A., Gujas, B., Kang, Y.H., Breda, A.S., Cattaneo, P., Depuydt, S., and Hardtke, C.S. (2014). Molecular genetic framework for protophloem formation. Proc. Natl. Acad. Sci. U. S. A. **111**.

Roschzttardtz, H., Paez-Valencia, J., Dittakavi, T., Jali, S., Reyes, F., Baisa, G., Anne, P., Gissot, L., Palauqui, J.-C., Masson, P., Bednarek, S., and Otegui, M.S. (2014). The VASCULATURE COMPLEXITY AND CONNECTIVITY (VCC) Gene Encodes a Plant-Specific Protein Required for Embryo Provasculature Development. Plant Physiol. **166**: 889–902.

Di Rubbo, S. et al. (2013). The clathrin adaptor complex AP-2 mediates endocytosis of brassinosteroid insensitive1 in Arabidopsis. Plant Cell **25**: 2986–97.

De Rybel, B. et al. (2009). Chemical inhibition of a subset of Arabidopsis thaliana GSK3-like kinases activates brassinosteroid signaling. Chem. Biol. **16**: 594–604.

De Rybel, B. et al. (2014a). Integration of growth and patterning during vascular tissue formation in Arabidopsis. Science (80-.). **345**: 1255215–1255215.

De Rybel, B., Breda, A.S., and Weijers, D. (2014b). Prenatal plumbing-vascular tissue formation in the plant embryo. Physiol. Plant. **151**: 126–33.

Ryu, H., Kim, K., Cho, H., Park, J., Choe, S., and Hwang, I. (2007). Nucleocytoplasmic shuttling of BZR1 mediated by phosphorylation is essential in Arabidopsis brassinosteroid signaling. Plant Cell **19**: 2749–62.

Sachs, T. (1981). The Control of the Patterned Differentiation of Vascular Tissues. Adv. Bot. Res. **9**: 151–262.

De Saint Exupery, A. (1943). Le Petit Prince.

Savaldi-Goldstein, S., Peto, C., and Chory, J. (2007). The epidermis both drives and restricts plant shoot growth. Nature **446**: 199–202.

Scacchi, E., Osmont, K.S., Beuchat, J., Salinas, P., Navarrete-Gómez, M., Trigueros, M., Ferrándiz, C., and Hardtke, C.S. (2009). Dynamic, auxin-responsive plasma membrane-to-nucleus movement of Arabidopsis BRX. Development **136**: 2059–67.

Scacchi, E., Salinas, P., Gujas, B., Santuari, L., Krogan, N., Ragni, L., and Berleth, T. (2010). Spatio-temporal sequence of cross-regulatory events in root meristem growth. PNAS **107**: 22734–22739.

Scarpella, E., Francis, P., and Berleth, T. (2004). Stage-specific markers define early steps of procambium development in Arabidopsis leaves and correlate termination of vein formation with mesophyll differentiation. Development **131**: 3445–55.

Scarpella, E., Marcos, D., Friml, J., and Berleth, T. (2006). Control of leaf vascular patterning by polar auxin transport. Genes Dev. **20**: 1015–27.

Scheres, B., Laurenzio, L. Di, Willemsen, V., Hauser, M., Janmaat, K., Weisbeek, P., and Benfey, P.N. (1995). Mutations affecting the radial organisation of the Arabidopsis root display specific defects throughout the embryonic axis. Development **121**: 53–62.

Scheres, B., Wolkenfelt, H., Willemsen, V., Terlouw, M., Lawson, E., Dean, C., and Weisbeek, P. (1994). Embryonic origin of the Arabidopsis primary root and root meristem initials. Development **2487**: 2475–2487.

Schlereth, A., Möller, B., Liu, W., Kientz, M., Flipse, J., Rademacher, E.H., Schmid, M., Jürgens, G., and Weijers, D. (2010). MONOPTEROS controls embryonic root initiation by regulating a mobile transcription factor. Nature **464**: 913–6.

Schuetz, M., Smith, R., and Ellis, B. (2013). Xylem tissue specification, patterning, and differentiation mechanisms. J. Exp. Bot. **64**: 11–31.

Sieburth, L.E., Muday, G.K., King, E.J., Benton, G., Kim, S., Metcalf, K.E., Meyers, L., Seamen, E., and Van Norman, J.M. (2006). SCARFACE encodes an ARF-GAP that is required for normal auxin efflux and vein patterning in Arabidopsis. Plant Cell **18**: 1396–411.

Siegfried, K.R., Eshed, Y., Baum, S.F., Otsuga, D., Drews, G.N., and Bowman, J.L. (1999). Members of the YABBY gene family specify abaxial cell fate in Arabidopsis. Development **126**: 4117–28.

Sjolund, R.D. (1997). The Phloem Sieve Element: A River Runs through It. Plant Cell **9**: 1137–1146.

Smith, R. a, Schuetz, M., Roach, M., Mansfield, S.D., Ellis, B., and Samuels, L. (2013). Neighboring parenchyma cells contribute to Arabidopsis xylem lignification, while lignification of interfascicular fibers is cell autonomous. Plant Cell **25**: 3988–99.

Stagljar, I., Korostensky, C., Johnsson, N., and Heensen, S.H. (1998). A genetic system based on split-ubiquitin for the analysis of interactions between membrane proteins in vivo. Proc. Natl. Acad. Sci. U. S. A. **95**: 5187–5192.

Sun, Y. et al. (2010). Integration of brassinosteroid signal transduction with the transcription network for plant growth regulation in Arabidopsis. Dev. Cell **19**: 765–77.

Sweetlove, L. (2011). Number of species on Earth tagged at 8.7 million. Nat. News.

Symons, G.M. and Reid, J.B. (2004). Brassinosteroids do not undergo long-distance transport in pea. Implications for the regulation of endogenous brassinosteroid levels. Plant Physiol. **135**: 2196–206.

Symons, G.M., Ross, J.J., Jager, C.E., and Reid, J.B. (2008). Brassinosteroid transport. J. Exp. Bot. **59**: 17–24.

Szekeres, M., Németh, K., Koncz-Kálmán, Z., Mathur, J., Kauschmann, A., Altmann, T., Rédei, G.P., Nagy, F., Schell, J., and Koncz, C. (1996). Brassinosteroids rescue the deficiency of CYP90, a cytochrome P450, controlling cell elongation and de-etiolation in Arabidopsis. Cell **85**: 171–82.

Taelman, V.F., Dobrowolski, R., Plouhinec, J.-L., Fuentealba, L.C., Vorwald, P.P., Gumper, I., Sabatini, D.D., and De Robertis, E.M. (2010). Wnt signaling requires sequestration of glycogen synthase kinase 3 inside multivesicular endosomes. Cell **143**: 1136–48.

Tang, W. et al. (2011). PP2A activates brassinosteroid-responsive gene expression and plant growth by dephosphorylating BZR1. Nat. Cell Biol. **13**: 124–31.

Tang, W., Kim, T.-W., Oses-Prieto, J. a, Sun, Y., Deng, Z., Zhu, S., Wang, R., Burlingame, A.L., and Wang, Z.-Y. (2008). BSKs mediate signal transduction from the receptor kinase BRI1 in Arabidopsis. Science (80-.). **321**: 557–60.

Truernit, E., Bauby, H., Belcram, K., Barthélémy, J., and Palauqui, J.-C. (2012). OCTOPUS, a polarly localised membrane-associated protein, regulates phloem differentiation entry in Arabidopsis thaliana. Development **139**: 1306–15.

Truernit, E., Bauby, H., Dubreucq, B., Grandjean, O., Runions, J., Barthélémy, J., and Palauqui, J.-C. (2008). High-resolution whole-mount imaging of three-dimensional tissue organization and gene expression enables the study of Phloem development and structure in Arabidopsis. Plant Cell **20**: 1494–503.

Turner, S. and Sieburth, L.E. (2003). Vascular patterning. Arabidopsis Book **2**: e0073.

Ulmasov, T., Murfett, J., Hagen, G., and Guilfoyle, T.J. (1997). Creation of a Highly Active Synthetic AuxRE. Plant Cell **9**: 1963–1971.

Vanmierlo, T., Husche, C., Schött, H.F., Pettersson, H., and Lütjohann, D. (2013). Plant sterol oxidation products--analogs to cholesterol oxidation products from plant origin? Biochimie **95**: 464–72.

Vanstraelen, M. and Benková, E. (2012). Hormonal interactions in the regulation of plant development. Annu. Rev. Cell Dev. Biol. **28**: 463–87.

Vatén, A. et al. (2011). Callose biosynthesis regulates symplastic trafficking during root development. Dev. Cell **21**: 1144–55.

Vert, G. and Chory, J. (2006). Downstream nuclear events in brassinosteroid signalling. Nature **441**: 96–100.

Vert, G., Nemhauser, J.L., Geldner, N., Hong, F., and Chory, J. (2005). Molecular mechanisms of steroid hormone signaling in plants. Annu. Rev. Cell Dev. Biol. **21**: 177–201.

Vert, G., Walcher, C.L., Chory, J., and Nemhauser, J.L. (2008). Integration of auxin and brassinosteroid pathways by Auxin Response Factor 2. Proc. Natl. Acad. Sci. U. S. A. **105**: 9829–34.

Vilarrasa-Blasi, J., González-García, M.-P., Frigola, D., Fàbregas, N., Alexiou, K.G., López-Bigas, N., Rivas, S., Jauneau, A., Lohmann, J.U., Benfey, P.N., Ibañes, M., and Caño-Delgado, A.I. (2014). Regulation of Plant Stem Cell Quiescence by a Brassinosteroid Signaling Module. Dev. Cell: 1–12.

Voinnet, O., Rivas, S., Mestre, P., and Baulcombe, D. (2003). An enhanced transient expression system in plants based on suppression of gene silencing by the p19 protein of tomato bushy stunt virus. Plant J. **33**: 949–956.

Völker, a, Stierhof, Y.D., and Jürgens, G. (2001). Cell cycle-independent expression of the Arabidopsis cytokinesis-specific syntaxin KNOLLE results in mistargeting to the plasma membrane and is not sufficient for cytokinesis. J. Cell Sci. **114**: 3001–12.

Vriet, C., Russinova, E., and Reuzeau, C. (2013). From squalene to brassinolide: the steroid metabolic and signaling pathways across the plant kingdom. Mol. Plant **6**: 1738–57.

Wang, X. and Chory, J. (2006). Brassinosteroids regulate dissociation of BKI1, a negative regulator of BRI1 signaling, from the plasma membrane. Science **313**: 1118–22.

Wang, X., Kota, U., He, K., Blackburn, K., Li, J., Goshe, M.B., Huber, S.C., and Clouse, S.D. (2008). Sequential transphosphorylation of the BRI1/BAK1 receptor kinase complex impacts early events in brassinosteroid signaling. Dev. Cell **15**: 220–35.

Wang, X., Li, X., Meisenhelder, J., Hunter, T., Yoshida, S., Asami, T., and Chory, J. (2005). Autoregulation and homodimerization are involved in the activation of the plant steroid receptor BRI1. Dev. Cell **8**: 855–65.

Wang, X., Zhang, J., Yuan, M., Ehrhardt, D.W., Wang, Z., and Mao, T. (2012). Arabidopsis microtubule destabilizing protein40 is involved in brassinosteroid regulation of hypocotyl elongation. Plant Cell **24**: 4012–25.

Wang, Z., Seto, H., Fujioka, S., Yoshida, S., and Chory, J. (2001). BRI1 is a critical component of a plasma-membrane receptor for plant steroids. Nature **410**: 380–383.

Wang, Z.Y., Nakano, T., Gendron, J., He, J., Chen, M., Vafeados, D., Yang, Y., Fujioka, S., Yoshida, S., Asami, T., and Chory, J. (2002). Nuclear-localized BZR1 mediates brassinosteroid-induced growth and feedback suppression of brassinosteroid biosynthesis. Dev. Cell **2**: 505–13.

Weijers, D., Benkova, E., Jäger, K.E., Schlereth, A., Hamann, T., Kientz, M., Wilmoth, J.C., Reed, J.W., and Jürgens, G. (2005). Developmental specificity of auxin response by pairs of ARF and Aux/IAA transcriptional regulators. EMBO J. **24**: 1874–85.

Wengier, D.L. and Bergmann, D.C. (2012). On fate and flexibility in stomatal development. Cold Spring Harb. Symp. Quant. Biol. **77**: 53–62.

Went, F.W. (1927). Wuchsstoff und Wachstum.

Wenzel, C.L., Schuetz, M., Yu, Q., and Mattsson, J. (2007). Dynamics of MONOPTEROS and PIN-FORMED1 expression during leaf vein pattern formation in Arabidopsis thaliana. Plant J. **49**: 387–98.

Wolf, S. et al. (2014). A receptor-like protein mediates the response to pectin modification by activating brassinosteroid signaling. Proc. Natl. Acad. Sci.

Wolf, S., Hématy, K., and Höfte, H. (2012a). Growth control and cell wall signaling in plants. Annu. Rev. Plant Biol. **63**: 381–407.

Wolf, S., Mravec, J., Greiner, S., Mouille, G., and Höfte, H. (2012b). Plant cell wall homeostasis is mediated by brassinosteroid feedback signaling. Curr. Biol. **22**: 1732–7.

Xie, B., Wang, X., Zhu, M., Zhang, Z., and Hong, Z. (2011). CalS7 encodes a callose synthase responsible for callose deposition in the phloem. Plant J. **65**: 1–14.

Xu, W., Purugganan, M.M., Polisensky, D.H., Antosiewicz, D.M., Fry, S.C., and Braam, J. (1995). Arabidopsis TCH4, regulated by hormones and the environment, encodes a xyloglucan endotransglycosylase. Plant Cell **7**: 1555–67.

Xue, Y., Liu, Z., Cao, J., Ma, Q., Gao, X., Wang, Q., Jin, C., Zhou, Y., Wen, L., and Ren, J. (2011a). GPS 2.1: enhanced prediction of kinase-specific phosphorylation sites with an algorithm of motif length selection. Protein Eng. Des. Sel. **24**: 255–60.

Xue, Y., Liu, Z., Cao, J., Ma, Q., Gao, X., Wang, Q., Jin, C., Zhou, Y., Wen, L., and Ren, J. (2011b). GPS 2.1: enhanced prediction of kinase-specific phosphorylation sites with an algorithm of motif length selection. Protein Eng. Des. Sel. **24**: 255–60.

Yamamoto, R., Demura, T., and Fukuda, H. (1997). Brassinosteroids induce entry into the final stage of tracheary element differentiation in cultured Zinnia cells. Plant Cell Physiol. **38**: 980–3.

Yan, Z., Zhao, J., Peng, P., Chihara, R.K., and Li, J. (2009). BIN2 Functions Redundantly with Other Arabidopsis GSK3-Like Kinases to Regulate. Plant Physiol. **150**: 710–721.

Yin, Y., Vafeados, D., Tao, Y., Yoshida, S., Asami, T., and Chory, J. (2005). A new class of transcription factors mediates brassinosteroid-regulated gene expression in Arabidopsis. Cell **120**: 249–59.

Yin, Y., Wang, Z.Y., Mora-Garcia, S., Li, J., Yoshida, S., Asami, T., and Chory, J. (2002). BES1 accumulates in the nucleus in response to brassinosteroids to regulate gene expression and promote stem elongation. Cell **109**: 181–91.

Young, S.G. and Fielding, C.J. (1999). The ABCs of cholesterol efflux. Nat. Genet. **22**: 316–8.

Yu, X., Li, L., Zola, J., Aluru, M., Ye, H., Foudree, A., Guo, H., Anderson, S., Aluru, S., Liu, P., Rodermel, S., and Yin, Y. (2011). A brassinosteroid transcriptional network revealed by genome-wide identification of BESI target genes in Arabidopsis thaliana. Plant J. **65**: 634–46.

Zhu, J.-Y., Sae-Seaw, J., and Wang, Z.-Y. (2013). Brassinosteroid signalling. Development **140**: 1615–20.

ANNEXES

The *VASCULATURE COMPLEXITY AND CONNECTIVITY* Gene Encodes a Plant-Specific Protein Required for Embryo Provasculature Development[1][C][W][OPEN]

Hannetz Roschzttardtz*, Julio Paez-Valencia, Tejaswi Dittakavi, Sathya Jali, Francisca C. Reyes, Gary Baisa, Pauline Anne, Lionel Gissot, Jean-Christophe Palauqui, Patrick H. Masson, Sebastian Y. Bednarek, and Marisa S. Otegui*

Department of Botany (H.R., J.P.-V., T.D., F.C.R., M.S.O.), Department of Genetics (S.J., P.H.M., M.S.O.), and Department of Biochemistry (G.B., S.Y.B.), University of Wisconsin, Madison, Wisconsin 53706; Great Lakes Bioenergy Research Center, Madison, Wisconsin 53706 (H.R., S.J., G.B.); and Institut National de la Recherche Agronomique and AgroParisTech, Institut Jean-Pierre Bourgin, Unité Mixte de Recherche 1318, Saclay Plant Science, 78000 Versailles, France (P.A., L.G., J.-C.P.)

ORCID IDs: 0000-0001-7465-1787 (S.Y.B.); 0000-0003-4699-6950 (M.S.O.).

The molecular mechanisms by which vascular tissues acquire their identities are largely unknown. Here, we report on the identification and characterization of *VASCULATURE COMPLEXITY AND CONNECTIVITY* (*VCC*), a member of a 15-member, plant-specific gene family in Arabidopsis (*Arabidopsis thaliana*) that encodes proteins of unknown function with four predicted transmembrane domains. Homozygous *vcc* mutants displayed cotyledon vein networks of reduced complexity and disconnected veins. Similar disconnections or gaps were observed in the provasculature of *vcc* embryos, indicating that defects in vein connectivity appear early in mutant embryo development. Consistently, the overexpression of *VCC* leads to an unusually high proportion of cotyledons with high-complexity vein networks. Neither auxin distribution nor the polar localization of the auxin efflux carrier were affected in *vcc* mutant embryos. Expression of *VCC* was detected in developing embryos and procambial, cambial, and vascular cells of cotyledons, leaves, roots, hypocotyls, and anthers. To evaluate possible genetic interactions with other genes that control vasculature patterning in embryos, we generated a double mutant for *VCC* and *OCTOPUS* (*OPS*). The *vcc ops* double mutant embryos showed a complete loss of high-complexity vascular networks in cotyledons and a drastic increase in both provascular and vascular disconnections. In addition, VCC and OPS interact physically, suggesting that *VCC* and *OPS* are part of a complex that controls cotyledon vascular complexity.

Coloration à l'iodure de propidium (d'après Truernit et al. 2008)

Le matériel végétal est fixé dans un tampon de fixation méthanol/acide acétique/eau (v/v/v 50/10/40) de 24h à 15 jours à 4°C et rincé deux fois à l'eau pendant 5 minutes. Un bain de 20 minutes sous agitation dans de l'acide périodique 1% (w/v) permet l'oxydation les aldéhydes. Les échantillons sont ensuite rincés deux fois à l'eau. Les échantillons baignent ensuite quelques secondes dans le réactif de Schiff (1.9g de bisulfite de sodium, 3mL de HCl 5M, qsp 100mL) avant d'y ajouter l'iodure de prodidium à une concentration finale 0.1mg/mL. Les échantillons sont incubés 1h sous agitation. Les échantillons sont rincés 2 fois à l'eau, puis décolorés au chloral hydrate pendant environ 1h (Chloral hydrate 4g, glycerol 1mL, eau 2mL). Le matériel est finalement monté entre lame et lamelle dans une solution de Hoyer (30 g de gomme arabique, 200g de chloral hydrate, 20g de glycerol, 50mL d'eau). Les échantillons sont observés quelques jours plus tard afin de laisser sécher le milieu de montage.

Coloration GUS (d'après Jefferson et al. 1987)

Les plantules sont infiltrées sous vide dans une solution 100mM de phosphate de sodium pH7.2, 10mM d'EDTA, 0.1% Triton X-100 et 1mg/mL d'acide 5-bromo-4 chloro-3-indolyl-β-D-glucuronic (X-gluc, Dushefa) à laquelle une concentration variable de potassium ferrocyanure et de potassium ferrocyanure est ajoutée. Les échantillons sont incubés 12-16h à 37°C à l'obscurité puis sont rincés deux fois à l'eau. Ils sont soit utilisés pour une coloration à l'iodure de prodidium soit décolorés dans des bains croissant d'ethanol (10% à 90%) puis réhydratée dans les mêmes bains successifs (90% à 10%). Les échantillons sont alors montés entre lame et lamelle dans de l'eau avant d'être observés.

Liste des primers (5'-3')

Clonage

OPS CDS gtw	F	GGGGACAAGTTTGTACAAAAAAGCAGGCTCCATGAATCCAGCTACTGACCCA
	R wo stop	GGGGACCACTTTGTACAAGAAAGCTGGGTCTTAAGTTCCAGATTGATTCAAGAAGC
	R STOP	GGGGACCACTTTGTACAAGAAAGCTGGGTCTCAATACAGCCTCATTACACTCCTCGC
OPS CDS$^{49-685}$ gtw	F	GGGGACAAGTTTGTACAAAAAAGCAGGCTCCATGGAACGTCTCTCAGTCTTAGATCAG
	R wo stop	GGGGACCACTTTGTACAAGAAAGCTGGGTCTTAAGTTCCAGATTGATTCAAGAAGC
OPS CDS$^{1-51}$ gtw	F	GGGGACAAGTTTGTACAAAAAAGCAGGCTCCATGAATCCAGCTACTGACCCA
	R wo stop	GGGGACCACTTTGTACAAGAAAGCTGGGTCGAGACGTTCACAGAGACAAGA
CDS OPSL1- gtw	FB1OPSL1cDNA	GGGGACAAGTTTGTACAAAAAAGCAGGCTCCATGGTTATGAATAATCCTGC
	RB2OPSL1cDNA wo stop	GGGGACCACTTTGTACAAGAAAGCTGGGTCGTAAAAGTTCATAACATTTC
CDS OPSL2- gtw	FB1OPSL2cDNA	GGGGACAAGTTTGTACAAAAAAGCAGGCTCCATGAATCTCTCCGCCGACCA
	RB2OPSL2cDNAdsto wo stop	GGGGACCACTTTGTACAAGAAAGCTGGGTCATACAGCCTCATAACCCTCC

2kB promoteur pOPSL1- gtw	B1 pOPSL1	GGGGACAAGTTTGTACAAAAAAGCAGGCTCCATTGAACTGAACCAGTTATTG
	pOPSL1 - R	GGGGACCACTTTGTACAAGAAAGCTGGGTCAAGAGGAAAGGATGAGTGATAAGACTTC
2kB promoteur pOPSL2- gtw	B1 pOPSL2	GGGGACAAGTTTGTACAAAAAAGCAGGCTCCCCTCGCATGTTTTGAATTCC
	pOPSL2 - R	GGGGACCACTTTGTACAAGAAAGCTGGGTCCCCGTGGCTCATATCGGG
CDS CDG1-gtw	Po27_CDG1-FB1	GGGGACAAGTTTGTACAAAAAAGCAGGCTCCATGGTTAGTTGCTTGTGTTTTCG
	Po28_CDG1-RB2 STOP	GGGGACCACTTTGTACAAGAAAGCTGGGTCTCATGGAGTCGGAGTTGG
	Po29_CDG1-RB2 wo stop	GGGGACCACTTTGTACAAGAAAGCTGGGTCTGGAGTCGGAGTTGGTGGCG
BIN2 CDS gtw	F	GGGGACAAGTTTGTACAAAAAAGCAGGCTCCATGGCTGATGATAAGGAGATGCCTGC
	R wo stop	GGGGACCACTTTGTACAAGAAAGCTGGGTCAGTTCCAGATTGATTCAAGAAGC
	R STOP	GGGGACCACTTTGTACAAGAAAGCTGGGTCTTAAGTTCCAGATTGATTCAAGAAGC
OPS pBT3-N or pPR3-N SfiI	F	ATTAACAAG GCC ATT ACG GCCATGAATCCAGCTACTGACCCAGTCTCCGCC
	R	AACTGATTGGCCGAGGCGGCCTCAATACAGCCTCATTACACTCCTCGCTATAGAATGCCCG
BIN2 pPR3N SfiI	F	ATTAACAAGGCCATTACGGCCATGGCTGATGATAAGGAGATGCCTGCTGCTG
	R	AACTGATTGGCCGAGGCGGCCTTAAGTTCCAGATTGATTCAAGAAGCTTAGACCC

RT-q-PCR

DWF4 qPCR	F	AGGGAATCATCGTCGACACC
	R	GGCTGAGATCACCGGTAACA
SAURAC1 qPCR	F	AGGGAATCATCGTCGACACC
	R	TGGTATTGTTAAGCCGCCCA
qPCR reference genes	F SAND	AAC TCT ATG CAG CAT TTG ATC CAC T
	R SAND	TGA TTG CAT ATC TTT ATC GCC ATC
	F APT1	CGGGGATTTTAAGTGGAACA
	R APT1	GAGACATTTTGCGTGGGATT
	F PP2A-A3	GCAATCTCTCATTCCGATAGTC
	R PP2A-A3	ATACCGAACATCAACATCTGG

Génotypage

Salk mutants genotyping	LbB1.3	ATTTTGCCGATTTCGGAAC
génotypage *opsl2-1*	R part1 cDNA L2 mutant allele	CCGAAACCCTACCAGCATCAAGCG
	opsl2_r612 WT allele	CGTCGATTACACTTCTGGGTTCC
	opsl2_F-841 WT allele	CAAGCGAGAGCCCCTAGAC
génotypage *opsl1-1*	opsl1_R463 WT allele	CTCACTCACGCTAGACTCCC
	opsl1_F-134 WT et mutant allele	GTCCGTTGGTAAAAGACG
génotypage *opsl1-2*	opsl1-Up2 WT et mutant allele	GCGTTTCTCCGGTTTCTGTCC
	opsl1-Lo2 WT alelle	TCCTCCTCCTTCTCCATTCC
génotypage *opsl2-1*	R part1 cDNA L2 mutant allele	CCGAAACCCTACCAGCATCAAGCG
	opsl2_r612 WT allele	CGTCGATTACACTTCTGGGTTCC
	opsl2_F-841 WT allele	CAAGCGAGAGCCCCTAGAC

Genotypage *cdl1-2*	Po75_cdl1_R218	ggctcacaggaatcagaaag
	Po76_cdl1-f135	CAGCGATTGGCTTGGCGTG

bri1-116 sequencing	F	GATTCCGAAATGGATTGGCCG
	R	GGCGAAGTGTGACCTCCATA
bin2-1D sequencing	F	GTTGCTGGAGTTTGTCACAGAG
	R	GCGCTGTGCATCTTAGACTTGG
bes1-D sequencing	F	TCCCGAGTCCTTCTCGAGTT
	R	GACAATTGCTGTGGTGCAGG
bzr1-D sequencing	F	CGCCGACTTCTAAGAACCCG
	R	CCACGAGCCTTCCCATTTCC

génotypage de colonies dans vecteur pDONR207	attL1	TCG CGT TAA CGC TAG CAT GGA TCT C
	attL2	GTA ACA TCA GAG ATT TTG AGA CAC

Résumé

Les tissus vasculaires sont d'une grande importance pour la physiologie et le développement de la plante. Le xylème et le phloème composent ce tissu. En assurant le transport des sèves brutes et élaborées, ils permettent ainsi de redistribuer minéraux et métabolites entre les différents organes de la plante. La régulation de la mise en place de ces deux tissus est hautement contrôlée tant d'un point de vue génétique que spatio-temporel. Parmi les gènes impliqués dans la mise en place des tissus vasculaires, le gène *OCTOPUS (OPS*) intervient très précocement au cours du développement dans la mise en place du patron vasculaire ainsi que différenciation du phloème (Bauby et al., 2007; Truernit et al., 2012). *OPS* appartient à une famille de gènes spécifiques des plantes supérieures. Cependant la fonction moléculaire de la protéine OPS reste inconnue.

Une combinaison d'approches physiologique, biochimique, moléculaire, cytologique et génétique a permis de montrer que le gène *OPS* est un nouveau régulateur positif de la voie signalisation des brassinostéroïdes (BR). Les BR sont des hormones végétales impliquées dans de nombreux processus développementaux incluant l'élongation cellulaire ou encore l'organisation des tissus vasculaires. Bien que la découverte des BR date seulement de 1970 (Mitchell et al., 1970; Mitchell and Gregory, 1972; Grove et al., 1979), l'intérêt commun que les scientifiques lui ont porté fait que sa voie de signalisation est aujourd'hui très détaillée. Parmi les composants de la voie des BR, la protéine kinase BIN2 en est le régulateur clef (Li et al., 2001) réprimant la voie par son action sur les facteurs de transcription BES1 et BZR1 (Yin et al., 2002; Wang et al., 2002). OPS interagit physiquement avec la protéine BIN2 au niveau de la membrane plasmique, pouvant créer une inhibition par délocalisation de la protéine BIN2 de son site d'activité. A ce titre, les défauts de phloème observés chez le mutant *ops* sont restaurés lorsque l'activité de BIN2 est abolie ou lorsque la voie est induite en dessous de *BIN2*. Ainsi nous montrons que la voie des BR est directement impliquée dans la différenciation du phloème. Plus généralement, une étude de la redondance fonctionnelle d'autres membres de la famille *OPS* semble indiquer qu'ils pourraient exercer une fonction similaire de régulateurs positifs de la voie des BR au sein d'autres tissus de la plante.

Summary

Vascular tissues play an important role in plant physiology and development. Vascular tissues consist on xylem and phloem that ensure sap transport and permit to redistribute mineral and metabolites between different organs. Regulation of vascular tissues establishment is highly controlled in space and time. Among genes involved in vascular tissues formation, *OCTOPUS (OPS*) gene operates early during development to control vascular patterning and to induce phloem differentiation (Bauby et al., 2007; Truernit et al., 2012). OPS belongs to a multigenic family conserved in high plant. However, molecular function of OPS protein remains unclear.

A combination of physiological, biochemical, molecular, cytological and genetic approaches allowed to show that *OPS* gene is a new positive regulator of brassinosteroid (BR) signaling pathway. BR are phytohormones involved in many developmental processes such as cell elongation or vascular tissues organization. Although BR were discovered in 1970 (Mitchell et al., 1970; Mitchell and Gregory, 1972; Grove et al., 1979), interest of researchers for this hormone permitted its detailed description. Among the component of BR signaling, the BIN2 kinase is the key regulator (Li et al., 2001) which represses the pathway through its action on BES1 and BZR1 transcription factors (Yin et al., 2002; Wang et al., 2002). OPS interacts physically with BIN2 at the plasma membrane which could create an inhibition by delocalization of the BIN2 protein from its activity place. As such, *ops* phloem defects are restored when the activity of BIN2 is inhibited or when the pathway is induced downstream of *BIN2*. Thus, we show that BR pathway is directly involved in phloem differentiation. More generally, a study of the functional redundancy of other *OPS* family members suggests that they could have a similar function as positive regulators of BR pathway in other plant tissues.